AN ABSTRACT OF THE THESIS OF

Hugo Rafael Groening (Name of Student) for the Doctor of Philosophy (Degree)

in Chemistry (Major) presented on 4 December 1973 (Date)

Title: The Structure of the Fission Transition Nucleus ^{227}Ra.

Abstract approved: Redacted for Privacy

Dr. Walter D. Loveland

The character and positions of the first few single particle levels in the transition nucleus ^{227}Ra have been deduced from the available experimental data on the ^{226}Ra (n,f) reaction at neutron energies between 3.6 and 4.1 MeV. A Hauser-Feshbach calculation was carried out in which the fission cross section and the fission fragment angular distributions were simultaneously fitted. In order to calculate the probability of neutron emission from the ^{227}Ra compound nucleus, the excitation energy dependence to the level density in Ra was assumed to be similar to the one in thorium. The level density in the latter was deduced from neutron evaporation data at low energies in ^{232}Th, and neutron resonance information in ^{230}Th. The Hauser-Feshbach calculation was conducted for two different assumptions regarding the nuclear shape at the saddle point. In one case,

the shape of the transition nucleus was assumed to be reflection-symmetric, in the other, asymmetric. The results of our calculation agree well with the theoretical predictions of Nix and Möller as to the number and character of the single particle levels and the height of the fission barrier for ^{227}Ra which was found to be $E_f = 8.2 \pm 0.1$ MeV.

Calculations extended to higher incident neutron energies ($4.7 \text{ MeV} < E_n < 9.0 \text{ MeV}$) indicate that collective effects in the nuclear level density have been consistently underestimated at the equilibrium, as well as at the saddle point deformations by a factor of about 10^3. Analysis of the fission fragment angular distributions at moderate energies tentatively suggest a value of the pairing gap parameter Δ_f considerable larger than the corresponding one at the equilibrium deformation ($\Delta_f \sim 1.7\Delta_o$).

The Structure of the Fission Transition Nucleus ^{227}Ra

by

Hugo Rafael Groening

A THESIS

submitted to

Oregon State University

in partial fulfillment of
the requirements for the
degree of

Doctor of Philosophy

June 1974

APPROVED:

Redacted for Privacy

Assistant Professor of Chemistry

Redacted for Privacy

Chairman, Department of Chemistry

Redacted for Privacy

Dean of Graduate School

Date thesis is presented Dec. 4th, 1973.

Types by Deanna L. Cramer for Hugo Rafael Groening

ACKNOWLEDGEMENTS

At this time I would like to thank my major professor, Dr. Walter Loveland, for his help and guidance and also for having suggested this project. To the Venezuelan Government for its financial backing during the time taken for the completion of my studies. To the International Atomic Energy Agency and the National Research Council of the United States for having partially supported two years of my stay at the University.

My deep appreciation goes to Drs. J. R. Nix and P. Möller for making available to me their ^{226}Ra calculations. Important suggestions and useful discussions with Dr. R. Vandenbosch are gratefully acknowledged. I would also like to thank Dr. M. Bolsterli for having made available his computer program to me, and to Dr. H. C. Britt for his cooperation.

It is a pleasure to acknowledge the help and cooperation from the personnel at the Computer Services Department of the EPA Water Research Laboratory in Corvallis, and also at the Bonneville Power Administration in Portland whose computer was employed in carrying out the present calculations.

Finally, I would like to acknowledge my wife, in spite of whom I was able to carry out this work to its happy completion.

TABLE OF CONTENTS

LIST OF ILLUSTRATIONS

LIST OF TABLES

THE STRUCTURE OF THE FISSION TRANSITION NUCLEUS ^{227}Ra

I. INTRODUCTION

A. Preliminary Considerations

In 1938, Hahn and Strassman (Ha 39) discovered that the bombardment of uranium with neutrons produced several radioactive nuclides which were chemically indistinguishable from elements in the middle of the periodic table, such as barium and lanthanum. Although at first they believed these nuclides to be isotopes of radium and actinium, soon they were convinced that the radioactive products were isotopes of much lighter elements formed by the splitting of the uranium nucleus into two parts of comparable size.

The mechanics of nuclear fission was first described in detail in a classic paper by Bohr and Wheeler (Bo 39). On the basis of a liquid drop model of the nucleus, they developed a fission theory which gives a satisfactory picture of many aspects of nuclear fission. This theory was centered on the idea that for the heaviest group of nuclei, the repulsion of the long range coulombic forces opposes, to a large extent, the short range nuclear forces which operate in a manner analogous to a surface tension.

The immediate implication of the theory was that as the nucleus distorted in a given direction, a point was reached in which the coulomb repulsive forces became equal

to the forces holding the nucleus together, and from here, the nucleus could either undergo fission or collapse back to its equilibrium shape. This critical point was called the "saddle point" in the potential energy surface, and the net increase in potential energy necessary to reach that point was termed the "fission barrier".

The passage over the saddle point is the rate determining step in fission. A nucleus at the saddle point is known as a "transition state nucleus" (see Figure 1). If the transition state nucleus is further deformed, it will eventually divide into at least two fragments. The deformation at which division into two fragments occurs is called the "scission point". The fragments are of intermediate mass and contain various amounts of excitation energy. At the time of scission, the nuclear deformation has increased beyond that of the transition state nucleus and at the instant of separation, the primary fragments possess, in some cases, considerable deformation energy, in addition to their other forms of energy. A wide variety of division in fragment mass, charge, and energy is observed, depending upon the initial mass and excitation energy of the fissioning nucleus.

In this work we are mainly interested in the properties of the transition state nucleus, i.e., the nucleus at the saddle point. Historically, we should begin by pointing out that in 1952, Winhold et al. (Wi 52) experimentally

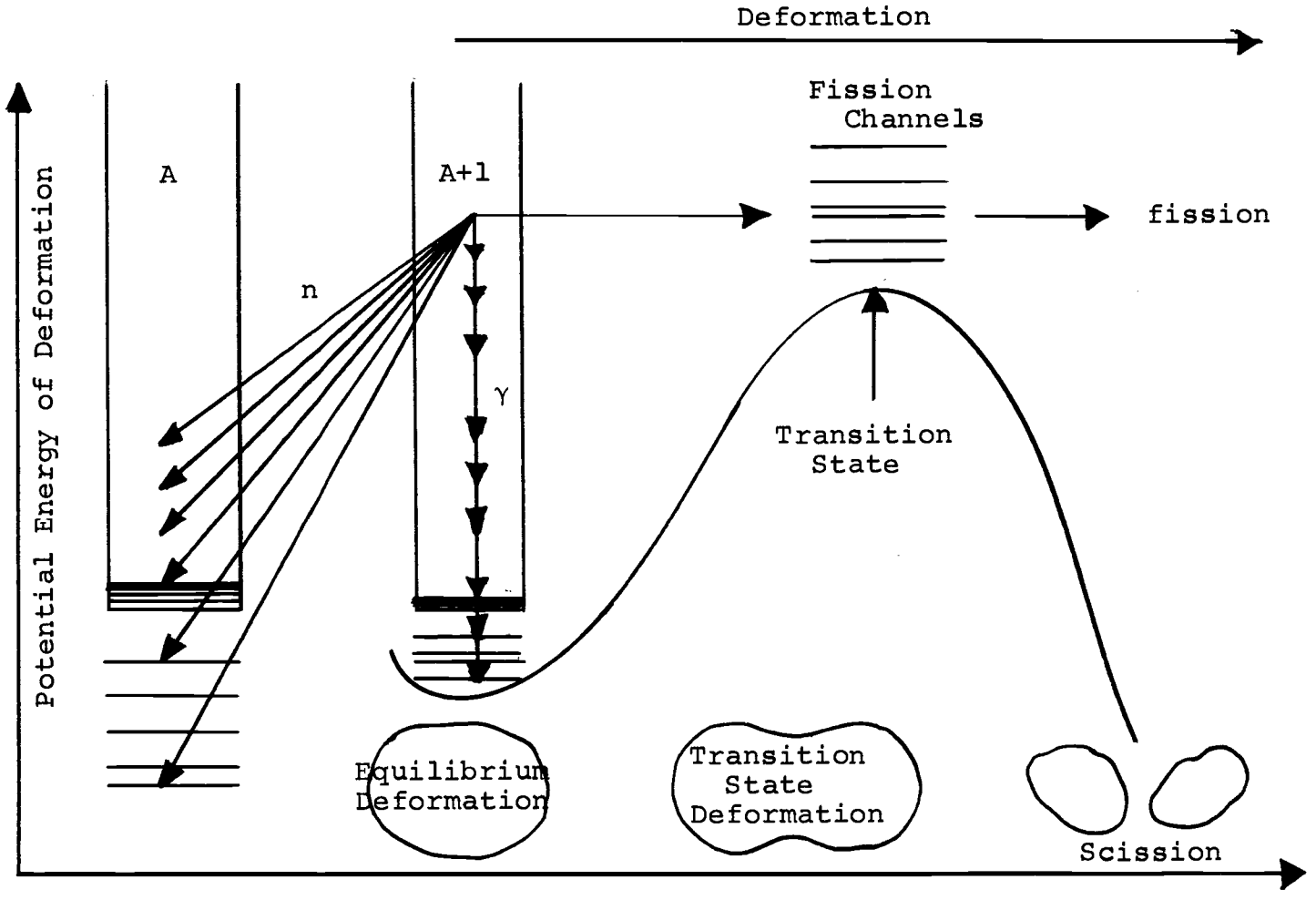

Figure 1. Schematic Overview of the Fission Process.

observed that the angular distribution of ^{232}Th and ^{238}U fission fragments induced by photofission was clearly anisotropic. In order to explain the observed angular distribution, Bohr (Bo 55) proposed a theory in which he suggested that fission proceeded through definite states in the transition state nucleus characterized by well defined quantum numbers, which were responsible for many of the properties of the final fragments. Basically, the spectrum of excited states of the nucleus at the saddle point could be simply explained in terms of the collective and unified models, which had worked so well for the low lying states of stably deformed nuclei (see Figure 1). These quantum states of the nucleus at the saddle point were termed "channels". According to Bohr, a fission event passing through a fission channel might exhibit a marked anisotropy in the angular distribution of the fission fragments, depending on the angular momentum quantum numbers of the channel.

In order to explain this situation, let us start by supposing for a moment that the nucleus is spherical. The simple shell model of the nucleus assumes that each nucleon moves in a potential well (also spherical), which is an approximate representation of the interaction of that nucleon with all of the others. By solving the Schrödinger equation for particles in such a potential well, and introducing a spin-orbit interaction, a set of energy

levels is obtained. These levels are characterized by their principal quantum number, orbital angular momentum, and total spin. An odd nucleon in a given shell model state can have several different projections of its angular momentum on a symmetry axis. These projections are called Ω. For example, a $d_{5/2}$ single nucleon can have values 1/2, 3/2, and 5/2 for its Ω quantum number. When the potential well is undeformed, the energy of the nucleon is independent of Ω. However, this is no longer the case when the potential well is deformed. Each shell model level of angular momentum j breaks into j + 1/2 levels (called Nilsson levels), each of which may contain up to two nucleons of each type. The angular momentum of the odd-A deformed nuclei is due to both the rotational angular momentum (if any) and to the angular momentum of the odd nucleon. The projection Ω of the nucleon's angular momentum adds vectorially to the rotational angular momentum R, to give the total angular momentum J. The projection of J on the nuclear symmetry axis is called K. As shown in Figure 2, R is actually perpendicular to the symmetry axis in an axially symmetric nucleus, and hence, Ω is equal to K. When the rotational angular momentum is zero, J, Ω, and K are all equal. Thus, each Nilsson level may form the ground state of a rotational band. Except for cases where K = 1/2, the energies of the members of the band are given by[1]

[1]The case of K = 1/2 is more complicated and a more complete discussion of this case is given in the next chapter.

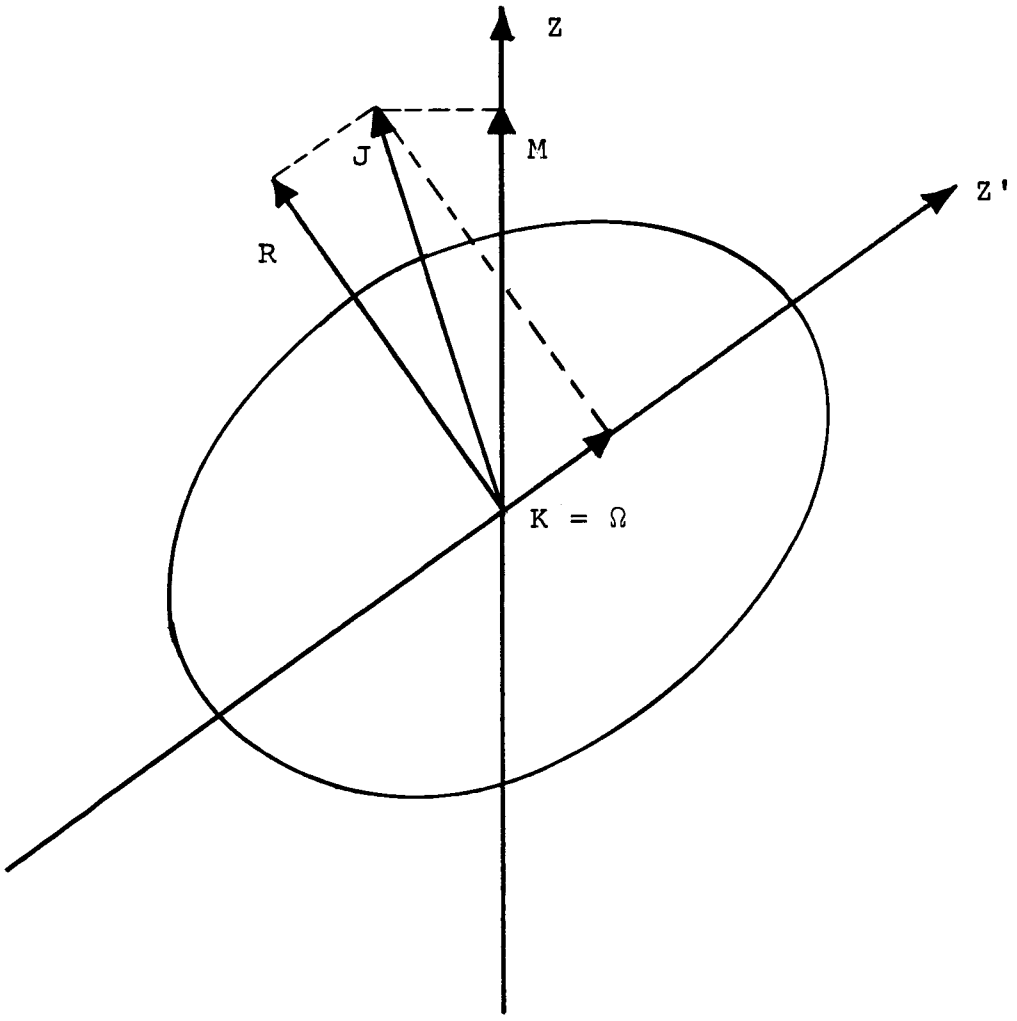

Figure 2. Schematic Diagram for Angular Momenta in Deformed Nuclei.

$$E_{K,J} = E_o + \frac{\hbar^2}{2\mathcal{J}} (J(J+1) \qquad (I-1)$$

where E_o is a constant, and $\mathcal{J}$ is the moment of inertia of the nucleus. This latter quantity depends on the nuclear deformation. For the ground states of the very heavy elements, the value of $\hbar^2/2\mathcal{J}$ is about 7 keV; for saddle point deformations, this figure becomes two or three times smaller. For an even-even nucleus, the ground state of the nucleonic structure has K = 0, corresponding to a paired nuclear configuration. Assuming a reflection-symmetric shape, the spectrum contains for K = 0, only the rotational levels with even J values 0, 2, 4..., which all have positive parity. If the nuclear shape is reflection-asymmetric, the situation is somewhat different and we shall discuss this problem later in more detail.

Thus, assuming axial symmetry for the nuclear shape at the saddle point, the channels could then be characterized by the quantum number K, representing the component of the nuclear angular momentum J about the symmetry axis, and M, the projection of J onto a space-fixed axis.

The probability distribution of the fission fragments as a function of direction is identical to the probability distribution of the direction of the symmetry axis of a symmetric top, having the same quantum numbers J, M, and K. This probability distribution can be expressed in terms

of a differential cross section[2], $W^J_{K,M}(\Theta)$, in the reaction plane, at a given angle Θ by:

$$W^J_{K,M}(\Theta) \propto (2J+1) \quad |D^J_{M,K}(\phi, \Theta, \gamma)|^2 \qquad (I\text{-}2)$$

where $D^J_{K,M}(\phi, \Theta, \gamma)$ are the symmetrical top wave functions, and (ϕ, Θ, γ) are Euler angles of rotation. $W^J_{K,M}(\Theta)$ is independent of the polar angle ϕ, the angle γ of rotation about the symmetry axis, and the moments of inertia of the transition nucleus.

In 1956, Henkel and Brolley (He 56) observed that the angular distribution of fragments in neutron induced fission of ^{232}Th near threshold, was concentrated in a direction normal to the incident neutron direction. Wilets and Chase (Wi 56) interpreted these results in terms of the Bohr model. They assumed that only a few rotational states were excited in the transition nucleus, and also that the direction of the separating fission fragments was that of the nuclear symmetry axis. Under these assumptions, the angular distributions could be described by the relation:

$$W^J_K(\Theta) \propto \int |\psi|^2 d\phi d\Omega \propto |D^J_{K,\ 1/2}|^2 + |D^J_{-K,\ 1/2}|^2 \qquad (I\text{-}3)$$

From the shape of the experimental distribution, they deduced the identity of two channels which appeared to be

---

[2]Differential cross section is defined as the cross section per unit solid angle, and it is given in millibarns per steradian (mb/sr).

involved and also determined the contributions of different J values to the intensity by a curve fitting procedure.

Hittmair (Hi 60), in a further development of the theory went back to first principles to determine relative intensities. He considered the problem in terms of the absolute probabilities for fission through the various channels. The probability amplitude was identified as being the product of the following factors:

1. Amplitude associated with the partial wave in the incident plane wave.
2. An element of reaction matrix for a transition from the state associated with the original even-even nucleus in its ground state, and the incident neutron in the state with quantum numbers $(\ell, s, 0, \mu)$ to the particular exit channel with quantum numbers JKM. This element of reaction matrix is represented by:

   $$\langle JKM|R|\ell s0\mu\rangle = \langle JK|R|\ell s\rangle\langle \ell s0\mu|JM\rangle$$

   where the second factor is the Clebsch-Gordan vector coupling coefficient.
3. The probability amplitude for the transition from the specified exit channel to a state in which the axis of nuclear symmetry lies within a certain solid angle.

Given the above factors then, the differential cross section would be given by the following expression:

$$\frac{d\sigma}{d\Omega}(\Theta) = 1/4\pi\lambda^2(2\ell+1)\,|\langle JKM|R|\ell s0\mu\rangle|^2 \times \frac{(2J+1)}{8\pi}\left[\,|d^J_{1/2,K}|^2 + |d^J_{1/2,-K}|^2\right] \qquad \text{(I-4)}$$

The $d^J_{1/2,K}$ functions will be defined in the next chapter.

In his classical review paper on fission, Wheeler (Wh 63) discussed, among other things, the types of channels which could be expected to contribute to the fission process at the saddle point. He gave great importance to the collective modes in fission, and particularly, developed a relatively simple theory in which he predicted different types of collective vibrations, by borrowing, in part, from the molecular theory. He discussed the roles of bending, sloshing, and of gamma vibrations (in which symmetry about the axis of extension is lost), and quantum numbers associated with each. Wheeler also gave estimates of the types of energies involved with the different kinds of motion, which he predicted by assuming the nucleus to be a liquid drop, and applying the hydrodynamic theory of motion. The role of the moment of inertia in the rotational spectrum and the couplings between different kinds of collective motion were also discussed. Wheeler recognized the fact that an accurate channel analysis of the fission process could not be carried out without including competition factors corresponding to other modes of decay, such as neutron and γ-ray emission. Under these circumstances, for neutron induced fission, he replaced the element of the reduced matrix in the treatment of Hittmair with an expression in terms of effective number of channels:

$$|\langle JK|R|\ell s 0\mu\rangle|^2 \propto \frac{N_{n_1} N_f(K,J)}{N_n + N_f + N \ldots} \qquad \text{(I-5)}$$

where the quantity N_{nl} measures the chance for the compound nucleus to break into a neutron plus the residual nucleus in its ground state. N_n measures the "yield effective number" of channels for all processes of emission of a neutron from a compound nucleus of the given J and parity π of excitation. Similarly, the quantity $N_f(J, \pi, K)$ in the numerator is but one of the contributions to the quantity $N_f(J, \pi)$ in the denominator corresponding to a sum over various fission channels.

Wheeler also summarized the information needed for channel analysis in the following terms:

1. Accurate measurement of the fission cross section as a function of angle and energy.
2. The cross section for the formation of the compound nucleus with a specified spin and parity as a function of energy for each (J, π) that contributes significantly to the fission cross section.
3. The saddle point energy of each fission channel, and the characteristic barrier curvature $\hbar\omega$.
4. The effective number of fission channels leading out from a compound nucleus of given spin and parity. This is found by adding up the openings of all the channels which are accesible from that (J, π).
5. The effective number of neutron channels accessible to a compound nucleus of given spin and parity.
6. The other levels of the residual nucleus and the opening of the channel leading to each of them as a function of energy.

In 1962, Lamphere (La 62) measured the fission cross section and fragment anisotropies[3] in the reaction $^{234}U(n,f)$ for neutron energies between 0.4 and 3.8 MeV. He found that for incident energies between 850 and 1050 keV, the fission cross section was depressed in relation to other energies. He interpreted this in terms of the argument by Wheeler, that neutron inelastic scattering competes with fission to an extent dependent, in part, on available levels in the residual ^{234}U nucleus.[4]

Lamphere derived expressions connecting the measured shape of the anisotropy, with the structure of the transition nucleus. His analysis combined the probability of compound nucleus formation of a certain spin J, with an expression describing the shape of the angular distribution of the fission fragments expected for a certain combination of K and J. The result was an explicit expression for the differential cross section for fission which assumed no other types of competing processes such as neutron emission and γ-ray decay.

$$\sigma_K(\Theta) = \frac{1}{4} \lambda\!\!\!^{-2} \sum_{\ell J} (2J+1) T_{\ell J} W_K^J(\Theta) \qquad \text{(I-6)}$$

---

[3] Anisotropy is defined as the ratio of the differential cross section at an angle near 0° to that at 90°.

[4] Since then, this observation has been determined to be false. Recent developments in the theory of fission attribute the peaking and sudden depression in $\sigma_f(E)$ to the presence of resonances caused by the existence of a doubly humped fission barrier.

Here, the $T_{\ell J}$'s are spin-dependent penetrabilities. These measure the probability that a particle with angular momentum 'ℓ' will penetrate the nuclear potential of the target and create a compound nucleus of spin J. $\lambda\!\!\!^{-}$ represents the rationalized wave length of the projectile (a neutron in this case), and $W_K^J(\Theta)$ is a function which describes the angular distribution of the fission fragments, in a similar manner as in expression (I-3). Lamphere recognized the fact that only relative strengths (i.e., proportions) of the various K bands could be estimated since no allowance had been made for other types of decay of the compound nucleus, mainly neutron emission which was considered to be much more probable than fission.

This situation was very much improved by Vandenbosch (Va 67) who introduced fission barrier penetrability factors into the calculation and also accounted for competition from other modes of decay. The barrier penetrability factors were necessary because the old theory by Bohr had predicted that the fission excitation function should resemble the shape of a staircase, where the sudden jumps in the cross section would be caused by the sudden opening of new fission channels. Wheeler had earlier pointed out that actually these expected sudden leaps in the probability of fission should be smoothed out because the penetration of a quantum mechanical barrier is a gradual process which increases with energy at a rate that depends on the physical

characteristics of the fission barrier. The barrier was assumed to have the shape of an inverted harmonic oscillator potential, whose penetrability is given by the Hill-Wheeler expression (Hi 53):

$$T_f(E) = 1/(1+\exp[2\pi(E_f-E)/\hbar\omega]) \qquad (I-7)$$

where E_f represents the height of the barrier, E is the excitation energy, and $\hbar\omega$ is a parameter which describes the curvature of the parabola. By using the fission data from Lamphere, Vandenbosch attempted to relate the K-band fission probabilities at one incident neutron energy to that at other incident energies. This was done by simultaneously fitting the fission cross section and the relative angular distributions as a function of energy, and by defining barrier heights E_f and curvatures $\hbar\omega$ for each fission channel. Although this analysis proved to be very innovative, no firm, unique K band assignments were possible. Instead, a number of choices were left available.

In 1968, Behkami et al. (Be 68) published a paper resembling, in form, that of Vandenbosch, in which the ^{235}U fission transition nucleus was analyzed. Although similar in form, two important variations are noted. First of all, new data on fission fragment angular distributions at 16 angles and 9 neutron energies between 200 and 1184 keV were obtained. Secondly and most importantly, the analysis was done by simultaneously fitting, instead of the relative

angular distributions, the differential cross sections and total fission cross section, as a function of energy. The introduction of the absolute fission fragment angular distributions permitted the elimination of many of the ambiguities in the analysis, and brought more coherence into the calculations. The result was, that within the framework of a simple and approximate mode of barrier penetration, it was possible to uniquely and firmly make assignments of the K values and parities of the channels in the transition nucleus ^{235}U. The use of differential cross sections instead of relative angular distributions is important because in the former, absolute growth in the strength of a given channel is observed progressively with excitation energy. The use of relative angular distributions only permits one to observe the relative increases in the strength of a certain band in relation to others. This practice also presents the problem that, if the 90° point is in error, it throws the whole distribution off, making the analysis somewhat unreliable, especially if only a few points are available in the data.

Until a few years ago the liquid drop model of fission provided the only base for the study of the fission process. According to this theory, a nucleus tends to assume a spherical shape under the influence of a surface tension, but in heavy nuclei it is prevented from doing so completely, by the strong repulsion provided by the coulomb force between

the protons, which acts as an agent of deformation in the nucleus.

In 1966, Strutinsky (St 66) developed a theory concerning shell effects[5] in nuclear masses and energies of deformation, which proved to have far reaching consequences in the understanding of the nuclear fission process.

He argued that the old liquid drop model of the nucleus, which had been so convenient in describing nuclear masses and fission theories, was not sufficient anymore. The LDM was based on the assumption of a classically uniform distribution of nucleons in phase space, and thus ignored completely nucleon shell effects. He then decided to treat nucleon shell effects as small deviations from a uniform distribution. These deviations were termed "shell corrections". Under these conditions, the total energy of the nucleus was written as the sum of the LDM energy, the pairing correction δP, and the shell correction δE, for both protons and neutrons:

$$E = E_{LDM} + \sum_{p,n} (\delta E + \delta p) \qquad (I-8)$$

Using a simplified Nilsson level scheme for his calculations, Strutinsky obtained some startling results. He obtained large fluctuations for the shell correction as a

[5] These are the effects caused by the non-uniformities of the spacings between the single particle levels in the nucleus.

function of nuclear deformation, especially for nuclei near magic numbers or midshells. He reached the important conclusion that the oscillations of δE reflected periodic changes in the single particle level density near the Fermi energy.

In near magic or midshell nuclei, the equilibrium deformation corresponds closely to the minimal density of nucleon states at the Fermi energy. Strutinsky pointed out that normally, the density fluctuations do not produce essential minima of the deformation energy because of the large dependence on the LDM surface energy. He observed however, that there were certain exceptions. One of these corresponds to the so called "fissionable" nuclei, where the effective LDM surface tension is small. The result was the appearance of a second minimum in the potential energy of deformation, as is shown in Figure 3.

Strutinsky's calculations were born out by the observation that, in many heavy nuclei (U, Pu, Am isotopes), one can populate an isomeric state of the nucleus that decays by spontaneous fission. These isomeric states are known to be states of the nucleus trapped in the minimum in the fission barrier. Their γ-ray decay to the ground state is greatly inhibited because it involves a change in the nuclear shape, while their spontaneous fission decay is enhanced because they have already partially passed over the fission barrier.

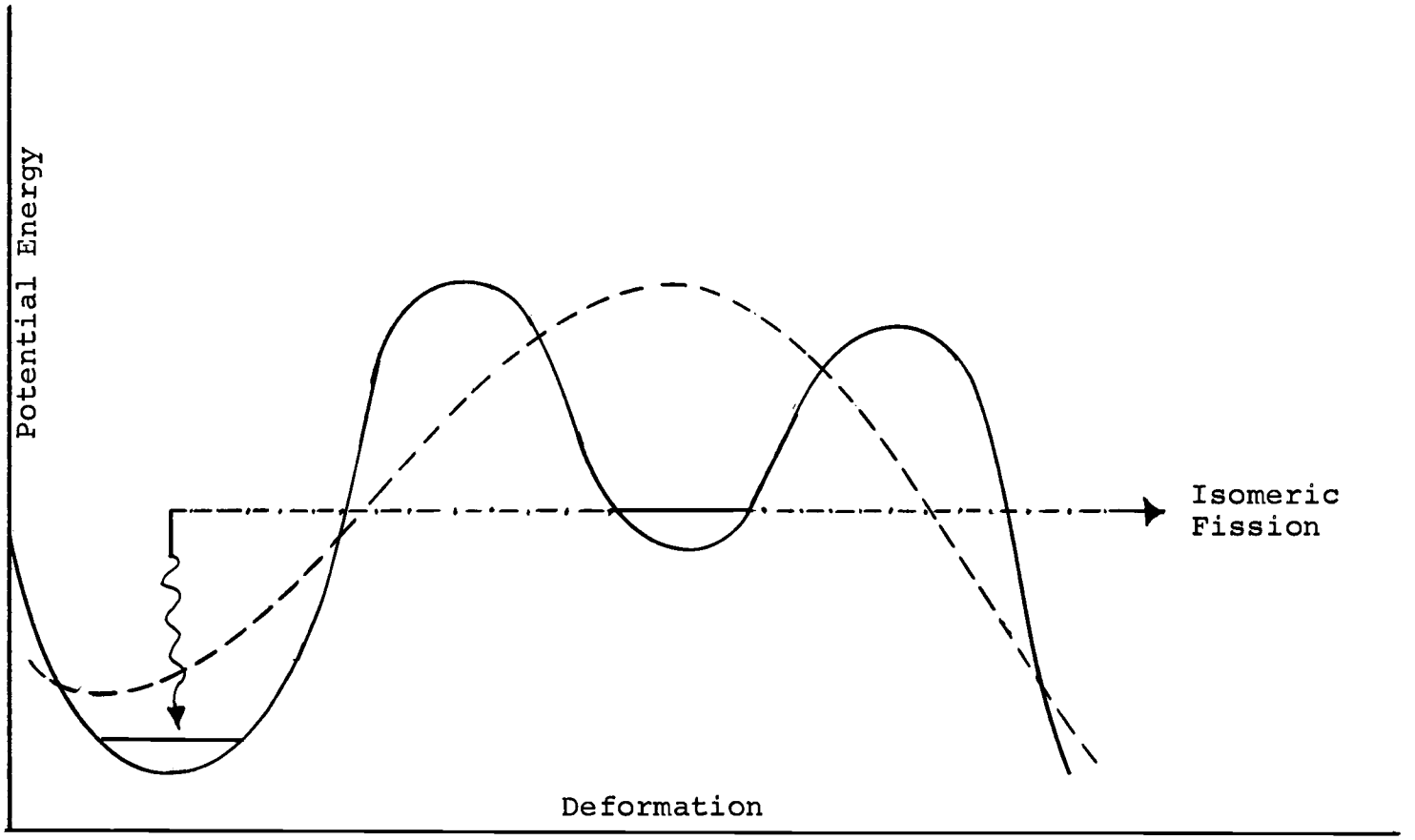

Figure 3. Effects of Shell and Pairing Corrections on the Shape of the Fission Barrier. The dashed line represents the LDM calculation, while the full line corresponds to the LDM + shell corrections.

The presence of a doubly humped fission barrier is responsible for the observation of strongly grouped subbarrier fission resonances in capture reactions with low energy neutrons. This is suggestive evidence for the existence of two weakly coupled sets of excited levels (Bj 69). In terms of Bohr's channel theory of fission, the pronounced structure in excitation functions for fission at energies near the barrier, introduces complications in the analysis of fission fragment angular distributions. Under these conditions, the penetrability expression (I-7) is no longer appropriate, but has to be replaced by a more complicated one which takes into account the penetration through two barriers instead of one. This immediately suggests that, unless the two humps in the fission barrier are not comparable in size, all previous calculations regarding channel analysis of fission are in error.

As the excitation energy above the fission barrier increases, the structure in the fission fragment angular distributions and cross section decreases rapidly, and the nucleus effectively "sees" only one barrier. According to Vandenbosch (Va 73), fragment anisotropies at moderate excitation energies are characteristic of the outer barrier deformation, while at very high energies (>50 MeV) shell effects disappear and the liquid drop barrier becomes determinative.

Recent statistical model calculations (Ba 73) of fission probabilities at moderate energies, taking into account competition between fission, neutron emission, and γ-ray de-excitation of the compound nucleus, suggest that fission widths which are greater by about a factor of four than those calculated, are necessary to reproduce the magnitude of the measured fission probabilities. This development implies that up to now, theoretical considerations have underestimated the number of fission channels above the fission barrier by a factor of about four. Recent theories (Bj 73) resulting from this observation suggest that arguments regarding the symmetry of the nuclear shape at high deformations are partially responsible for the noted increase in the number of fission channels. The basic reason for this increase lies in the fact that, the number of rotational energy levels in a nucleus, or for that matter, in a molecule, increases with the degree of asymmetry offered by the body shape. Recent calculations (Ni 72) regarding the nuclear shape tend to indicate that the nucleus has a reflection-asymmetric shape at the deformation, corresponding to the second barrier. This would immediately increase rotational contributions to the channel spectrum by a factor of two. Not only is the high number of channels caused perhaps by non-counted rotational states, but also possibly by the neglect of vibrational contributions. It is even possible, as we shall see in a later chapter, that important

collective effects have consistently been neglected at the nuclear equilibrium deformation.

B. Short Overview of Fission Barrier Calculations

Shortly after Strutinsky developed his theory concerning fission barrier shapes, people around the world began studying the applications of the shell corrections to the liquid drop model and some very sophisticated theoretical calculations have been carried out in connection with many fissioning systems. Most of them have adopted the so called macroscopic-microscopic approach, in which the average behavior of the sum of the single particle level energies is normalized to that of the liquid drop.

As pointed out by Nix (Ni 72), the calculations of the potential energy of deformation by means of this approach consist of five steps:

1. Specify nuclear shape.
2. Calculate macroscopic (LDM) energy.
3. Generate single particle potential felt by nucleus.
4. Solve Schrödinger equation for single particle energies.
5. Calculate microscopic (shell and pairing) corrections.

The total potential energy is then given by the sum of the macroscopic energy calculated in step two, and the microscopic corrections calculated in step five.

Until recently, these calculations were carried out including only shapes of the nucleus that were symmetric with respect to reflection in the x-y plane. The results in

these cases were that the predicted second barrier height appeared systematically too high in relation to the experimental evidence. Although several people had previously conjectured that at very high P_2 deformations, the liquid drop energy surface was "soft" to asymmetric shape distortions that involve a certain combination of P_3 and P_5 deformations,[6] it was not until recently, that it was specifically determined that for nuclei in the actinide region, the asymmetric deformations were responsible for a general decrease in the potential energy of the second barrier (Mo 70, 72, 73). The mass asymmetry associated with the second peak was first demonstrated by Moller and Nilsson with a modified harmonic oscillator potential (Mo 70). Also, whereas the first saddle point is stable with respect to reflection asymmetry it is found to be unstable with respect to axial symmetry (γ-deformations), in some cases lowering the energy by about one MeV (Ni 72).

Calculations in this region also show that as the proton number decreases towards thorium, the second barrier increases in height systematically and becomes significantly larger than the first barrier. This qualitative trend has been observed experimentally and reported in a recent paper by Back et al. (Ba 73, 73a). Although theoretical

---

[6] P_2 deformations are those associated with stretching of the nucleus in the fission degree of freedom, while P_3 and P_5 distortions signify right-left asymmetry.

calculations of the two barriers for these elements agree remarkably well with experimental findings, ^{230}Th presents the problem that both its secondary minimum and first saddle point are higher by about 3 MeV than the theory predicts. These discrepancies constitute the "thorium anomaly".

In the case of radium, calculations predict that for all intents and purposes, the fission barrier is essentially single humped. Theoretically, Brack et al. (Br 72) estimate the height of the inner barrier in the case of ^{228}Ra to be about 2.4 MeV, compared to an outer barrier height of 8.2 MeV. This latter figure would agree very well with recent calculations by Moller and Nix (Ni 73), which tentatively place the outer barrier height in ^{226}Ra at about 8.2 MeV also. Some inconclusive evidence supporting the concept of a comparatively small inner barrier for radium is reported by Kuks et al. (Ku 73) who, after irradiating ^{226}Ra with neutrons at various energies, found no evidence of isomeric fission present in the samples. We will come back to this point as we develop the statement of the problem concerning the present work.

C. Statement of a Problem

While these fission barrier calculations appear to describe reasonably well the experimental data on spontaneously fissioning isomeric states, they have not, in general, been rigorously tested as to how well they predict the low energy

single particle level spacings at the saddle point, and few if any, tests have been made concerning predictions of fission barrier structure in nuclei with $Z \lesssim 90$.

In the search for systems that could yield important information in this respect, the isotopes of radium stand out. They are considered to be in the intermediate region between heavy and light fissioning nuclei, and they are endowed with a series of unique properties in relation to other nuclei. For example, we might comment briefly in phenomena related to the mass distribution of fission fragments in connection with this mass region. Low excitation energy fission of higher Z-actinide nuclei is typically asymmetric, characterized by a double humped mass distribution. On the contrary, nuclei near Pb and Bi exhibit a symmetric mass distribution. However, for fission of nuclei in the intermediate region (Ra and Ac), a triple humped mass distribution with well established minima between the three mass yield peaks is observed. As the excitation energy is increased, the yield of symmetric fission increases rapidly. The origin of these phenomena is still being debated. It has been suggested that the triple-humped mass distribution is the result of a superposition of two different fission components, a symmetric one, appropriately described by the liquid drop model, and an asymmetric component, whose origin is believed to be determined by the influence of the shells in the nascent heavy fragments. The

question arises as to when, in the fission process, is the mass distribution decided? Or, what set of conditions determines the mode of fission which the nucleus will exhibit? There are those who believe that the mass distributions are decided at the saddle point, while others prefer to think that it is actually decided by the nucleus on its way towards scission from the saddle point.

The experimental data obtained recently by Konecny et al. (Ko 73) for excitation energies up to 15 MeV on the compound systems ^{225}Ra, ^{227}Ra, ^{226}Ac, ^{227}Ac, and ^{228}Ac would tend to support the argument that the mass distributions are decided at the saddle point. For all the above systems, they find that the variation of $\sigma_f(E^*)$ as a function of excitation energy is quite different when both mass components are considered separately.(see Figure 22). The asymmetric component dominates totally at low energies; as the energy increases, symmetric fission increases at a relatively slow rate until, at about 12 MeV of excitation, the contributions from both modes are about equal. Presumably, then two barriers would be available; a lower asymmetric barrier, and a higher symmetric barrier, two or three MeV above the former.

The data obtained by Nobles and Leachman (No 58) on the ^{226}Ra(n,f) reaction also shows that the mass distribution changes from one asymmetric in character at neutron energies below 4.6 MeV, to one predominantly symmetric at energies above E_n = 10 MeV. A complete analysis of the structure of

the ^{227}Ra transition nucleus in this region might yield evidence concerning the nature of the corresponding mass distribution. That is, the existence of a mass symmetry dependent path to fission for the transition nucleus, might be reflected in the energy dependence of the parameters that describe the state of the transition nucleus over the appropriate energy range.

Recently, Babenko and coworkers (Ba 68, 69, 70) and also Ippolitov et al. (Ip 72) have reported some very unusual data concerning the ^{226}Ra(n,f) reaction. Their published data on the energy variation of the fission cross section and angular distributions is shown in Figures 4 and 5. Of great interest are the sharp variations in the anisotropy as the cross section steadily increases at neutron energies, E_n, between 3.6 and 3.9 MeV. It is also important to notice the steady decrease in the anisotropy as the cross section remains relatively unchanged in the region $3.9 \leq E_n \leq 4.7$ MeV. Then there is a step in the cross section corresponding to En = 4.7 Mev, and for neutron energies ranging between 5.4 and 9.0 MeV, the fission cross section increases slowly and monotonically. We also notice that anisotropies remain relatively constant between E_n = 5.4 MeV and En = 7.1 MeV, with certain changes observed for $E_n > 7.1$ MeV. From 9.0 MeV to the last point at 14.8 MeV, the cross section increases more rapidly, and very unusual features in the

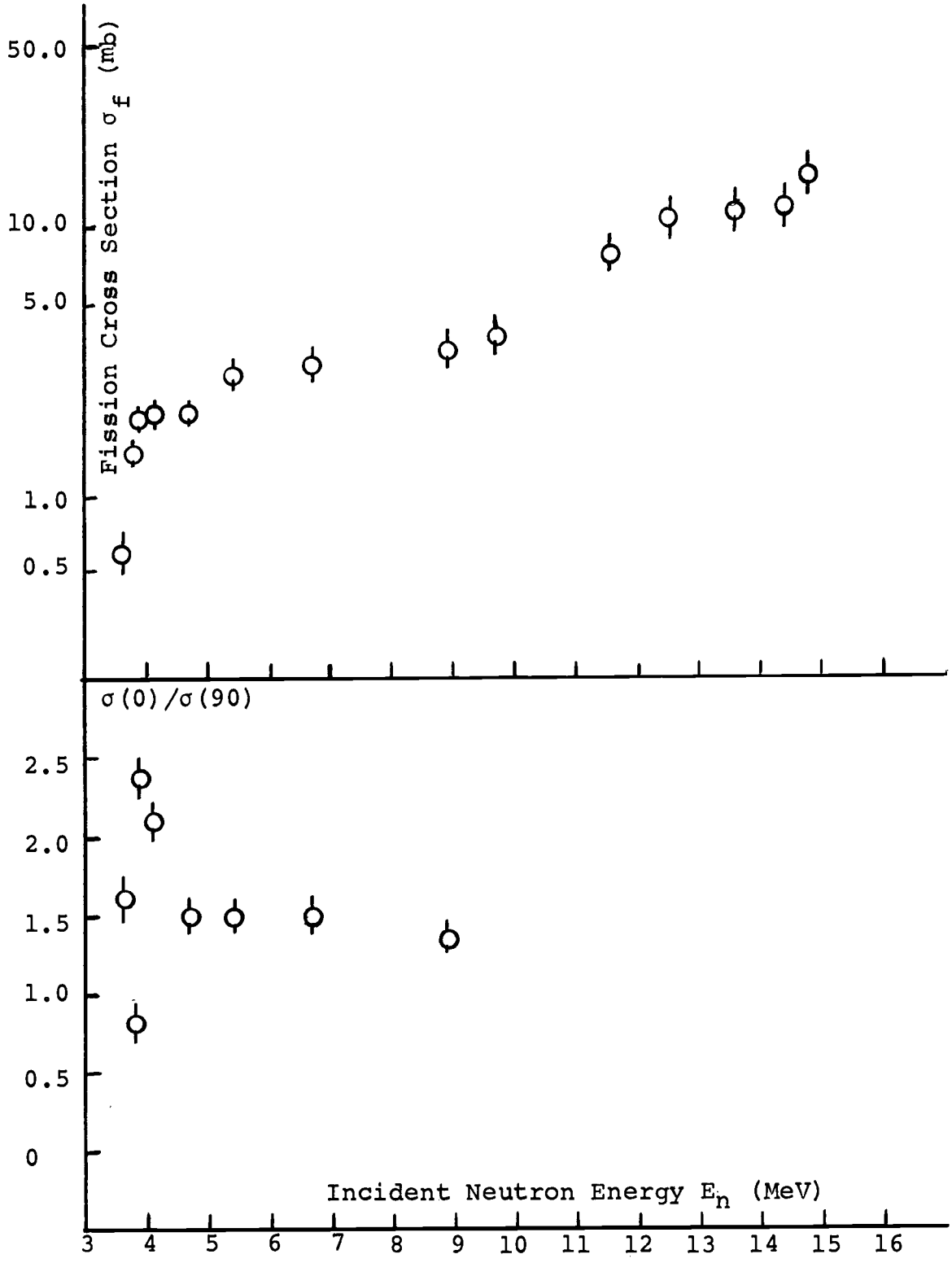

Figure 4. Fission Cross Section and Anisotropy vs. Neutron Energy for Neutron Induced Fission of ^{226}Ra from References (Ba 68, Ba 69 and Ip 72).

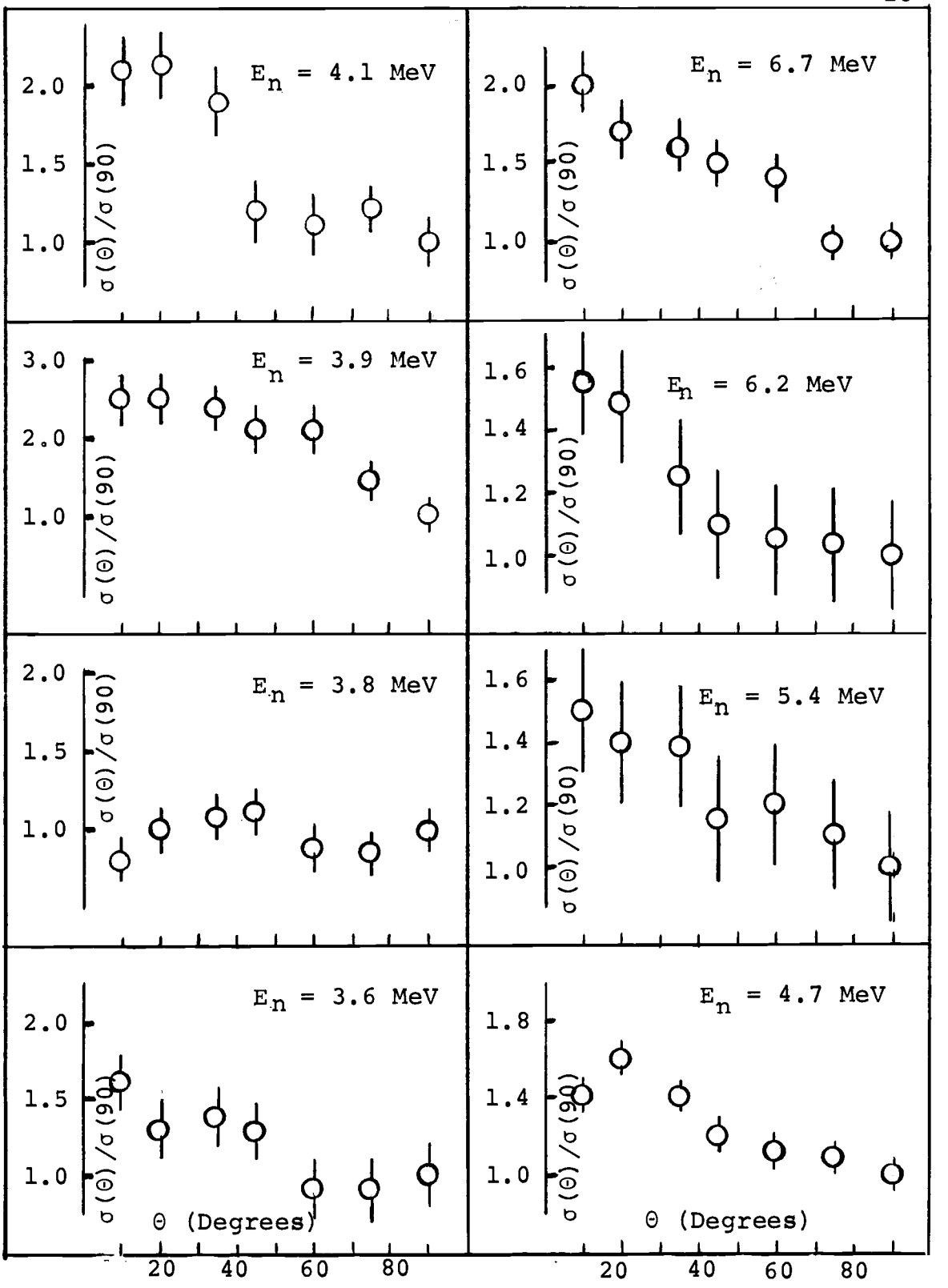

Figure 5a. Fission Fragment Angular Distributions in Neutron Induced Fission of ^{226}Ra for Neutron Energies between 3.6 and 6.7 MeV from References (Ba 68, Ba 69 and Ip 72).

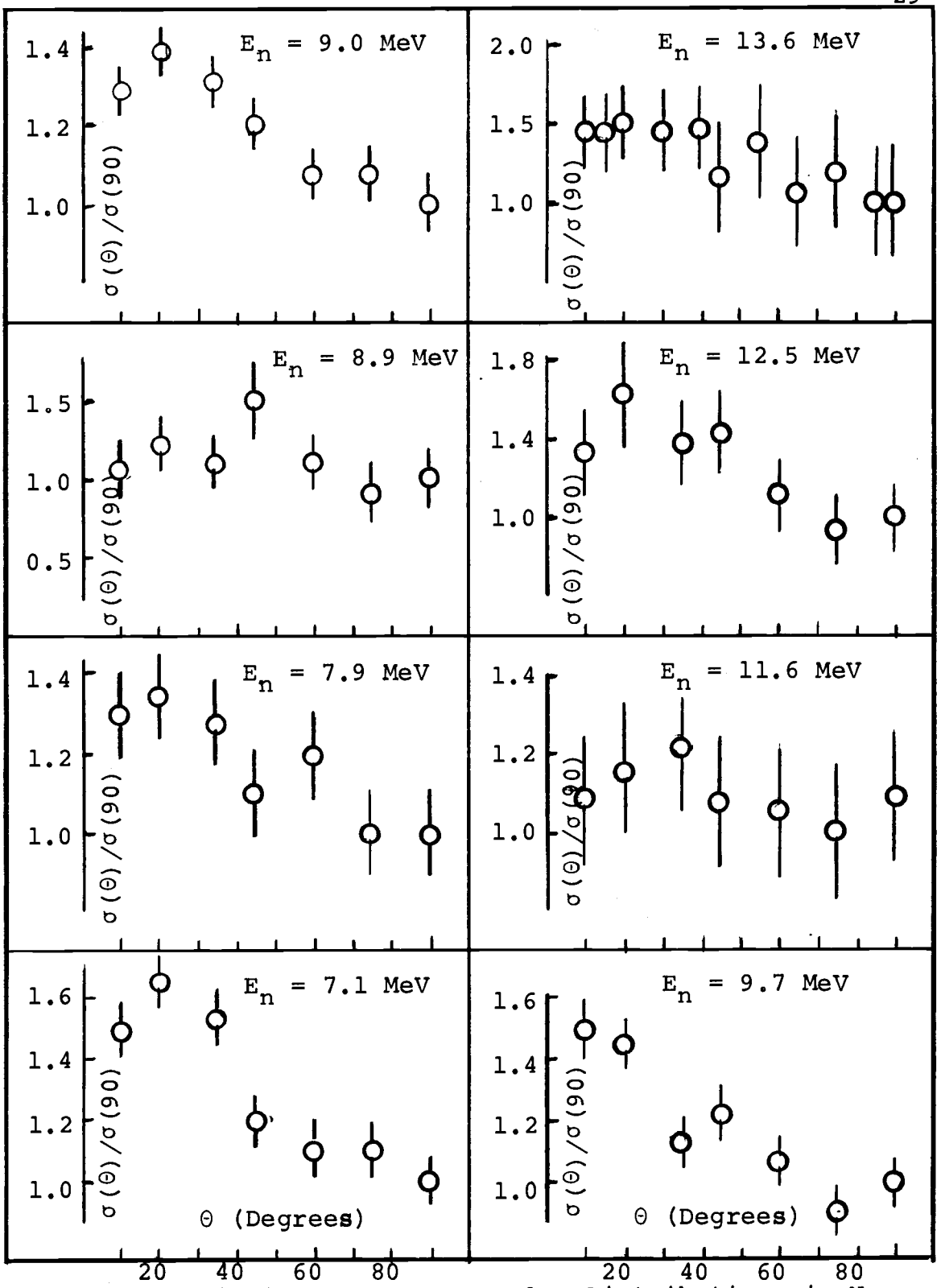

Figure 5b. Fission Fragment Angular Distributions in Neutron Induced Fission of ^{226}Ra for Neutron Energies between 7.1 and 13.6 MeV from References (Ba 68, Ba 69 and Ip 72).

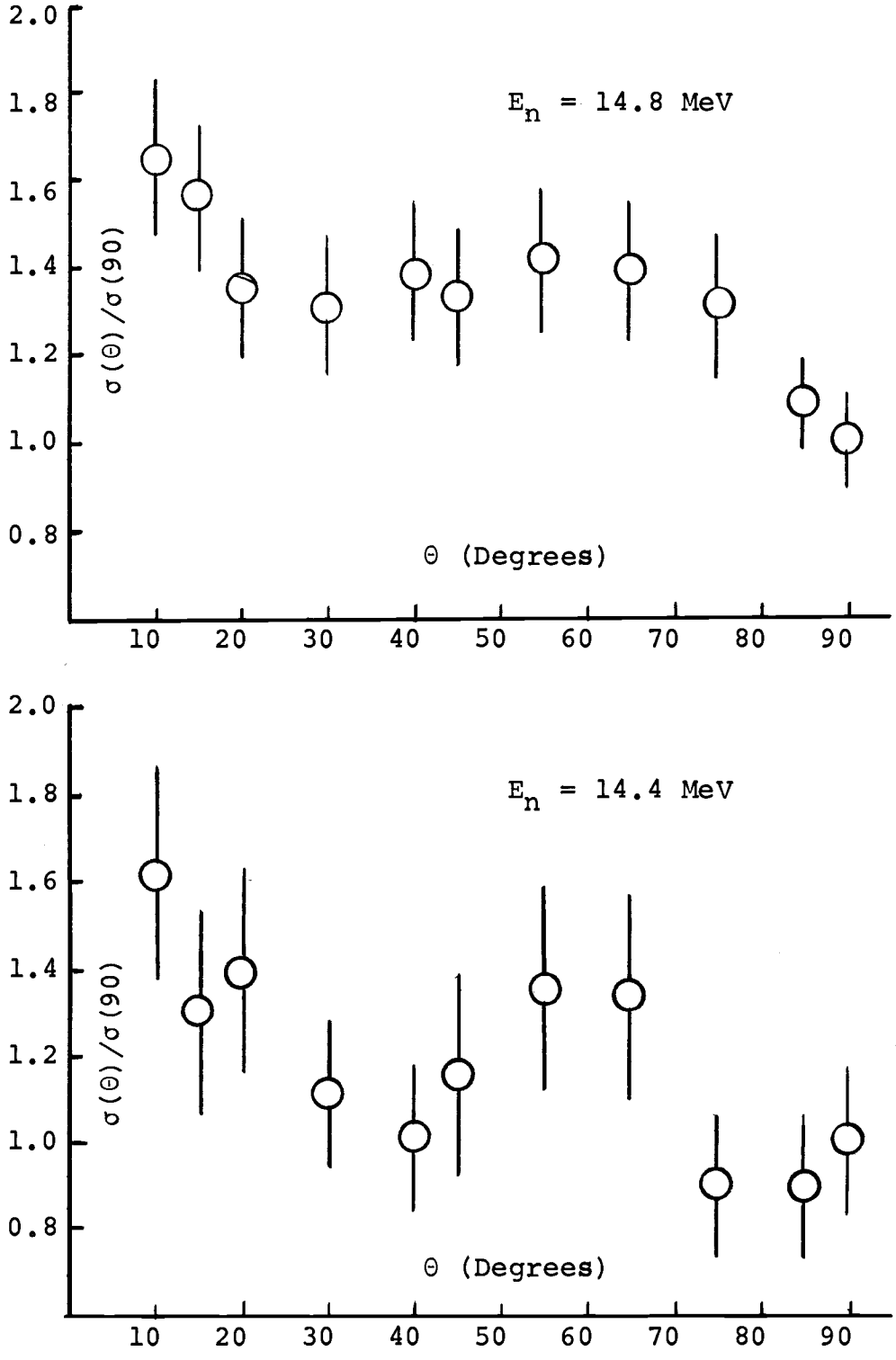

Figure 5c. Fission Fragment Angular Distributions in Neutron Induced Fission of ^{226}Ra for Neutron Energies between 14.4 and 14.8 MeV from References (Ba 68, Ba 69 and Ip 72).

angular distributions are noticeable at neutron energies equal to 14.4 and 14.8 MeV.

Babenko et al. correctly point out that the rapid changes in the cross section near the threshold are usually due to the opening of new fission channels. From the raw data, they estimate the fission barrier to be about 8.5 MeV high. Normally, a step in the cross section, such as the one observed above E_n = 4.7 MeV is interpreted as being caused by fission after neutron evaporation. In the case of radium, this interpretation is completely ruled out. Assuming that the binding energy released when a neutron is added to the ^{226}Ra nucleus is about 4.5 MeV, an incident neutron with a kinetic energy of 4.7 MeV produces a compound nucleus with an excitation of about 9.2 MeV. If the nucleus decays by neutron emission, the average energy of the outgoing neutron is roughly 1.5 MeV. This means that the residual nucleus is left with an average excitation of about 3.2 MeV, which is considerably less than the fission barrier height of 8.5 MeV and thus second chance fission is very improbable.

Their analysis of the data includes some over-simplifying assumptions. The expression for the fission cross section in their analysis was written in the following form:

$$\sigma_f(E_n) = \sum_{J\pi} \sigma_c\,(J, \pi, E_n)\, \frac{N_f(J, \pi, E_n)}{N_n(J, \pi, E_n)}$$

where N_f and N_n are the effective numbers of fission and neutron channels respectively (neutron emission is assumed to be overwhelming dominant in relation to other modes of decay), σ_c is the capture cross section for neutrons, and J,π are the angular momentum and parity of the nucleus respectively. They assumed that the quantity $N_n(J, \pi, E_n)$ remained constant for incident neutron energies between 3.5 and 5.0 MeV. As we shall demonstrate later, this is a poor assumption, since the energy levels in the residual nucleus increase exponentially with excitation energy.

The angular distributions of the fission fragments were analyzed by fitting Legendre polynomials to the $\sigma(\Theta)/\sigma(90)$ data. Although this method gives an idea of the nature of some of the channels involved, it does not predict their positions. In the same manner, no account was taken of the energy differences between the different J members of a given K rotational band. Also the fits to cross sections and angular distributions were carried out not simultaneously, but separately. As we mentioned before, this latter procedure presents the problem that we are constrained in the amount of information that can be extracted regarding the absolute contributions to the cross sections from individual channels. We are allowed only to speculate about the relative strengths of certain K bands in relation to others.

Finally, it was assumed that the step in the cross section is caused by the existence of two barriers, one lower,

characterized by negative parity states, and another one, higher, characterized by positive parity states at higher energies. In reality, there is no physical reason for adopting such a scheme.

The development of this introductory part has led us to the following conclusions:

1. Very peculiar features are observed in the cross section and angular distribution data reported by Babenko and co-workers and Ippolitov et al. regarding the $^{226}Ra(n,f)$ reaction.

2. The triple humped mass distribution in the fission of radium isotopes might be caused by two different components, each being characteristic of a particular mass region.

3. There is no agreement between theoretical calculations and experimental observations regarding the fission barrier in the thorium isotopes, while the agreement is good for heavier nuclei.

4. The fission barrier in radium is predicted to be double humped, but the first hump can be considered, for all intents and purposes, negligible in relation to the second hump; the latter is predicted to have a height of 8.2 MeV above the ground state.

5. Recent evidence indicates that the number of channels at the saddle point is underestimated by a factor

of about four, possibly because of the neglect of collective contributions to the fission width.

It is the purpose of this work to study the fission transition nucleus ^{227}Ra by analyzing the experimental data reported by Babenko et al., and Ippolitov et al. The analysis should be facilitated by the fact that the fission barrier can be assumed to be single humped. It should give some degree of indication as to whether the anomaly reported for thorium is only observed for Z = 90, or in radium also. At the same time, it is the intention of this work to investigate the problem regarding the collective contributions in fission. Finally, it is hoped that the analysis of the experimental data might yield some tentative evidence regarding the stage at which the mass distribution is decided in fission. We hope to accomplish this, by what we think is a substantial improvement over the method of analysis employed by Babenko, Ippolitov and collaborators.

D. Scope

It is clear that the ^{226}Ra(n,f) data measured in references (Ba 68, 69, 70) and (Ip 72), covers a fairly complete range of energies. Near the fission threshold, the nature of the transition nucleus structure requires that the analysis be discrete, since we are dealing with only a few channels above the fission barrier. As the excitation of the nucleus increases, the system must be described in terms of

parameters that emphasize the statistical behavior of the nucleus. This behavior will then be compared with theoretical predictions based on different assumptions regarding the nuclear shape at the transition state.

As we shall see later, the question regarding the nuclear shape is not a trivial one. The symmetry of the nucleus plays an important role in determining the degree of freedom involved in the fission process, which are associated with that part of the wave function that describes the collective motion of the nucleons.

Therefore, we shall proceed now to develop the model and, as we go along, a description will be made of the assumptions employed in this calculation.

II. DEVELOPMENT OF THE CALCULATIONAL MODEL

A. General Aspects of the Calculations

We might begin to develop the model for transition state spectroscopy by describing the fate of the compound nucleus formed by the absorption of a low energy neutron. The nucleus is excited to an energy which is equal to the sum of the neutron binding energy, plus the kinetic energy of the neutron, minus a negligible amount corresponding to the recoil energy. The excited nucleus then has essentially three modes of decay available for de-excitation. It might emit γ-rays, in which case only levels of the compound nucleus will be populated; it also has the possibility of emitting one or more neutrons, depending upon the excitation energy, and thereby population levels in the residual nucleus of lower A; or it might alternatively, choose the path to fission, in which case, given channels in the transition nucleus will be population.

If we assume that statistical equilibrium is reached before the compound nucleus has a chance to decay, then we can describe the probability for a particular type of de-excitation as a suitably weighted fraction of the neutron absorption cross section. The suitably weighted fraction of the absorption cross section is formed by computing the ratio of the relative number of a particular type of

de-excitation channels to the total possible number of de-excitation channels.

The number of available channels can effectively be described in terms of the average width for a particular process, and the average level spacing between resonances of given total angular momentum and parity. Mathematically, the effective number of channels for a certain process may be written in the following way:

$$N_f = 2\pi \frac{\langle \Gamma_{J\ell}{}^{\pi} \rangle}{\langle D_J{}^{\pi} \rangle} \qquad \text{(II-1)}$$

where N_f is equal to the effective number of channels. $\langle \Gamma_{J\ell}{}^{\pi} \rangle$ is equal to the average width for a certain channel of total angular momentum J, orbital angular momentum ℓ and parity π; and $\langle D_J{}^{\pi} \rangle$ is equal to the average level spacing between compound nuclear resonances of given spin and parity. As we will show, the effective number of channels can be computed using the transmission coefficients for given processes. If then, we wish to calculate the partial cross section for a given process, we can incorporate these transmission coefficients into a Hauser-Feshbach calculation in an appropriate manner (Ha 52).

In 1964, Moldauer et al. (Mo 64) created a computer code for calculating energy averages of integrated compound nucleus scattering, capture, and fission cross sections. This code incorporated features from the Hauser-Feshbach approach to particle scattering, the Blatt-Weisskopf theory

for γ-ray emission, and the effects of level width fluctuations. The partial cross sections for the given processes could be obtained from the expression:

$$\langle \sigma_{\ell}^{\alpha\alpha'} \rangle = \frac{\pi^2}{k^2} (2J+1) \frac{\langle \Gamma_{\lambda J\ell}^{\alpha} \rangle \langle \Gamma_{\lambda J\ell}^{\alpha'} \rangle}{\langle D_{\lambda J} \rangle \langle \Gamma_{\lambda J} \rangle} \times S\alpha\alpha' \qquad \text{(II-2)}$$

where $\sigma_{J\ell}^{\alpha\alpha'}$ is equal to the cross section for partial wave ℓ, entrance channel α, exit channel α' near an isolated resonance λ of total angular momentum J. k is equal to the wave number of the incident neutron, $\langle \Gamma_{\lambda J\ell}^{\alpha} \rangle$ to the partial width for entrance channel α, $\langle \Gamma_{\lambda J\ell}^{\alpha'} \rangle$ to the average partial width for the exit channel α', $\langle \Gamma_{\lambda J} \rangle$ to the average total width of the resonance, and $\langle D_{\lambda J} \rangle$ is equal to the average level spacing between resonances of given spin and parity.

$S\alpha\alpha'$ represents the level width fluctuation correction factor. Its magnitude depends on the number of degree of freedom, if it is assumed that the partial widths are distributed according to a χ^2 family of distributions. This quantity arises from the fact that the average of a ratio is not in general equal to the ratio of the averages, and the original Hauser-Feshbach expression is as follows:

$$\langle \sigma_{J\ell}^{\alpha\alpha'} \rangle = (2J+1) \left(\frac{\pi^2}{k^2}\right) \frac{1}{\langle D_{\lambda J} \rangle} \left\langle \frac{\Gamma_{\lambda J\ell}^{\alpha} \Gamma_{\lambda J\ell}^{\alpha'}}{\Gamma_{\lambda J}} \right\rangle \qquad \text{(II-3)}$$

and therefore:

$$S\alpha\alpha' = \frac{\langle \Gamma_{\lambda J\ell}^{\alpha} \Gamma_{\lambda J\ell}^{\alpha'} / \Gamma_{\lambda J} \rangle}{\langle \Gamma_{\lambda J\ell}^{\alpha} \rangle \langle \Gamma_{\lambda J\ell}^{\alpha'} \rangle / \langle \Gamma_{\lambda J} \rangle} \qquad \text{(II-4)}$$

In the particular case of the ^{226}Ra(n,f) reaction analysis, where the number of neutron exit channels is very large, $S_{\alpha\alpha'}$ becomes essentially unity, and therefore, it will be neglected in the analysis.

In 1968, Behkami et al. (Ba 68) extended the above formalism to allow a microscopic description of the fission exit channels in terms of the states of the transition nucleus, and to allow the calculation of fission fragment angular distributions.

In the calculations described in the present work, the same approach has been adopted with some important changes. The computer program of Behkami et al. was modified (see Appendices III and IV) to take into account up to 60 fission channels instead of the original five. In addition (as we shall describe in more detail in another section), an option has been added to the program that permits the exit neutron channels to be treated in a statistical manner. This was done because in the original program it was only possible to treat up to 26 neutron exit channels.

Because of the wide range of excitation energies studied in this project, it was also necessary to extend the formalism in such a way as to include a statistical treatment of the fission channels when they could no longer be treated discretely. This at the same time, called for the extension of the subprogram that calculates the angular distributions, to treat any desired values of the (K,J) quantum numbers.

It is important to point out that although the shape of the formalism remains basically the same, the substance and depth are somewhat changed. For the sake of completeness and clarity, we have decided to proceed with the description of both what is old and what is new in the substance of the calculation, with the hope that it will provide a better understanding of the theory behind this work.

In order to express the partial reaction probabilities in terms of transmission coefficients, Moldauer et al. proceeded to replace the neutron and exit channel partial widths with optical model transmission coefficients using the relation:

$$T_{\lambda J \ell} = \frac{2\pi}{\langle D_{\lambda J \ell} \rangle} \langle \Gamma^{\alpha}_{\lambda J \ell} \rangle \qquad \text{(II-5)}$$

The partial widths for γ-ray decay of the compound nuclear state λ, spin J, parity π, and excitation energy U in equation (II-5) were replaced by transmission coefficients using the expression:

$$T_{\lambda\gamma}(J,\pi,U) = 2\pi \langle \Gamma_{\lambda\gamma}(J,\pi,U) \rangle \rho(J,\pi,U) \qquad \text{(II-6)}$$

where $\rho(J,\pi,U)$ is the density of (J,π) levels at excitation energy U. The energy dependence of the average radiation width was given by the Blatt-Weisskopf formula for dipole γ-ray emission:

$$\Gamma_{\lambda\gamma}(U) = C_1 \int_0^U \frac{\rho(U-E)}{\rho(U)} E^3 dE \qquad \text{(II-7)}$$

with Ericson's formulation of the energy dependence of the level density

$$\rho(U) = C_2 \exp (2\pi^2 U/3\delta)^{\frac{1}{2}} \qquad \text{(II-8)}$$

In the above equations, C_1, C_2, and δ are constants, the latter being of the order of the average spacing between single particle levels. Thus, the energy dependence of $T_{\lambda \ell}$ was given by the function:

$$X(U,\delta) = e^{x}[x^4-10x^3+45x^2-105x+105] \qquad \text{(II-9)}$$

where $x \equiv \sqrt{2\pi^2 U/3\delta}$. The functional form of the angular momentum dependence of the level density was given by:

$$F(J) = \exp (-J^2/2\sigma^2) - \exp [-(J+1)^2/2\sigma^2] \qquad \text{(II-10)}$$

where σ is the familiar spin cutoff parameter. Combining the above equations we get:

$$T_{\lambda\gamma}(J,\pi,E) = 2\pi \left(\frac{\Gamma_\gamma}{D}\right)_o \frac{F(J,\sigma)X(U_o+E,\delta)}{[F(\frac{1}{2},\sigma)]X(U_o,\delta)} \qquad \text{(II-11)}$$

where $(\Gamma_\gamma/D)_o$ is the measured ratio of the average radiation width to level spacing for compound nuclear states populated by s-wave neutrons of zero energy, E is the neutron energy, and U_o is the neutron binding energy. For the case of radium at high excitation energies, γ-ray emission contributes very little to the total cross section. Therefore, the accuracy of the parameters used is not crucial to the calculation of the fission cross section. However, the parameter δ can be related to the level density parameter

a_n, which determined the slope of the log of the level density vs. the excitation energy in the compound nucleus.

The partial widths for fission through an exit channel of given (J,K,π) were replaced by transmission coefficients given by:

$$T_{\lambda f}(J,K,\pi,E) = (2\pi/\langle D_{\lambda J}\rangle)\langle \Gamma_{\lambda f}(J,K,\pi,E)\rangle \qquad \text{(II-12)}$$

As was mentioned before, in order to calculate the transmission coefficients for fission, the fission barrier was assumed to have the shape of an inverted parabola. Hill and Wheeler (Hi 53) have shown that the penetrability is then given by:

$$T_f(J,K,\pi,E) = \{1+\exp[2\pi(E_f(J,K,\pi)-E_n)/\hbar\omega]\}^{-1} \qquad \text{(II-13)}$$

where E_n is equal to the incident neutron energy, $E_f(J,K,\pi)$ is the fission barrier height relative to the neutron binding energy, associated with the state (J,K,π) of the transition nucleus, and $\hbar\omega$ is equal to the barrier curvature parameters.

We can see that for small values of $\hbar\omega$, the barrier is thick, and penetration only takes place close to the top of the barrier. As $\hbar\omega$ increases, the barrier becomes thinner, and penetration becomes a more gradual function of energy. The barrier height is usually calculated assuming the following expression:

$$E_f(J,K,\pi) = E_o+(h^2/2\mathcal{J}_\perp)[J(J+1)-\alpha(-1)^{J+\frac{1}{2}}(J+\tfrac{1}{2})\delta_{K,\frac{1}{2}}] \qquad \text{(II-14)}$$

where E_o is the constant representing the base of the rotational band, $\mathcal{J}_\perp$ is equal to the nuclear moment of inertia about an axis of rotation perpendicular to the nuclear symmetry axis, α is the decoupling constant for $K=\frac{1}{2}$ bands, and δ is the familiar Kronecker delta.

It is worth mentioning that as the nucleus becomes more and more elongated, $\mathcal{J}_\perp$ increases. The effect of this increase for highly deformed shapes is to lower the effective barrier corresponding to the different members of the rotational band, and thereby increasing the fission probability.

Once the transmission coefficients have been defined, they can be replaced in the Hauser-Feshback expression, to obtain the cross section for neutron induced fission through a state (K,J,π) of the transition nucleus, in the following manner:

$$\sigma_f(K,J,\pi) = \pi\lambda\!\!\!^{-2} \frac{(2J+1)}{2} T_{\ell J}(E_n) \times \frac{2T_f(K,J,\pi)}{\sum_K 2T_f(K,J,\pi) + T_\gamma(E,J,\pi) + \sum_{E'} \sum_{\ell' J'} T_{\ell' J'}(E')} \qquad \text{(II-15)}$$

where E_n is equal to the incident neutron energy, $\lambda\!\!\!^{-}$ is the reduced wave length of the neutron, and T_f, T_γ, and $T_{\ell j}$ have already been defined. The primed quantities refer to energy levels in the residual nucleus. Therefore, these neutron transmission coefficients are "inverse reaction coefficients". They are evaluated at an energy which is the

difference between the incident neutron energy, and that of the level which is being fed. In the calculation, angular momentum and parity are, of course, conserved, and only certain values of ℓ are allowed to populate levels in the residual nucleus. The transmission coefficients for fission are counted twice, in order to account for the possibilities of two projections of the angular momentum over the nuclear symmetry axis.

The question regarding the angular distribution of the fission fragments hinges on the assumption that when the nucleus reaches the saddle point, the K quantum number, which is the projection of the total angular momentum over the nuclear symmetry axis, becomes a constant of the motion. This assumption would clearly become invalid in the event that the nucleus lost axial symmetry.

Assuming then, axial symmetry, the dynamics of the dividing nucleus is compared with the dynamics of a symmetric top. In other words, the probability distribution in space of the fission fragments is taken to be the same as the probability distribution in direction of the symmetry axis of a symmetric top, which has: (1) The same total angular momentum quantum number J; (2) The same quantum number M for the component of the angular momentum about the space fixed axis "s"; and (3) The same quantum number K for the component of the angular momentum about the symmetry axis of extension.

The wave equation of the rotator is given by the expression for the symmetric top:

$$\psi = D^J_{MK}(\phi,\Theta,\chi) = e^{iM\phi}\, d(\Theta) e^{iK\chi} \qquad \text{(II-16)}$$

where ϕ, Θ, and χ are the familiar Euler angles, and $d(\Theta)$ will be defined later.

The probability that a fissioning nucleus will be oriented in a certain way will be given by an expression:

$$d(\text{probability}) = \frac{2J+1}{4\pi} \left| D^J_{M,K}(\phi,\Theta,\chi) \right|^2 2\pi \sin\Theta d\Theta \qquad \text{(II-17)}$$

For neutron induced fission of even-even nuclei, the above two equations yield the following relation for the angular distribution:

$$W^J_{M,K}(\Theta) = \frac{1}{4}(2J+1)\left[\left| d^J_{M=\frac{1}{2},K}(\Theta) \right|^2 + \left| d^J_{M=-\frac{1}{2},K}(\Theta) \right|^2 \right] \qquad \text{(II-18)}$$

where the d functions are given by:

$$d^J_{M,K}(\Theta) = \left[(J+M)!\,(J-M)!\,(J+K)!\,(J-K)! \right]^{\frac{1}{2}} \qquad \text{(II-19)}$$

$$\times \sum_{x=o} \frac{(-1)^x \left[\sin(\tfrac{1}{2}\Theta)\right]^{K-M+2x} \left[\cos(\tfrac{1}{2}\Theta)\right]^{2J-K+M-2x}}{(J-K-x)!\,(J+M-x)!\,(x+K-M)!\,x!}$$

where the sum is over $x = 0, 1, 2, 3, \ldots$ and contains all terms in which no negative value appears in the denominator, for any one of the quantities in parentheses.

Some typical $W^J_{M,K}$ functions are shown in Figure 6. These serve to illustrate the point that the fission fragment angular distributions can be used as "fingerprints" to

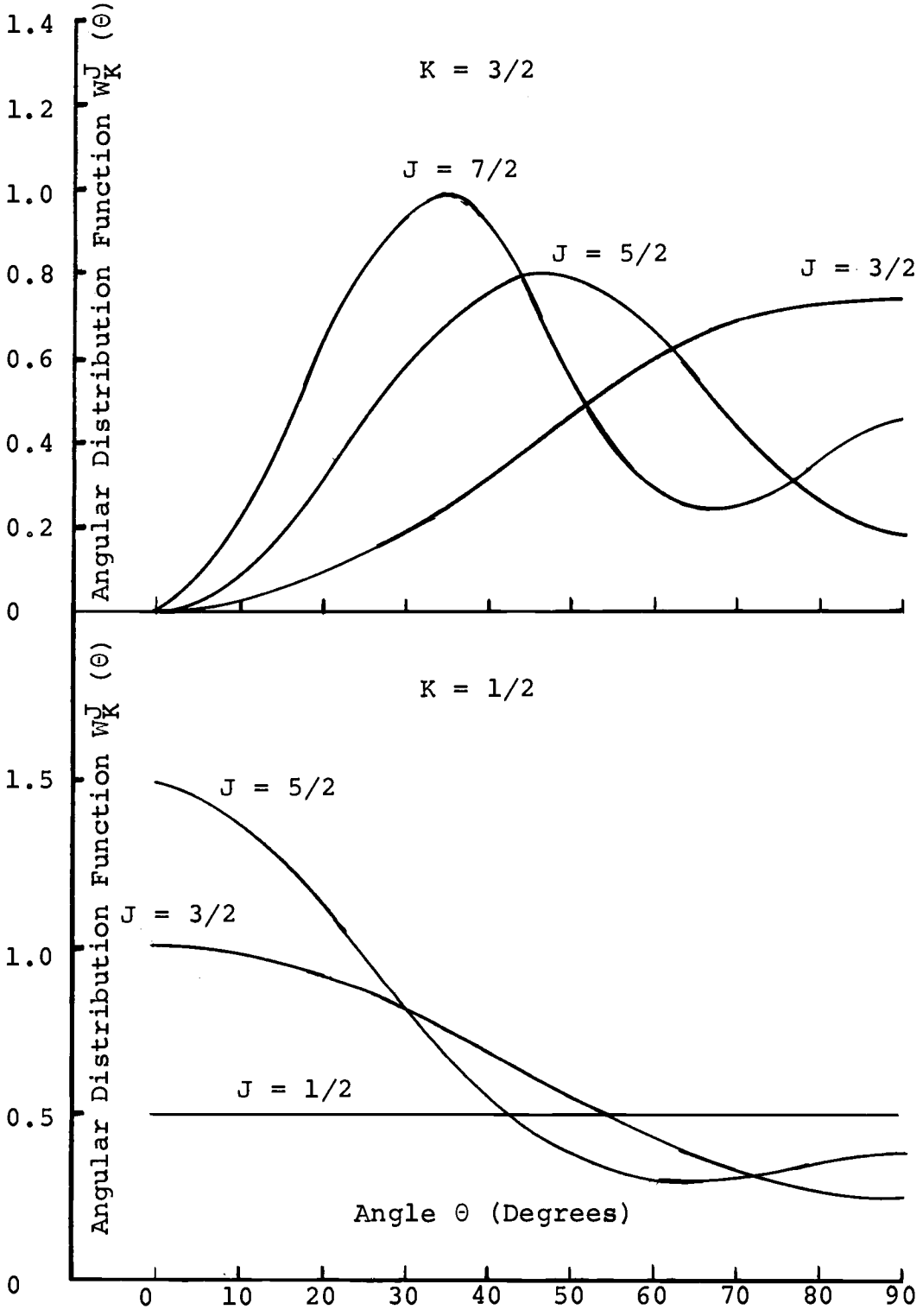

Figure 6. Theoretical Fission Fragment Angular Distributions for Neutron Induced Fission of Even-Even Targets Assuming Fission Proceeds through a State of Given (K,J,M) in the Transition Nucleus.

clarify the identity of the fission channels. For example, $K = \frac{1}{2}$ bands are the only ones responsible for angular distribution peaking at 0°. Therefore, when forward peaking is observed, this represents the unqualified signature of $K = \frac{1}{2}$ character in the transition state spectrum. Assuming that all the parameters are known, the fragment distribution associated with fission through a channel of given K can readily be computed from the expression:

$$W_K(\Theta) = \sum_{J,\pi,M} \sigma_f(J,K,\pi) W^J_{MK}(\Theta) \qquad \text{(II-20)}$$

once the various partial fission cross sections have been determined.

In reality though, some of the variables are not known, and the way the calculation is carried out is to assume, in a trial and error basis, values for some of the parameters, until the experimental data have been fit in the most statistically significant manner. The free parameters in the two regions singled out for calculation, namely, moderate and low energies, are not the same. They will be specified as each section of the calculation is individually described.

B. The Role of Neutron Emission

By far, the dominant mode of decay of the excited compound nucleus for incident neutron energies between 3.6 and 14.8 MeV, is the emission of neutrons to energy levels in

the residual nucleus. This neutron emission represents ∿95% of the decay events observed in this region. Therefore, in computing the cross section for fission, we see that the denominator in the Hauser-Feshbach expression (II-15) will be largely determined by the neutron emission probability factor.

Under normal circumstances, the neutron emission term in the denominator of the Hauser-Feshbach expression (II-15) represents a summation of transmission coefficients for decay to levels of energy E' in the residual nucleus in the range of excitation energies from 0 to the incident neutron energy. Because not all combinations of (ℓ', J') are allowed due to momentum conservation arguments, the sum only takes place over a restricted selection of these values. If these energy levels in the residual nucleus are known, the sum can be made in an exact manner; however, at moderate excitation energies encountered in this work, two complications come into play. In the first place, the residual nucleus levels are only known up to a relatively low value of the excitation energy, and secondly, even if the levels were known accurately, their number would seriously lengthen the calculation in terms of computer time, making it impractical. In the individual case of ^{226}Ra, the energy levels are only known to 0.445 MeV. The lowest neutron energy for which we have data available corresponds to 3.6 MeV. This means that any summation in terms of energy levels should be

performed up to this energy. Of course, the same situation applies for the whole set of neutron energies.

The way in which we have decided to treat this problem is to assume a continuous distribution of levels from the ground state to the incident neutron energy. In this manner, for a given neutron partial wave with a (ℓ', J') combination and kinetic energy (E_k), decaying into a small number interval of levels dN of spin and parity $J\pi$ and energy (E_n-E_k) of the target nucleus, the effective number of channels dP is given by the relation:

$$dP = T_{\ell',J'}(E_k)\, dN_{I\pi}(E_n-E_k) \qquad \text{(II-21)}$$

For a small enough energy interval the number of levels $dN_{I\pi}(E_n-E_k)$ can be expressed in terms of the local level density:

$$dN_{I\pi}(E_n-E_k) = \rho(E_n-E_k)\, d(E_n-E_k) \qquad \text{(II-22)}$$

Substituting the above expression in (II-21) and integrating over E_k, we get:

$$P_{\ell',J'}(I\pi) = \int_o^{E_n} T_{\ell',J'}(E_k)\, \rho(E_n-E_k)\, d(E_n-E_k) \qquad \text{(II-23)}$$

By reversing the limits of integration and differentiating (E_n-E_k) with respect to E_k, we get:

$$P_{\ell',J'}(I\pi) = \int_{E_n}^{o} T_{\ell',J'}(E_k)\, \rho(E_n-E_k)\, dE_k \qquad \text{(II-24)}$$

The effective number of neutron channels of all (ℓ', j') decaying into all (I,π) levels of the residual nucleus for all allowed excitation energies is given by the relation:

$$\sum_{E'} \sum_{\ell' J'} T_{\ell' J'}(E') \rightarrow \sum_{I,\pi} \sum_{\ell' J'} \int_{E_n}^{O} [T_{\ell' J'}(E_k) \rho_{I\pi} (E_n - E_k) dE_k] \qquad \text{(II-25)}$$

In order to be able to evaluate this expression we must know the dependence on energy of the different neutron transmission coefficients, and that of the level density.

1. The neutron transmission coefficients

The evaluation of the different $T_{\ell' j'}(E_k)$, requires the use of an appropriate optical model code. To make use of such a code in a continuous manner as would be required in the evaluation of an integral would prove cumbersome because of the complexity of the calculation. For neutron energies below 3 MeV, the tables produced by Perey and Auerbach (Au 62) of neutron transmission coefficients, are very useful, and have enjoyed widespread use. However, as we have pointed out, neutron energies encountered in the ^{226}Ra(n,f) data go up to almost 15 MeV, and therefore the above tables are not appropriate for our use. Meldner and Lindner (Me 64) have calculated values of the transmission coefficients for several values of the atomic mass, and for values of ℓ corresponding to $0 \leq \ell \leq 7$, as a function of

neutron energy. We have used the Meldner-Lindner $T_{\ell',j'}$ values for A = 232 to represent the $T_{\ell',j'}$ values needed in our calculation for these reasons. In the first place, we have not been able to find any specific data for $T_{\ell j}$ values corresponding to A = 226 specifically. Secondly, the dependence of the transmission coefficients is expected to be on $A^{1/3}$ rather than on A and therefore, the use of values corresponding to A = 232 rather than A = 226 should make very little difference in the final results (Bo 69). Finally, quite good agreement is obtained between the calculations of total reaction cross sections using the Meldner-Lindner $T_{\ell',j'}$ values and the experimental data on ^{232}Th of Batchelor et al. (Ba 65). This agreement is shown in Table I.

Table 1. Inelastic Cross Sections for ^{232}Th(n,n') Reaction.

E_n(MeV)	Experimental*	Theory**
3	2.96 b.	3.11 b.
4	2.85 b.	2.90 b.
7	2.77 b.	2.90 b.

* Batchelor et al. (Ba 65)

** Meldner and Lindner (Me 65)

In order to simulate analytically the energy dependence of the transmission coefficients for the purpose of evaluating the compound expression (II-24) we fitted this energy dependence using a non-linear least squares calculation with five free parameters. Fits were made for each value of ℓ

between 0 and 7. In all cases the same functional form was used, but of course, with different values of the free parameters. The general form of this relation is:

$$T_\ell(E_k) = \frac{\alpha}{1+\exp[\beta(\gamma-E_k)]} + \delta E_k^{\xi} \qquad \text{(II-26)}$$

where α, β, γ, δ and ξ are free parameters. Table II shows the best values of these constants for the different ℓ waves, and Figures 7 through 10 show plots of the real neutron transmission coefficients and our empirical fits using expression (II-26).

Table II. Parameters used in Calculating Compound Neutron Transmission Coefficients.

ℓ	α	β	γ	δ	ξ
0	0.30	-0.2272	-5.250	0.36900	0.27150
1	1.00	8.1300	0.257	-0.05030	0.08210
2	0.35	2.8530	1.242	0.08972	0.49590
3	1.00	3.0550	1.574	-0.03078	0.48730
4	0.50	1.5220	3.099	0.00933	0.06276
5	0.50	1.1720	3.855	-0.04660	-0.50000
6	1.00	1.0939	6.865	0	0
7	1.00	0.6743	7.305	-0.00008	-1.00000

For some of the ℓ values, the fits deviate from the original curves at energies above 5 MeV. This however, does not introduce an important source of error in the calculation of the "compound transmission coefficients" because of

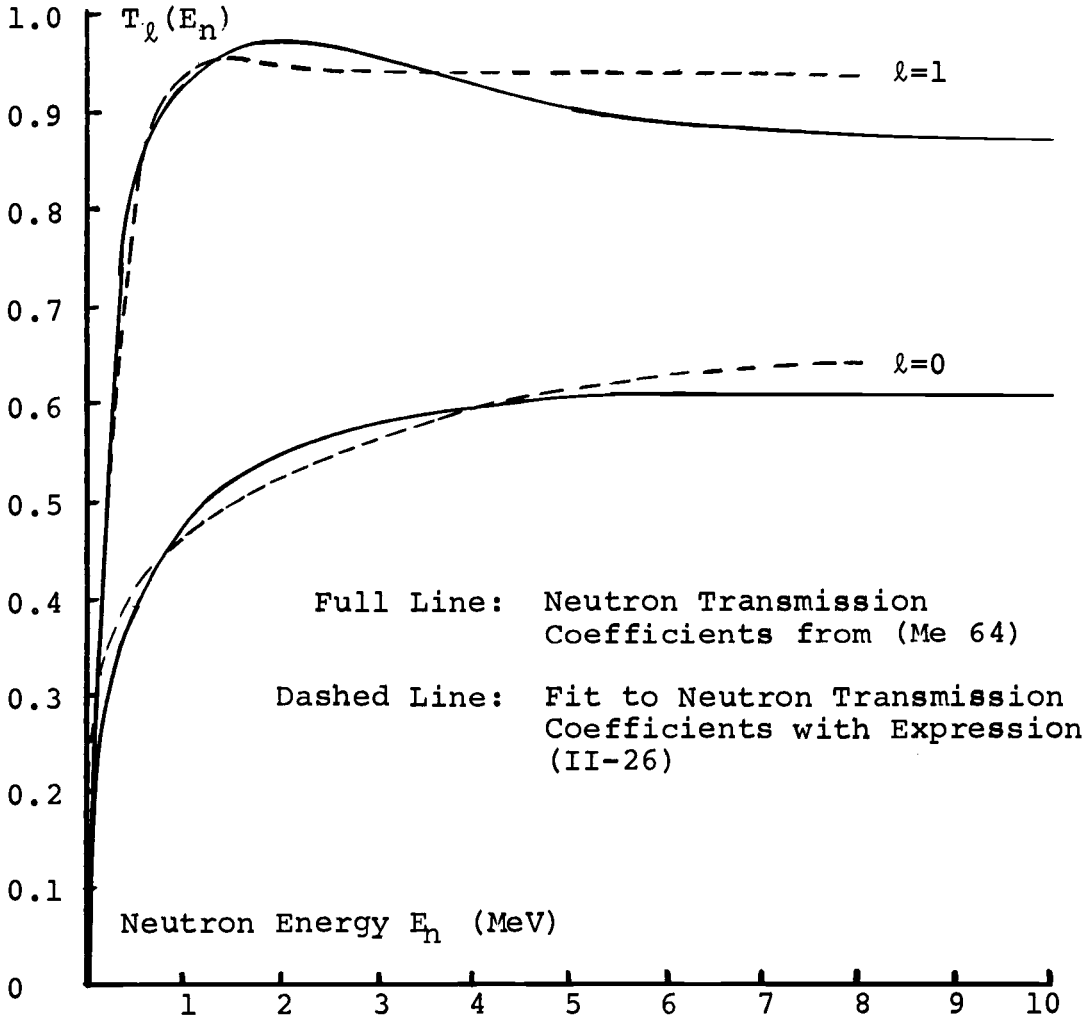

Figure 7. Neutron Transmission Coefficients for A=232 Corresponding to ℓ=0 and ℓ=1.

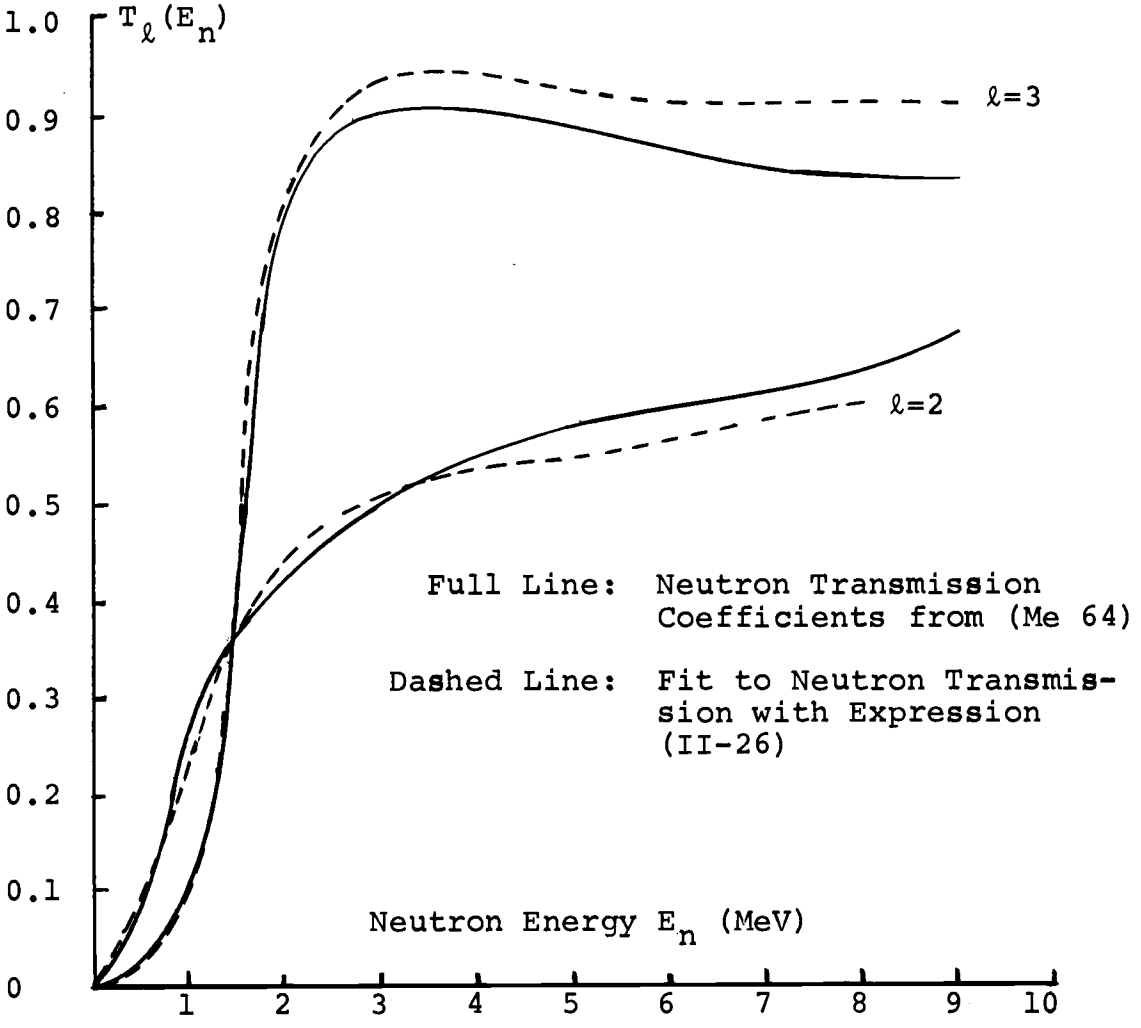

Figure 8. Neutron Transmission Coefficients for A=232 Corresponding to ℓ=2 and ℓ=3.

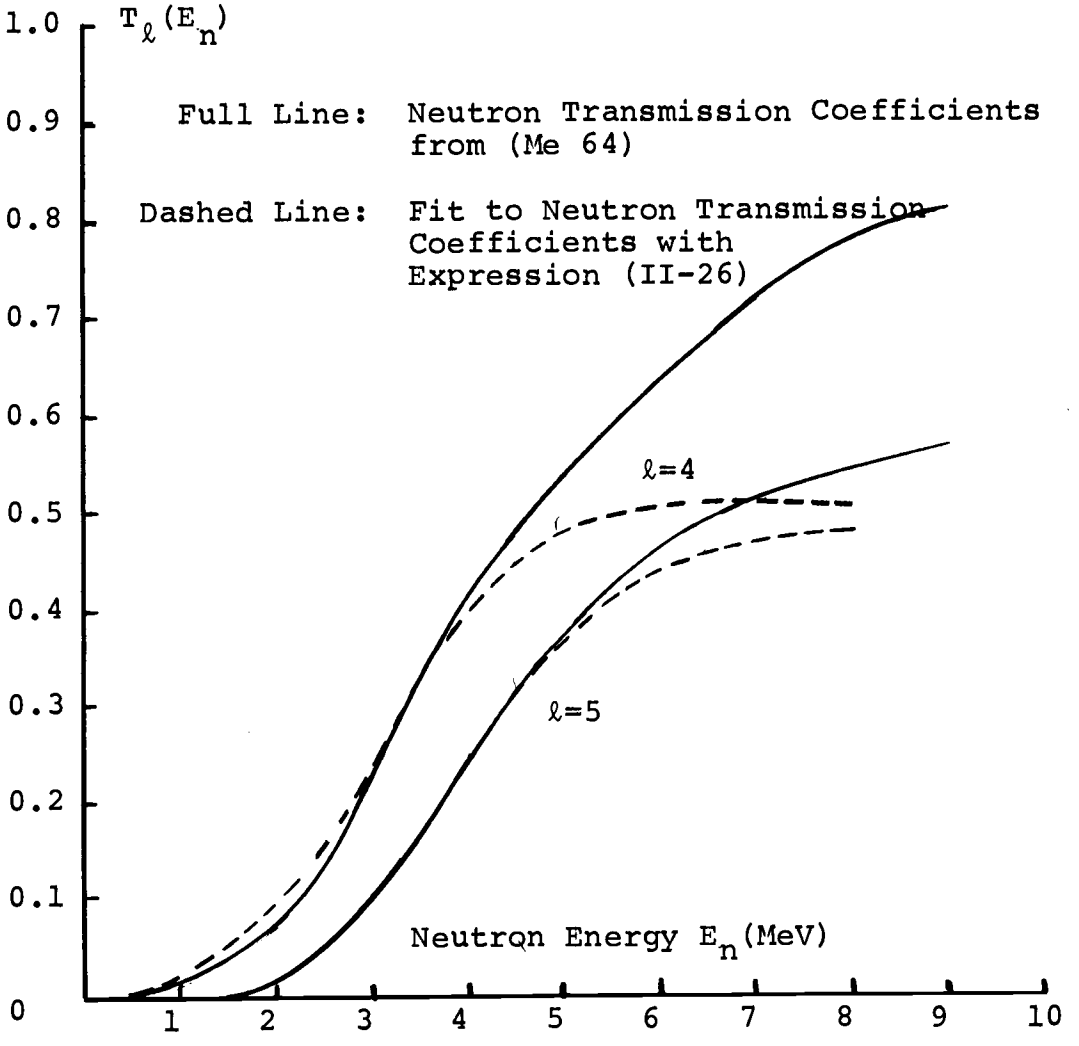

Figure 9. Neutron Transmission Coefficients for A=232 Corresponding to ℓ=4 and ℓ=5.

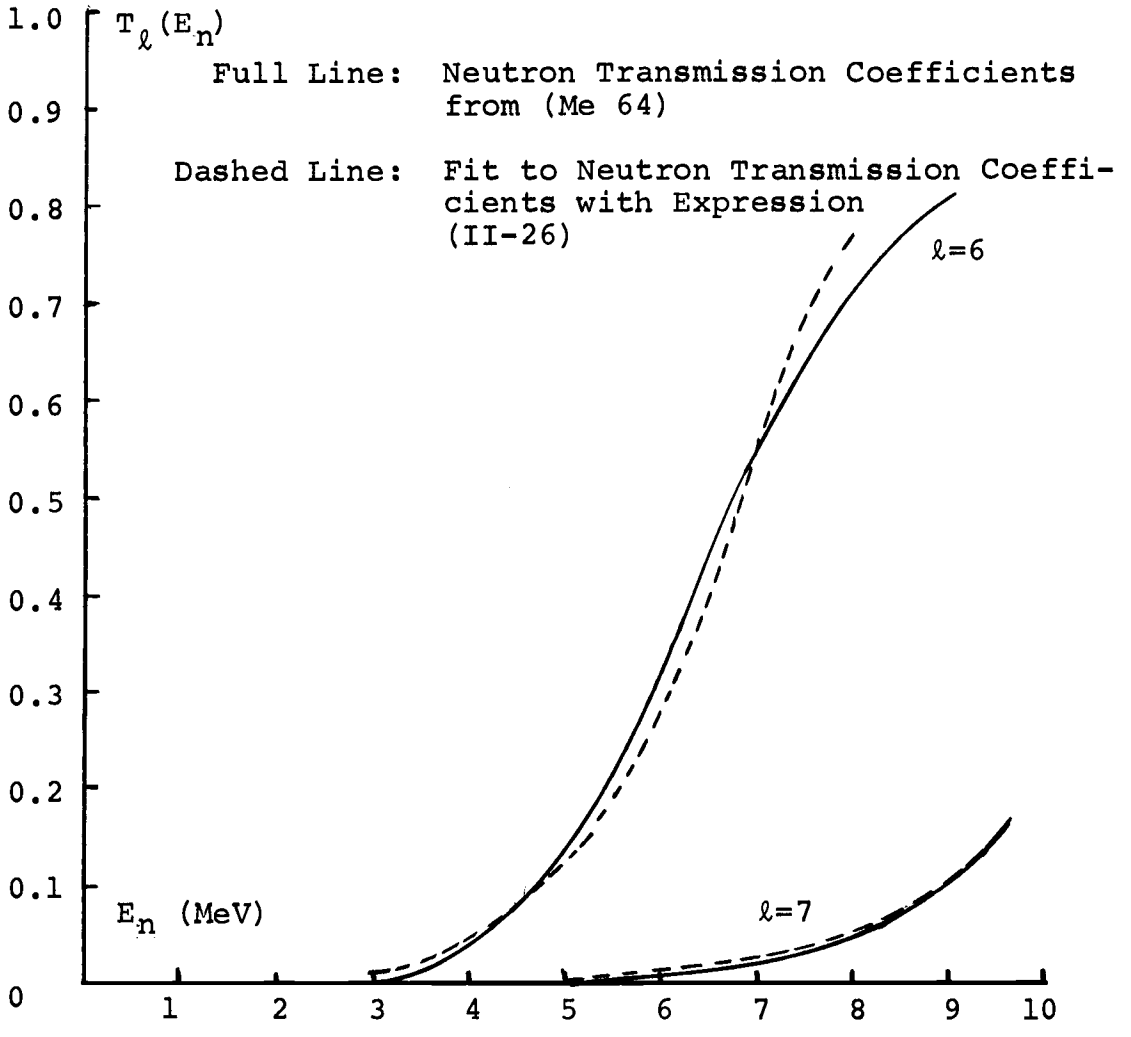

Figure 10. Neutron Transmission Coefficients for A=232 Corresponding to ℓ=6 and ℓ=7.

the sharp dependence of the level density on the excitation energy. See Appendix I.

2. The level densities in the residual nucleus

To evaluate expression (II-25) we need to know $\rho_{I\pi}$, the level density of the residual nucleus. The problem concerning the evaluation of this level density is a complex one because of the almost non-existent data in the mass region around A = 226. In the case of radium in particular, there is no information that can be used in determining the densities. Experimental data relating to state densities and their dependence upon excitation energy was available for thorium and this data was used in the present calculation because it is felt that it should closely approximate the case of ^{226}Ra. As we shall see in a moment, a justification for this assumption is found in the fact that neutron resonance data for the even-odd elements in the region around uranium are quite similar in magnitude.

The detailed study of neutron resonances provides information about level densities that is confined to a very narrow energy interval at the neutron binding energy. Evidence concerning the nuclear level densities over a much wider energy interval can be obtained from the analysis of the energy spectra of evaporated particles in nuclear reactions. The level density $\rho(E)$ at the excitation energy E

is deduced from the yield of neutrons $N(E_n')$ of energy E_n' by employing the statistical relation:

$$N(E_n') \propto \rho(E) E_n' \sigma_c(E_n', E) \qquad \text{(II-27)}$$

where $\sigma_c(E_n', E)$ is the inverse cross section for formation of the compound nucleus at excitation energy E by bombardment with neutrons of energy E_n.

The dependence of the level density on excitation e energy can be obtained naturally by plotting log $N(E_n')/E_n'$ $\sigma_c(E_n', E)$ vs. E. The paper by Batchelor et al. (Ba 65) contains plots of log $N(E_n')/E_n'$ vs. E for various incident energies in the ^{232}Th(n,n') reaction. Fission components were subtracted from the total non-elastic neutron spectrum to give the spectrum of the evaporation neutrons. The incident neutron energies were 3, 4, and 7 MeV, and plots are shown in Figure 11. All these plots show linear dependences of log $N(E_n')/E_n'$ vs. $\sqrt{E}$ in the energy regions considered; however, the ordinate is not directly proportional to the level density because the inverse cross section is absent in the denominator of the expression plotted in this figure. We have made a correction by including this factor, which was obtained from the ^{232}Th capture cross section calculation by Meldner and Lindner[7] (Me 64). The shapes of the lines are only slightly changed as shown in Figure 12. In

[7]The magnitude of the error incurred by neglecting σ_c fluctuates between 6 and 14% for the energy range considered.

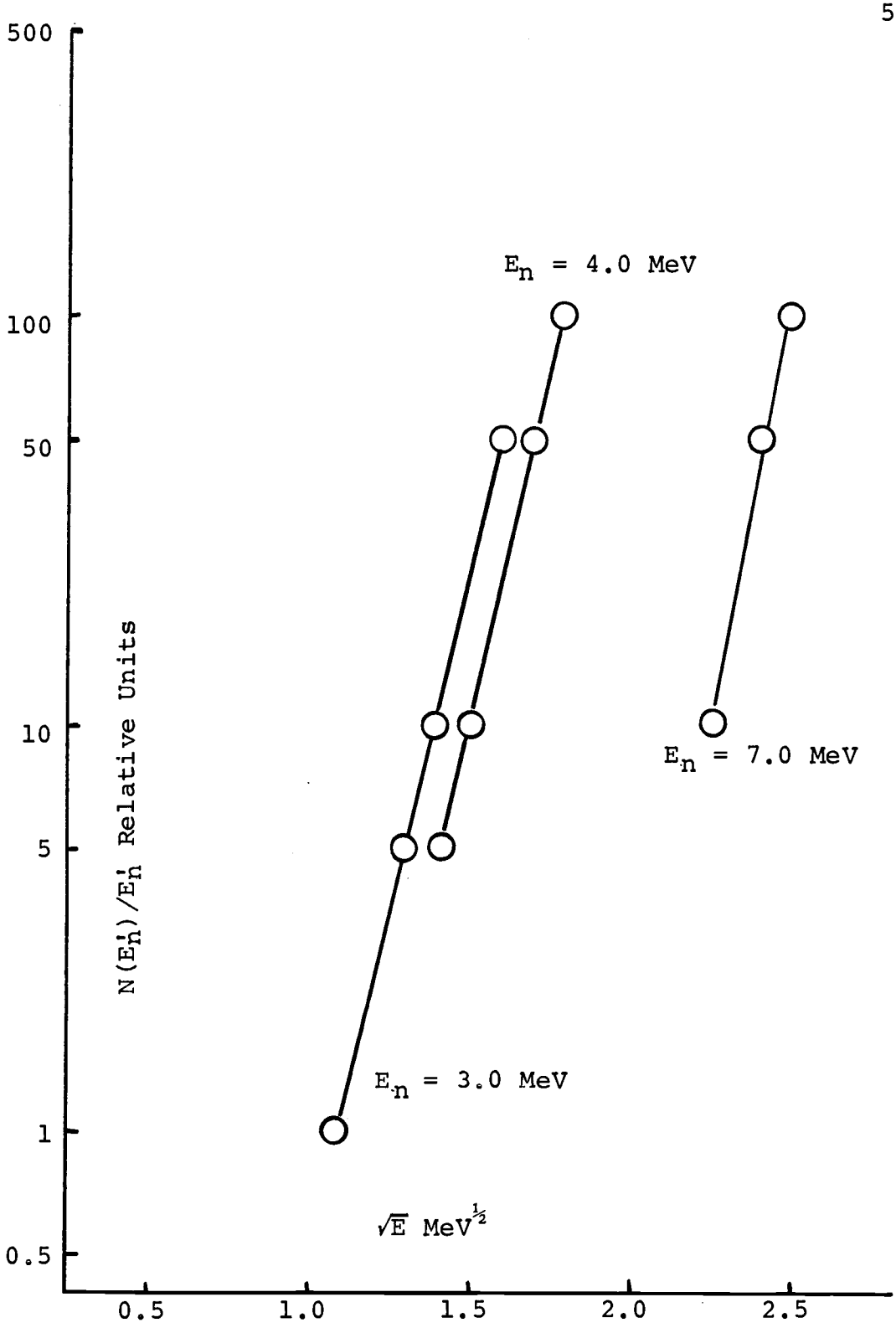

Figure 11. $N(E_n')/E_n'$ vs. Square Root of the Excitation Energy for the Evaporation Spectra from ^{232}Th at 3, 4, 7 MeV Incident Neutron Energy, from Reference (Ba 65).

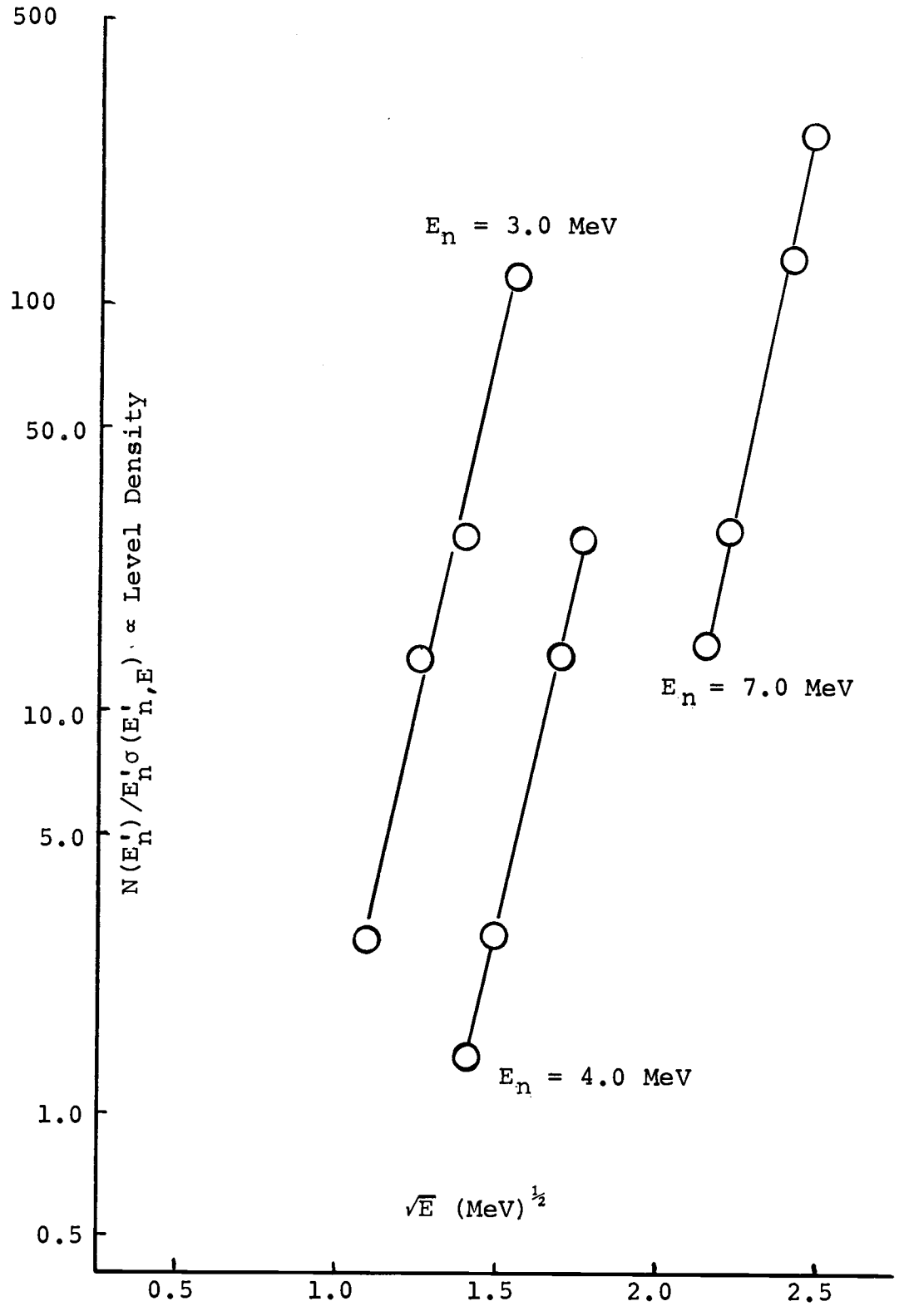

Figure 12. Relative Level Density vs. (Excitation Energy)$^{\frac{1}{2}}$ for the Evaporation Spectra from ^{232}Th at 3, 4, 7 MeV Incident Neutron Energy.

order to obtain the dependence of the continuous density on energy, these lines are superposed on each other at the overlapping excitation energies. The ^{232}Th data however, presents the problem that there is a lack of data in the curves for 1.6 $MeV^{\frac{1}{2}} \leq \sqrt{E} \leq 2.1\ MeV^{\frac{1}{2}}$. This problem was solved by an extrapolation procedure that joins both curves smoothly at the crossing point. The result is shown in Figure 13. The data drawn in Figure 13 was then replotted in the form: $\log N(E_n')/E_n'\sigma_c(E_n',E)$ vs. E, as shown in Figure 14. Having the dependence of the level density on excitation energy, one needs to find the absolute level densities. These absolute level densities were obtained by normalizing the curve showing the energy dependence of the level density to one measured value of the level density at a given excitation energy.

Vorotnikov (Vo 69) has tabulated neutron resonance data for a series of nuclei in the radium region. This data is shown in Table III. The even-even nucleus closest to ^{226}Ra

Table III. Neutron Resonance Data for Nuclei in the Th Region*.

Compound Nucleus	I_o	Binding Energy (MeV)	Interval of E_n, eV	Number of Resonances	$N/\Delta E_n$, eV^{-1}
Th^{230}	5/2	6.72	0-10	14	1.40±0.37
U^{234}	5/2	6.78	20.5-62.8	68	1.60±0.10
U^{236}	7/2	6.40	0-25	42	1.68±0.16
Pu^{242}	5/2	6.21	0-30	25	0.83±0.10

*Vorotnikov (Vo 69)

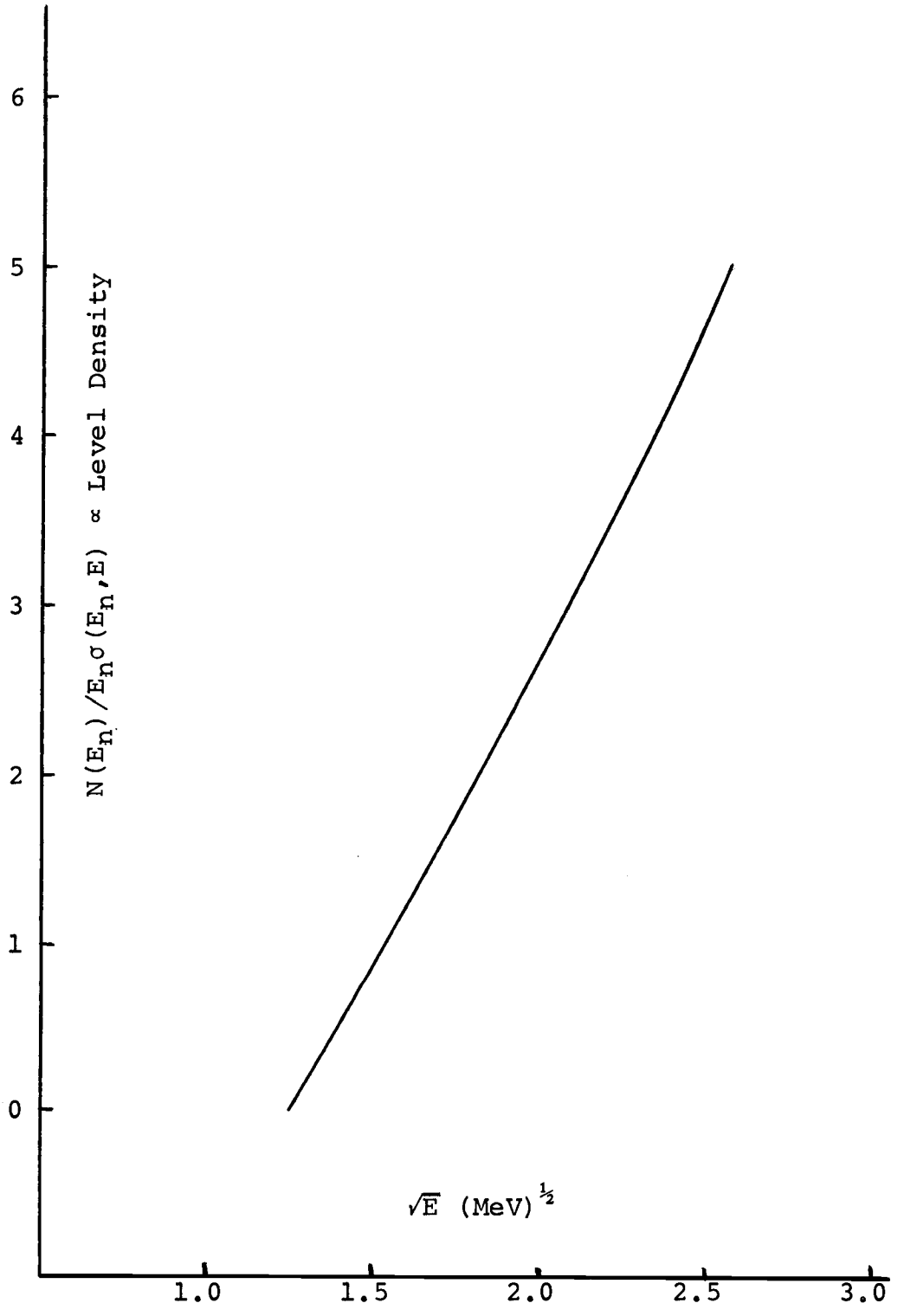

Figure 13. Same as in Figure 12 Except that Lines have been Smoothly Joined.

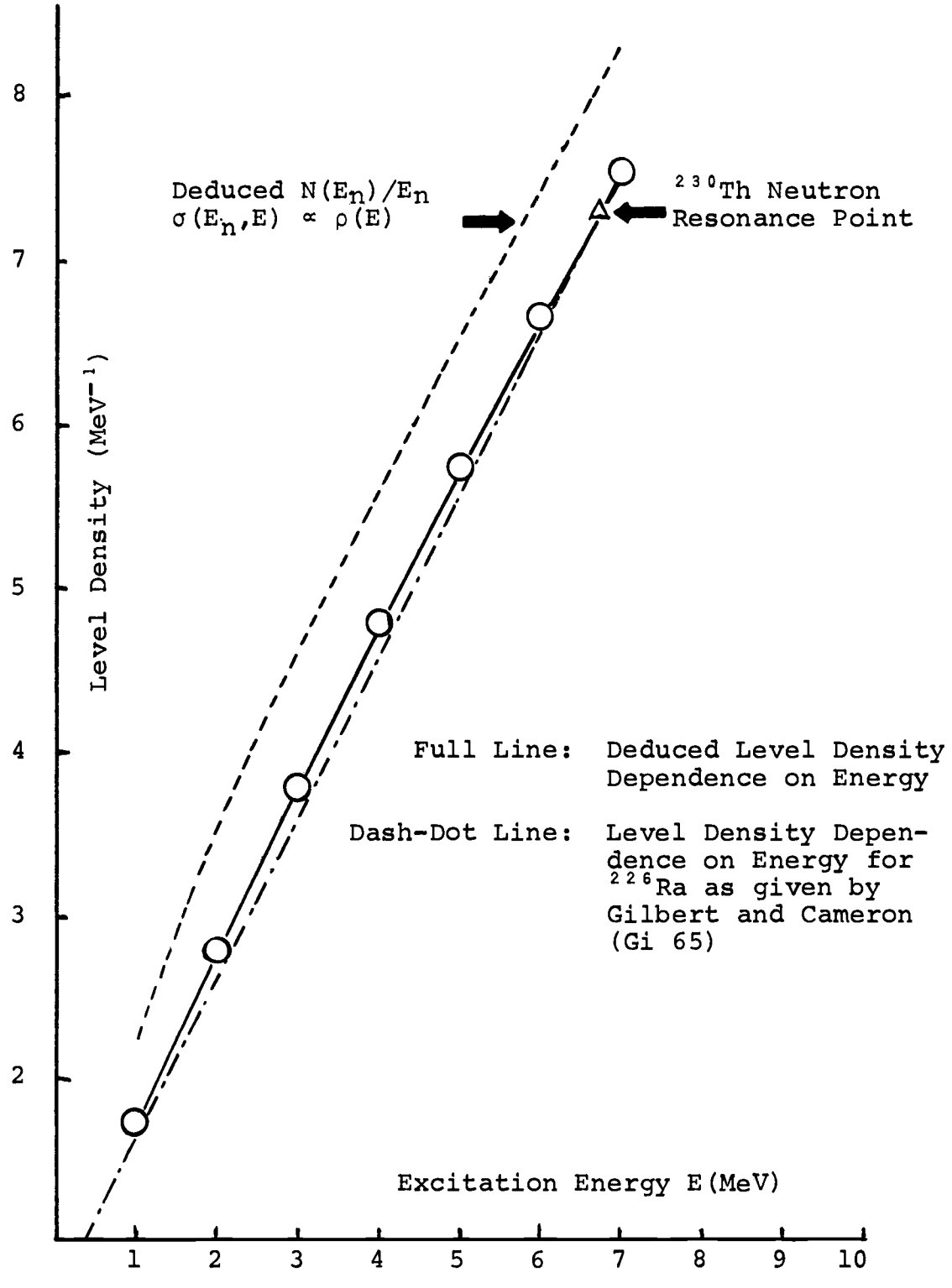

Figure 14. Deduced Level Density Dependence on Excitation Energy for ^{226}Ra.

for which this kind of information exists is ^{230}Th. The data in Table III are the observed density of levels excited when an s-wave neutron strikes a target of spin I_o, to form a compound nucleus of resulting spin $I_o \pm 1/2$ if $I_o \neq 0$, and of spin 1/2 if $I_o = 0$ with the parity of the compound system being determined by the parity of the ground state of the target nucleus. In the case of the compound nucleus ^{230}Th, the angular momenta and parities of the levels excited are J = 2+ and J = 3+, because the spin and parity of ^{229}Th are J = 5/2+. Knowing the local density of these states at the neutron binding energy, we can determine the total level density provided we also know the spin distribution. The spin distribution is usually assumed to be Gaussian in shape, and it is given in the form:

$$\rho(J) \propto \frac{(2J+1)}{2\sigma^2} e^{-J(J+1)/2\sigma^2} \qquad \text{(II-28)}$$

where J is the total spin, and σ is the spin cutoff parameter that determines the width of the distribution. Gilbert and Cameron (Gi 65) give the following expression to calculate σ^2:

$$\sigma^2 = 0.0888\ (aU)^{\frac{1}{2}} A^{2/3} \qquad \text{(II-29)}$$

where a is equal to the level density parameter, in the order of A/8; U is equal to E-P(Z)-P(N): E is equal to the excitation energy of the nucleus and P(Z) and P(N), are proton and neutron pairing corrections respectively. Assuming

that we know all these values, we can calculate the total density of levels at the binding energy from the relation:

$$(E,\text{all } J,\pi) = 2\rho(E,J=2,3;\pi=+) \times \frac{\rho(\text{all } J;\pi=+)}{\rho(J=2,3;\pi=+)} \qquad \text{(II-30)}$$

We have made the assumption that the density of positive levels is equal to that of negative levels. $\rho(\text{all } J,\pi=+)$ can be calculated by integrating (II-28) over all J's to give:

$$\rho(\text{all } J,\pi=+) = 1$$

In the calculation of σ^2 we have used the parameters given by Gilbert and Cameron: $a_n = 29.65$, $P(Z) = 0.89$, $P(N) = 0.79$ for ^{226}Ra. These values are very close to other estimates (Ne 62). Using these values, we find:

$$\rho(E,\text{all } J\pi) = 15\rho(E,J=2,3;\pi=+)$$

and $\rho(B_n=6.72 \text{ MeV}, \text{all spins}) = 2.05 \times 10^7 \text{ MeV}^{-1}$

The normalized level density curves is shown in Figure 14. For purposes of comparison we also show the one estimated for ^{226}Ra by Gilbert and Cameron (Gi 65).

We analytically parameterized the level density dependence on excitation energy so that it could be used to compute expression (II-24). For this purpose we have chosen the standard Fermi-gas expression for the level density, and left one parameter, a_n, to vary as a function of energy, At excitation energies below 3 MeV, where the log of the level

density is a linear function of energy, we have chosen to use a constant temperature formula of the same form as that used by Gilbert and Cameron (Gi 65). We have also added a spin dependence to this expression of the form given by (II-28). The two models are made to join smoothly at 3 MeV. On account of the above, we have the following expressions:[8]

$$\text{Below 3 MeV} \quad \rho(E) = \frac{1}{T} e^{(E-E_o)/T} \qquad \text{(II-31)}$$

$$\text{Above 3 MeV} \quad \rho(E) = \frac{\sqrt{\pi}}{12} \frac{e^{2\sqrt{a_n U}}}{a_n^{1/4} U^{5/4}} \times \frac{1}{\sqrt{2\pi\sigma^2}} \qquad \text{(II-32)}$$

where E_o is an empirical constant and T is equal to the nuclear temperature (also to be determined empirically). Upon fitting these expressions to the level density curve, we find the following values for the parameters:

$$E_o = -0.29$$

$$T = 0.415$$

The variation of a_n with E is shown in Figure 19, and it seems to follow the empirical relation:

$$a_n(E) = 29.2 + 205.62\, e^{-1.003E} \qquad \text{(II-33)}$$

or

$$a_n(U) = 29.2 + 38\, e^{-1.003U}$$

---

[8] A somewhat more complicated formula due to Lang and Le Couteur (La 54) is sometimes found in the literature instead of equation II-32, in which $U^{5/4}$ is expressed as $(U + t)^{5/4}$. According to (Gi 65), this formula contains an error regarding the procedure used in conducting the saddle point integration

The total fit to the level density is given in Figure 14. Individual J contributions are obtained from the relation:

$$\rho(E,J) = \rho(E) \frac{(2J+1)}{2\sigma^2} e^{-J(J+1)/2\sigma^2}$$

C. Extension of the Model to High Energies

As the excitation energy above the fission barrier increases, the number of fission channels increases to the point where the statistical properties of the levels must be considered rather than the discrete ones. This is done by extending the calculation by defining "statistical transmission coefficients" for fission in the same spirit in which we defined the "compound transmission coefficients" of expression (II-24). These compound fission penetrabilities would then play the same role as the individual penetrabilities in the case of the discrete fission channels, and the parameters (K, J, π, E) describing them would be determined in a similar way.

These compound fission transmission coefficients are given by the expression:

$$T_f(K,J,\pi,E) = \int_0^{U-B_f+\epsilon} \rho_F(E,K,J,\pi) T'_f(E) dE \qquad \text{(II-35)}$$

where $\rho_F(E, K, J, \pi)$ is the density of channels with quantum numbers K, J, and π at an energy E. $T'_f(E)$ is of the same form as the expression given in (II-13). U represents

the excitation energy of the nucleus, B_f represents the height of the fission barrier, and ε is a small energy increment to the excitation energy interval over which the integration is carried out to account for the contributions of channels at higher energies.

The transition nuclear level density expression $\rho_F(E, K, J, \pi)$ takes the form of the Fermi-gas expression for two different types of particles for the sake of consistency with the calculation used for the case of the neutron exit channels. We assume that we have an equal number of positive and negative parity levels.

For a rotating system of total energy E, the level density follows the relation:

$$\rho_{J,K}(E) \propto \exp\left[(E-E_{rot}^{J,K})/T\right] \qquad \text{(II-36)}$$

where $E_{rot}^{J,K}$ is the energy which is tied up in the rotation of the deformed nucleus, and T is the temperature. This expression can be transformed to yield (Gi 68):

$$\rho_{J,K}(E) \propto \exp\{E/T-\hbar^2J^2/2\mathcal{J}_\perp T-(\hbar^2K^2/2T)[1/\mathcal{J}_{||} -1/\mathcal{J}_\perp]^{-1}\} \qquad \text{(II-37)}$$

where J is the total angular momentum. The quantity $[1/\mathcal{J}_{||} - 1/\mathcal{J}_\perp]^{-1}$ is usually termed the effective moment of inertia and it is symbolized by $\mathcal{J}_{eff}$. If we assume that the distribution in K for a fixed value of J is Gaussian, then we can set:

$$\rho_{J,K} \propto \exp\ (-K^2/2K_o^2) \tag{II-38}$$

and

$$K_o^2 = \frac{\mathcal{J}_{eff} T}{\hbar^2} \tag{II-39}$$

This leads to the following expression for the total level density of the transition nucleus:

$$\rho_f(E,K,J) = \frac{1}{24\sqrt{2}} \frac{(2J+1)}{a_f^{1/4} E^{5/4} \sigma^3} \exp\ [2\sqrt{a_f E} - \frac{(J+\frac{1}{2})^2}{2\sigma^2} - K^2/2K_o^2] \tag{II-40}$$

where a_f is the level density parameter related to the local density of levels in the transition nucleus near the Fermi surface, and σ is the spin cutoff parameter. It is calculated from the expression:

$$\sigma^2 = \frac{\mathcal{J}_\perp T}{\hbar^2} \tag{II-41}$$

$\mathcal{J}_\perp$ is the moment of inertia for rotation about an axis perpendicular to the nuclear symmetry axis.

The evaluation of the temperature, T, for use in (II-41) above, is not as completely straightforward as it might seem. The temperature is usually calculated directly as the inverse of the partial derivative of the log of the state density, ω, with respect to the excitation energy. In this respect then:

$$\frac{1}{T} = \frac{\partial \ln \omega(E)}{\partial E} \tag{II-42}$$

For a Fermi-gas of two kinds of particles with equidistant levels the state density is given by the expression (Gi 65):

$$\omega(E) \frac{\sqrt{\pi}}{12} \frac{\exp(2\sqrt{aE})}{a^{\frac{1}{4}} E^{5/4}} \qquad \text{(II-43)}$$

From this definition, the resulting formula for the temperature is:

$$\frac{1}{T} \approx \sqrt{\frac{a}{E}} - \frac{5}{4E} \qquad \text{(II-44)}$$

The problem with this relation is that it assumes the parameter 'a' to be a constant, independent of energy, and this is not necessarily so. We have seen in the neutron emission discussion that a_n is a very sharp function of excitation energy at low energies, tending to a constant value at higher excitation. This is a result of fluctuations of the local level density around the Fermi surface, and reflects the fact that the level spacings are not uniform as is usually assumed.

The same is true in the transition nucleus and there is no reason why we should expect a_f to be a constant, at least <u>a priori</u>. This fact also poses a problem in the sense that there is no convenient analytical expression which defines a_f in terms of excitation energy, and therefore we have to resort to empirical fits of the same nature that we used in the neutron emission case. Under these conditions, we might define a general form for a_f in terms of a flexible

function which would be expected to yield a constant asymptotic value of a_f at the limits of higher excitation. As we did before, and for convenience, we choose the function to be of the form:

$$a_f(E) = \alpha+\beta e^{-\gamma E} \qquad \text{(II-45)}$$

where α, β, γ are free parameters. In terms of this function and (II-42), the temperature becomes:

$$\frac{1}{T} = \left(\frac{\alpha+\beta e^{-\gamma E}}{E}\right)^{\frac{1}{2}} - \left(\frac{E}{\alpha+\beta e^{-\gamma E}}\right)^{\frac{1}{2}}\beta\gamma e^{-\gamma E} + \frac{\beta\gamma e^{-\gamma E}}{4(\alpha+\beta e^{-\gamma E})} - \frac{5}{4E} \qquad \text{(II-46)}$$

and as the excitation energy E reaches high values, the inverse of the temperature approaches the form:

$$\frac{1}{T} \rightarrow \left(\frac{\alpha}{E}\right)^{\frac{1}{2}} - \frac{5}{4E} \qquad \text{(II-47)}$$

where α represents then the asymptotic limit of $a_f(E)$. So, we see that at high excitation energies, the temperature is expected to follow the uniform spacing model prediction but, to deviate from this prediction for lower energy regions. Of course, these conclusions are model dependent, and it might very well be that our choice of an analytic function for $a_f(E)$ might not be right, but it provides us with a start. Figure 21 shows results from calculating T from both constant a_f and variable a_f assumptions. It will be discussed later.

The resulting level density expression must be normalized in K. This is done by dividing the level density

by the sum of all the relative K contributions up to the maximum value of the angular momentum. The resulting expression for the statistical transmission coefficients for fission is then:

$$T_f(K,J,\pi,E) = \frac{\int_0^{U-B_f+\varepsilon} \rho_F(E,K,J,\pi) T'_F(E)\,dE}{\sum_{-J\ max}^{J\ max} \exp\ (-K^2/2K_o^2)} \qquad \text{(II-48)}$$

Note that we are summing over a range of $-J_{max} \leq K \leq J_{max}$ because we must include both K projections, in the same manner as we did in the case of the individual channels.[9]

K_o^2 measures the mean square value of the project of the angular momentum on the nuclear symmetry axis. It can be extracted from the shape of the angular distribution of fission fragments. The flatter this distribution is, the higher K_o^2 will be, reflecting the width of the distribution in K. As the anisotropy increases, K_o^2 decreases, because proportionally, we find more bands with low values of K. Rapid and sudden shifts in K_o^2 as a function of excitation energy in the statistical region are usually associated with either the creation of new quasiparticle states, or the occurrence of multiple chance fission.

---

[9] In many instances the normalization in K is done by integrating the denominator in (II-48) between the limits of $-\infty$ and $+\infty$. This is basically incorrect, because in certain cases, the value of J_{max} may be relatively small and the sum will not approximate the value of the integral as is usually assumed.

D. Final Comments on the Model

In the three previous sections we have described the determination of the parameters involved in evaluating the "compound transmission coefficients" as given by (II-24) and (II-35). The integrals in these expressions were solved numerically by Simpson's rule of integration, using a total of 30 terms. This was done for all neutron energies involved in the calculations. Computer programs used in the calculations are listed in Appendices III and IV. Calculated "compound transmission coefficients" for neutrons were read into the modified version of the transition state spectroscopy code WILDCAT as part of the total calculation.

In this chapter we have discussed the main assumptions adopted in the calculational model. We have also described in detail how neutron emission is treated in the calculation, but have not yet shown how the total calculation is carried out. We have so far assumed in the development of the formalism that the fission channels are discrete, and have not said anything regarding their statistical behavior in the limit of high energies above the barrier. This we shall do as the need arises. A description of the practical aspects of the calculation, starting in the limit of a few channels will be shown in the next chapter.

III. RESULTS OF THE CALCULATIONS

The problem of determining the nature of the fission channels from experimental data has been shaded with some ambiguity lately because of the uncertainty in the shape of the transition state nucleus. If the transition nucleus has a reflection-symmetric shape, then one would expect the usual form of the allowed (J,π) values for a rotational band, i.e., 0+, 2+, 4+, 6+... or 3/2-, 5/2-, 7/2-, etc. However, if, as predicted by calculations (Ni 72), the transition nuclei in this region have asymmetric shapes, then the number of levels in the rotational band are doubled. For example, asymmetric e-e nuclei rotational bands have the form 0+, 1-, 2+, 3-, 4+, 5-, etc., while odd-A nuclei rotational bands have the form $3/2^{\pm}$, $5/2^{\pm}$, $7/2^{\pm}$, etc. The argument is that additional collective degrees of freedom result from deformations that are not reflection symmetric. A deformation violating either of these symmetries leads to a doubling of the energy levels, and hence to an increase of the level density by a factor of two. Thus, each (K,R) level of transition nucleus is fourfold degenerate, i.e., $\pm$ parity and $\pm$ K value (Er 58). This effect was pointed out by Vandenbosch (Va 73a), and later confirmed by Bjornholm, Bohr, and Mottelson (Bj 73).

Although some theoretical predictions, as we have mentioned, favor an asymmetric shape for the ^{227}Ra transition

nucleus, it would not be correct to, a priori, rule out the symmetric shape. For this reason we have carried out the calculations using both assumptions separately.

Before going directly on to the substance of the calculations, we should describe the procedure followed in practical terms, and tell also how the constant parameters involved in the calculations are obtained.

A. The Analysis of the Experimental Data at Low Energies

From the theory that has been developed in the preceding sections it is clear that angular distributions of fission fragments observed experimentally should be determined by weighted contributions of curves similar to the types shown in Figure 6. At low energies, close to the fission barrier, the distributions are determined by the parameters characterizing the first few individual levels, and we do not know, a priori, what values these parameters assume; in fact, this is exactly what we are seeking.

The procedure which is followed in this work is to leave four free parameters for each channel and then, by trial and error, to find the set of parameters that will give us the best fit simultaneously to both the fission cross sections and the corresponding angular distributions at various energies. The parameters that are left to vary are: (a) the single particle energy, E_o, which is the base of the rotational band; (b) the K quantum number, or projection of the angular momentum over the nuclear symmetry axis;

(c) the parity of the band, if reflection symmetry is assumed; and finally, (d) the parameter $\hbar\omega$ which measures the curvature of the parabola simulating the fission barrier. Small values of $\hbar\omega$ imply a thick, almost impenetrable, barrier and vice versa.

The values of other constants, such as the rotational constant $h^2/2\mathcal{J}_\perp$, the decoupling constant α, the level density parameter δ, the spin cutoff parameter σ for γ decay, and $(\Gamma_\gamma/D)_o$ are inserted into the calculation. The moment of inertia is calculated from the formula given by Brack *et al.* for a rigid body (Br 72):

$$<\mathcal{J}_\perp^{RB}> = \tfrac{1}{2}<\mathcal{J}_\parallel^{RB}> + \frac{1}{5} mAR_o^2 [c^2+4/35\ c^5(c-1)] \qquad \text{(III-1)}$$

and

$$<\mathcal{J}_\parallel^{RB} = \frac{2}{5} mAR_o^2 [c^{-1}-2/35\ c^2(c-1)+4/525\ c^5(c-1)^2] \qquad \text{(II-2)}$$

where $<\mathcal{J}_\parallel^{RB}>$ is equal to the nuclear moment of inertia around nuclear symmetry axis, m is equal to the mass of the nucleon, R_o is equal to the nuclear radius at zero deformation (8.5f), and c equal to the nuclear elongation parameter taken at the saddle point in the potential energy surface (1.65, from estimates by Brack *et al.* [Br 72]).

The above expressions yields a value of the rotational constant at the saddle point equal to about 2 keV. The value of the decoupling constant is not really known, but it makes little difference in the calculation.[10] A value of $\alpha=2$ was used.

[10] This was confirmed by assuming values of $-2 \leq \alpha \leq +2$.

The contribution of γ-ray emission to the total cross section is very small in relation to neutron evaporation. This means that if the denominator of the Hauser-Feshbach expression (II-15) is almost totally controlled by neutron emission, the cross section for γ-ray emission may be written as:

$$\sigma_{n,\gamma}(E_n) \approx \sigma_c(E_n)\left(\frac{\Gamma_\gamma}{\Gamma_n}\right)_{E_n} \qquad \text{(III-3)}$$

where Γ_γ and Γ_n are the widths for γ-ray de-excitation and neutron evaporation respectively, and $\sigma_c(E_n)$ is the neutron capture cross section. Because Γ_γ increases slowly with energy around 7 MeV (Gi 68), and σ_c decreases slowly with energy, the dependence of $\sigma_{n,\gamma}(E_n)$ on energy will be almost totally dependent on $(\Gamma_n)^{-1}$. Since Γ_n is directly proportional to the allowed sum of "compound transmission coefficients" for neutron emission, a partial test of the empirically determined level density, would be to compare the experimental and calculated dependences of $\sigma_{n,\gamma}(E_n)$ on E_n. In reality, what we have done is to deduce the parameter δ by fitting the slope of the experimentally determined cross section for γ-ray emission as a function of incident neutron energy. This is shown in Figure 15. The curve yields a value of δ=0.07, and $(\Gamma_\gamma/D)_o$ is estimated to be approximately equal to 0.0002, while σ, the spin cutoff parameter was assumed to have a value of about 6.0. On the basis of the level density systematics, the value of δ can be equated

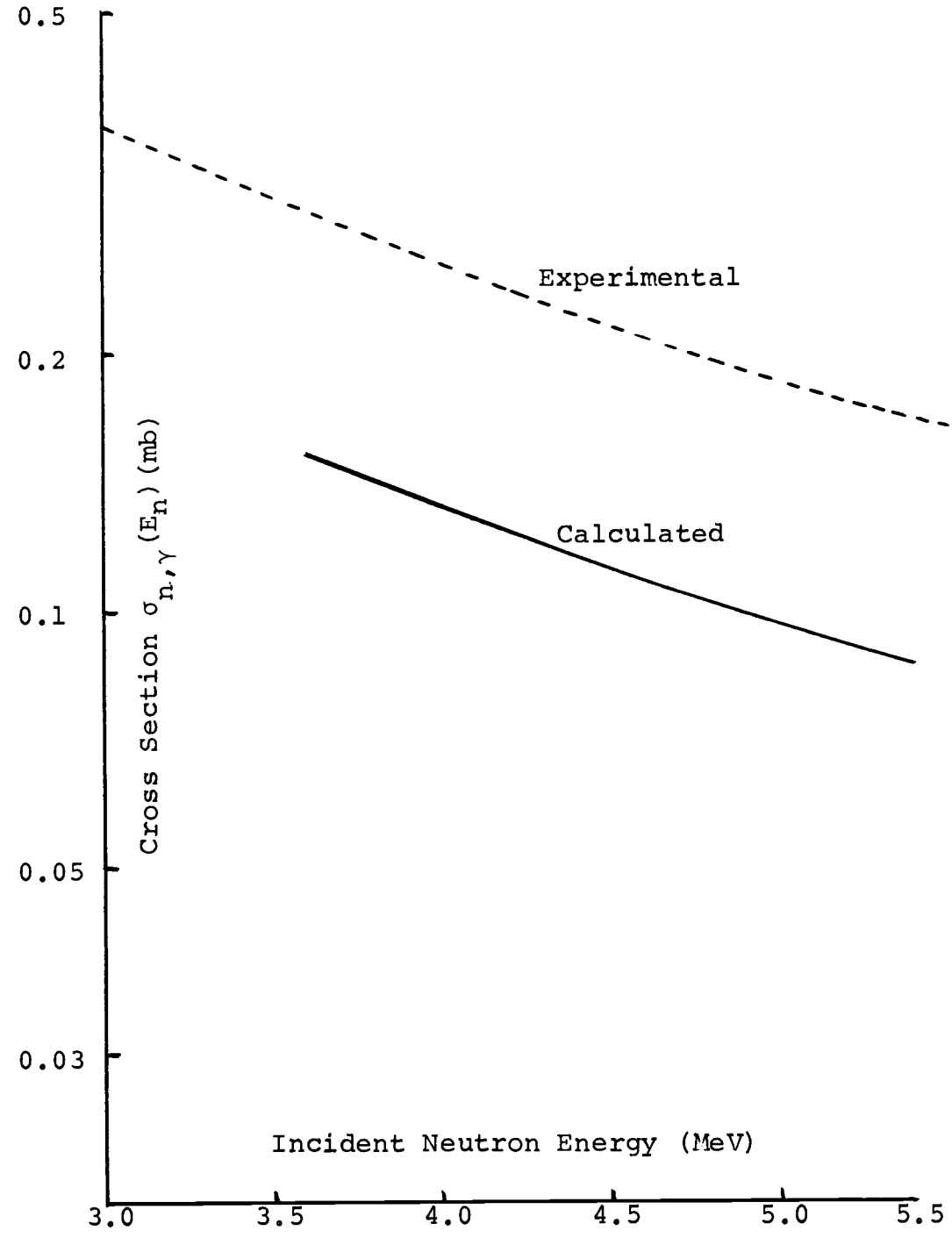

Figure 15. Experimental and Calculated Dependence of $\sigma_{En}(n,\gamma)$ on Neutron Energy for ^{226}Ra.

with a value of $a_n \approx 29$ at an excitation energy $\sim$9 MeV, if it is assumed that:

$$2\sqrt{a_n U} \simeq \sqrt{\frac{2\pi^2 E}{3\delta}} \qquad \text{(III-4)}$$

where E represents the excitation energy of the nucleus and U-E-P(Z)-P(N). P(Z) and P(N) are pairing corrections, previously defined. This relation is deduced from a comparison of expressions (II-8) and II-39) for the level density. The value of a_n deduced in this form is consistent with the one estimated from the neutron evaporation data, $a_n \simeq 29.5$. Since the slopes of the lines in Figure 15 remain roughly parallel in the energy range in question, this can be considered as partial indication that the treatment given to the level density of the residual nucleus and the "compound transmission coefficients" for neutron evaporation is basically correct.

The experimental data of Babenko et al. concerning angular distributions is given in the form of differential cross section ratios. In order to carry out the analysis properly, these must be converted into absolute differential cross sections. The procedure followed for this purpose is outlined in Appendix II. Resulting differential cross sections are shown in Figures 16a, b, c and d.

The best fit to the experimental data was determined by a χ^2 or "goodness of fit" test. Unsatisfactory fits were rejected at the 99% level of confidence. A problem that

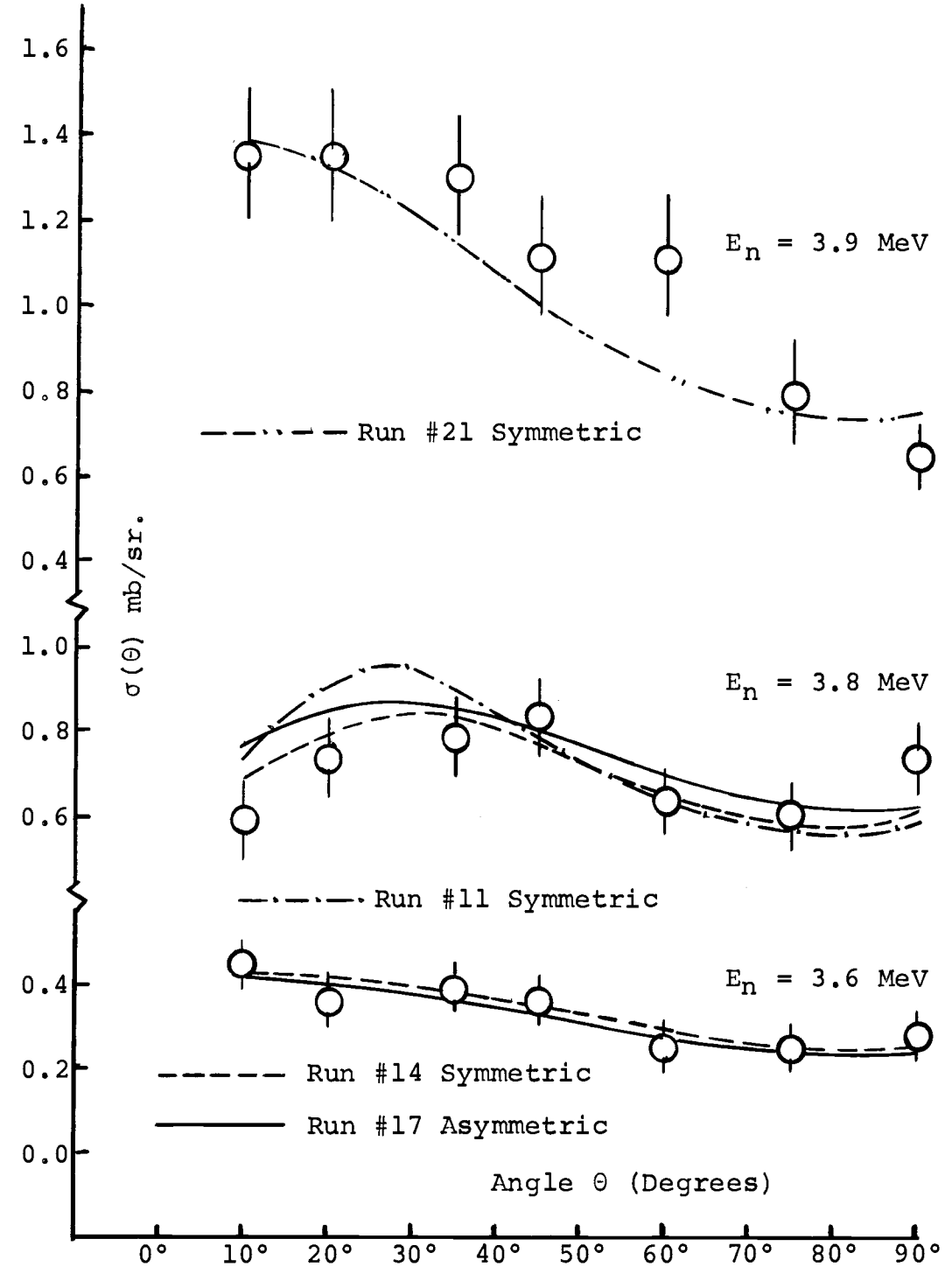

Figure 16a. Differential Cross Sections and Fits for the ^{226}Ra(n,f) Reaction.

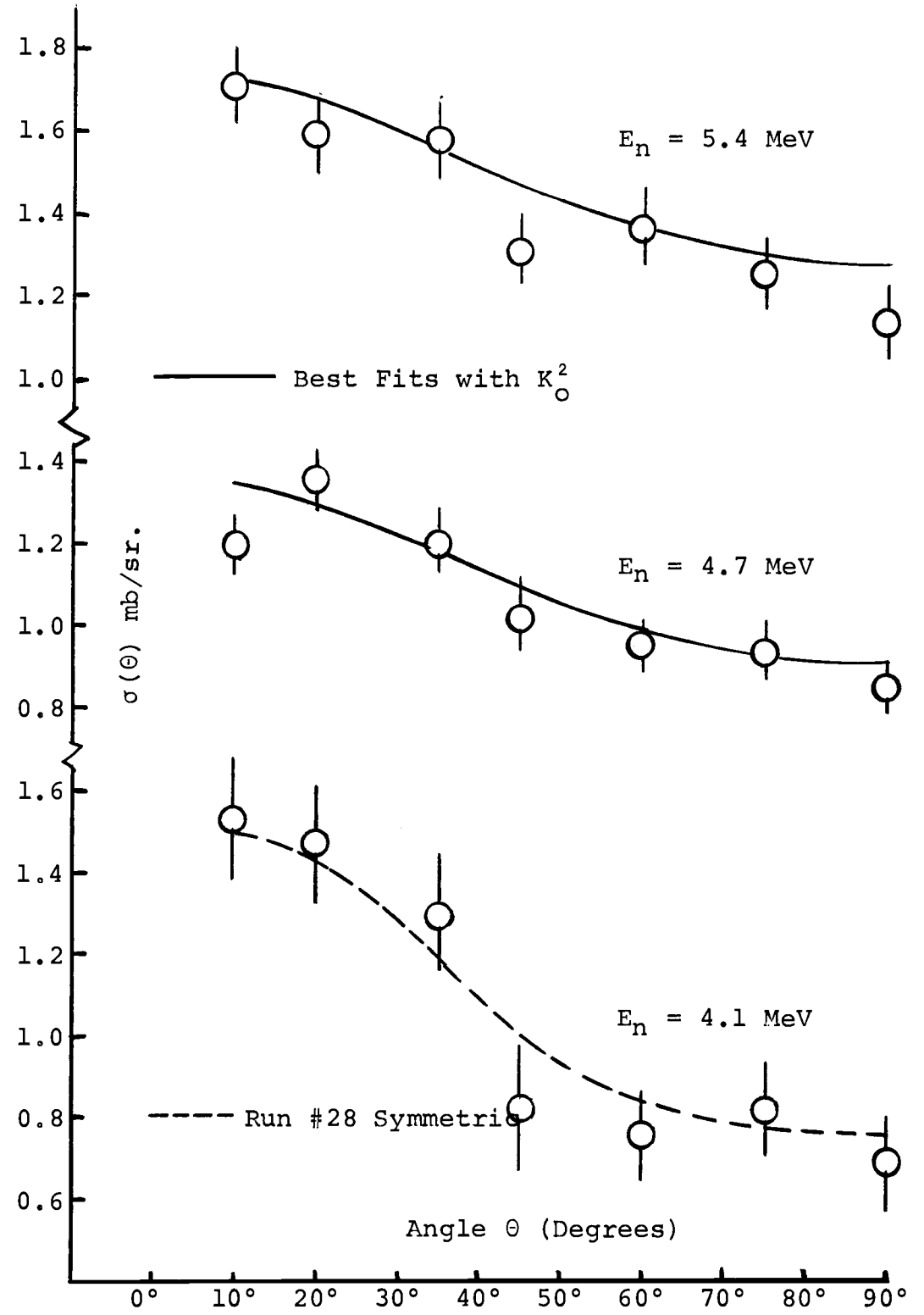

Figure 16b. Differential Cross Sections and Fits for the ^{226}Ra(n,f) Reaction for neutron energies 4.1 to 5.4 MeV.

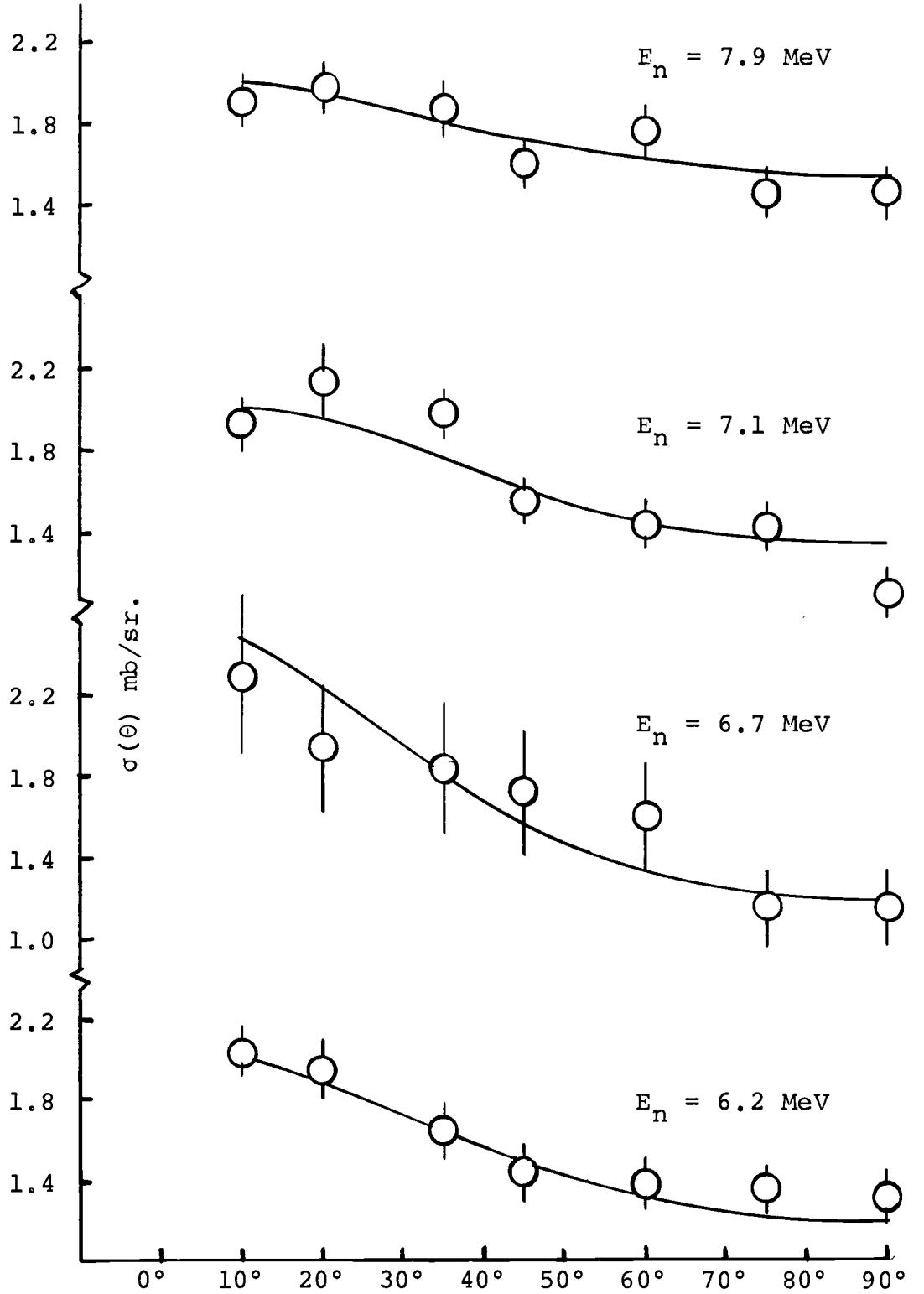

Figure 16c. Differential Cross Sections and Fits for the $^{226}Ra(n,f)$ Reaction for neutron energies 6.2 to 7.9 MeV.

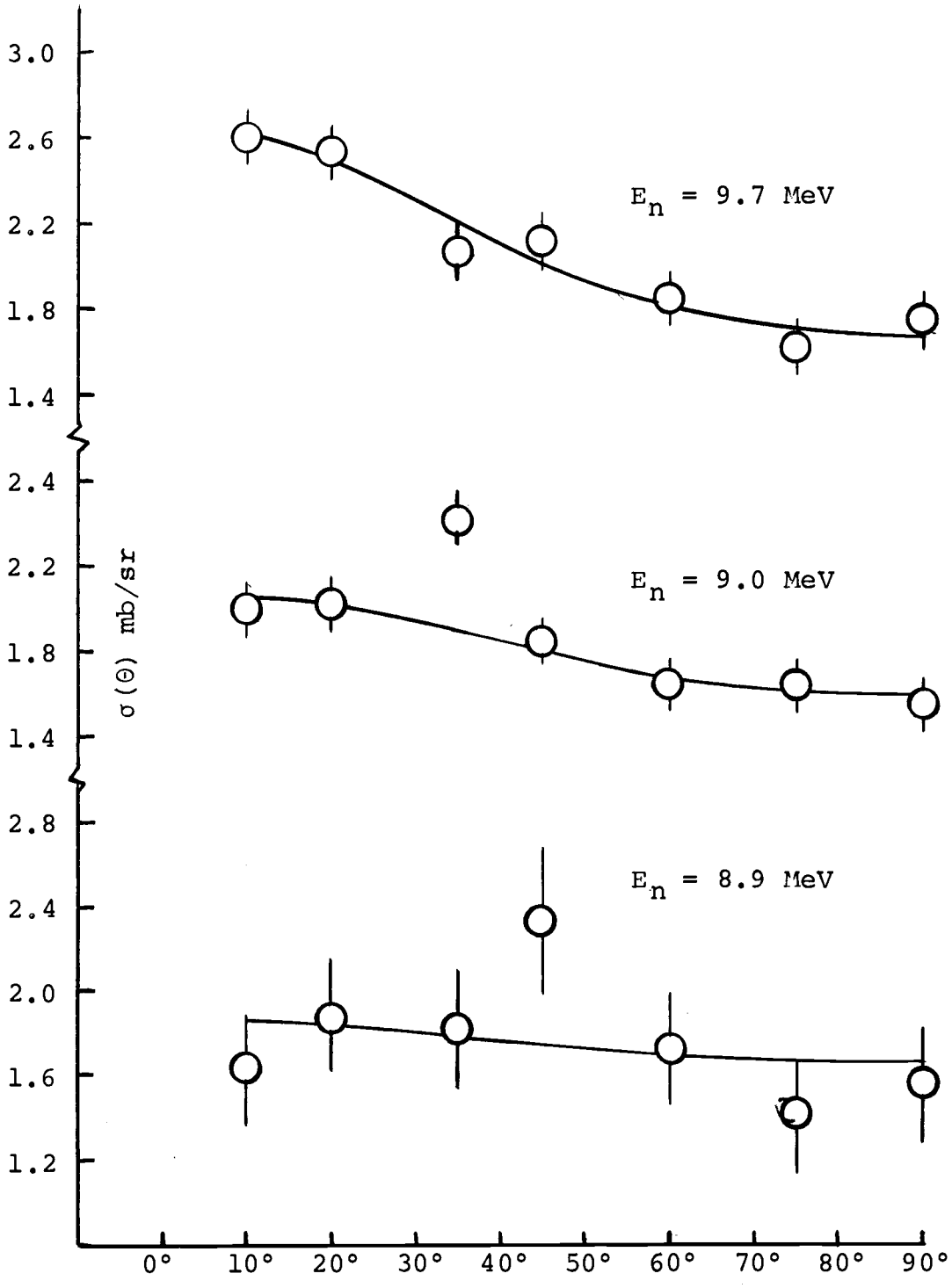

Figure 16d. Differential Cross Sections and Fits for the ^{226}Ra(n,f) Reaction for neutron energies 8.9 to 9.7 MeV.

arose in using the χ^2 test was to estimate the numbers of degrees of freedom in fitting the data. For a given number of data points, the number of degrees of freedom is represented by the total number of experimental points minus the effective number of free parameters used in the calculation. There are a total of seven experimental points for every neutron energy, and we are trying to find optimal values for four variables, K, π, E_o and $\hbar\omega$ for every fission channel. Two of these, E_o and $\hbar\omega$ are unrestricted in the number of values that they can assume. K can only take a few values and π can only be either positive or negative. The interpretation of this problem becomes a little different when we consider the argument in terms of symmetric vs. asymmetric saddle point shapes. In the latter case, both parities are available for every channel, and π is no longer a free parameter. With the above in mind, we can now proceed to carry out a search for the parameters that best fit the experimental data assuming both symmetric and asymmetric shapes at the saddle point.

1. Fission channels in the symmetric nucleus ^{227}Ra

The technique that we have used is to try to fit the data simultaneously for, at first one neutron energy, then two, three, etc., by using the minimum number of channels possible in each case. It is clear that as the number of angular distributions and cross sections increases, the

chance of obtaining a statistically significant fit to the data decreases very rapidly. The reason for this is that we need an ever increasing number of channels, and each channel introduces four free parameters. Since we only have a total of seven experimental points at each energy, the number of degrees of freedom left in each case is exhausted quickly. We can obtain fits to the data but they are statistically meaningless.

The data listed in Table IV shows the different combinations of parameters tried. We note that it is possible to fit the experimental data meaningfully only for two energies, 3.6 and 3.8 MeV. Statistically speaking, nothing can be said about the parameters characterizing the distributions at neutron energies equal to 3.9 and 4.1 MeV. We can, however, resort to common sense to discover a few items. Figure 16a shows that $d\sigma/d\Omega$ at about 10° in the 3.8 MeV data takes a value of about 0.60, and it is about 0.42 for E_n = 3.6 MeV. However, it jumps to 1.35 for E_n = 3.9 MeV. The calculations show that it is not possible to reproduce this sudden rate of increase in cross section in $d\sigma/d\Omega$ at 10° with only three channels. Since only K = 1/2 bands peak at forward angles, we conclude that there must be some nearby K = 1/2 band which produces a sharp increase in cross section around 3.9 MeV. In order to produce such a sharp increase and not affect the distribution at 3.8 MeV, the channel must open only very close to the top of the

Table IV. Summary of Calculations Describing the Symmetric Nucleus ^{227}Ra.

		RUN 1	2	3	4	5	6	7	8	9	10
# of Energ.		one	one	two	two	two	two	two	two	two	two
Channel #											
	K	3/2-	3/2-	3/2-	3/2-	3/2+	3/2+	3/2-	3/2-	3/2-	3/2-
1	E_o	3.650	3.650	3.650	3.630	3.600	3.600	3.650	3.650	3.650	3.650
	$\hbar\omega$	0.400	0.400	0.400	0.400	0.400	0.400	0.400	0.400	0.400	0.400
	K	1/2+	1/2+	1/2+	1/2+	1/2+	1/2+	1/2+	1/2+	1/2+	1/2+
2	E_o	3.675	3.675	3.675	3.675	3.675	3.675	3.675	3.675	3.675	3.675
	$\hbar\omega$	0.750	0.750	0.750	0.750	0.750	0.750	0.750	0.750	0.750	0.750
	K		5/2+				3/2+	3/2+	3/2+	3/2+	3/2+
3	E_o		3.800				3.800	3.800	3.775	3.750	3.750
	$\hbar\omega$		0.400				0.400	0.400	0.400	0.400	0.300
	K										
4	E_o										
	$\hbar\omega$										
	K										
5	E_o										
	$\hbar\omega$										
	K										
6	E_o										
	$\hbar\omega$										
	χ^2	3.23	2.91	35.9	35.7	86.7	47.8	19.75	18.84	19.37	18.37
Satisfactory		no	no	no	no	no	no	no	no	no	no

Table IV. continued

		RUN 11	12	13	14	15	16	17	18	19	20
# of Energ.		two	two	two	two	two	two	two	three	three	three
Channel #											
	K	3/2-	3/2-	3/2-	3/2-	3/2-	3/2-	3/2-	3/2-	3/2-	3/2-
1	E_o	3.650	3.650	3.650	3.650	3.650	3.650	3.650	3.650	3.650	3.650
	$\hbar\omega$	0.400	0.400	0.400	0.400	0.400	0.400	0.400	0.400	0.400	0.400
	K	1/2+	1/2+	1/2+	1/2+	1/2+	1/2+	1/2+	1/2+	1/2+	1/2+
2	E_o	3.675	3.675	3.675	3.675	3.675	3.675	3.675	3.675	3.675	3.675
	$\hbar\omega$	0.750	0.750	0.750	0.750	0.750	0.750	0.750	0.750	0.750	0.750
	K	3/2+	3/2+	5/2-	5/2+	5/2-	5/2-	5/2-	5/2+	5/2+	5/2+
3	E_o	3.750	3.725	3.800	3.700	3.800	3.800	3.800	3.700	3.700	3.700
	$\hbar\omega$	0.200	0.200	0.400	0.300	0.400	0.400	0.400	0.300	0.300	0.300
	K					3/2-	5/2-	1/2-	1/2-	1/2-	1/2-
4	E_o					3.975	3.900	3.880	3.880	3.850	3.860
	$\hbar\omega$					0.400	0.400	0.150	0.100	0.050	0.075
	K							3/2-			
5	E_o							3.975			
	$\hbar\omega$							0.400			
	K										
6	E_o										
	$\hbar\omega$										
	χ^2	18.06	21.81	12.68	8.64	11.59	9.91	5.99	29.0	30.4	27.5
Satisfactory		no	no	yes	yes	no	no	no	no	no	no

Table IV. continued

		RUN 21	22	23	24	25	26	27	28	29	30
# of Energ.		three	three	three	three	three	three	three	three	three	three
Channel #											
	K	3/2-	3/2-	3/2-	3/2-	3/2-	3/2-	3/2-	3/2-	3/2-	3/2-
1	E_o	3.650	3.650	3.650	3.650	3.650	3.650	3.650	3.650	3.650	3.650
	$\hbar\omega$	0.400	0.400	0.400	0.400	0.400	0.400	0.400	0.400	0.400	0.400
	K	1/2+	1/2+	1/2+	1/2+	1/2+	1/2+	1/2+	1/2+	1/2+	1/2+
2	E_o	3.675	3.675	3.675	3.675	3.675	3.675	3.675	3.675	3.675	3.675
	$\hbar\omega$	0.750	0.750	0.750	0.750	0.750	0.750	0.750	0.750	0.750	0.750
	K	5/2+	5/2+	5/2-	5/2-	5/2+	5/2+	5/2+	5/2+	1/2-	5/2-
3	E_o	3.700	3.700	3.740	3.740	3.700	3.700	3.700	3.700	3.880	3.800
	$\hbar\omega$	0.300	0.300	0.250	0.200	0.300	0.300	0.300	0.300	0.150	0.400
	K	1/2-	1/2-	1/2-	1/2-	1/2-	1/2-	1/2-	1/2-	3/2-	1/2-
4	E_o	3.870	3.875	3.875	3.875	3.875	3.875	3.875	3.875	3.975	3.880
	$\hbar\omega$	0.075	0.075	0.075	0.075	0.075	0.075	0.075	0.075	0.400	0.150
	K						3/2-	3/2-	3/2-		3/2-
5	E_o						3.950	3.950	3.950		3.975
	$\hbar\omega$						0.200	0.200	0.200		0.400
	K							1/2-	1/2-		
6	E_o							4.050	4.090		
	$\hbar\omega$							0.300	0.300		
	χ^2	26.4	26.7	27.24	28.0	72.15	41.6	35.7	32.8	59.0	30.0
Satisfactory		no	no	no	no	no	no	no	no	no	no

Table IV. continued

		RUN 31	32	33	34	35	36	37	38	39	40
# of Energ.		three	three	three	three	three	three	three	three	three	three
Channel #											
	K	3/2-	3/2-	3/2-	3/2-	3/2-	3/2-	3/2-	3/2-	3/2-	3/2-
1	E_o	3.650	3.650	3.650	3.650	3.650	3.650	3.650	3.650	3.650	3.650
	$\hbar\omega$	0.400	0.400	0.400	0.400	0.400	0.400	0.400	0.400	0.400	0.400
	K	1/2+	1/2+	1/2+	1/2+	1/2-	1/2+	1/2+	1/2+	1/2+	1/2+
2	E_o	3.700	3.650	3.675	3.675	3.675	3.675	3.675	3.675	3.675	3.675
	$\hbar\omega$	0.750	0.750	0.850	0.650	0.750	0.750	0.750	0.750	0.750	0.750
	K	5/2-	5/2-	5/2-	5/2-	5/2-	5/2-	5/2-	5/2-	5/2-	5/2-
3	E_o	3.800	3.800	3.800	3.800	3.800	3.800	3.800	3.800	3.800	3.800
	$\hbar\omega$	0.400	0.400	0.400	0.400	0.400	0.400	0.400	0.400	0.400	0.400
	K	1/2-	1/2-	1/2-	1/2-	1/2-	1/2-	1/2-	1/2-	1/2+	1/2+
4	E_o	3.880	3.880	3.880	3.880	3.880	3.930	3.880	3.880	3.880	3.830
	$\hbar\omega$	0.150	1.150	0.150	0.150	0.150	0.150	0.100	0.200	0.150	0.150
	K	3/2-	3/2-	3/2-	3/2-	3/2-	3/2-	3/2-	3/2-	3/2-	3/2-
5	E_o	3.975	3.975	3.975	3.975	3.975	3.975	3.975	3.975	3.975	3.975
	$\hbar\omega$	0.400	0.400	0.400	0.400	0.400	0.400	0.400	0.400	0.400	0.400
	K										
6	E_o										
	$\hbar\omega$										
	χ^2	30.0	35.5	30.6	30.7	164.3	54.6	29.0	32.4	38.6	36.3
Satisfactory		no	no	no	no	no	no	no	no	no	no

Table IV. continued

		RUN 41	42	43	44
# of Energ.		three	three	three	four
Channel #					
	K	3/2-	3/2-	3/2-	3/2-
1	E_o	3.650	3.650	3.650	3.650
	$\hbar\omega$	0.400	0.400	0.400	0.400
	K	1/2+	1/2+	1/2+	1/2+
2	E_o	3.675	3.725	3.625	3.675
	$\hbar\omega$	0.750	0.750	0.750	0.750
	K	5/2-	5/2-	5/2-	5/2-
3	E_o	3.800	3.800	3.800	3.800
	$\hbar\omega$	0.400	0.400	0.400	0.400
	K	1/2+	1/2-	1/2-	1/2-
4	E_o	3.830	3.880	3.880	3.880
	$\hbar\omega$	0.100	0.150	0.150	0.150
	K	3/2-	3/2-	3/2-	3/2-
5	E_o	3.975	3.975	3.975	3.975
	$\hbar\omega$	0.400	0.400	0.400	0.400
	K				1/2-
6	E_o				4.090
	$\hbar\omega$				0.300
	χ^2	31.2	34.8	47.3	37.4
Satisfactory		no	no	no	no

barrier; if so, then the barrier must be wide and therefore $\hbar\omega$ small.

In the case of E_n = 4.1 MeV, the fits become statistically meaningless; combination 28 of Table IV shows the best fit that can be obtained with six channels, but with the condition that we not be allowed to say much about them.

For the case in which only two neutron energies are considered, the combination that gives us the best fit is combination 14. However, we have some ambiguity present with regard to the K = 5/2 channel; the table shows that the parity is not defined, thereby making the energy and curvature parameter uncertain. We tried to fit the angular distribution with K = 3/2 channels instead of the K = 5/2 appearing in the table, but it was not possible to obtain an acceptable value of χ^2 for any combination tried. Figure 16a shows the best fits obtained for three energies, 3.6, 3.8, and 3.9 MeV, and also other combinations of each channel with energy. Figure 17 represents a fit of channel cross section vs. neutron energy for the optimum set of parameters. The uncertainties in the deduced parameters are hard to evaluate in an exact manner because the search would have to become much more extensive and the meaning of the information gathered in this fashion would not be entirely accurate in any case, due to the other uncertainties in the calculation. However, from the information available in Table IV we have made a compilation of the best

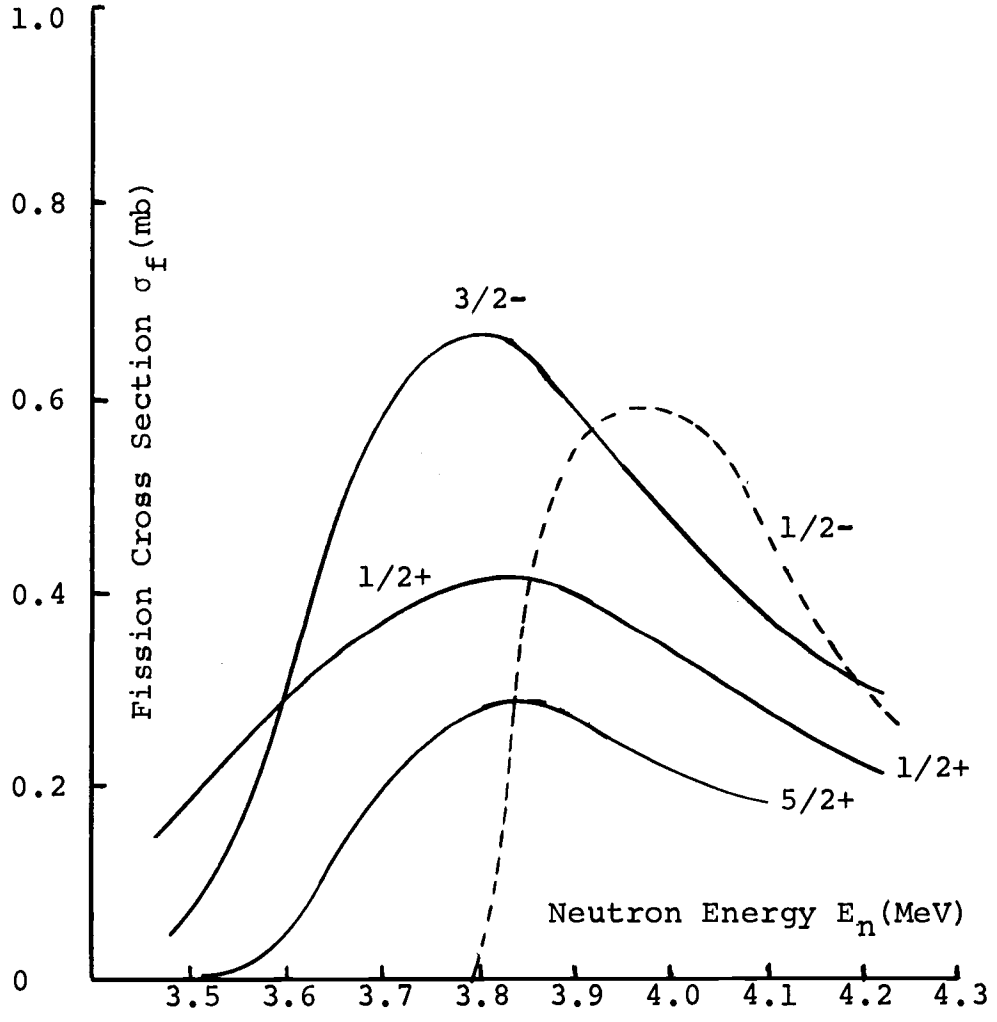

Figure 17. Partial Fission Cross Sections for Four Open Channels.

parameters and most likely errors for every channel. This is shown in Table VI. The best fit to the fission cross section is shown in Figure 18.

2. Fission Channels in the asymmetric nucleus ^{227}Ra

The search for a best fit in this case was done in the same manner as in the symmetric case, with one exception; for every channel both parities were allowed in the calculation. It was done in this fashion in order to simulate the doubling in the rotational band as was mentioned before. The same problems were encountered as in the symmetric case, and Table V shows a list of all the combinations tried. The best fit is obtained for E_n = 3.6 and 3.8 MeV with the use of three channels as indicated by combination 17. When the third energy, E_n = 3.9 MeV, comes into play, the ground state, and the one above, are pushed upwards in energy a little bit in order to obtain the best fit for three energies simultaneously. As was pointed out for the symmetric case, we cannot specify the parameters with any statistical significance when the third neutron energy is included. The uncertainties in the parameters as extracted from Table V are shown in Table VI. Figure 16a shows the best fit obtained for two energies. Other fits are also shown for purposes of comparison and illustration. The best fit to the cross section is shown in Figure 18.

Table V. Summary of Calculations Describing Asymmetric Nucleus ^{227}Ra at Low Energies.

		RUN 1	2	3	4	5	6	7	8	9	10
# of Energies		two	two	two	two	two	two	two	two	two	two
Channel #											
	K	3/2	5/2	5/2	5/2	3/2	3/2	3/2	5/2	3/2	5/2
1	E_o	3.750	3.700	3.700	3.700	3.750	3.740	3.730	3.730	3.725	3.675
	$\hbar\omega$	0.600	0.600	0.600	0.400	0.600	0.600	0.600	0.450	0.500	0.500
	K	1/2	1/2	1/2	1/2	1/2	1/2	1/2	1/2	1/2	1/2
2	E_o	3.875	3.890	3.890	3.890	3.890	3.910	3.910	3.910	3.910	3.910
	$\hbar\omega$	0.900	1.200	1.000	0.900	1.000	1.000	1.000	1.000	1.000	1.000
	K										
3	E_o										
	$\hbar\omega$										
	K										
4	E_o										
	$\hbar\omega$										
	K										
5	E_o										
	$\hbar\omega$										
	χ^2	44.3	114.0	39.5	60.5	35.3	30.2	28.4	34.3	28.12	28.5
Satisfactory		no	no	no	no	no	no	no	no	no	no

Table V. continued

		RUN 11	12	13	14	15	16	17	18	19	20
# of Energ.		two	two	two	two	two	two	two	two	two	two
Channel #											
	K	5/2	3/2	3/2	3/2	3/2	3/2	3/2	3/2	3/2	3/2
1	E_o	3.665	3.740	3.740	3.740	3.740	3.750	3.755	3.755	3.758	3.760
	$\hbar\omega$	0.500	0.500	0.600	0.600	0.550	0.600	0.600	0.600	0.600	0.600
	K	1/2	5/2	5/2	5/2	5/2	5/2	5/2	5/2	5/2	5/2
2	E_o	3.910	3.850	3.850	3.850	3.850	3.840	3.830	3.830	3.830	3.830
	$\hbar\omega$	1.000	0.400	0.400	0.400	0.500	0.500	0.500	0.500	0.500	0.500
	K		1/2	1/2	1/2	1/2	1/2	1/2	1/2	1/2	1/2
3	E_o		3.910	3.910	3.915	3.915	3.915	3.915	3.915	3.915	3.915
	$\hbar\omega$		1.000	1.000	1.000	1.000	1.000	1.000	1.050	1.025	1.025
	K										
4	E_o										
	$\hbar\omega$										
	K										
5	E_o										
	$\hbar\omega$										
	χ^2	26.7	21.0	16.8	15.6	15.6	13.9	13.4	15.2	13.8	13.65
Satisfactory		no	no	no	no	no	yes	yes	no	yes	yes

Table V. continued

		RUN 21	22	23	24	25	26	27	28	29	30
# of Energ.		two	three	three	three	three	three	three	three	three	three
Channel #											
	K	3/2	3/2	3/2	3/2	3/2	3/2	3/2	3/2	3/2	3/2
1	E_o	3.770	3.755	3.755	3.755	3.755	3.755	3.755	3.755	3.755	3.755
	$\hbar\omega$	0.600	0.600	0.600	0.600	0.600	0.600	0.600	0.600	0.600	0.600
	K	5/2	5/2	5/2	5/2	5/2	5/2	5/2	5/2	5/2	5/2
2	E_o	3.830	3.830	3.830	3.830	3.830	3.830	3.830	3.830	3.830	3.840
	$\hbar\omega$	0.500	0.500	0.500	0.500	0.500	0.500	0.500	0.500	0.550	0.550
	K	1/2	1/2	1/2	1/2	1/2	1/2	1/2	1/2	1/2	1/2
3	E_o	3.915	3.915	3.900	3.925	3.915	3.910	3.905	3.915	3.915	3.915
	$\hbar\omega$	1.025	1.000	0.150	0.150	0.100	0.100	0.100	1.000	1.000	1.000
	K			1/2	1/2	1/2	1/2	1/2	1/2	1/2	1/2
4	E_o			3.915	3.915	3.915	3.915	3.915	3.925	3.925	3.925
	$\hbar\omega$			1.000	1.000	1.000	1.000	1.000	0.150	0.150	0.150
	K								3/2		
5	E_o								4.000		
	$\hbar\omega$								0.200		
	χ^2	13.7	45.5	51.0	37.5	37.5	38.4	41.1	38.4	37.1	36.1
Satisfactory		yes	no	no	no	no	no	no	no	no	no

Table V. continued

		RUN 31	32	33	34	35	36	37	38	39	40
# of Energ.		three	three	three	three	three	three	three	three	three	three
Channel #											
	K	3/2	3/2	3/2	3/2	3/2	3/2	3/2	3/2	3/2	3/2
1	E_o	3.755	3.755	3.755	3.755	3.755	3.775	3.765	3.775	3.780	3.780
	$\hbar\omega$	0.600	0.600	0.600	0.600	0.600	0.630	0.625	0.630	0.630	0.650
	K	5/2	5/2	5/2	5/2	5/2	5/2	5/2	5/2	5/2	5/2
2	E_o	3.850	3.860	3.870	3.870	3.880	3.880	3.880	3.880	3.880	3.880
	$\hbar\omega$	0.600	0.600	0.600	0.600	0.625	0.625	0.625	0.675	0.700	0.700
	K	1/2	1/2	1/2	1/2	1/2	1/2	1/2	1/2	1/2	1/2
3	E_o	3.915	3.915	3.915	3.915	3.915	3.915	3.915	3.915	3.915	3.915
	$\hbar\omega$	1.000	1.000	1.000	1.000	1.000	1.000	1.000	1.000	1.000	1.000
	K	1/2	1/2	1/2	1/2	1/2	1/2	1/2	1/2	1/2	1/2
4	E_o	3.925	3.925	3.925	3,905	3.905	3.905	3.905	3.905	3.905	3.905
	$\hbar\omega$	0.150	0.150	0.150	0.100	0.100	0.100	0.100	0.100	0.100	0.100
	K										
5	E_o										
	$\hbar\omega$										
	χ^2	35.1	34.6	34.4	35.6	34.8	34.8	34.2	33.5	33.4	33.1
Satisfactory		no	no	no	no	no	no	no	no	no	no

Table V. continued

		RUN 41	42	43	44	45	46	47	48	49	50
# of Energ.		three	three	three	three	four	four	four	four	four	four
Channel #											
	K	3/2	3/2	3/2	3/2	3/2	3/2	3/2	3/2	3/2	3/2
1	E_o	3.780	3.790	3.790	3.790	3.790	3.790	3.790	3.790	3.790	37.90
	$\hbar\omega$	0.650	0.650	0.675	0.675	0.675	0.675	0.675	0.675	0.675	0.675
	K	5/2	5/2	5/2	5/2	5/2	5/2	5/2	5/2	5/2	5/2
2	E_o	3.880	3.880	3.880	3.880	3.880	3.880	3.880	3.880	3.880	3.880
	$\hbar\omega$	0.750	0.775	0.775	0.775	0.775	0.775	0.775	0.775	0.775	0.775
	K	1/2	1/2	1/2	1/2	1/2	1/2	1/2	1/2	1/2	1/2
3	E_o	3.915	3.915	3.915	3.915	3.915	3.915	3.915	3.915	3.915	3.915
	$\hbar\omega$	1.000	1.000	1.000	1.000	1.000	1.000	1.000	1.000	1.000	1.000
	K	1/2	1/2	1/2	1/2	1/2	1/2	1/2	1/2	1/2	1/2
4	E_o	3.905	3.905	3.905	3.900	3.900	3.925	4.000	4.100	4.050	4.075
	$\hbar\omega$	0.100	0.100	0.100	0.100	0.100	0.150	0.200	0.400	0.400	0.450
	K										
5	E_o										
	$\hbar\omega$										
	χ^2	32.5	32.6	32.6	34.0	69.3	69.5	76.6	57.6	53.7	53.1
Satisfactory		no	no	no	no	no	no	no	no	no	no

Table V. continued

		RUN 51	52	53	54	55	56	57	58	59	60
# of Energ.		four	four	four	four	two	two	two	two	two	two
Channel #											
	K	3/2	3/2	3/2	3/2	3/2	3/2	3/2	3/2	3/2	3/2
1	E_o	3.790	3.790	3.790	3.790	3.755	3.730	3.780	3.755	3.755	3.755
	$\hbar\omega$	0.675	0.675	0.675	0.675	0.600	0.600	0.600	0.500	0.700	0.700
	K	5/2	5/2	5/2	5/2	5/2	5/2	5/2	5/2	5/2	5/2
2	E_o	3.880	3.880	3.880	3.880	3.830	3.830	3.830	3.830	3.830	3.805
	$\hbar\omega$	0.775	0.775	0.775	0.775	0.500	0.500	0.500	0.500	0.500	0.500
	K	1/2	1/2	1/2	1/2	1/2	1/2	1/2	1/2	1/2	1/2
3	E_o	3.915	4.025	3.925	3.850	3.915	3.915	3.915	3.915	3.915	3.915
	$\hbar\omega$	1.000	0.600	0.600	0.600	1.000	1.000	1.000	1.000	1.000	1.000
	K	1/2									
4	E_o	4.060									
	$\hbar\omega$	0.450									
	K										
5	E_o										
	$\hbar\omega$										
	χ^2	52.3	324.0	167.5	86.8	13.4	19.5	15.5	18.7	15.4	14.4
Satisfactory		no	no	no	no	yes	no	no	no	no	yes

Table V. continued

		RUN 61	62	63	64	65	66	67	68
# of Energ.		two	two	two	two	two	two	two	two
Channel #									
	K	3/2	3/2	3/2	3/2	3/2	3/2	3/2	3/2
1	E_o	3.755	3.755	3.755	3.755	3.755	3.755	3.755	3.755
	$\hbar\omega$	0.700	0.700	0.700	0.700	0.700	0.700	0.700	0.700
	K	5/2	5/2	5/2	5/2	5/2	5/2	5/2	5/2
2	E_o	3.855	3.830	3.830	3.830	3.830	3.830	3.830	3.830
	$\hbar\omega$	0.500	0.400	0.600	0.600	0.600	0.600	0.600	0.600
	K	1/2	1/2	1/2	1/2	1/2	1/2	1/2	1/2
3	E_o	3.915	3.915	3.915	3.890	3.940	3.915	3.915	3.940
	$\hbar\omega$	1.000	1.000	1.000	1.000	1.000	0.800	1.200	1.000
	K								
4	E_o								
	$\hbar\omega$								
	K								
5	E_o								
	$\hbar\omega$								
	χ^2	14.6	14.8	13.8	22.3	12.2	26.5	30.5	29.3
Satisfactory		yes	yes	yes	no	yes	no	no	no

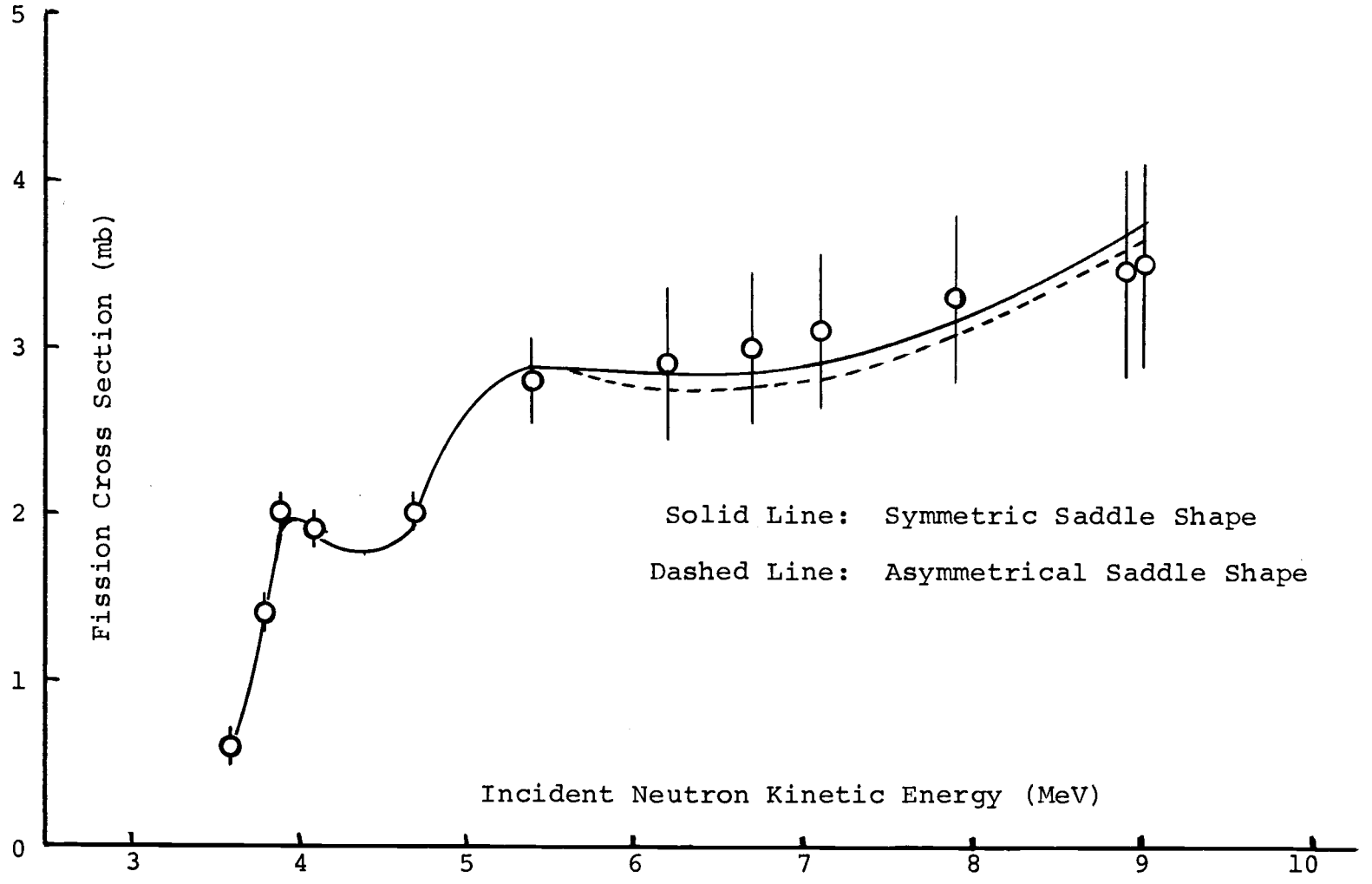

Figure 18. Best Fits to the Fission Cross Sections at Low and High Energies.

Table VI. Parameters Describing the Low Lying Single Particle States in the ^{227}Ra Transition Nucleus.

Part A. Symmetric Saddle Point Deformation			
State No.	(K,π)	E_o (MeV)	$\hbar\omega$ (MeV)
1	3/2-	3.65±0.1	0.4 ±0.1
2	1/2+	3.67±0.1	0.75±0.2
3	5/2±	3.70±0.1	0.3 ±0.2
4	1/2-	3.88±0.1	∿0.1 ±0.05

Part B. Asymmetric Saddle Point Deformation			
State No.	K	E_o (MeV)	$\hbar\omega$ (MeV)
1	3/2	3.76±0.05	0.6 ±0.1
2	5/2	3.83±0.05	0.4 ±0.2
3	1/2	3.92±0.05	1.0 ±0.1

B. Parameters Describing the ^{227}Ra Transition Nucleus at Moderate Excitation Energies

The discussion concerning the excited transition nucleus in this energy region follows basically the same pattern used in describing the region where only a few channels are available for fission. The calculations are carried out on a trial and error basis. In this manner the values of certain free parameters which best fit the experimental data are chosen; the fit is judged according to the χ^2 criteria. As we did before, we have to allow for two basic possibilities: in one case the shape of the transition nucleus is assumed to be symmetric, in the other the nuclear

shape will be asymmetric. The number of levels in each rotational band is doubled in the latter case.

One question that immediately comes to mind is in relation to where the "statistical region" lies. In other words, at what point are we justified in using the statistical approximations developed above" We know that there is in fact a "twilight zone" between the "discrete" and "statistical worlds". Conservatively speaking, we might expect the application of a statistical model for $E^* < 1$ MeV to be questionable and that for $E^* \geq 3$ MeV, such an application should be quite acceptable. The excitation energy range $1 \leq E^* \leq 2$ MeV constitutes a "twilight zone". Unfortunately the interestingly large step in the cross section is observed at the point corresponding to $E_n = 4.7$ MeV ($E^* \simeq 1$ MeV). This "discontinuity" in the cross section assures the existence of a large jump, in the number of fission channels available, within a short energy range.

What we have done to treat this lower energy region is to feed discrete channels into the undefined region (from $\sim$3.9 MeV to $\sim$4.7 MeV), with the idea of fitting the cross section in this range in a way which will reproduce the angular distribution of fragments at 4.7 MeV (the next point where data of this kind is available). Of course, the use of discrete levels in fitting the data in this region has no meaning other than perhaps giving us a vague idea of the relative K strengths required to reproduce the

anisotropy at 4.1 and 4.7 MeV. From 4.7 MeV on, we apply the statistical formalism in a way such that all the data points are fitted. The two models are made to join smoothly in a region (E_n = 4.7 MeV) where some of the parameters describing the behavior of the system lose some of their significance. This is the best that we can do under the circumstances and it might be a small price to pay in return for the overall information which we will finally obtain.

As the excitation energy of the nucleus increases, the cross section reaches a point where its variations with energy is relatively small, because of the relative constancy of (Γ_f/Γ_n). Large jumps in the slope of the curve can be associated with fission after neutron evaporation. In the case of ^{227}Ra we see that at neutron energies above approximately 9.0 MeV, the cross section increases very rapidly; this rapid change takes place in a region where we can expect second chance fission to begin occurring. Qualitatively it can be shown that this is the case. An incident 9 MeV neutron excites the ^{227}Ra nucleus to about 13.5 MeV. An evaporated neutron would, on the average, possess a kinetic energy of about 1.5 MeV, leaving the residual nucleus excited to about 7.5 MeV. However, the range of excitation is wide, and, for example, the most probable kinetic energy would be in the order of about 0.75 MeV, which would leave the residual nucleus with 8.25 MeV of excitation energy. This is more or less the height of the fission barrier in

the residual nucleus and thus where we would expect fission to begin to be observed.

Therefore, the region over which the statistical calculation can be used is for excitation energies corresponding to neutron energies between 4.7 and 9.0 MeV. Another reason why the formalism in this calculation cannot be used at higher energies is that we simply do not know the shape of the level density of the residual nucleus at energies much higher than the neutron binding energy, because no experimental data is available.

As might have been anticipated, the free parameters left to vary in our calculation are a_f and K_o^2. The determinations of the parameters can be carried out separately, also very conveniently, because the value of the fission cross section does not depend strongly on K_o^2, as can be inferred from the normalization implied in (II-48). Therefore, we can proceed to fit the cross sections independent of the angular distributions.

It is clear that the variation of a_f with energy must be simulated analytically such that it is a continuous function of energy. For this purpose we make use of expression (II-45). As we have already mentioned, this form has three free parameters, α, β, and γ. The variable α represents the asymptotic value of a_f as the energy becomes very high: γ reflects the sharpness of the variation of a_f with energy; and β reflects the magnitude of the energy dependence

itself. The excitation energy is evaluated from the barrier heights (3.650 and 3.755 MeV), which were estimated from the discrete calculations, for both the symmetric and asymmetric shapes. The parameters extracted from the best fits are listed in Table VII, while the fits themselves are shown in Figure 18. The dependence of a_f on the excitation energy is shown in Figure 19.

Table VII. Statistical Parameters for ^{227}Ra

Mode	α	β	γ	$\hbar\omega$	$\hbar^2/2\mathcal{J}_\perp$
Asym.	28.9	58.0	1.055	0.400	0.002
Symm.	30.0	55.0	0.960	0.400	0.002

The fit to the point at E_n = 4.7 MeV (E^* = 1.5 MeV), may be somewhat artificial, as we have explained, because it is not possible to define a clear-cut transition point between the single particle calculations and the statistical calculations. In order to fit this point, 15 channels are added individually to the calculation between 4.0 and 4.7 MeV in the symmetric case, while ten are used in the asymmetric case.

In the symmetric case, the integration of the statistical expression (II-35) starts at E_n = 4.650, while in the asymmetric case the integral is evaluated beginning at E_n = 4.7 MeV. Fixed parameters used in the calculation are the rotational constant $\hbar^2/2\mathcal{J}_\perp$, assumed to be the same as before ($\sim$2 keV); the curvature parameter $\hbar\omega$, which assumes a

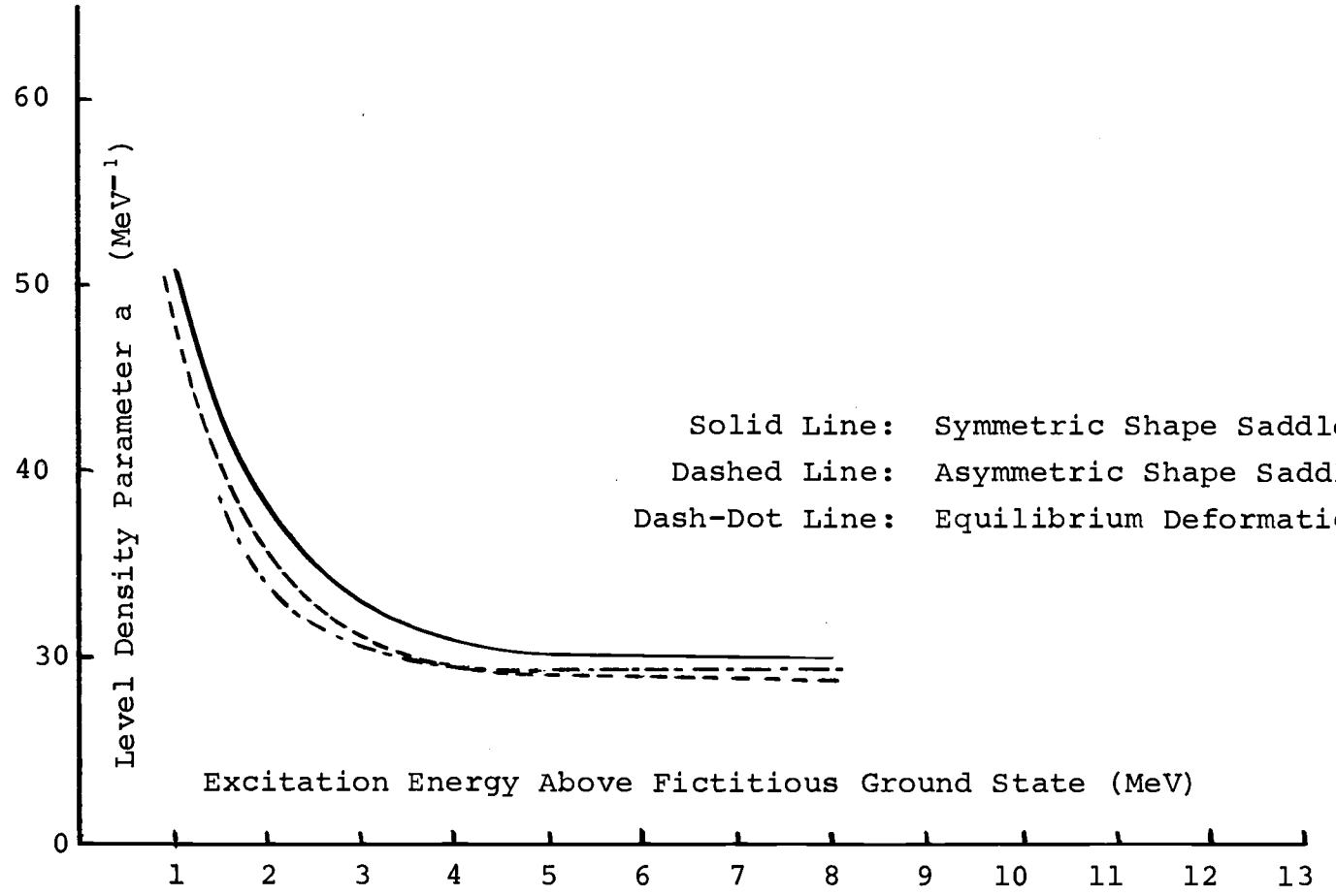

Figure 19. Excitation Energy Dependence of the Level Density Parameters a_f and a_n.

value of 0.400 MeV (Be 68), and the upper integration limit, ε, used in the evaluation of expression (II-35). Although in most calculations done by others (Gi 68) the fission channels are assumed to be completely open, up to the nominal excitation energy, with higher lying channels completely closed, we have not adopted this approximation because it is not physically correct. The nucleus in the transition state at a given excitation energy samples the character of the barriers immediately above that energy because of the nature of the penetrability implied by (II-13). The value of ε was chosen by noting that if, for example, we integrate up to 0.400 MeV above the incident neutron energy, and have used a value of $\hbar\omega$ = 0.400 MeV, then the barrier penetration factor at that point would be:

$$T_f' = \{1+\exp[(2\pi/0.400)(0.400)]\}^{-1} = e^{-2\pi} \sim 0.002$$

which is small enough to cause no appreciable error. Hence, the upper integration limit has been chosen for an excitation energy 0.4 MeV above $(E_n + B_n - B_f)$, where E_n is the neutron kinetic energy, B_n is the neutron binding energy, and B_f is the height of the fission barrier. Since the values for some of these constants have been assumed, we have decided to determine the effect of varying them. We express this effect as the percentage of change in a_f in relation to the original value, needed to reproduce the experimental data when the constants in question have been

varied by a certain specified amount. Thus, when $\hbar\omega$ changes by ±0.200 MeV, a_f varies by about 0.5%. In the same manner, a variation in the rotational constant $\hbar^2/2\mathcal{J}_\perp$ from 2 to 5 keV, requires a decrease in a_f of about 13%. Similarly, a decrease in ε from 0.4 MeV to zero, requires a change in a_f of roughly 1%.

From the fission fragment angular distributions we can infer the values of K_o^2 for every energy. Since, as we mentioned previously, the evaluation of both, a_f and K_o^2 are separable, the best value for K_o^2 is obtained by fitting the fission cross section by varying a_f, and then varying K_o^2 until the smallest χ^2 value is obtained for every angular distribution individually. The error limits in K_o^2 are deduced in a similar manner by finding the values of this parameter corresponding to the points where the fits are no longer considered to be acceptable using a χ^2 criterion. Table VIII lists the best values deduced for K_o^2 in this energy region, together with the upper and lower limits of error. Figures 16b, c, d how best fits to the angular distributions of the fission fragments at the different energies, and Figure 20 is a plot of K_o^2 vs. the kinetic energy of the incident neutron.

Figure 20 shows how K_o^2 oscillates with energy in a manner not expected from the theory developed in the previous section, although the character of the energy dependence is not very precise because of the uncertainty in the values

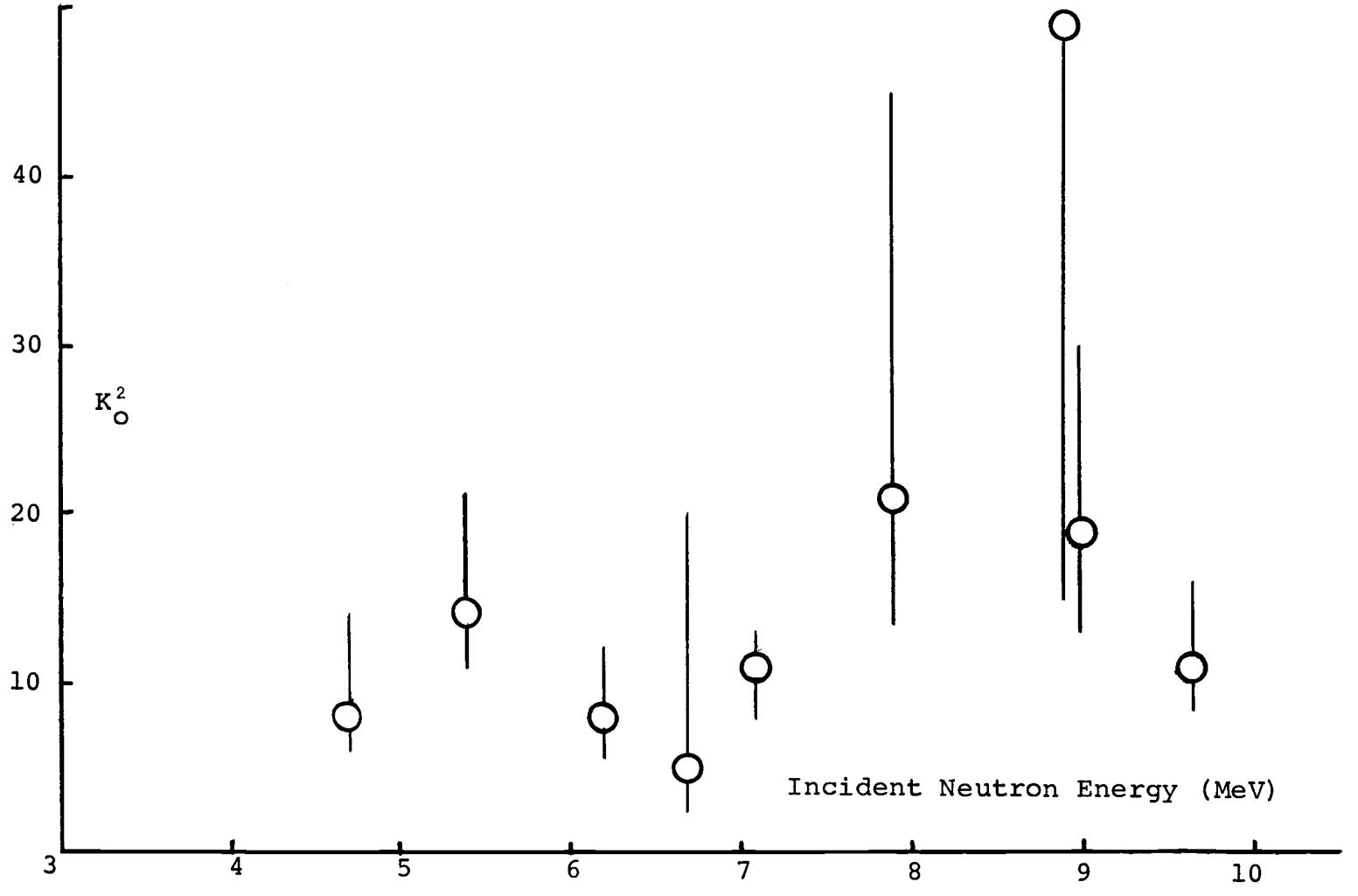

Figure 20. Incident Neutron Energy Dependence of K_o^2.

Table VIII. K_o^2 Values Describing Angular Distribution of Fission Fragments.

E_n	Best	χ^2	Low	χ^2	High	χ^2
4.7	8.0	8.2	6.5	12	14.0	12.8
5.4	14.0	9.0	11.0	13	21.0	12
6.2	8.0	6.6	6.0	13	12.0	12.7
6.7	5.0	3.0	3.0	12	20.0	12
7.1	11.0	9.9	8.0	12	13.0	11.6
7.9	21.0	5.8	13.5	12.5	45.0	12
8.9	50.0	7.7	15.0	9.0	Very High	-
9.0	19.0	6.1	13.0	12	30.0	12.7
9.7	11.0	4.2	8.5	∿12	16.0	∿12

deduced. However, for energies below 7.1 MeV, the value of K_o^2 fluctuates around an average of about 8, and of about 24 for energies between 7.9 and 9.0 MeV. Above this region, at 9.7 MeV, K_o^2 decreases substantially as the contribution from second chance fission becomes more significant.

One final parameter which we have not commented on is the nuclear temperature. The dependence of T on excitation energy follows directly from (II-46). Figure 21 shows the behavior of T(U) vs. U, where U is the excitation energy above the fission barrier. For comparison, we also show the behavior of the temperature when a uniform Fermi gas model is assumed, in which a_f remains constant (at a value of $\sim 30\ MeV^{-1}$), with varying energy. As we can see, the

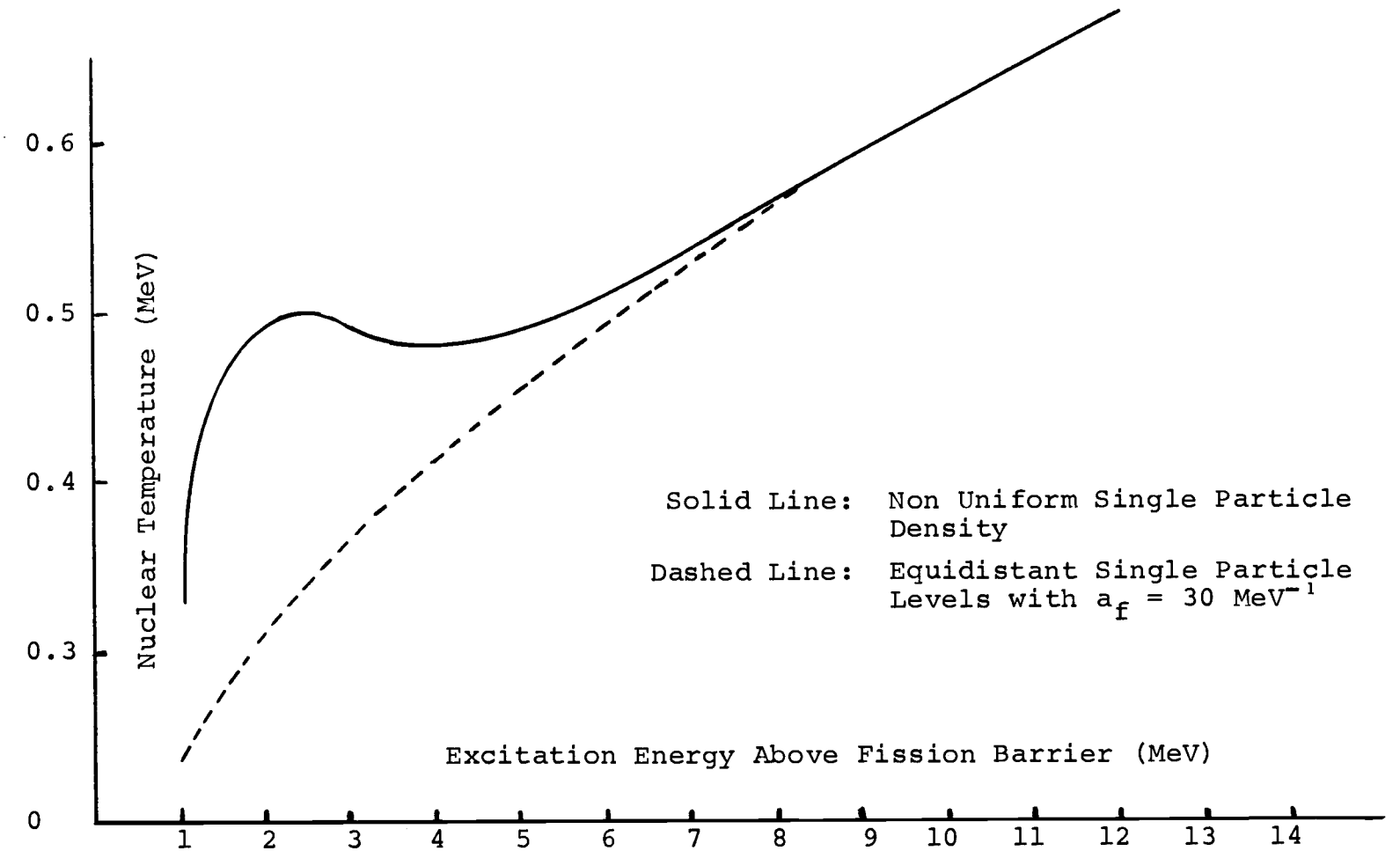

Figure 21. Excitation Energy Dependence of the Temperature using two Different Assumptions Regarding a_f.

non-uniformity of the single particle levels near the Fermi surface seems at first sight to be responsible for the plateau and slight decrease in T. As the energy increases, T approaches the value predicted by the constant a_f model. We shall discuss this problem in more detail in the next chapter.

Before we enter the discussion of the results reported in this chapter, it is important that we point out and clarify some of the terminology that will be used in relation to the excitation energies.

A plot of level densities vs. excitation energy for even-even, odd-A and odd-odd nuclei in the same mass region shows that at a given excitation energy, $\rho_{o-o} > \rho_{o-A} > \rho_{e-e}$. Moreover, the shape of the density functions is very similar in all cases, the difference arising from a shift in the energy axis. This phenomenon is associated with the fact that an even-even nucleus has all its nucleons paired, and its only low lying states are collective in nature. When the excitation energy becomes sufficiently large to break a nuclear pair, the level density begins to exhibit the characteristic exponential increase with energy. An odd-odd nucleus, by contrast, already has two unpaired nucleons and intrinsic states associated with different orbits of the unpaired nucleons can therefore be immediately excited. The effective excitation energy, U, is thus related to the excitation energy measured from the true ground state by:

$$U = E \quad \text{for o-o nuclei}$$

$$U = E - \Delta_{(n \text{ or } p)} \quad \text{for odd-A nuclei}$$

$$U = E - \Delta_n - \Delta_p \quad \text{for e-e nuclei}$$

It is very useful to be able to compare some of the statistical parameters on a common ground of intrinsic excitation. Therefore, in the coming discussion we will refer to the quantity U as the energy "above the unpaired ground state", or the "fictitious excitation energy".

IV. DISCUSSION OF RESULTS

A. Interpretation of Results at Low Excitation Energies

In the discussion of the preceding chapter, we deduced the sets of parameters which describe the ^{227}Ra transition nucleus at the saddle point for two types of deformations. Since the neutron binding energy has a value of 4.5 MeV, this calculation places the fission barrier height at about 8.2 MeV. How do our results compare with those obtained independently by other investigators?

The most recent experimental data regarding fission of ^{227}Ra is that of Konecny and co-workers (Ko 73), whose results are shown in Figure 22 for the reaction ^{226}Ra(d,p) ^{227}Ra $\rightarrow$ f. The "elbow" in the Γ_f/Γ_n curve observed in their experimental data would place the fission barrier at approximately 8.2 MeV of excitation. This estimate agrees substantially well with our own previously stated result.

Theoretical predictions of the single particle levels and the barrier height have come from the calculations done by Drs. Nix and Moller (Ni 73) (who have very kindly made these available to us). The results involve calculations for two deformations, one corresponding to the ground state, and another corresponding to a very deformed, highly asymmetric saddle point shape. The potential energies of deformation were evaluated according to the macroscopic-microscopic method. The macroscopic part was calculated for two

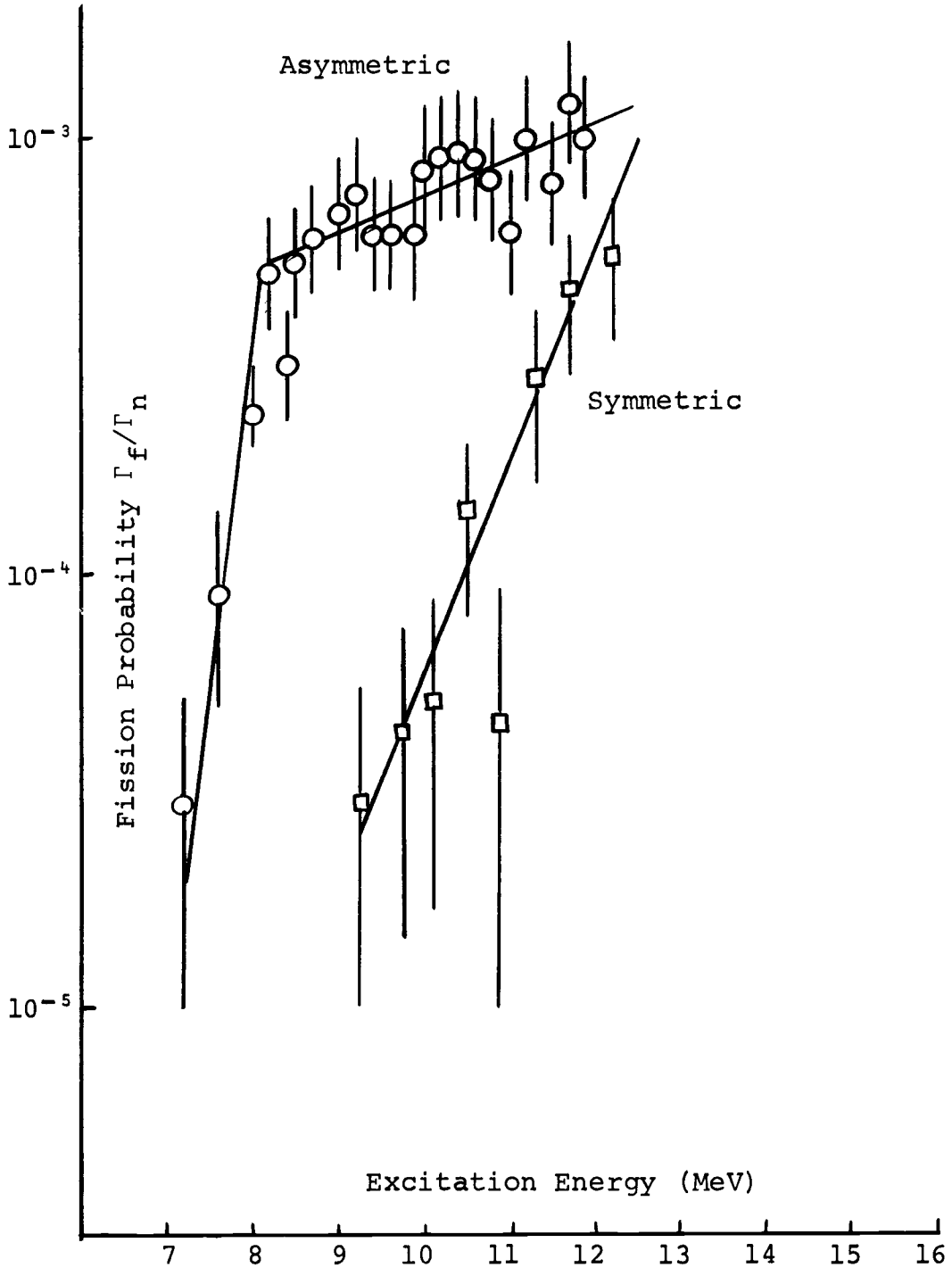

Figure 22. Fission Probabilities vs. Excitation Energy for ^{227}Ra Showing Two Possible Fission Components, from (Ko 73).

orders of approximation. In one case the nuclear energy is evaluated by including the Coulomb and surface energies, expressed in terms of lower order shape dependent quantities; this approximation leads to the liquid drop model (LDM). The inclusion of higher order terms in the expansion leads to the droplet model, which takes into account effects that are associated with the finite size of nuclei, such as nuclear compressibility and curvature corrections.

From the nuclear shape specified by the macroscopic calculation, a potential is generated, and the Schrödinger equation is solved to obtain the single particle energies. From these, the shell and pairing corrections are calculated. They arise because of fluctuations in the actual distribution of levels relative to a smooth distribution. A partial potential energy surface diagram for ^{226}Ra, as calculated by Nix and Moller, is given in Figure 23, and arrows indicate the most probable path to fission. The "s" indicates the probable saddle point. Table IX lists the

Table IX. Macroscopic-Microscopic Calculations for ^{226}Ra*.

	Ground State**	Saddle Point**	Total**
Shell Correction	-2.394	- 3.524	
Pairing Correction	+0.276	+ 0.698	
LDM Energy	+2.637	+13.780	
Droplet Energy	+2.720	+11.550	
Potential Energy (LDM)	+0.518	+10.950	+10.43
Potential Energy (Droplet)	+0.602	+ 8.72	+ 8.12

* Nix and Moller (Ni 73)
** All energies in MeV.

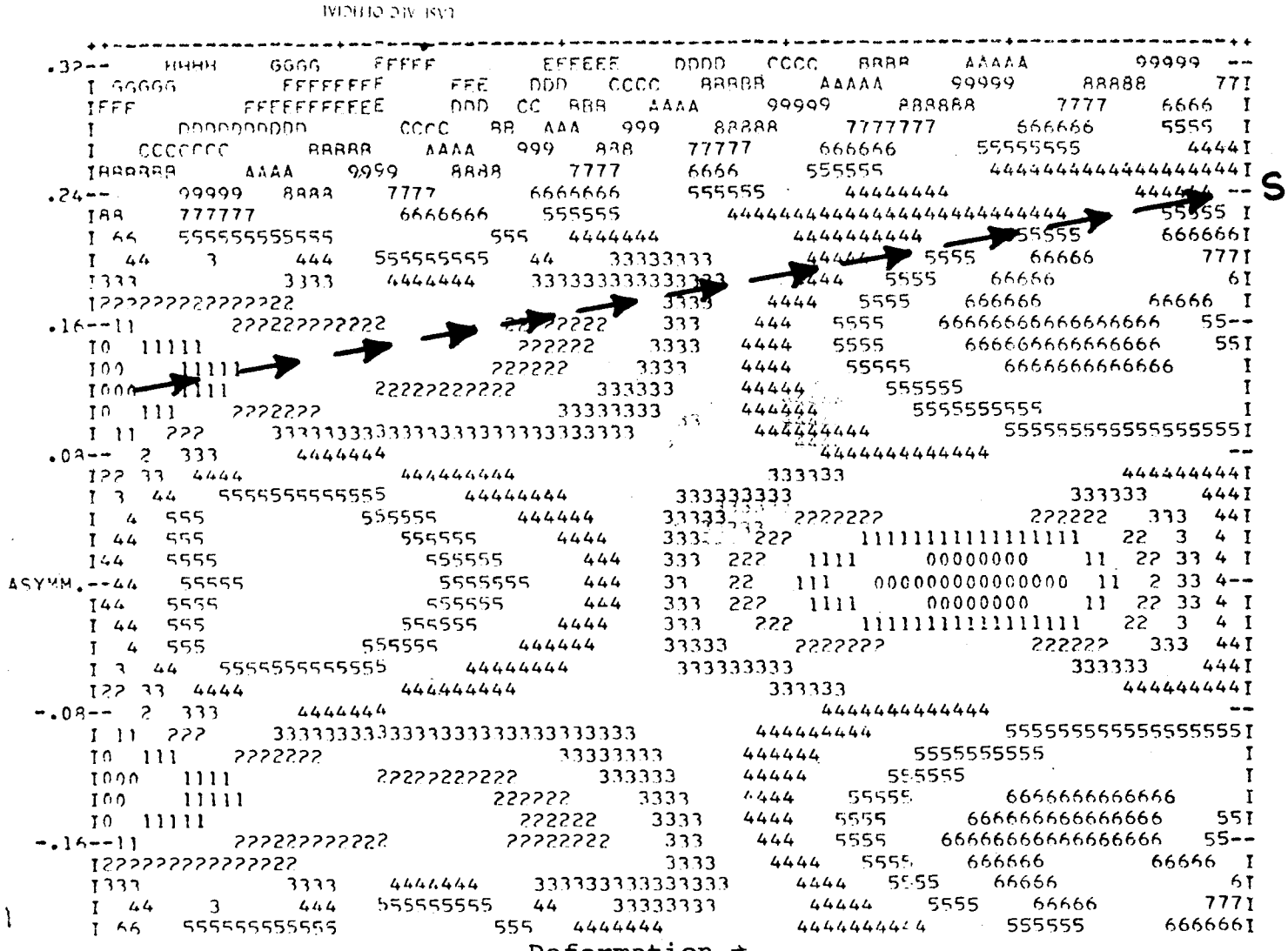

Figure 24. Partial Potential Energy Diagram for ^{226}Ra. Arrows Indicate Probable Path to Fission. Contours Are in Arbitrary Units.

values for the shell and pairing corrections, the liquid drop and droplet energies, and the resulting potential energies at the ground state and saddle point deformations. It is interesting to notice the difference between the barriers calculated by the droplet model and the LDM. The latter is higher by over 2 MeV. Therefore, it seems that the introduction of higher order correction terms into the LDM introduces a significant difference in the results of the calculations at high deformations. The shell corrections for the ground state and fission deformations can be interpreted to mean that the calculations predict a lower than average single particle level density around the Fermi surface at these deformations.

In comparing these results with the ones extracted from the experimental data, we notice that our estimate of the fission barrier height is in very good agreement with the calculations by Nix and Möller, whose barrier estimate is 8.12 MeV in the droplet approximation.

Other fission barrier results are summarized in Table X. Apart from the calculations that we have described, good agreement is also obtained with the estimates of Brack et al. (Br 72) for ^{228}Ra. It is important to note the height of the inner barrier derived in this calculation. It is only calculated to be 2.2 MeV. Also, not listed in Table X, but worth mentioning is the magnitude of the shell correction for ^{228}Ra, which according to Brack et al., is

Table X. Fission Barrier Heights (In MeV) for Various Ra Isotopes.

Nucleus	Source	Inner Barrier	Outer Barrier Symmetric	Outer Barrier Asymmetric	Reference
^{226}Ra	Experimental	-	8.5±0.5		Zhagrov (Zh 71)
^{226}Ra	Theory	4.5	10.0	10.0	Adeev (Ad 72)
^{226}Ra	Theory	4.2	10.5	9.0	Moller (Mo 72)
^{226}Ra	Theory	3.7	10.7	-	Mosel & Schmitt (Mo 71)
^{226}Ra	Theory	-	10.2	10.2	Pauli (Pa 73)
^{227}Ra	Experimental	-	8.2±0.1		This work
^{228}Ra	Theory	2.4	-	8.2	Brack et al. (Br 72)

-0.4 MeV at the ground state. This is to be compared with a shell correction of -2.394 MeV as estimated by Nix and Möller and listed in Table IX. We shall comment more on the subject of the shell corrections in a subsequent section.

If the independent estimates of the fission barrier in ^{227}Ra show such good agreement, it will be interesting to see how well the single particle level calculations carried out by other people compare with those deduced in this work. We might begin by noting that the gradual decrease in the anisotropy with decreasing energy from a maximum at 8.6 MeV of excitation (E_n = 4.1 MeV) observed by Konecny et al., (Ko 73) would qualitatively support the notion that the first channel at the barrier is not a K = 1/2 channel. In both our estimates (symmetric and asymmetric), the lowest lying channel is K = 3/2. Figure 24 shows the neutron single particle levels calculated theoretically for the saddle point deformation by Nix and Möller and also Pashkevich (Ip 72), in comparison with those determined in the present work, which assumes symmetric and asymmetric saddle point deformations. The agreement between the Nix-Möller set of data and ours can be considered remarkably good, and perhaps fortuitous. In the symmetric case, the order of the levels is predicted by the theory, even though the energy differences are not well reproduced. In order to empirically reproduce the level spacings, the level

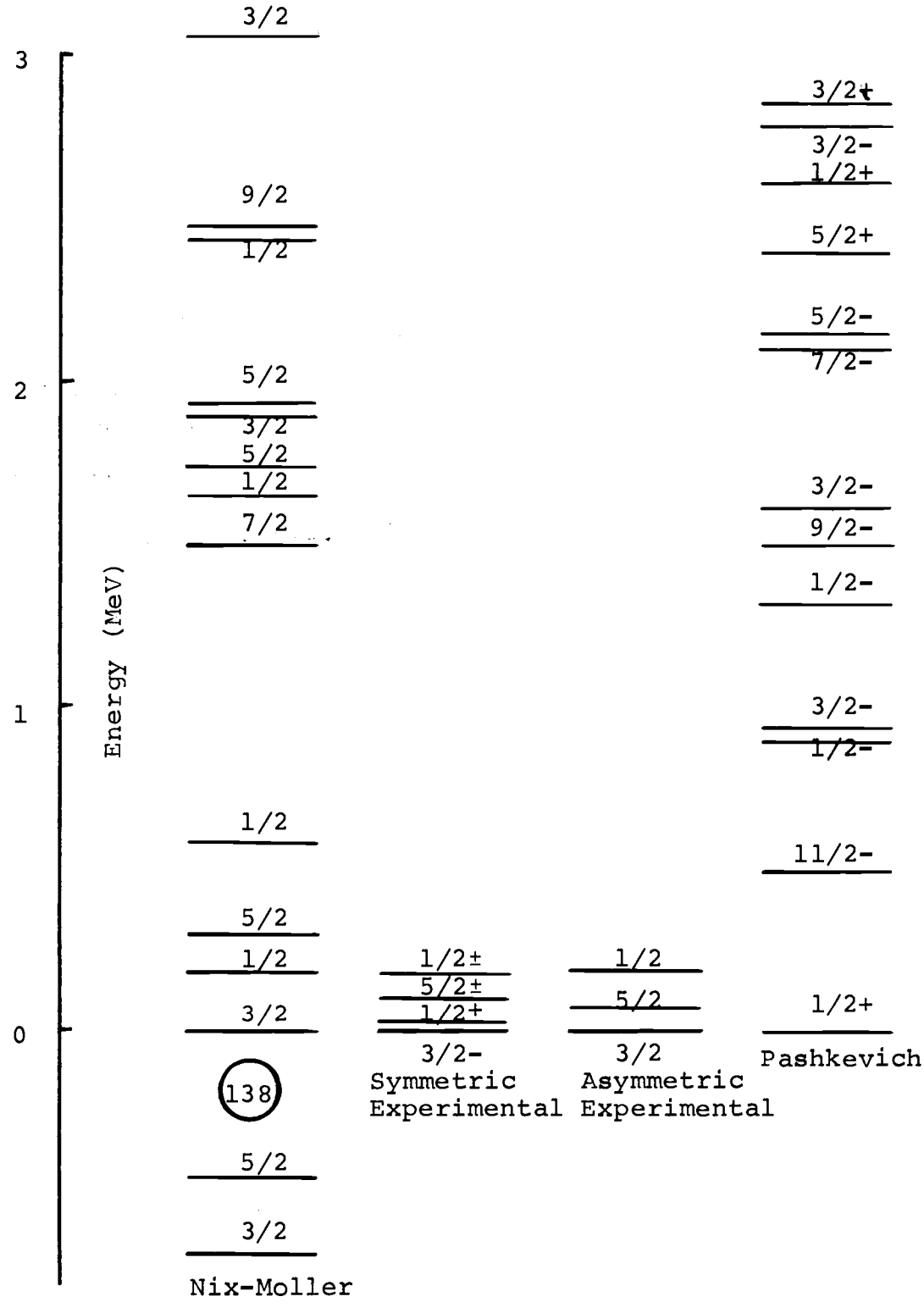

Figure 24. Theoretical and Experimentally Deduced Single Particle Levels for the ^{227}Ra Transition Nucleus.

density of ^{226}Ra would have had to be reduced. This would have caused a rise in the height of the barrier which would have been necessary in order to fit the experimental data. In the asymmetric case, the level spacings are better reproduced by the theory; however, the ordering of the 5/2 and 1/2 levels would have to be reversed. Considering the numerous approximations that have been made in these calculations, we must say that the agreement is quite reasonable.

Very little or no agreement is observed between our set of levels and that resulting from Pashkevich's calculations. Sources of discrepancy between the theoretical and empirically determined single particle levels would involve the accuracy of the deformation at which these levels are calculated in comparison to the one corresponding to the precise saddle point. From looking at Nilsson-type diagrams it is easy to see that a small displacement in deformation can substantially alter the spacings between the levels and even reverse their order if there are nearby crossings.

Now we return to one of the important points in the purpose of this project. In the introductory part of this work it was suggested that even if the problem of the "thorium anomaly" could not be resolved, we could perhaps at least determine whether this disagreement between the theory and experiment persisted in the case of radium. The evidence displayed in this section would indicate that it

does not. The agreement between different theoretical calculations, particularly those of Nix and Möller, and experimental analysis for ^{227}Ra in this work is very good. This observation would lead us to conclude that there is something peculiar in thorium which does not seem to be present in other nearby elements.

B. Interpretation of Results at Moderate Excitation Energies

A great proportion of the results obtained from the calculations outlined in the previous sections are based upon the validity of the assumptions regarding the evaluation of the level density of the ^{226}Ra nucleus at equilibrium deformation. Under these circumstances we might spend some time discussing the parameters that entered in this particular part of the calculation.

The fit to the experimental level density dependence on energy had made use of a back-shifted Fermi-gas model expression with one free parameter, a_n, at energies above 3 MeV. We have pointed out previously that in this fit, a dependence of a_n on excitation energy is obtained as shown in Figure 19. In the derivation of the Fermi-gas level density expression, this parameter is proportional to the density of single particle levels in the nucleus in the following form:

$$a_n = \frac{\pi^2}{6} g_o$$

where g_o represents the single particle density for both neutrons and protons. We have assumed that these particle levels are equidistant and therefore g_o is a constant.

However, from fits to experimental data we know that this is not the case and that in many cases a_n is indeed a function of excitation energy. At low energies the nucleus only samples the levels close to the Fermi surface, and the level density of the nucleus is therefore characterized by the single particle levels in a short energy interval above and below the Fermi surface. However, as the energy increases, the nucleus begins sampling regions far from the surface, with the effect that it now "sees" an average single particle density, in which the local density fluctuations are effectively washed out.

In the case of ^{226}Ra, values of a_n decrease steadily as the excitation energy increases, until asymptotic values are reached. The real location at which the a_n dependence on energy becomes flat is not known because we do not have any more experimental data above this region, and therefore our fit is not reliable at energies a little above the neutron binding energy, or about 7.0 MeV of excitation energy. The main point to be emphasized, is the meaning of this steady decrease with energy.

Under normal circumstances, this energy dependence of the level density could be equated with a high local density of single particle levels at the Fermi surface, in the

order of $40/1.5 \sim 24$ levels/MeV, or about 12 MeV^{-1} for each nucleon type. This is quite high if we look at other systems above and below the radium mass region and see that the a_n dependence is in a sense reversed. In other words, what is observed is that a_n increases with excitation energy; the interpretation of this is based on the argument that at ground state deformations, the Strutinsky shell correction is negative because the local density of levels at the Fermi surface is lower than average. Therefore, unless the interpretation given to the experimental data is wrong, it is clear that we have at hand a system which shows some peculiar properties.

The problem becomes more important when we realize that the behavior of the fissioning system depends directly on the level density of the residual nucleus. For example, the evaluation of Γ_f depends totally on what Γ_n values are used in the calculations and Γ_n is, of course, directly proportional to ρ_n, the level density of the residual nucleus.

Our version of the energy dependence of a_f, the density parameter at the saddle point, is therefore strongly bound to what we may determine regarding a_n, as we have implied previously. The result, as we have already seen, is shown in Figure 19. As in the case of a_n, we observe a monotonic decrease of a_f with energy in both the asymmetric and symmetric calculations. It is interesting to notice

that the symmetric curve does not cross the a_n line at any point, while the asymmetric line crosses it at a point corresponding to about 4.25 MeV of excitation above the unpaired ground state: from there on, $a_f^{asym} < a_n$. We will discuss the meaning associated with this observation a little later.

The derivation of the Fermi-gas expression (II-32) assumes that the overwhelming contribution to the level density is provided by the random coupling between single particle excitations in the nucleus. This assumption could be tested by theoretically calculating the level density dependence on energy and comparing it with the results deduced from the experimental data.

Single particle levels can be used to calculate microscopically the nuclear level density. An important formalism has been established by Decowski et al. (De 68) which properly takes into account the effect of the pairing correlations. Based on this formalism a computer code has been developed by Bolsterli (Bo 73, Br 73) which calculates the density of intrinsic levels as a function of excitation energy. Input parameters in this calculations are the single particle levels and the pairing strengths, which are obtained from the macroscopic-microscopic calculations of Nix and Möller. We have used this computer code for calculating the density of states at the ground state and saddle point deformations in ^{226}Ra. Table XI lists the values of

Table XI. State Density Parameters for ^{226}Ra from Microscopic Calculation

Part A. Equilibrium Deformation				
E (MeV)	$\log_{10}\omega$	Δ_n	Δ_p	T
0.50	-0.605	1.230	0.89	0.353
1.00	-0.080	1.210	0.83	0.388
1.50	0.418	1.190	0.78	0.416
2.00	0.895	1.160	0.73	0.439
2.50	1.354	1.140	0.68	0.460
3.00	1.796	1.120	0.62	0.478
3.50	2.224	1.100	0.56	0.495
4.00	2.641	1.070	0.50	0.510
4.50	3.046	1.050	0.43	0.524
5.00	3.442	1.030	0.34	0.538
5.50	3.840	0.998	0.21	0.552
6.00	4.271	0.968	-	0.567
6.70	4.797	0.924	-	0.586
7.00	5.015	0.895	-	0.598
8.00	5.702	0.811	-	0.628
10.00	6.995	0.615	-	0.680
Part B. Highly Deformed Saddle Point				
E(MeV)	$\log_{10}\omega$	Δ_n	Δ_p	T
0.50	-0.510	1.320	0.54	0.355
1.00	0.010	1.300	0.44	0.390
1.50	0.505	1.280	0.32	0.418
2.00	0.979	1.260	0.15	0.442
2.50	1.486	1.240	-	0.467
3.00	1.911	1.210	-	0.490
3.50	2.318	1.180	-	0.511
4.00	2.715	1.150	-	0.531
4.50	3.099	1.120	-	0.549
5.00	3.472	1.090	-	0.565
5.50	3.835	1.060	-	0.581
6.00	4.191	1.030	-	0.595
6.70	4.676	0.990	-	0.615
7.00	4.879	0.970	-	0.623
8.00	5.542	0.900	-	0.648
10.00	6.801	0.750	-	0.693

the excitation energies, the resulting state density, the pairing gap for both protons and neutrons, and the nuclear temperature. The calculated state density does not include

collective contributions such as rotations and vibrations, and these would have to be included separately. Figure 25 shows a plot of the intrinsic state densities calculated in this fashion, in comparison with those obtained empirically from the experimental data. It is apparent from this graph that the difference in magnitude between the experimental and theoretical level densities is immense.

The recent paper by Bjornholm et al. (Bj 73) may shed some light on the problem. This work discussed the relative enhancements in the total level density of the nucleus based on the degrees of asymmetry associated with certain nuclear shapes. Thus, a spherical nucleus would possess the lowest density of levels because of its high symmetry. For example, they point out that if the spin cutoff parameter σ has a value of five, a nucleus with no rotational symmetry would be expected to have a level density:

$$(8\pi)^{\frac{1}{2}}\sigma^3 \approx 625$$

times higher than its spherical counterpart at comparable excitation energies. In the same manner, the total density of levels of energy E would be enhanced by vibrational contributions to the level density, expressed by the factor:

$$Z_{vib}(T) = (1-e^{-\hbar\omega/T})^{-g} \qquad \text{(IV-1)}$$

where $\hbar\omega$ is the frequency of the vibration, T is the temperature, and g is a degeneracy factor equal to $2\lambda+1$; λ is

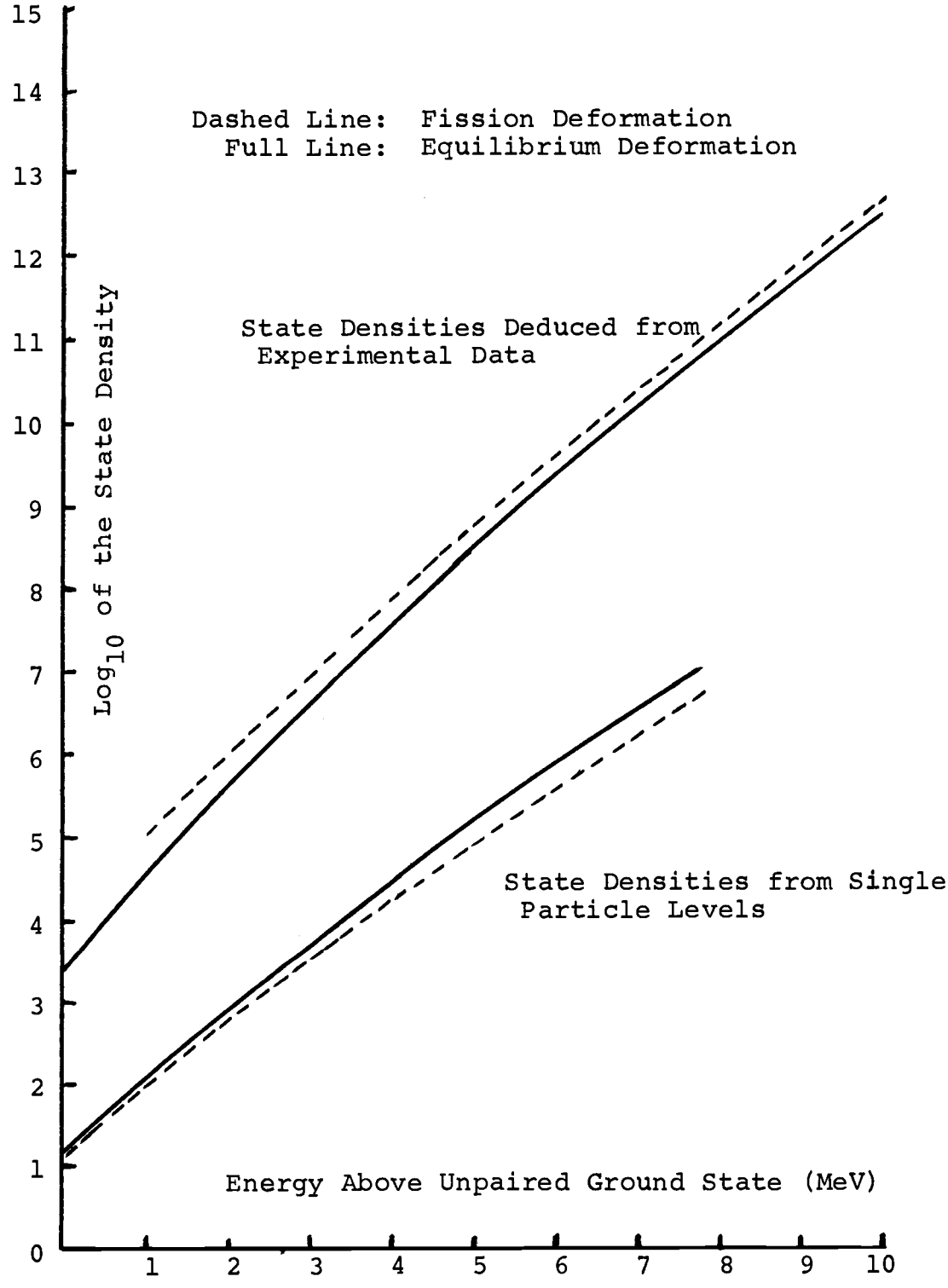

Figure 25. Theoretical and Experimentally Deduced State Density Dependence on Energy.

in the multipole order. It is clear then, that the degree of enhancement provided by the collective degrees of freedom can be very substantial, particularly in cases where values of the vibrational frequency are small, and multipole orders are high, and also in cases where asymmetries are found in the nuclear shape, particularly if the deformations are large. For nuclei in the actinide region the characteristic ground state deformations is prolate. The rotational enhancement provided for such a shape is equivalent to σ^2, which is proportional to the temperature. Although σ^2 can be large, its variation with energy is not expected to be very significant in a relatively short range of energy because the temperature T varies approximately as $T \propto \sqrt{E}$. However, intrinsic excitations increase very rapidly with energy because of the exponential dependence of ρ_{intr} on E. The degree of variation of the vibrational enhancement with energy is not expected to be nearly as large as for the intrinsic excitations, but larger than in the case of rotations, particularly if λ in (IV-1) is relatively high. Therefore, the slope of the $\log_{10}$ of the level density curve is expected to be largely determined by the dependence of the internal excitations on energy with relatively small deviations provided by the other contributions to the level density. The degree to which these deviations are observed should depend, to a great extent, on the mass region to which a certain nucleus belongs. This is clearly indicated

by the characteristic low energy spectra noted in certain areas of the periodic table. These spectra are determined largely by the corresponding nuclear shapes (see for example [Ma 70]).

The "transitional character" of radium in relation to other nuclei can be described in terms of the fact that other nuclei of lower atomic number do not exhibit rotational levels because of their sphericity. In contrast, vibrational states are observed. In the case of radium and thorium, both types of levels are present and the vibrations are low in energy ($\sim$0.25 MeV for the first octupole state in radium). We might say that radium is "soft" to octupole deformations (Jo 61). As we can see, the enhancement of the level densities predicted by (IV-1) can be considerable, particularly if $T >> \hbar\omega$. The same is true of the rotational contribution to the level density, which is in the order of σ^2. Now it is possible to begin answering the question which was posed before, namely why does the Fermi-gas expression (II-32) yield a value for the level density parameter a_n which implies a much larger than expected single particle level density around the Fermi surface? The answer lies in the fact that our method of deducing a_n does not distinguish between single particle levels and collective levels and thus, some of the collective effects may be "absorbed" into the deduced a_n value, thereby causing a rise in the value of a_n. This effect would be expected to be large

at low energies because the proportion of single particle excitations is relatively low in relation to other types of excitations.

To demonstrate this, we could ask ourselves how the different types of excitations exist in proportion to each other as the energy of the nucleus increases. What ratios of collective to quasiparticle excitations are expected at different temperatures? One typical type of motion is the octupole vibration as we mentioned before. In the case of thorium, from which we have borrowed our functional level density, the first octupole vibration is observed at about 500 keV above the ground state. The partition function for this type of motion is given by (IV-1), where g = 7; since $\lambda = 3$. If we assume that the temperature is approximately 400 keV, we find that:

$$Z_{vib} \ (T=0.4) \sim 10$$

If we now assume that the temperature is about 500 keV, or in the order of the vibration quantum energy,

$$Z_{vib} \ (T=0.5) \sim 25$$

Switching for a moment into the BCS formalism, we could compare these two quantities with the partition functions corresponding to quasiparticle excitations evaluated at these same values of the temperature. For $T \geq \Delta/2$, where Δ is the pairing gap parameter, the partition function may be approximated by the following expression (K1 64);

$$\log Z(\beta) \approx 4g_o \Delta \sum_{n=1}^{\infty} (-1)^{n+1} K_1(n\beta\Delta)/n - \log 4 \qquad \text{(IV-2)}$$

where β is the inverse of the temperature, and K_1 is the modified Bessel function of first order. If $g_o\Delta \approx 5$ then it is found that:

$$Z_{intr}(\beta) \sim \begin{cases} 3.9 \text{ for } T = 0.4 \\ \\ 24 \text{ for } T = 0.5 \end{cases}$$

The result is that the ratio of Z_{intr} to Z_{vib} increases by a factor of about 2.6 when the temperature increases by 25%. We have made this rough calculation to show that collective excitations are extremely important, and that their contribution is very large, particularly at low energies. In the mass region $A \sim 230$, octupole vibrations seem to play a significant role; other types of excitation might also contribute, but for purposes of illustration we have only chosen to discuss one mode. So far, that is how the situation regarding the level density appears at the equilibrium deformation. However, we have not yet said anything regarding collective effects at the transition state deformation. The number of levels that are required to fit the fission cross section and angular distributions goes up rapidly as the energy increases. This is a direct consequence of the high number of neutron exit channels which are present in the residual nucleus.

Just as in the previous case of a_n, we observe a general decrease of a_f with increasing excitation energy as shown in Figure 19. The state density at the saddle point deformation, calculated theoretically (Figure 25), follows closely that corresponding to the ground state deformation, crossing the latter at about 5.0 MeV of excitation (in relation to the unpaired ground state). Again, in this calculation we seem to be badly underestimating the collective contributions to the level density. The single particle level densities at the saddle point are too large in relation to what is normally expected. It is possible to develop an argument similar to the one which we expressed before, relating a_n, with some minor variations. In the first place, the nuclear shape is very elongated and the moment of inertia large; secondly, two types of deformations can be discussed, symmetric and asymmetric; whereas before one could only talk about symmetric distortions. Finally, little is known about the vibrational effects.

The elongated shape of the transition nucleus provides for a great enhancement of the rotational contributions to the level density, because the moment of inertia of the transition nucleus is about three times larger than that corresponding to the residual nucleus. If the transition nucleus is reflection-asymmetric, as the theoretical calculations predict, this enhancement increases automatically by a factor of two. This explains why a_f^{asym} is

consistently lower than a_f^{sym}. In calculating the transition state level density, all contributions, collective and intrinsic, were thrown together, and accounted for in one parameter, a_f. When we multiplied the level density by a factor of two in order to include the asymmetry factor, this had the effect of effectively removing one of the collective factors (the one corresponding to x-y asymmetry) from a_f and accounting for it externally and artificially by doubling the total density of levels. Actually this is a step in the right direction because the nature of the level density parameters a_f and a_n requires that only intrinsic contributions be accounted for in their use, while collective effects should appear as multiplicative factors to the internal level density. We will return to this particular point shortly. Similarly, the fact that a_f^{asym} crosses a_n at some point in our empirical level density is not indicative of anything, except the fact that we have accounted externally for the asymmetric degree of freedom predicted for the shape of the transition nucleus.

At this point we do not know anything regarding vibrational effects at the saddle point. Calculations by Nix and Swiatecki (Ni 65) based exclusively on the liquid drop model would indicate that certain modes of vibration with frequencies in the order of 1 MeV are possible at the saddle point. We simply cannot say anything more in this respect.

The variation of a_f and a_n with excitation energy has been interpreted by Vandenbosch and Mosel (Va 72), and Bishop et al. (Bi 72) as a reflection of the close relationship between the sign and magnitude of the shell correction energy and the local single particle level density near the Fermi energy. If the single particle level density is unusually low, the shell correction is negative, and vice versa. However, as the excitation energy increases, single particle levels farther away from the Fermi surface begin playing a role, and shell effects tend to disappear.

From the decreasing trend of a_f and a_n with increasing energy, it might have appeared natural to predict positive shell corrections for both the ground state and saddle point deformations. We have pointed out however, that because of the relatively high contribution of collective states to the level density in both cases, it is hard to say what the real dependence of a_n and a_f on energy is. In the previous section we briefly mentioned that the theoretically calculated values of the shell corrections are negative (see Table IX). If these theoretical results are realistic, it is clear that either one of two things is happening. Either our estimates of a_f and a_n are wrong, in which case our level density calculation is also wrong; or the extent to which collective states are "absorbed" into the a_f or a_n values is fairly substantial. From the very rough calculations involving the two partition functions which were shown in the last section,

we note that there is, in fact, a large probability that the latter argument can be accepted. We might have made substantial errors in determining the level density of ^{232}Th. However, if anything these errors should have gone in the direction of underestimating the number of resonances at the neutron binding energy. The reason for this observation is that, in counting these resonances, there is always a danger of missing some resonances because of resolution problems. Alternatively, the dependence of the level density in the low energy region might have been overestimated, in which case the treatment of the neutron evaporation data would have been in error.

On the other hand, Lynn and Bjornholm (Br 72) have experimentally deduced a positive ground state shell correction for thorium. They find that the values of the ground state shell correction decrease rapidly as a function of Z, such that they are all negative for U, Pu, and Cm. From this trend it would be expected that the ground state shell correction energy would be positive in the case of radium. This observation conflicts sharply with the results from Nix and Möller who predict a large negative shell correction for radium. It is conceivable that the Nix-Möller calculation might have failed to take into account effects of which we are not aware. However, it is hard to forget that such good agreement is found between their results and those deduced in this work regarding the height of the fission

barrier and the single particle levels as discussed in the previous section.

From the above discussion, we conclude that at this point we cannot infer much about the shell correction in radium. All what can be said is that because of the similar dependences of a_f and a_n vs. energy, and because of the occurrence of low energy collective phenomena, at both deformations, the sign of the shell correction is perhaps the same in these two cases. Because of the predominance of collective excitations at low energies over intrinsic excitations, and the subsequent relative increase of the latter with energy, it is worthwhile to point out that the real variation of a_n and a_f (or g_o) with energy is surely less than what is observed in the empirical dependence shown in Figure 19.

The behavior of the nuclear temperature as a function of excitation energy is a direct result of the sharp dependence of the nuclear level density parameters a_f and a_n on energy. In the case of the ground state deformation, there is a rapid increase in T up to about 2 MeV of excitation (Figure 26). Between 2 and 4.5 MeV, the curve levels off into a plateau, and then it begins to climb again at a relatively slow rate. In the case of a_f, there actually seems to be a small dip in the curve (Figure 27). It is hard to say whether it is realistic to expect such an occurrence in the excitation energy dependence of the

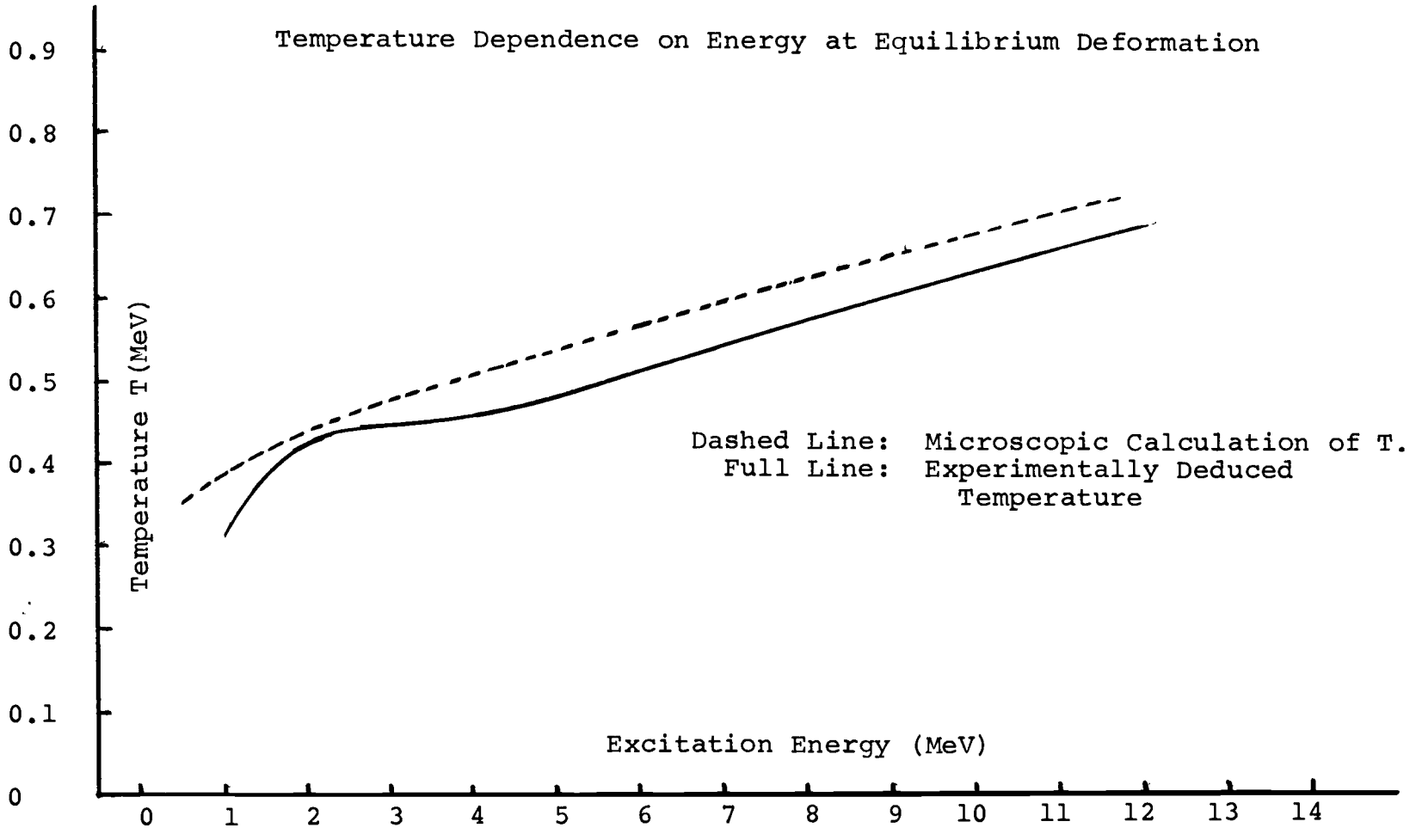

Figure 26. Temperature Dependence on Excitation Energy for ^{226}Ra at Equilibrium Deformation.

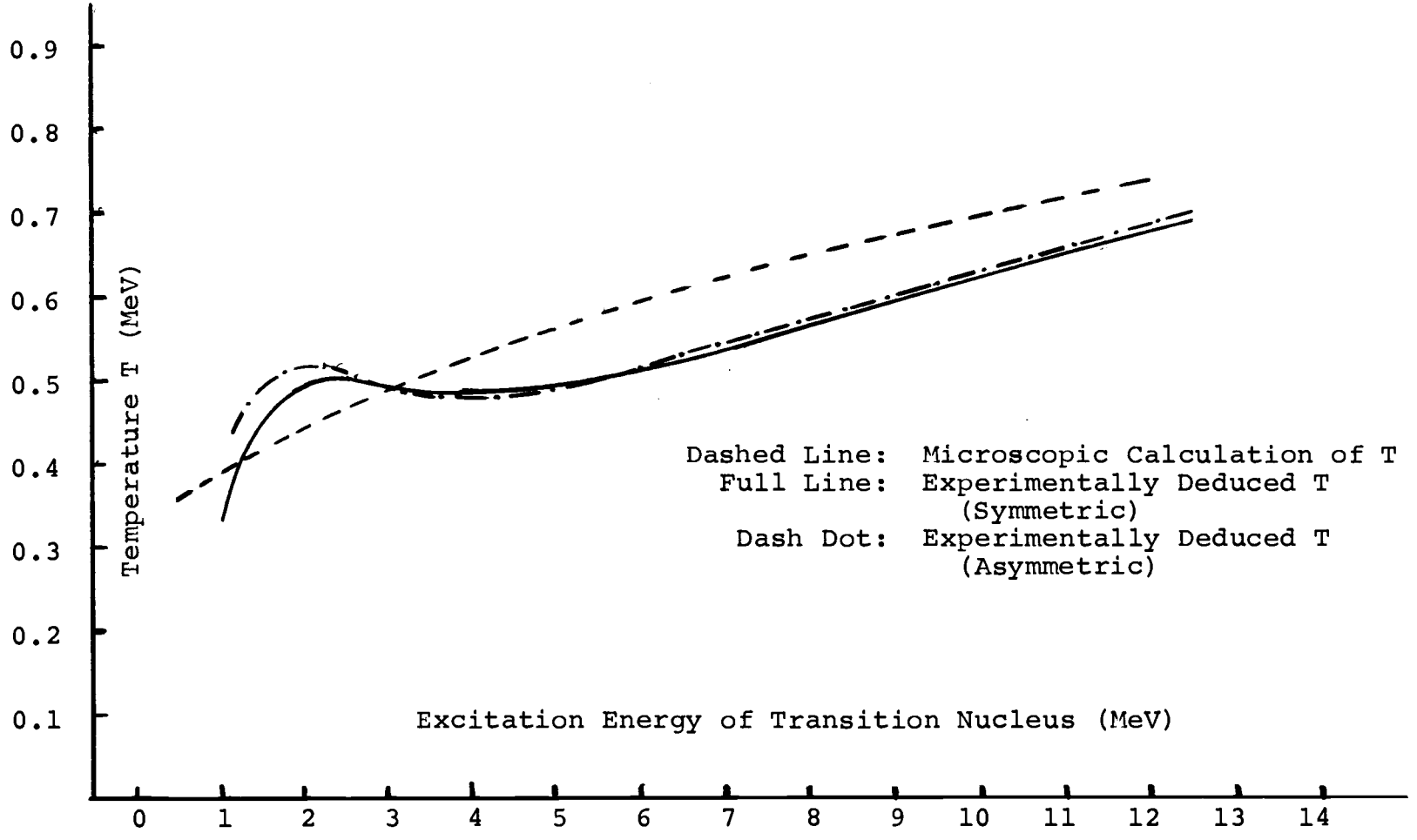

Figure 27. Temperature Dependence on Energy for the Transition Nucleus ^{227}Ra.

temperature. If realistic, it could be interpreted as meaning only that within the small range of energy in which T decreases, there is a very small increment in the rate at which the level density increases with excitation energy. This behavior is not normally expected, and the temperature is usually assumed to follow the smooth dependence:

$$T \propto \sqrt{E} \qquad \text{(IV-3)}$$

Deviations from this dependence can be observed, for example, in the values derived from the experimental data on lighter nuclei by Tsukada and co-workers (Ts 66), who obtained nuclear temperatures by fitting the level density dependence on energy, and then computing the inverse of the nuclear temperature according to the expression;

$$\frac{1}{T} = \frac{\partial \ln \rho(E)}{\partial E} \qquad \text{(IV-4)}$$

where $\rho(E)$ is the level density. Qualitatively, the deduced energy dependences of the temperatures are similar to that which we observe for ^{226}Ra. It is worthwhile to also point out that values of a_n obtained by Tsukada et al. are in some cases strongly dependent on excitation energy. Although the calculations and experimental data which we have mentioned concern lighter masses (Co, Ag, In, Ta, and Au), the results reported serve to illustrate the point that in many cases the expected energy dependence of the temperatures does not follow the simpler relation (IV-3).

Let us now see if it is possible by simple calculations to numerically account for the degree of discrepancy between the experimentally determined and theoretically calculated state densities shown in Figure 25. For this purpose, we make use of the temperature information described previously, and for simplicity, only the ground state deformation is chosen. For two different temperatures, 400 and 500 keV, the excitation energies relative to the unpaired ground state are 1.65 and 5.6 MeV respectively. Vibrational contributions, which are assumed to be mainly octupole, provide us with the partition functions;

$$Z_{vib}^{\lambda=3}\ (1.65\ \text{MeV}) \simeq 10$$

$$Z_{vib}^{\lambda=3}\ (5.6\ \text{MeV}) \approx 25$$

The partition function for rotations can be derived to be $Z_{rot} = 2\sigma^2/S$, where σ is the familiar spin cutoff parameter, and S represents a symmetry factor which is equal to 2 when the nucleus is reflection-symmetric, and 1 when it is reflection-asymmetric. Under these circumstances, the rotational partition functions are:

$$Z_{rot}\ (1.65\ \text{MeV}) \sim 30$$

$$Z_{rot}\ (5.6\ \text{MeV}) \sim 41$$

The degree of collective enhancement over the intrinsic level density is the product of the partition functions

contributing to the entropy of the system. The predicted degrees of enhancement are now compared with the ratios of the experimental state densities to the calculated intrinsic densities shown in Figure 25 at the two energies in question. The results are listed in Table XII.

Table XII. Collective Enhancements in ^{226}Ra.

Energy	$\log_{10}(Z_{vib}\ Z_{rot})$	$\log_{10}(\omega_{exp}/\omega_{intr})$
1.65	2.48	2.65
5.60	3.20	3.40

These results are remarkable in view of the rough approximations used in calculating the collective enhancements from the partition functions. They seem to indicate that in principle the assumptions made regarding the predominance of the low frequency octupole mode over other vibrational modes are not at all unrealistic, and also that the single particle levels of Nix and Möller seem to correctly describe the ^{226}Ra nucleus at its equilibrium deformation.

For some time now we have relied on the experimentally deduced temperatures for conducting the partition function calculations. The evidence seems to indicate that they are fairly reliable. However, we should compare our estimates with those predicted by the theory.

Figures 26 and 27 show plots of temperature vs. energy for the two saddle point assumptions and for the ground state deformation as deduced from the experimental data.

Microscopically calculated temperatures are also shown for both nuclear deformations with no collective correction. It is clear from these figures that the theoretical estimates differ substantially from those obtained empirically. These differences in the separately evaluated temperatures are consistent with the argument that we have employed all along, namely that the general formalism has been neglecting contributions from degrees of freedom other than intrinsic excitations. Generally, the entropy in the exponential factor of the level density is expressed as the sum of several terms;

$$S = \ln Z + \beta E - \mu_n N_n - \mu_p N_p \qquad \text{(IV-16)}$$

where Z is the partition function, β is the inverse of the temperature, μ_p and μ_n are Lagrangian multipliers for the proton and neutron numbers N_p and N_n respectively. From this condition we could for example, establish:

$$-\frac{\partial \ln Z}{\partial \beta} = E_T$$

If all we are concerned with is intrinsic excitations, then the above expression remains as written. However, if other degrees of freedom are present, namely rotational motion and vibrations, the expression converts into:

$$-\frac{\partial \ln Z}{\partial \beta} = \left(\frac{\partial \ln Z_{intr}}{\partial \beta} + \frac{\partial \ln Z_{vib}}{\partial \beta} + \frac{\partial \ln Z_{rot}}{\partial \beta}\right) = \qquad \text{(IV-8)}$$

$$E_{intr} + E_{vib} + E_{rot} = E_T$$

When we include three terms into the partition function, the value of β must increase by some amount in order to conserve the total energy E_T, as opposed to the case where only the intrinsic excitations are included. In other words, the temperature of a system decreases with increasing number of degrees of freedom, when the total energy is conserved. This explains basically the reason why the temperatures calculated in the two manners, theoretically and empirically, differ as shown in Figures 26 and 27.

The entropy in a system is given in terms of the state density as:

$$S = k\ln\omega \qquad \text{(IV-9)}$$

where k is the Boltzmann constant, S is also given by the expression:

$$S = \frac{E}{t} + k\ln Z \qquad \text{(IV-10)}$$

where E is the total energy, and Z the partition function. From these two expressions, the state density becomes:

$$\omega(E) = Ze^{E/T} \qquad \text{(IV-11)}$$

and Z includes the contributions from all degrees of freedom. We have set T = kt for convenience in the above expression. If, for example, T = 0.400 MeV, the E-2Δ = 1.65 MeV, and E = 3.3 MeV. From previous discussions at the given temperature $Z_{intr} \sim 3.9$ and $Z_{vib} \sim 10$. $Z_{rot} = 2\sigma^2$ for a deformed symmetric nucleus and in the order of $Z_{rot} \sim 30$

in this case. Putting together all these quantities it is found that:

$$\omega(T=0.4) \approx (10)(3.9)(30)e^{(3.3/0.4)} = 4.56 \times 10^{6}$$

or $\log_{10}\omega\ (T = 0.400) = 6.66$. The experimentally deduced value is $\log_{10}\omega_{exp}\ (T = 0.400) = 5.25$. Analogously, we could calculate the state density at T = 0.500 MeV, which corresponds to $E - 2\Delta = 5.6$ MeV or E = 7.33 MeV. We found previously that $Z_{vib} \sim 25$, $Z_{intr} \sim 23$, and $Z_{rot} \sim 40$. These values give us an estimate of $\omega(T = 0.500) = 3 \times 10^{10}$ MeV^{-1}, or $\log_{10}\omega\ (T = 0.5) = 10.48$, as opposed to an experimentally deduced value, $\log_{10}\omega_{exp}\ (T = 0.5) = 8.95$). The differences between the calculated and experimental state densities are $10^{1.41}$ for T = 0.400 and $10^{1.53}$ for T = 0.500. This calculation indicates that the slope of the calculated density line remains roughly equal to that of the experimentally deduced one, through an energy interval of about 4 MeV. The constant difference in the state densities obtained by these two methods is in part explained by the fact that in our crude calculations we did not put any constraints regarding the total number of particles, which would have the effect of reducing the total density of states. Perhaps we have carried the statistical mechanical analogy too far, in view of the simplistic arguments involved. Nevertheless, it is important to notice that apart from a normalization factor, the correct dependence of the

density on excitation energy is predicted. This would argue that, in principle, the calculations of the temperature as a function of energy and the partition function arguments regarding the collective contributions to the level density are realistic.

C. Fission Fragment Angular Distributions at High Energies

In the last chapter we parameterized the fission fragment angular distributions for 4.7 MeV $\leq E_n \leq$ 9.0 MeV in terms of the variable K_o^2 which describes the width of the K distribution in the transition nucleus. For sufficiently high energies, the distribution in K is assumed to be Gaussian, as in expression (II-38).

Figure 28 shows the dependence of K_o^2 on excitation energy above the barrier for the transition nucleus ^{227}Ra, obtained by determining the values of K_o^2 which minimize χ^2 when the fission fragment angular distributions in Figures 16b, c, and d are fitted with expressions (II-15 (II-48). For comparison, we also show the values of K_o^2 deduced for the same system by Ippolitov et al. (Ip 72) who used the expression:

$$K_o^2 = (2.1\sqrt{E_n}+1)^2/8(A-1) \qquad \text{(IV-12)}$$

where A is the anisotropy and E_n is the incident neutron energy. It can be noted that good agreement is found between the two methods. The data shows that K_o^2 oscillates

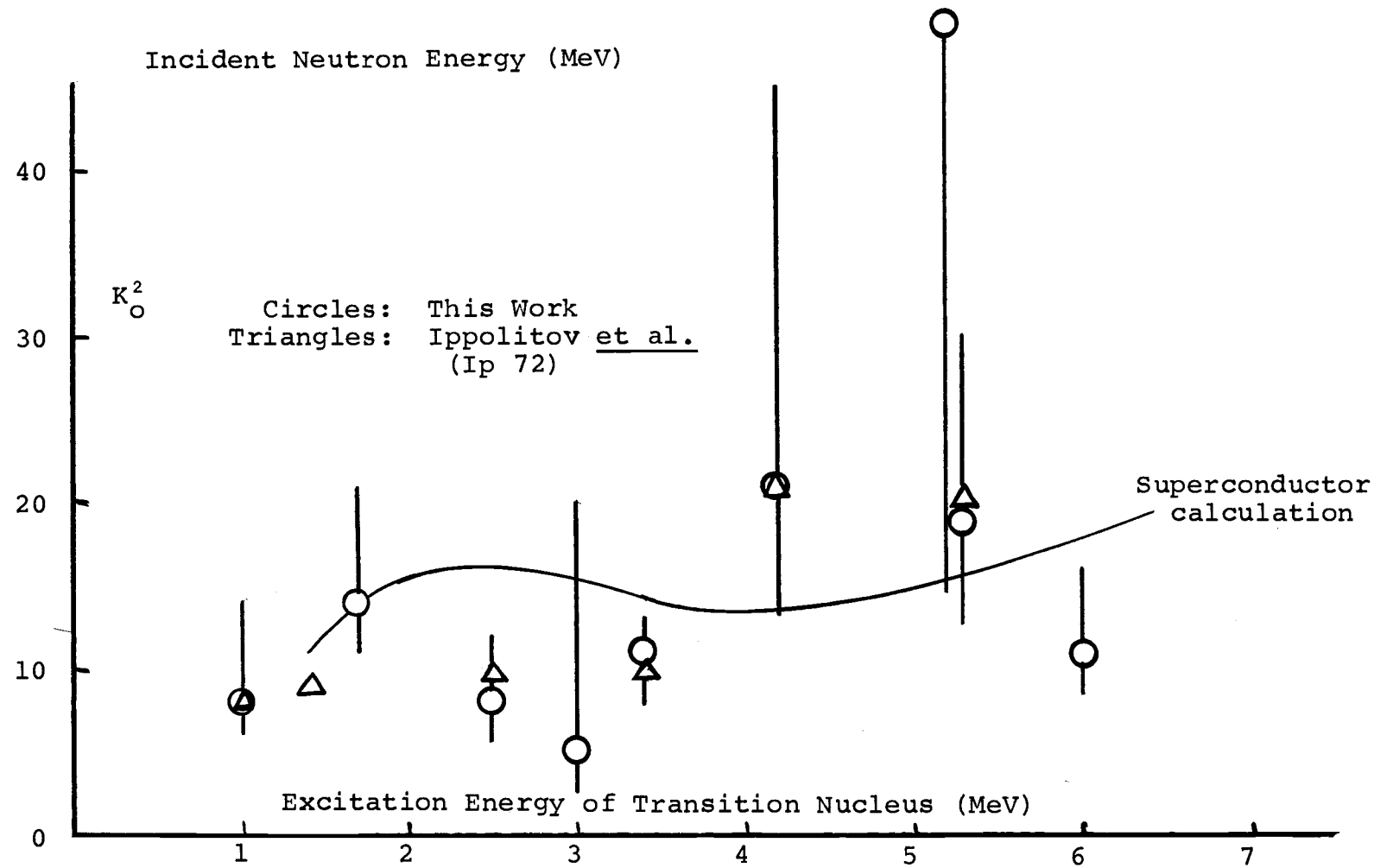

Figure 28. Experimentally Deduced Values of K_o^2.

around a value ∿8 for excitation energies $E_f^* \leq 4$ MeV and then it seems to jump to $K_o^2 \sim 24$ for $4 \leq E_f^* \leq 5.5$. The point at about 6 MeV has a value of $K_o^2 \sim 12$, and it shows strong contributions from second chance fission; therefore, we will disregard it in our discussion.

In terms of the Fermi-gas model, the behavior of K_o^2 as a function of energy is expected to follow the relation:

$$K_o^2 = \frac{\mathcal{J}_{eff}^{RB} T}{\hbar^2} \qquad \text{(IV-13)}$$

where $\mathcal{J}_{eff}^{RB}$ is the effective moment of inertia for a rigid body as defined in (II-37), and T is the nuclear temperature. Since $T \propto \sqrt{E}$, K_o^2 is also supposed to be directly proportional to E. However, at low excitation energies, a significant deviation from the behavior predicted by the Fermi-gas model is observed, and K_o appears generally depressed in relation to the Fermi-gas value (IV-13). This deviation is explained in terms of the BCS superconductivity theory, which takes into account the pairing interactions between nucleons. At excitation energies close to the fission barrier, K_o^2 is generally observed to increase in a step-like manner; as the energy increases the step-like structures smooth out and disappear rapidly and K_o^2 increases more or less linearly with energy until a point is reached at which the behavior of K_o^2 follows that predicted by expression (IV-13). This point of transition is labeled the critical energy, and in the BCS superconductivity theory,

it corresponds to the energy at which the pairing correlations between nucleons disappear and the nucleus behaves as a Fermi-gas. Figure 31 shows qualitatively the expected behavior of K_o^2 as a function of excitation energy for a highly deformed e-e nucleus. For even-even nuclei at low energies, the first observed intrinsic excitation corresponds to energies just above 2Δ, where Δ is the pairing gap parameter. Since the number of excited quasiparticles is low in relation to the number of available levels, the probability that a given level will be doubly occupied will be small, and configurations with the maximum allowed quasiparticle number are predominant. Therefore, in very simplistic terms, a "jump" in the value of K_o^2 should be observed every 2Δ energy interval such that:

$$K_o^2 \ (E^*) \approx 2 \ \bar{\nu} \ \overline{K_p^2}$$

where $\bar{\nu}$ is the average number of pairs of excited quasiparticles and K_p's are simply the quantum numbers characterizing the single particle levels in a deformed nucleus, the average of their squares being taken over an appropriate energy range. The observed steps in K_o^2 are more weakly pronounced than required by expression (IV-13), mainly because of the so-called "blocking effect", which leads to a decrease in Δ for individual excited nucleon states. In other words, the presence of an odd particle in a given level k' prevents pairs from scattering into this level, and the

level is said to be blocked; as the energy increases, more and more individual particles occupy levels above the Fermi surface, thereby increasing the blocking effect and causing a decrease in the pairing correlations. At energies above a few Δ_o the dependence of K_o^2 can be expressed in terms of a smooth function, $A(T/T_c)$, which roughly relates the effective moment of inertia to the moment of inertia of a rigid body, such that:

$$K_o^2 \approx \frac{\mathcal{J}_{eff}^{RB}}{\hbar^2} A(T/T_c) \qquad \text{(IV-14)}$$

The values assumed by $A(T/T_c)$ depend on the ratio of T/T_c where T_c is the nuclear temperature corresponding to the critical energy E_c^*, above which the nucleus behaves as a Fermi-gas. Suffice for the moment to say that for:

$$E^* < E_c^*, \; A(T/T_c) = f(T/T_c)$$

and for

$$E^* \geq E_c^*, \; A(T/T_c) = 1 \qquad \text{(IV-15)}$$

Numerical values for $A(T/T_c)$ as a function of T/T_c have been tabulated by Vonach et al. (Vo 64).

From the above discussion, it is clear that from the dependence of K_o^2 on energy it is possible to deduce some of the parameters that describe the transition state nucleus. In the case of ^{227}Ra we have few experimental points, and their uncertainties are relatively large; however, by tentatively identifying the points at which K_o^2 seems to show

"breaks" in its energy dependence, we might be able to offer an estimate for the pairing gap parameter, Δ_f. For excitation energies 1 MeV < E* < 3 MeV, the average value of K_o^2 is about 8, and it corresponds to the excitation of one quasiparticle. For 3 MeV < $E_n \leq$ 5.5 MeV, K_o^2 increases rapidly to an average value of about 25 which would be more or less the value of K_o^2 required from expression (IV-13) in the presence of three quasiparticles. Therefore, we tentatively place the value of pairing gap at the saddle point at $2\Delta_f \approx 3$ MeV. From single particle levels provided to us by Nix and Moller, $K^2_p \sim 6$. Ipolitov et al. (Ip 72) calculated K^2_p from sets of single particle levels with Nilsson and Pashkevich potentials, and obtained values of $K^2_p = 7.52$ and $K^2_p = 9.05$ respectively. These estimates tend to agree better with the experimental data, although the uncertainties in the latter are large. Ippolitov et al. estimate the pairing gap as $2\Delta_f = 2.7 \pm 0.7$ MeV which substantially agrees with our findings.

A value of the pairing gap in the order of 3 MeV contrasts sharply with values of the same quantity calculated for the equilibrium deformation. The question concerning the dependence of the pairing gap on nuclear deformation has been the subject of controversy for some time. On theoretical grounds, Δ may increase as the nucleus deforms. The calculations by Kennedy et al. (Ke 64) on the slab model of the nucleus show that while infinite nuclear matter

presents very small pairing effects, the slab model calculations predict a finite pairing gap, very sensitive to the slab thickness. However, from the experimental aspect there have been arguments favoring both points of view, and there is no conclusive evidence one way or the other. The classical paper by Griffin (Gr 53) in which the pairing gap at the saddle point is deduced for the compound nucleus ^{240}Pu, yielded a value of $\Delta_f = 1.36$. Subsequently this value was found to be lower. Huizenga et al. (Hu 68) determined $2\Delta_f \simeq 2.2$ MeV for ^{240}Pu, while Britt et al. (Br 68) placed $2\Delta_f \simeq 2.0$ MeV for the same nucleus, and $2\Delta_f \approx 2.10$ for ^{236}U. More recently, Shpak et al. (Sh 71) have found $2\Delta_f = 1.7$ MeV for ^{240}Pu; however, their estimate is based on the expression:

$$E_c^* \approx 0.78\, g\Delta_o^2 \qquad \text{(IV-16)}$$

where g is the single particle level density around the Fermi surface. They estimate this quantity from the Fermi-gas level density parameter $a = (\pi^2/6)g_o$ where they set $a = A/8$. It is clear from previous discussions that g may vary with excitation energy. Also because collective effects have been included in the empirical determination of 'a', the real value of 'g' may be somewhat inflated, which would have the effect of decreasing the value of Δ_f calculated in (IV-16).

Moretto et al. (Mo 69) have deduced the value of the pairing gap in ^{210}Po to be $\Delta_f \approx 1.62$ by identifying the breaks in the K_o^2 spectrum. Itkis et al. (It 73) have deduced $\Delta_f = 0.90$ for the same nucleus. This latter estimate offers the problem that the method used in its deduction relies on a good estimate of a_f which, again, is assumed to be in the order of $a \sim A/8$. Therefore, it seems that at present, the safest way of determining Δ_f is by identifying the breaks in the K_o^2 spectrum and comparing the jumps in K_o^2 with the predicted increases caused by quasiparticle break up. However, it is important to stress the fact that none of the results appear to be conclusive, there is a lot of controversy surrounding this topic and more work needs to be done in relation to the problem.

Finally, for purposes of illustration, we have calculated the predicted dependence of K_o^2 in ^{227}Ra, assuming the nucleus to be a Fermi-gas and also under the assumption of a superconductor (Figure 29). For the case of the latter, the quantity $A(T/T_c)$ in expression (IV-14) has been interpolated from a table given by Vonach et al. The value of the critical temperature T_c is calculated from the relation:

$$T_c = \frac{4}{7} \Theta_o \qquad \text{(IV-17)}$$

where according to Lang,[11] $\Theta_o \sim \Delta$. Therefore, $T_c \approx 0.87$ MeV.

[11] Vonach et al. tentatively set $\Theta_o = 1.3\Delta$ in order to obtain the experimental odd-even mass difference.

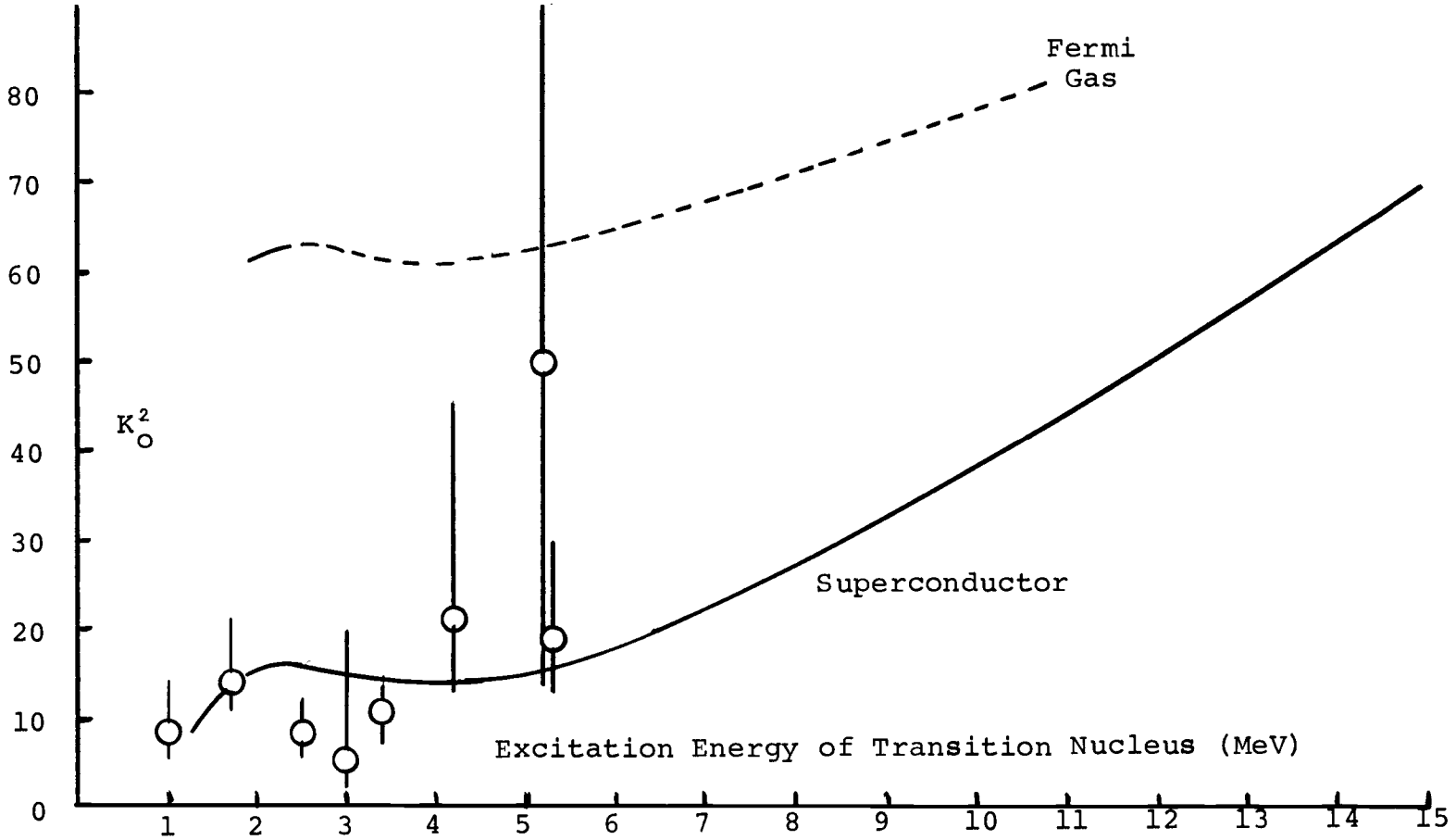

Figure 29. Calculated Values of K_o^2 at High Energies.

D. The Energy Region $3.9 \leq E_n < 4.7$ MeV

The region of the plateau in $\sigma_f(E_n)$ is in essence what we have termed the "twilight zone". The data in this region could not be analyzed discretely because the number of levels required to fit the experimental data would be too large for the analysis to have statistical significance. On the other hand, no statistical approximations are possible because the number of levels is still too small for the analysis to have any meaning. It is difficult to speculate about the significance of the plateau and subsequent step at 4.7 MeV. A step in the cross section could, under normal circumstances, be identified with the same type of pairing phenomena at low energies which we discussed in the previous section. Breaks in the cross section have been predicted by Strutinsky (St 58, 65). Kluge (Kl 64) has also qualitatively predicted jumps in the level density which are caused by the pairing correlations at low energies. Much in the same manner as in K_o^2, these breaks are expected at energies which are multiples of 2Δ. Because of the "blocking effect", the breaks quickly disappear as the energy increases. Under this interpretation, the sudden increase in σ_f would be expected not just above $E_n = 4.7$ MeV, but at about 6.7 MeV, where a second plateau has been reached. It is clear that a great increase in σ_f must occur at energies slightly above 4.7 MeV, but it is hard to speculate about the causes

of such a great increment. Figure 24 shows the single particle level spectrum calculated for the transition nucleus ^{226}Ra by Nix and Möller. As we have pointed out, the level sequence above the 69th neutron level is very similar to the one predicted in this work, and it goes 3/2, 1/2, 5/2, 1/2. However, above this last 1/2 level, there is a gap of about 0.9 MeV, before the next level is encountered, and then there is a sequence of fairly close levels. It may be possible that the region above E_n = 3.9 MeV, where the plateau begins, corresponds to the gap above the K = 1/2 level in Figure 24. While the sudden increase in the cross section corresponds to a region of high channel density at the end of the gap, which creates a great increase in σ_f at that point.

E. Comments on the Mass Distribution in the Fission of ^{227}Ra

The data reported by Konecny et al. (Ko 73) on the reaction ^{226}Ra(d,p) ^{227}Ra $\rightarrow$ f, shown in Figure 22 is interesting in the sense that it would seem at first sight to show that the so-called triple-humped mass distribution in fission is actually caused by fission proceeding through two different saddle points, one symmetric and the other asymmetric. The latter fission barrier height appears to be lower in energy than the former. The range of excitation energies studied is between 7 and about 12 MeV, which would correspond to neutron energies between 2.5 and 7.5 MeV. The

plateau in the fission excitation function which Babenko et al. observe between 4.1 and 4.7 MeV is not present in the (d, pf) data. An increase in the Γ_f/Γ_n function is observed however, and the uncertainties in the data do not permit any assertion as to whether the slight drop in Γ_f/Γ_n at an excitation energy of about 8.2 MeV (corresponding to E_n = 3.8 MeV in the (n,f) experiment) is related in any way to the features reported in the (n,f) cross section data.

The assertion made by Konecny et al. regarding the two different paths leading to scission would seem to be supported by the difference in the anisotropies observed for the symmetric and asymmetric fission components of the cross section extracted in the study of the ^{226}Ra (^{3}He, df) reaction. However, this problem is far from being resolved theoretically. Until recently, no account had been taken of the dynamics of the fission process. When dynamic variables are included into the calculation of spontaneous fission rates, the path to fission may not necessarily be the one where the energy remains lowest. Pauli and Ledergerber (Pa 73) in a very instructive paper argue that the trajectory adopted by the fissioning nucleus is really that of least action which does not necessarily correspond to that of lowest potential energy. In other words, it would seem that the fission process would be controlled not by the thermodynamics but, by the kinetics of the system. If this were to be true, many of the experimentally deduced fission

barrier heights might be in error, but as we pointed out previously, this argument is still a subject of heated debate.

Within the range of energies in which we so far have carried our analysis (3.6 MeV $\leq E_n \leq$ 9.0 MeV), we have not noted any irregular features which could be associated with fission through two different saddle points. However, the data by Konecny et al. indicates that we should not begin seeing these effects except for energies $E_n > 8.0$ MeV. Unfortunately, the energy region corresponding to second chance fission starts at about $E_n \sim 9.0$ MeV, and any effects caused by fission through a saddle point would be mixed with those corresponding to fission after neutron evaporation.

F. Parameters Describing Second Chance Fission

We previously pointed out that the steep rise in the fission cross section at incident neutron energies above 9 MeV is caused by the contribution from fission after neutron evaporation. This was shown in Figure 4. The corresponding angular distributions of fission fragments are displayed in Figure 5.

Before we are able to analyze the behavior of the fissioning nucleus ^{226}Ra, it is necessary to subtract the contribution to fission from ^{227}Ra. The evaluation of this contribution is dependent upon the assumption that since the

total fission cross section can be described by the function:[12]

$$^{227}\sigma_f(E_n) \simeq \sigma_c(\frac{\Gamma_f}{\Gamma_n})^{227} \qquad \text{(IV-18)}$$

then $\sigma_f(E_n)$ should remain relatively constant as a function of energy at moderate and high excitation. The reason for this is that Γ_f/Γ_n is predicted to increase only slowly with excitation energy, while σ_c decreases slowly with increasing incident neutron kinetic energy.

The result is that we can set σ_f for first chance fission as equal to an average over energy of the cross section in the plateau region between neutron energies of 5.4 and 9.0 MeV. This permits us to calculate $(\frac{\Gamma f}{\Gamma n})^{227}$ if we also know the neutron evaporation cross section $\sigma_n(E_n)$. The latter is given by the Hauser-Feshbach calculation as evaluated in (II-15). Within the region in question, $\sigma_n(E_n)$ remains fairly constant at about 2.92 barns. If we assume σ_f to be about 3.1 mb. between E_n = 5.4 and 9.0 MeV, then we can give an approximate value for $(\Gamma_f/\Gamma_n)^{227}$:

$$(\frac{\Gamma_f}{\Gamma_n})^{227} \approx \frac{\sigma_f}{\sigma_n} = \frac{3.1\text{x}10^{-3}}{2.92} = 1.061 \text{ x } 10^{-3}$$

Assuming $\Gamma_n >> \Gamma_f + \Gamma_\gamma$, the expression for $(\Gamma_f/\Gamma_n)^{226}$ becomes for, first and second chance fission:

---

[12] 226 and 227 written as superscripts mean reference to the corresponding Ra isotopes.

$$\left(\frac{\Gamma_f}{\Gamma_n}\right)^{226} \approx \frac{^{226,227}\sigma_f}{\sigma_c} - \left(\frac{\Gamma_f}{\Gamma_n}\right)^{227} \qquad \text{(IV-19)}$$

Table XIII lists the calculated values of $(\Gamma_f/\Gamma_n)^{226}$ and for $^{226}\sigma_f$ for the different incident neutron kinetic energies.

Table XIII. First and Second Chance Fission Cross Sections

E_n (MeV)	$(\Gamma_f/\Gamma_n)^{226}$	$^{226}\sigma_f$(mb)	$^{227}\sigma_f$(mb)
9.7	0.365×10^{-3}	0.985	2.865
11.6	1.994×10^{-3}	5.220	2.780
12.5	2.789×10^{-3}	7.250	2.750
13.6	3.299×10^{-3}	8.310	2.690
14.4	3.739×10^{-3}	9.350	2.650
14.8	5.339×10^{-3}	13.350	2.650

Similarly, the angular distributions of fission fragments corresponding to the fissioning nucleus ^{226}Ra are obtained by subtracting the predicted ^{227}Ra distributions from those observed experimentally from the combined system ^{226,227}Ra. In order to determine the first chance fission angular distributions at high excitation energies, it is necessary to know the dependence of K_o^2 with energy. This can be done because K_o^2 is directly related to the inverse of the anisotropy $\sigma(0°)/\sigma(90°)$ by the following approximation (Ip 72):

$$\sigma(0°)/\sigma(90°) \cong 1 + \frac{(2.1\sqrt{E_n}+1)^2}{8K_o^2} \qquad \text{(IV-20)}$$

The shape of the angular distribution can be obtained with sufficient accuracy if we assume that three points in $\sigma(\Theta)/\sigma(90)$ are known, namely those at 0°, 45°, and 90°. The one at 0° is the anisotropy calculated from (IV-20). The point at 90° is unity, by definition. The point at 45° can be assumed to be half way between $\sigma(0°)/\sigma(90°)$ and 1. We can easily prove this assumption by evaluating the anisotropies at the three angles from a second degree polynomial fit. First let us assume that the distribution can be simulated by a function:

$$\begin{aligned} \sigma(\Theta) &= a_o + a_2 P_2 (\cos \Theta) \\ &= a_o + (a_2/4)(3 \cos \Theta + 1) \end{aligned} \qquad \text{(IV-21)}$$

where a_o and a_2 are constants. From the above expression we find that:

$$\sigma(0°) = a_o + a_2$$

$$\sigma(90°) = a_o - \tfrac{1}{2}a_2$$

$$\sigma(45°) = a_o + a_2/4$$

The latter is equal to the average between $\sigma(0°)$ and $\sigma(90°)$. A basic assumption is, of course that the angular distribution of the fission fragments peaks only at 0°, and decreases smoothly towards 90°.

The three points are then fitted with a function of the form (IV-21) in which a_o and a_2 are free parameters to be obtained. Once these two are known, the distributions over

all angles can be simulated, and by using the methods of Appendix II we normalize all of those to the corresponding fission cross sections shown in Figure 4 for ^{227}Ra. The next and final step is to subtract point by point the calculated $^{227}\sigma(\Theta)$ from the experimental $^{226,227}\sigma_f(\Theta)$.

In the actual calculation we have made use of only the data obtained from the symmetric saddle point shape assumption. This decision was made for the sake of simplicity since the outcome of the calculation is not affected seriously, and because nothing new would be learned by carrying out both approaches to greater lengths. The uncertainties in some of the parameters, such as Δ_f and T_c, would not, in any case, permit great accuracy in the final results.

Table XIV lists the values of K_o^2 which are obtained by applying the formalism developed in the first section. The

Table XIV. Parameters for ^{226}Ra(n,f) at Moderate Energies.

E_n(MeV)	U(MeV)	K_o^2	$\sigma(0)/\sigma(90)$	a_o	a_2	Correction Factor
9.7	6.0	18.1	1.393	1.131	0.262	1.267
11.6	7.9	25.7	1.323	1.108	0.215	1.155
12.5	8.8	30.6	1.290	1.097	0.193	1.254
13.6	9.9	36.9	1.259	1.086	0.173	1.238
14.4	10.7	41.6	1.242	1.081	0.161	1.226
14.8	11.1	44.0	1.235	1.078	0.157	1.229

critical temperature is assumed to be in the order of 0.87 MeV as was estimated in the previous section, and this yields a critical energy of about 22 MeV. The dependence of K_o^2 on excitation energy is shown in Figure 29.

Table XIV lists the values of the anisotropies as calculated from expression (IV-20), together with those of the constants a_o and a_2 obtained from fits to the angular distributions, for different neutron energies. Correction factors as defined in Appendix II are also tabulated.

Table XV lists the differential cross sections as a function of angle (θ), for:

a) The unresolved ^{226,227}Ra fissioning data

b) The estimated ^{227}Ra distributions, and

c) The deduced ^{226}Ra values.

This last set of data is shown graphically in Figures 30a and b. We have fitted these ^{226}Ra(n,n'f) angular distributions with a Legendre polynomial function of sixth order, in the same manner as described previously, see Appendix II. The fits corresponding to 11.6, 12.5, 14.4, and 14.8 MeV are remarkable in the sense that they peak at side angles. Assuming the fission barrier in ^{226}Ra to be about the same as in ^{227}Ra, i.e., about 8.2 MeV, and also that evaporated neutrons have a mean energy of 1.5 MeV, the corresponding excitation energies are 0.9, 2.8, 4.7, and 5.1 MeV above the fission barrier. Such effects are not

Table XV. Deduced Angular Distribution for the Two Fissioning Systems ^{226}Ra and ^{227}Ra

	E_n = 9.7 MeV			E_n = 11.6 MeV			E_n = 12.5 MeV		
Angle	$\sigma(\Theta)_{TOT}$	$\sigma(\Theta)^{227}$	$\sigma(\Theta)^{226}$	$\sigma(\Theta)_{TOT}$	$\sigma(\Theta)^{227}$	$\sigma(\Theta)^{226}$	$\sigma(\Theta)_{TOT}$	$\sigma(\Theta)^{227}$	$\sigma(\Theta)^{226}$
0°	2.794	1.765	1.029						
10°	2.600	1.750	0.850	4.040	1.648	2.392	5.612	1.607	4.005
20°	2.521	1.707	0.814	4.278	1.613	2.665	6.886	1.575	5.311
35°	2.057	1.601	0.456	4.516	1.527	2.989	5.888	1.498	4.390
45°	2.109	1.517	0.592	4.000	1.458	2.543	6.070	1.436	4.634
60°	1.847	1.430	0.417	3.906	1.356	2.550	4.703	1.345	3.358
75°	1.613	1.300	0.313	3.720	1.282	2.438	3.946	1.319	2.627
90°	1.746	1.267	0.479	4.040	1.255	2.785	4.248	1.254	2.994

Table XV. continued

	E_n = 13.6 MeV			E_n = 14.4 MeV			E_n = 14.8 MeV		
Angle	$\sigma(\theta)_{TOT}$	$\sigma(\theta)^{227}$	$\sigma(\theta)^{226}$	$\sigma(\theta)_{TOT}$	$\sigma(\theta)^{227}$	$\sigma(\theta)^{226}$	$\sigma(\theta)_{TOT}$	$\sigma(\theta)^{227}$	$\sigma(\theta)^{226}$
10°	6.525	1.549	4.977	8.475	1.514	6.961	10.000	1.509	8.491
15°	6.525	1.537	4.988	6.839	1.503	5.336	9.534	1.498	8.036
20°	6.828	1.521	5.307	7.308	1.488	5.820	8.250	1.484	6.766
30°	6.525	1.478	5.047	5.845	1.448	4.357	7.976	1.446	6.530
40°	6.629	1.426	5.203	5.492	1.400	4.092	8.414	1.398	7.016
45°	5.274	1.398	3.876	6.082	1.374	4.708	8.110	1.373	6.737
55°	6.227	1.343	4.884	7.134	1.324	5.810	8.651	1.324	7.327
65°	4.772	1.295	3.475	7.013	1.279	5.734	8.451	1.281	7.170
75°	5.423	1.259	4.164	4.677	1.246	3.431	7.976	1.248	6.728
85°	4.519	1.248	3.270	4.682	1.235	3.447	6.625	1.238	5.387
90°	4.519	1.238	3.281	5.261	1.226	3.995	6.084	1.229	4.855

expected in these regions of excitation, where the angular distributions are expected to be forward peaked.

In order to investigate some of these effects we have attempted to calculate the relative strengths of K bands that are necessary to cause the observed irregularities. The J distribution is assumed to be the same as that of the initial compound nucleus ^{227}Ra, and the values of M, the projection of J over the neutron beam direction, are assumed to range from -1 to +1.

Under the above assumptions, we may write the differential cross section contributed by a given value of K for a certain energy in the following manner:

$$\sigma_K(\Theta) = {}^{226}\sigma_f f_K \sum_{J=0}^{J_{max}} (2J+1) T_J(E_n) \sum_{M=-1}^{+1} \varepsilon_K W^J_{K,M}(\Theta) \quad \text{(IV-22)}$$

where the f_K's are weighting coefficients corresponding to different values of K; ε_K takes a value of 2 for all values of K, except for K = 0, where it is unity. This accounts for the fact that K can normally be either positive or negative, except when K equals zero. The $T_J(E_n)$'s are transmission coefficients for the formation of the compound nucleus with neutrons of kinetic energy E_n, and values of the angular momentum J.

The actual calculation is carried out by separately evaluating the normalized angular distribution functions $W^J_{K,M}(\Theta)$, and summing them individually for $0 \leq K \leq 5$, and

weighting each J = ℓ wave correspondingly. The f_K parameters are left to vary independently, and the angular distributions are fitted using a non-linear least squares code. The results of these calculations are given in Table XVI for the different values of K, while the angular distribution

Table XVI. Partial K Fission Cross Sections for the ^{226}Ra (n,n'f) Reaction*

	Incident Neutron Energy (MeV)					
K	9.7	11.6	12.5	13.6	14.4	14.8
0	0.493	∿0	1.789	1.322	2.282	3.712
1	0.129	1.069	0.510	2.067	1.701	1.970
2	0.140	1.112	2.779	2.047	0.824	∿0
3	∿0	1.045	1.186	2.530	0.489	3.027
4	0.223	0.128	0.986	∿0	∿0	0.111
5	∿0	1.866	∿0	0.343	4.053	4.526

* in mb.

fits are shown in Figures 30a and b. As we can see, these results are very puzzling because of the zig-zagging in the cross section function.

The distribution corresponding to E_n = 9.7 MeV seems to peak at forward angles. The dominant channel excited corresponds to K = 0, and the distribution looks quite normal. However, as we go up in energy, side peaking is observed in the angular distribution data corresponding to 11.6 and 12.5 MeV. This is very unusual at these excitation energies (∿1.9 and ∿2.8 MeV above the fission barrier of ^{226}Ra),

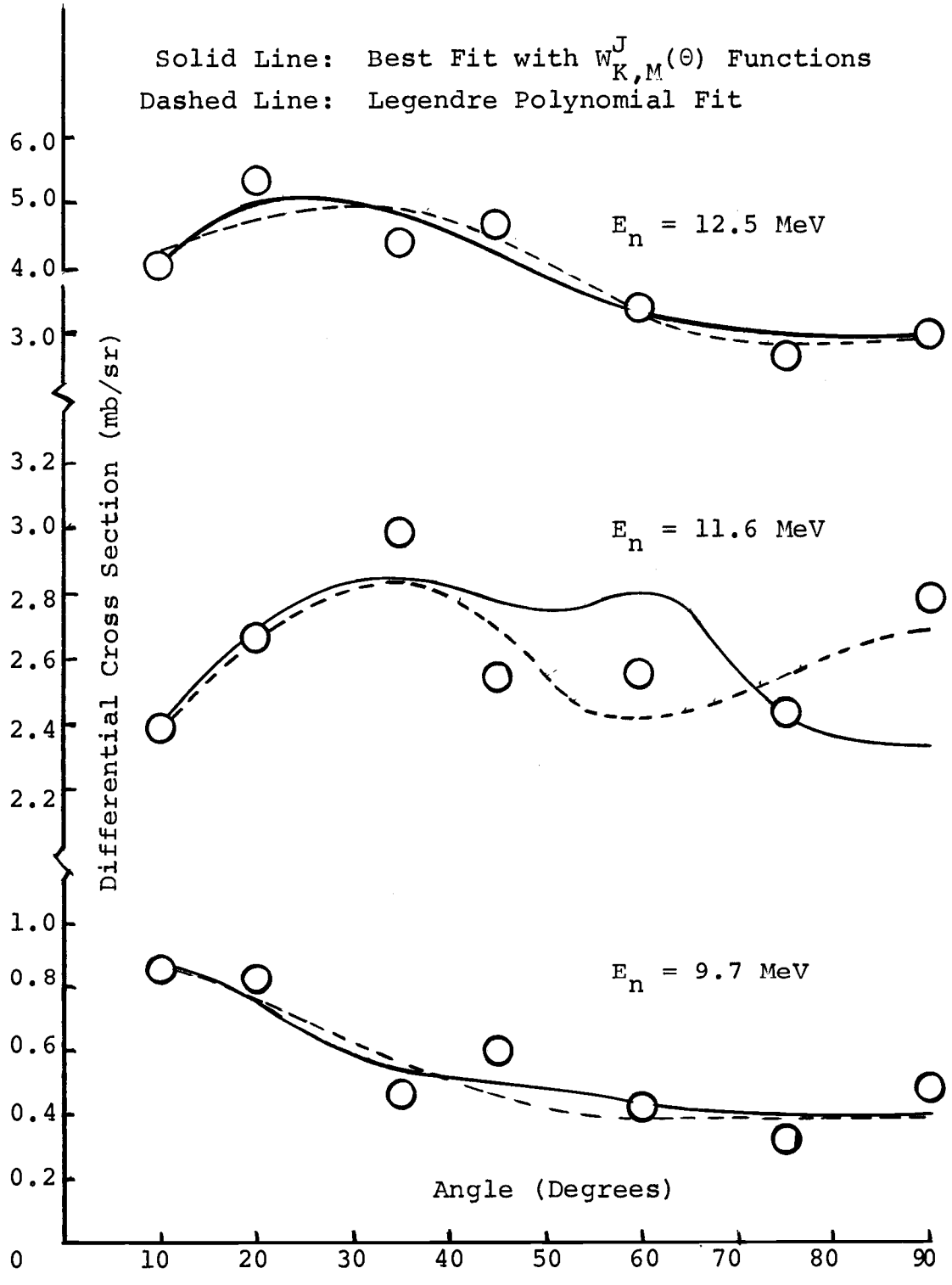

Figure 30a. Fits to the Angular Distribution Corresponding to Second Chance Fission.

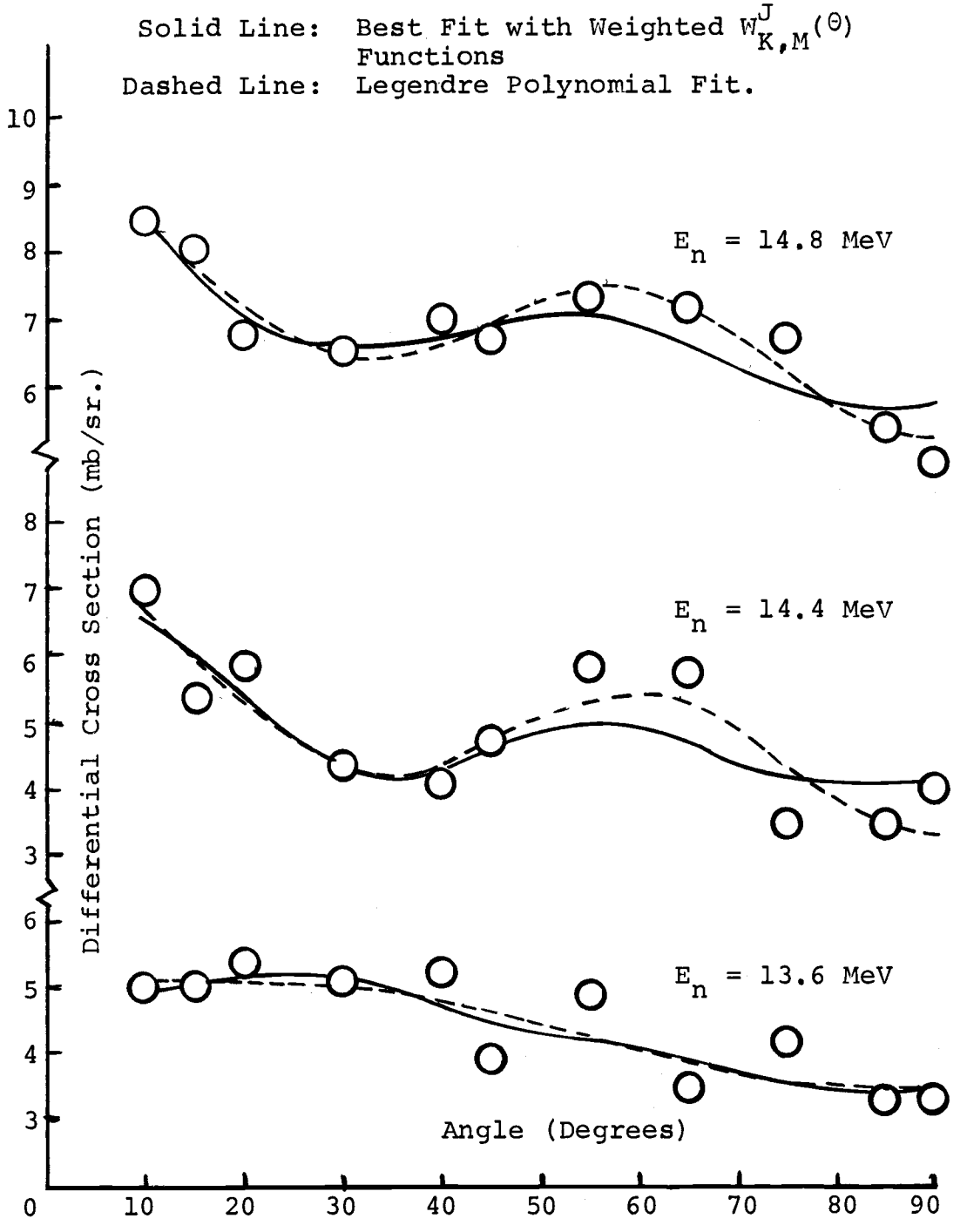

Figure 30b. Fits to the Angular Distributions Corresponding to Second Chance Fission.

where forward peaking would be expected if a Gaussian distribution in K is assumed. However, the percentage of K = 0 is very small at E_n = 11.6 MeV, in comparison with the contributions from all other bands, especially in relation to K = 5. At E_n = 12.5 MeV, K = 2 seems to predominate but, K = 0 again becomes significant. K = 3 strength increases to dominate at E_n = 13.6 MeV, but, K = 1 and K = 2 bands are important. The angular distributions at both 14.4 and 14.8 MeV are fairly similar in shape, showing peaking at 0 and at about 60 degrees. This requirement can only be met if large percentages of K = 0 and K = 5 are mixed. Strangely indeed, it seems that in three out of the six angular distributions analyzed, K = 5 bands predominate relative to others. These strange distributions at 14.4 and 14.8 MeV coincide with a relatively sharp increase in the cross section at a place where the cross section would be expected to level off. Clearly, this increase is not caused by third chance fission, since the energy available would require too small a fission barrier height (about 6.5 MeV).

In any case, the important point to notice is the strong predominance of certain $K \neq 0$ bands at some of these energies. Angular distributions in neutron induced fission of ^{232}Th at comparable energies ($12.18 \leq E_n \leq 18.26$ MeV) do not seem to show the anomalies observed in the case of radium (Em 73).

It is necessary to emphasize the fact that these calculations are by no means accurate. All we have pretended to do is to find out in a rough way what kinds of K strengths are necessary to assume in order to reproduce the unusual angular distributions which are observed in the fission of ^{226}Ra.

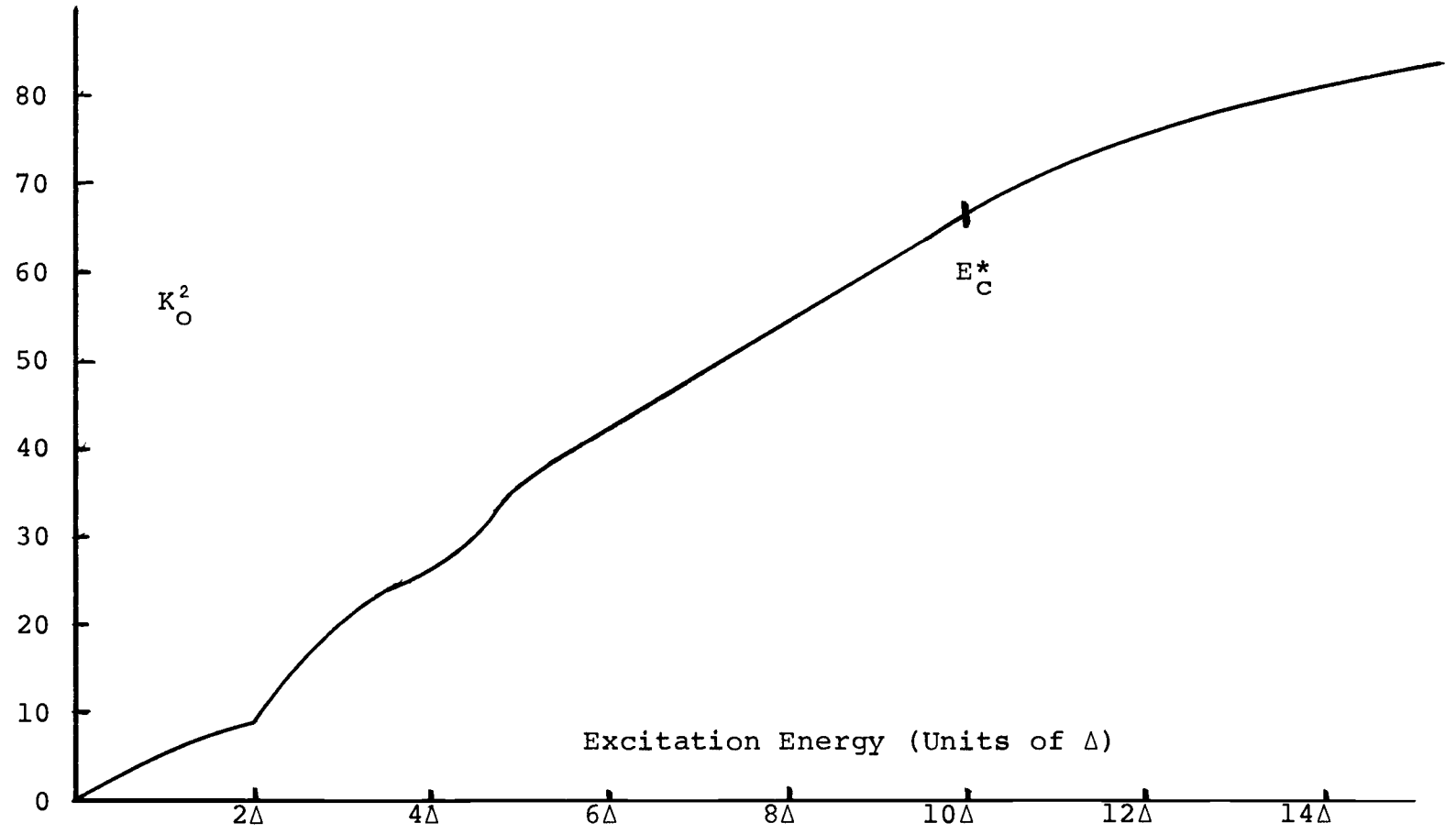

Figure 31. Schematic Dependence of K_o^2 as a Function of Energy.

V. CONCLUSIONS

The information obtained from the analysis of the experimental data can be summarized in a few paragraphs.

1. Our deduced height of the fission barrier stands in very good agreement with the estimates by Brack et al., and those of Nix and Möller. The ordering and nature of the single particle levels above the barrier are in near perfect agreement with those of Nix and Möller, although discrepancies are found in the level spacings. The anomaly found in thorium seems to be confined to this element. The disagreement found between theory and experiment concerning the fission barrier does not appear in radium.

2. The agreement between the theoretical calculations of Nix and Möller and the information deduced from the experimental data leads us to believe that the methodology employed in conducting the present analysis is a correct way of carrying out transition state spectroscopy.

3. We have obtained what we think is a reliable description of the excitation energy dependence of the level density of radium at the equilibrium deformation, up to energies around the neutron binding energies. This dependence was deduced from the neutron evaporation spectra in the ^{232}Th(n,n') process, and the neutron resonance data in ^{230}Th. From this information, and from the cross-section

information data in the $^{226}Ra(n,f)$ reaction, the level density dependence on energy at the saddle point was obtained.

4. The empirical dependence on energy of the parameters a_f and a_n in the Fermi-gas expression indicate that these decrease with excitation energy. Normally this would be interpreted as reflecting a higher than average single particle level density around the Fermi surface at the equilibrium and fission deformations. New calculations based on the macroscopic-microscopic method indicate that the shell correction is negative at both of these deformations, which signifies that, on theoretical grounds, the density of levels around the Fermi surface is expected to be lower than average.

5. The above discrepancy can be understood if we accept the premise that many of the levels that are seemingly missing in the microscopic calculation, are actually collective in nature. Level density calculations carried out microscopically show values at least 10^3 times smaller than those obtained from experimental data. Rough estimates of collective enhancements based on partition function arguments show that collective degrees of freedom could possibly account for the huge difference between the microscopic and empirical estimates of the level density. Calculations show that vibrational contributions are comparatively more important at low energies than at higher excitations. This might

explain in part the observed decrease of the level density parameters with increasing excitation energy at low energies.

6. From the K_o^2 dependence on excitation energy, we have deduced a tentative value for the pairing gap at the saddle point of about 3 MeV. This contrasts sharply with the value deduced at the equilibrium deformation of $2\Delta_o \sim$ 1.7 MeV. The estimate of $2\Delta_f$ at the transition state deformation may present a considerable degree of inaccuracy because of the scarcity of available data and also because of the large uncertainties in the experimental points. The dependence of the parameter Δ on nuclear deformation is still the subject of considerable controversy.

7. The fission fragment angular distributions corresponding to fission after neutron evaporation show very unusual shapes. This phenomenum is not observed in other systems and the question is still open to interpretation.

8. The problem concerning the origin of the mass distribution in fission has not been resolved in this work. There are indications that symmetric fission begins to contribute significantly in radium at energies where second chance fission is expected to become important, thereby making the analysis difficult.

In conclusion, we might say that many of the problems that have been observed in the study of the fission phenomena, are being explained with relative success by recent

theoretical developments. Particularly, impressive progress has been made in describing the topology associated with nuclear deformation, which has been born out by experimental confirmations. More study needs to be carried out in relation to the problem of the level density dependence on energy, and its connection with collective phenomena.

BIBLIOGRAPHY

Ad 72 Adeev, G. D., Gamalya, I. A., Cherdantsev, P. A., Sov. J. Nucl. Phys. 14, 637 (1972).

Au 62 Auerbach, E. and Perey, F., Brookhaven National Laboratory Report No. BNL-765(T-286), 1962 (unpublished).

Ba 65 Batchelor, R., Gilboy, W. B., and Towle, J. H., Nucl. Phys. 65, 236 (1968).

Ba 68 Babenko, Y. A., Nemilov, Y. A., Selitskii, Y. A. and Funshtein, V. B., Sov. J. Nucl. Phys. 7, 186 (1968).

Ba 69 Babenko, Y. A., Ippolitov, V. T., Nemilov, Y. A., Selitskii, Y. A., and Funshtein, V. B., Sov. J. Nucl. Phys. 10, 133 (1969).

Ba 70 Babenko, Y. A., Nemilov, Y. A., Pleskachevskii, L. A., Selitskii, Y. A., and Funshtein, V. B., Sov. J. Nucl. Phys. 11, 560 (1970).

Ba 73 Back, B. B., Britt, H. C., Garrett, J. D., and Hansen, O., Proc. Symp. Phys. Chem. Fission, Rochester, N. Y., (1973), Paper, SM-174/201. Intern. At. Energy Agency, Vienna.

Ba 73a Back, B. B., Hansen, O., Britt., H. C., and Garrett, J. D., Proc. Symp. Phys. Chem. Fission, Rochester, N. Y., (1973), Paper, SM-174/27, Intern. At. Energy Agency, Vienna.

Be 68 Behkami, A. N., Roberts, J. N., Loveland, W., and Huizenga, J. R., Phys. Rev. 171, 1267 (1968).

Bi 72 Bishop, C. J., Halpern, I., Shaw, R. W., and Vandenbosch, R., Nucl. Phys. A198, 161 (1972).

Bj 69 Bjornholm, S. and Strutinsky, V., Nucl. Phys. A136, 1 (1969)

Bj 73 Bjornholm, S., Bohr, A., and Mottelson, B., Proc. Symp. Phys. Chem. Fission, Rochester, N. Y., (1973), Paper, SM-174/205. Intern. At. Energy Agency, Vienna.

Bo 39 Bohr, N. and Wheeler, J. A., Phys. Rev. 56, 426 (1939).

Bo 55 Bohr, A., Proc. Int. Conf. Peaceful Uses At. Energy: Geneva, 2, 151 (1955).

Bo 69 Bohr, A. and Mottelson, B. R., Nuclear Structure Pt. I. W. A. Benjamin, Inc. (1969) New York.

Bo 73 Bolsterli, M., Private communication.

Br 68 Britt, H. C., Rickey, F. A., and Hall W. S., Phys. Rev. 175, 1525 (1968).

Br 72 Brack, M., Damgaard, J., Jensen, A., Pauli, H., Strutinsky, V., and Wong, C., Rev. Mod. Phys. 44, 320 (1972).

Br 73 Britt, H. C., Bolsterli, M., Nix, J. R., and Norton, J. L., Phys. Rev. 7C, 801 (1973).

De 68 Decowski, P., Grochulski, W., Marcinkowski, A., Siwek, K., and Wilhelmi, Z., Nucl. Phys. A110, 129 (1968).

Em 73 Emma, V., LoNigro. S., and Milone, C., Nucl. Phys. A199, 186 (1973).

Er 58 Ericson, T., Nucl. Phys. 6, 62 (1958).

Gi 65 Gilbert, A. and Cameron, A. G. W., Can. J. Phys. 43, 1248 (1965).

Gi 68 Gindler, J. E. and Huizenga, J. R., Nuclear Chemistry, (L. Yaffe, ed.) Pt. II., Academic Press, Inc. (1968) New York.

Gr 63 Griffin, J. J., Phys. Rev. 132, 2204 (1963).

Ha 39 Hahn, O. and Strassmann, F., Naturwissenschaften 27, 11 (1939).

Ha 52 Hauser, W. and Feshbach, H., Phys. Rev. 87, 366 (1952).

He 56 Henkel, R. and Brolley, J., Phys. Rev. 103, 1292 (1956).

Hi 53 Hill, D. L. and Wheeler, J. A., Phys. Rev. 89, 1102 (1953).

Hi 60 Hittmair, O., Nucl. Phys. 18, 346 (1960).

Hu 68 Huizenga, J. R., Behkami, A. N., Meadows, J. W., and Klema, E. D., Phys. Rev. 174, 1539 (1968).

Ip 72 Ippolitov, V. T., Nemilov, Y. A., Selitskii, Y. A. and Funshtein, V. B., Sov. J. Nucl. Phys. 14, 526 (1972).

It 73 Itkis, M. G., Kuvatov, K. G., Okolovich, V. N., Ruskina, G. Ya., Smirenkin, G. N. and Tishin, A. S., Sov. J. Nucl. Phys. 16, 144 (1973).

Jo 61 Johansson, S. A. E., Nucl. Phys. 22, 529 (1961).

Ke 64 Kennedy, R., Wilets, L., and Henley, E. M., Phys. Rev. 133B, B1131 (1964).

Kl 64 Kluge, G., Nucl. Phys. 51, 41 (1964).

Ko 73 Konecny, E., Specht, H. J., and Weber, J., Proc. Symp. Phys. Chem. Fission, Rochester, N. Y., (1973), Paper, SM-174/20. Intern. At. Energy Agency, Vienna.

Ku 73 Kuks, I. M., Matvienko, V. I., Nemilov, Y. A., Selitskii, Y. A., and Funshtein, V. B., Sov. J. Nucl. Phys. 16, 244 (1973).

La 54 Lang, J. M. B. and LeCouteur, K. J., Proc. Phys. Soc. A67, 586 (1954).

La 62 Lamphere, R., Nucl. Phys. 38, 561 (1962).

Ma 70 Marmier, P. and Sheldon, E., Physics of Nuclei and Particles, Vol. II., Academic Press, Inc. (1970) New York.

Me 64 Meldner, H. and Lindner, A. Z., Z. Physik 180, 362 (1964).

Mo 64 Moldauer, P. A., Engelbrecht, C. A., and Duffy, G. J., Argonne National Laboratory Report No. ANL-6978, 1964 (unpublished).

Mo 69 Moretto, L. G., Gatti, R. C., Thompson, S. G., Huizenga, J. R., Rasmussen, J. O., Phys. Rev. 178, 1845 (1969).

Mo 70 Moller, P. and Nilsson, S. G., Phys. Lett. 31B, 283 (1970).

Mo 71 Mosel, U. and Schmitt, H. W., Nucl. Phys. A165, 73 (1971).

Mo 72 Moller, P., Nucl. Phys. A192, 529 (1972).

Mo 73 Moller, P. and Nix, J. R., Proc. Symp. Phys. Chem. Fission, Rochester, N. Y., (1973), Paper, SM-174/202. Intern. At. Energy Agency, Vienna.

Ne 62 Nemirovsky, P. E. and Adamchuk, Y. V., Nucl. Phys. 39, 551 (1962).

Ni 65 Nix, J. R. and Swiatecki, W. J., Nucl. Phys. 71, 1 (1965).

Ni 72 Nix, J. R., Ann. Rev. Nucl. Sci., 22, 65 (1972).

Ni 73 Nix, J. R. and Moller, P., Private communication.

No 58 Nobles, R. A. and Leachman, R. B., Nucl. Phys. 5, 211 (1958).

Pa 73 Pauli, H. C., Phys. Rep. 7, 36 (1973).

Pa 73a Pauli, H. C. and Lederberger, T., Proc. Symp. Phys. Chem. Fission, Rochester, N. Y., (1973), Paper SM-174/206. Intern. At. Energy Agency, Vienna.

Sh 71 Shpak, D. L., Ostapenko, Yu. B., and Smirenkin, G. N., Sov. J. Nucl. Phys. 13, 547 (1971).

St 58 Strutinsky, V. M., Compt. Rend. Congr. Intern. Phys. Nucl., Paris, 1958, p. 617.

St 65 Strutinsky, V. M. and Pavlinchuk, V. A., Proc. Symp. Phys. Chem. Fission, Salzburg, Austria, (1965), p. 121. Intern. At. Energy Agency, Vienna.

St 66 Strutinsky, V., Nucl Phys. A95, 420 (1966).

Ts 66 Tsukada, K., Tanaka, S., Maruyama, M., and Tomita, Y., Nucl. Phys. 78, 369 (1966).

Va 67 Vandenbosch, R., Nucl. Phys. A101, 460 (1967)

Va 72 Vandenbosch, R. and Mosel, U., Phys. Rev. Lett. 28, 1726 (1972).

Va 73 Vandenbosch, R., Phys. Rev. C7, 2092 (1973).

Va 73a Vandenbosch, R., Private communication.

Vo 64 Vonach, H. K., Vandenbosch, R., and Huizenga, J. R., Nucl. Phys. 60, 70 (1964).

Vo 69 Vorotnikov, P. E., Sov. J. Nucl. Phys. 9, 179 (1969).

Wh 63 Wheeler, J. P., Fast Neutron Physics, (J. B. Marion and J. L. Fowler, eds.), Pt. II. Wiley (Interscience), New York (1963).

Wi 52 Winhold, E. J., Demos, P. T., and Halpern, I., Phys. Rev. 87, 1139 (1952).

Wi 56 Wilets, L. and Chase, D., Phys. Rev. 103, 1296 (1956).

Zh 71 Zhagrov, E. A., Nemilov, Yu. A., Nikitina, N. V., and Selitskii, Yu. A., Sov. J. Nucl. Phys. 13, 537 (1971).

APPENDICES

APPENDIX I

Error Incurred in the Approximation for the Exit Channel Neutron Transmission Coefficients Above 5.0 MeV

The fits made to the neutron transmission coefficients shown in Figures 7 through 10 are not very reliable at energies above 5 MeV. However, these fits are used in conjunction with the calculated level densities in order to calculate the neutron emission expression in the denominator of the Hauser-Feshbach relation (II-15).

For purposes of illustration we can make a rough evaluation of the magnitude of the of the error that we are introducing into the calculation due to poor fit to the T_ℓ values above 5 MeV by calculating the differential contribution to the average kinetic energy of the outgoing neutron, and comparing it with that of a 5 MeV outgoing neutron.

Assume that a nucleus absorbs a 7 MeV neutron; the excitation energy of the compound system is about 11.5 MeV, because the neutron binding energy is 4.5 MeV. If the spectrum of neutrons is assumed to be Maxwellian, then the emission probability is roughly given by the expression:

$$P(E) \propto Ee^{-E/T} \qquad \text{(AI-1)}$$

and the average neutron energy is twice the value of the temperature, T. The temperature may be estimated from the expression

$$\frac{1}{T} = \sqrt{\frac{a_n}{U}} - \frac{3}{2U} \qquad \text{(AI-2)}$$

where U is the excitation energy of the nucleus, a_n is the level density parameter and it roughly obeys the relation:

$$a_n \sim A/8 \qquad \text{(AI-3)}$$

Therefore $a_n \sim 226/8 = 28.3$, and $T \sim 0.62$ MeV, when $U = 11.5$ MeV. Then the average neutron kinetic energy is estimated to be 1.24 MeV. The residual nucleus excitation energy is about 5.76 MeV. If we assume the level density to be proportional to $e^{E/T}$, then we can calculate the ratio of the compound level densities at residual nucleus excitation energies corresponding to an average energy neutron being emitted ($U = 5.76$ MeV) and a 5 MeV neutron being emitted ($U = 2$ MeV). Then the ratio, R, becomes:

$$R \sim \exp\left[\frac{(5.76)}{0.51} - \frac{(2)}{0.33}\right]$$

In this case $R \propto e^{5.25}$ is equal to 200.

What this means is that, at most, the error introduced by neglecting contributions due to neutrons with $E_n = 5$ MeV is less than 0.5%. Of course, we are not neglecting this contribution, but merely saying that there is a deviation in the fit of T_ℓ, (E_n) above 5 MeV for certain ℓ' waves of outgoing neutrons. At worst, this deviation is about 25%, making the average total error in the calculation in the order of 0.12% which is certainly negligible.

We must also point out that the transmission coefficients for incoming neutrons are exact, and no calculational source of error appears in the evaluation of the Hauser-Feshbach expression (II-15).

APPENDIX II

Normalization of the Experimental Data

The experimental data shown in Figures 1 through 4 represent the ratios of the differential cross sections at the given angles to the corresponding ones at 90°. Although this representation might be useful in comparing angular distributions at different energies, it might also be misleading because the normalization is based on only one point, the one at 90°. Consequently, should this point be in error, it would throw off the relative strengths of the distributions for comparison at the different neutron energies. It follows that it is important and necessary that these angular distributions be expressed in a manner that reflects the variation of the total fission cross section with neutron energy, i.e., as differential cross sections.

Differential cross sections for nuclear reactions are expressed in terms of probability per unit solid angle; since the fission cross section for the ^{226}Ra(n,f) reaction is so low, we choose to express the data in terms of mb/sr. To compute the differential cross section from the observed data we begin by noting that the angular distribution functions are normalized in such a way that:

$$\int_{-1}^{+1} W_{K,M}^{J}(\Theta)\, d\,(\cos\Theta) = 1 \qquad \text{(AII-1)}$$

Following the same idea, we found a smooth function of cos Θ, which when integrated between the appropriate limits, yielded the observed total fission cross section. We begin

by defining the total fission cross section in the following manner:

$$\sigma_f(E) = \int_{-1}^{+1} f(\cos\,\theta)\, d\,(\cos\,\theta) \qquad \text{(AII-2)}$$

This function $f(\cos\,\theta)$ can be any useful function capable of reproducing the angular distribution pattern. Legendre polynomials are normally used for this purpose because of their simplicity. In our case, we have chosen to use a sixth order Legendre polynomial in which we only have even terms. The reason for this is that the angular distributions are symmetrical about 90°. Therefore, the integrating function would be:

$$f(\cos\,\theta) = a_o + a_2P_2(\cos\,\theta) + a_4P_4(\cos\,\theta) + a_6P_6(\cos\,\theta) \qquad \text{(AII-3)}$$

where the a's represent coefficients to be determined for each energy studied, and the P_n's are the Legendre polynomials of nth order.

Having chosen these functions, we proceeded to fit the angular distributions in their original form as shown in Figure 5, with expression (AII-3) using a non-linear least squares computer program, and leaving four free parameters (a_o, a_2, a_4, and a_6). Table XVII shows the values of parameters extracted in every case.

Once we obtained these fits we proceeded to place the polynomial functions into expression (AII-2) for integration. From expressions (AII-2) and (AII-3) it can easily

Table XVII. Parameters Derived in Fitting ^{226}Ra(n,f) Anisotropies

E_n (MeV)	a_o	a_2	a_4	a_6
3.6	1.154	0.4610	0.1210	0.1100
3.8	1.029	0.1220	-0.0684	-0.0248
3.9	1.668	0.8780	-0.5580	0.2645
4.1	1.306	0.7450	-0.3020	-0.1950
4.7	1.192	0.3620	0.0346	-0.0892
5.4	1.210	0.1750	0.0149	0.1020
6.2	1.075	0.2990	0.1421	-0.0188
6.7	1.323	0.5660	-0.1930	-0.0004
7.1	1.195	0.4270	0.0693	-0.1500
7.9	1.125	0.2230	-0.0460	-0.0090
8.9	1.108	0.2110	-0.2010	0.0610
9.0	1.138	0.2680	-0.0012	-0.0763
9.7	1.103	0.3320	0.0853	0.0483
11.6	1.075	0.1020	0.0118	-0.1381
12.5	1.177	0.4520	-0.1095	-0.1975
13.6	1.217	0.3630	-0.0725	-0.0139
14.4	1.140	0.1952	-0.0893	0.4275
14.8	1.315	0.1927	-0.1480	0.3650

be shown that the following relation is obtained:

$$\sigma_f(E) = \int_{-1}^{+1} f(\cos\,\theta)\, d\,(\cos\,\theta) = 2a_o \qquad \text{(AII-4)}$$

This conclusion is very useful because we can now relate in a very simple manner the fission cross section to one of the parameters in the fit, and therefore normalize the angular distribution, point by point, through a constant factor, to the total fission cross section. From the above we then find:

$$\sigma(E,\theta) = \frac{\sigma_f(E)}{2a_o} \times \frac{\sigma(E,\theta)}{\sigma(E,90°)} \qquad \text{(AII-5)}$$

where $\sigma(E,\theta)$ represents the differential cross section for a given neutron energy, E, at the angle θ. The resulting angular distributions are shown in Figure 16.

APPENDIX III

Computer Program for Calculating Compound Transmission Coefficients and Sample Output

```
                PROGRAM WILDCAT(INPUT,OUTPUT,TAPE7=INPUT,TAPE6=OUTPUT)
      C         WILDCAT, A CODE FOR TRANSITION STATE SPECTROSCOPY IN (N,F) REACTI      002
      C         ONS                                                                   003
      C                                                                               004
      C         1184/RE257 BY C.ENGELBRECHT,P.MOLDAUER,G.DUFFY, W.LOVELAND            004*
      C         THIS IS THE 3300 VERSION(FORTRAN 32 COMPATIBLE)OF THE MODIFICATION
      C         OF NEARREX CALLED WILDCAT WHICH
      C         WILL RUN ON 704 FORTRAN II WITH A FEW MINOR MODIFICATIONS.           R1050006
      C         TO RUN THIS CODE ON A 704 OR 7090/94,MAKE THE FOLLOWING CHANGES-     R1050007
      C         (1)CHANGE THE INITIALIZE TEMPORARY STORAGE SECTION BY REPLACING      R1050008
      C            ALL MULTIPLE EQUALITIES WITH A SUITABLE SUBSTITUTE.               R1050010
      C         (2) CHANGE ALL IF EXPONENT FAULT STATEMENTS TO IF ACCUMULATOR        R1050011
      C            OVERFLOW STATEMENTS.                                              R1050012
      C         (3)THE 2 STATEMENTS FOLLOWING STATEMENT 9500 SET UP AN ERROR         R1050013
      C            TERMINATION JUMPED TO FROM 20 DIFFERENT LOCATIONS IN THE CODE.    R1050014
      C            CHANGE THIS SUBROUTINE, CALLED Q8QERROR,TO SUIT YOUR SYSTEM.      R1050015
      C         THIS VERSION INCLUDES CORRECTIONS IN NEARREX TO AUGUST,1964 AND IN
      C         WILDCAT TO DECEMBER,1966
      C                                                                             R1050017
000003          DIMENSION R(26),HI(26),PI(26),PE(20),EM(20),PAFO(19),
               X          AMFO(19),PAF1(19),AMF1(19),PAHO(19),AMHO(19),           R1050019
               X PAH1(19),G(30),XK(30),FINT(13,7),EN(36),FLIM(10),
               X  FHALF(14,7),P(36,19),Q0(36,19),Q1(36,19),
               XENSIG(26,15,15),RGP(19),RRR(19),AGPLUS(19),AGMIN(19),RGM(19),
               XATEMPP(26,15),AMH1(19),          RECORD(12),GFUNG(30),
               XENSIGN(10,26),ESURP(10),ENSIGE(36),DIST(9),NEW(6),XNOW(6),E(10),
               XTOTAL(10),A(26,15),QQ(19),CWCALC(10,9),
               XATEMPM(26,15),GSIGN(35),GSIG(19),
               XUSIGMF(15),SIGTO(15),CSS(10),VAR(10),
               XWCALC(10,9),SIGMAF(10),WEXP(10,9),SIGMAW(10,9),IOPTION(1),
               X       RN(10,2),HIN(10,2),PIN(10,2),IN(2,15,10),
               XFNU(40),FKAY(40),PSP(40),PSM(40),FZERO(40),HBARO(40),HBOTI(40),
               XALPHA(60),AKPLUS(40,15),AKMIN(40,15),NFTR(60),TCOEFF(40,15),
               XFSIG(40,15),TEMPFA(60),ASUBFF(60),TEMPNE(60),FSIGE(60),
               X FSIGN(10,60),COMPTR(26,15),RHO(20,10),AMEV(10),ESUP(15)
000003          COMMON/C/XJ(9),W1(19,9),W2(19,9),W3(19,9),W4(19,9),WS(19,19,10),
               XW5(19,9),W6(19,9)
               X /R/SIGST(20,20)
      C                                                                             R1050028
      C              COMPUTE TABLE OF J-COEFFICIENTS                                R1050029
      C
000003          DO3331N=1,7                                                         R1050030
000005    3331  FHALF(1,N)=0.0                                                      R1050031
000012          DO3332N=1,13                                                        R1050032
```

```
000266          R(I)=RI(I)=PI(I)=EN(I)=ENSIGE(I)=0.0
000275          DO 401 N=1,2
000276          DO 401 NIE=1,10
000277          RN(NIE,N)=RIN(NIE,N)=PIN(NIE,N)=0.0
000305     401  TN(N,NN,NIE)=0.0
000315          DO 17 J=1,9
000316          AMEV(J)=0.0
000317       17 XJ(J)=0.0
000322          DO 9010 J=1,19
000323                P(I,J)=QQ(I,J)=Q1(I,J)=ATEMPP(I,J)=ATEMPM(I,J)=0.0          R1050073
000336          DO 9010 K=1,19
000340    9010 ENSIG(I,J,K)=0.0                                                   R1050075
000354          DO 9011 I=1,19                                                  R1050076
000355    9011 PAEO(I)=AMEO(I)=PAE1(I)=AME1(I)=PAHO(I)=AMHO(I)=PAH1(I)=BGP(I)=  R1050077
              C                                   AGPLUS(I)=AGMIN(I)=BGM(I)=    R1050078
              CAMH1(I)=PE(I)=EM(I)=     0.0
000416          DO 9012 I=1,30                                                  R1050081
000417    9012 G(I)=XK(I)=GEUNG(I)=0.0                                          R1050082
000424          DO 9013 I=1,19
000426    9013 BBB(I)=GSIG(I)=0.0
000432          DO 9014 I=1,35                                                  R1050085
000434    9014 GSIGN(I)=0.0
000437          DO 9015 I=1,20
000440          ESUBP(I)=0.0
000441          DO 9015 J=1,36
000443    9015 ENSIGN(I,J)=0.0                                                  R1050088
000453          DO 8667 I=1,60
000454          ENU(I)=EKAY(I)=PSP(I)=PSM(I)=EZERO(I)=RBARO(I)=RBOII(I)=
              XALPHA(I)=NETR(I)=TEMPFA(I)=ASURFE(I)=TEMPNE(I)=FSIGE(I)=0.0
000511          DO 3010 J=1,20
000513    3010 AKPLUS(I,J)=AKMIN(I,J)=TCOEFF(I,J)=FSIG(I,J)=0.0
000524          DO 8667 L=1,20
000526          FSIGN(L,I)=0.0
000532    8667 CONTINUE
          C
          C     ZERO OUT FIXED POINT TEMPORARIES.                               R1050089
          C
000536          IAFGH = IAF   = IAG   = IAH   = IAN   = IBG   = IEJPI = INAWT =  R1050090
                CINO  = IPHI  = ISIGMA= ITPT  = JPI   = J     = JUPPER= KC    =  R1050091
                CKKK  = K     = LMAX12= LMAX  = L     = MR    = ME    = MJ    =  R1050092
                CMN   = MP    = M     = NCAE  = NE    = NIF   = NINT  = NLKN  =  R1050093
                CNLK=NMAX1=NMAX=NN=NOJ1=NOJ=N=IAI=0                               094
000606          IOPTION=0
          C
          C     PREPARATION OF  W(K,J) TABLES
```

```
000013          K=N+1                                                                   R1050033
000015          FINT(N,1)=1.0                                                           R1050034
000016     3332 FHALF(K,1)=1.0                                                          R1050035
000022          SS=2.0                                                                  R1050036
000023          DO3334N=2,6                                                             R1050037
000025          DO3333J=1,13                                                            R1050038
000026          AHEL=FLOAT(J-1)
000030          AHAL=AHEL+0.5                                                           R1050040
000032          K=J+1                                                                   R1050041
000033          C   =0.5/(SS*SS)                                                        R1050042
000035          FINT(J,N)=EXP(-C   *AHEL*AHEL)-EXP(-C   *(AHEL+1.0)
                X*(AHEL+1.0))                                                           R1050044
000055     3333 FHALF(K,N)=EXP(-C   *AHAL*AHAL)-EXP(-C   *(AHAL
                X+1.0)*(AHAL+1.0))                                                      R1050046
000076     3334 SS=SS+2.0                                                               R1050047
000101          FINT(1,7)=1.0                                                           R1050048
000103          FHALF(2,7)=1.0                                                          R1050049
000104          DO3335J=1,12                                                            R1050050
000105          K=J+1                                                                   R1050051
000107          L=K+1                                                                   R1050052
000110          FINT(K,7)=FINT(J,7)+2.0                                                 R1050053
000113     3335 FHALF(L,7)=FHALF(K,7)+1.0                                               R1050054
          C                                                                             R1050055
          C     INITIALIZE TEMPORARY STORAGE.                                           R1050056
          C     ZERO OUT FLOATING POINT TEMPORARIES.                                    R1050057
          C
000120      301 AE    = AFPHI = AGSUPO= AHAL  = AHEL  = AMTOT = ANAWTA= ANAWTM=        R1050058
              CANAWTP= AN   = AQEN  = ASUBFE= ASUBH = ATEMP = AWTA  = AWT   =         R1050059
              CAXA  = AYA   = C     = DBPROD= DELTA = EJPI  = D     = EYE   =        R1050060
              XFINAWT= FKN   = FLN   = FNINT =                 FTEMP1= FTEMP2=
              X   PHIU=  PHIUE=   PATOT=  GELTA=   TEMP3=
              CPHPHP = PHPH  = PIFK  = PIEN  = PIE   = PROD11= PROD12= PROD21=        R1050063
              XPROD22=PSIBAR=SIGMA=SS=SUMINM=SUMINP=SUMINV=SUMK=
              CSUMOTM= SUMOTP= SUMOPM= SUMOPP= TEMP1 = TEMP2 = TEMP3 = TEMP4 =        R1050065
              CTEMP5 = TEMPAG=          TEMPAO= TEMPA = TEMPBG=          TEMPJ =      R1050066
              CTEMPM =                  TEMPP = TEMP  = TEMPT = TEMPX = U     =      R1050067
              CVEK  = VEL   = VI    = VJ    = VKN   = VK    = VLN   = VL    =        R1050068
              C WQEN=XK1=ZMIN=ZPLS=                                          EXPSUM
              C=CALSUM=CHISQW=CHISQS=      0.0
000247          DO 9999 I=1,26
000251          DO 9999 NN=1,15
000252          COMPTR(I,NN)=0.0
000256          A(I,NN)=0.0
000261     9999 CONTINUE
000264          DO 9010 I=1,36
```

```
C
C                                                                      094*
C          READ INPUT                                                  R1050095
C                                                                      R1050096
C
C     READ IN TITLE                                                    96*
C                                                                      96*
000607      READ INPUT TAPE 7,3001,KKK,(RECORD(I),I=1,12)              R1050097
000622      IF(KKK .EQ. 999) 9205,9206
000627   9205 CALL EXIT
000630   9206 CONTINUE
000630      WRITEOUTPUTTAPE6,3002                                      R1050098
000634      WRITEOUTPUTTAPE6,8006                                      R1050099
000640      WRITEOUTPUTTAPE6,8027,(RECORD(I),I=1,12)                   R1050100
000652      READ(7,3003)IAG,IAF,NOK,NMAX,LMAX,NCAE,KC,ITPT,NE,Q,MN,
           XNINT,NANGL,LIPRNT,LEVDEN,GSS
000716      READ(7,1815)LIO,KINDEX,JSTAT,IMAX,EPSIL,SING,NLEV,AFFCTN
000742   1815 FORMAT(4I3,2F3.1,I2,F3.1)
000742      IF(LEVDEN.EQ.1)READ(7,795)DFACT,DOBLE
000754    795 FORMAT(2F10.5)
C
C          READ STATISTICAL PARAMETERS
C
000754      IF(JSTAT.EQ.0)GO TO 1846
000755      READ(7,70)ATOMW,A1,A2,E0,AE,EX,TEMPER,HBAROS,RIGIDI ,A3,EMINI
001007     70 FORMAT(8F10.5)
001007      WRITE(6,8006)
001013      IC=(4.0/7.0)*1.3*(PZ+PN)/2.0
001021      ALITF=AE
001022      DO 1844 IM=1,NE
001024   1844 READ(7,1845)VAR(IM),ESUP(IM),AMEV(IM)
001040   1845 FORMAT(3F10.5)
001040      WRITE(6,8006)
001043   1846 CONTINUE

001043      LMAX1=LMAX+1
001045      IEJPI=KC                                                   R1050103
001047      NOKK=NOK
001050      IF(MN-1)3701,3702,3702                                     R1050104
001052   3701 NINT=12                                                  R1050105
001053   3702 CONTINUE                                                 R1050106
001053      LMAX12=2*LMAX+1                                            R1050107
001055      NMAX1=NMAX+1                                               R1050108
001057      IF(LEVDEN.EQ.1)NMAX1=NMAX*2
001061      NLIM=NMAX1+NLEV
```

```
001063          NMAX2=NMAX1+1
001065          WRITE(OUTPUT,TAPE6,8006)                                R1050109
001070          WRITE(OUTPUT,TAPE6,8006)                                R1050110
001074          WRITE(OUTPUT,TAPE6,3004 ,KC                             R1050111
001102          WRITE(OUTPUT,TAPE6,8006)                                R1050112
001106          IF(LEVDEN)912,917,912
001107      917 DO 914 N=1,NMAX1
001111          READ(7,27)B(N),HI(N),PI(N)
001122      914 WRITE(6,27)B(N),HI(N),PI(N)
001137          WRITE(5,8006)
001142          GO TO 780
001143      912 CONTINUE
001143          IF(SING.EQ.0.0)GO TO 780
001144          DO 750 N=NMAX2,NLIM
001146          READ(7,27)B(N),HI(N),PI(N)
001157      750 WRITE(6,27)B(N),HI(N),PI(N)
001174          WRITE(6,8006)
001177      780 CONTINUE
001177          HI(1)=GSS
            C                                                           116*
            C       TEST IF G.S. SPIN IS INTEGRAL
            C                                                           116*
001201          SS=HI(1)+0.75
001203      305 IF(SS-1.0)306,307,307                                   R1050118
            C                                                           118*
            C       G.S. SPIN IS 1/2 INTEGRAL                           118*
            C                                                           118*
001206      306 INAWT=1                                                 R1050119
001207          AWT=0.5                                                 R1050120
001211          GOTO310                                                 R1050121
001211      307 SS=SS-0.5                                               R1050122
001213          IF(SS-1.0)308,309,309                                   R1050123
001215      308 INAWT=0                                                 R1050124
001216          AWT=0.0                                                 R1050125
001217          GOTO310                                                 R1050126
001217      309 SS=SS-0.5                                               R1050127
001221          GOTO305                                                 R1050128
001222      310 TEMP=FLOAT(LMAX+1)
001225          TEMP=TEMP+HI(1)
001227          IF(INAWT-1)311,312,312                                  R1050131
001231      311 TEMP=TEMP+0.5                                           R1050132
001233      312 TEMP=TEMP+0.25                                          R1050133
            C
            C       NOJ  IS TRUNC(TOTAL NO. L WAVES + G.S. SPIN  + 0.25)
            C       NOJ IS NO. J-S  IN  CALC
```

```
      C
001235        NOJ=XINTF(TEMP)                                          R1050134
001241        PRINT 1222,NOJ
001246   1222 FORMAT(I3)
001246        NOJ1=NOJ+1                                               R1050135
001250        IF(IAG-1)313,314,314                                     R1050136
001252    313 AGSUPO=0.00005                                           R1050137
001254        GOTO315                                                  R1050138
      C                                                                    138*
      C     READ IN GAMMA CHANNEL DATA
      C                                                                    138*
001254    314 READINPUTTAPE7,3101,AGSUPO,MJ,ME,MB,MP,SIGMA,U,DELTA,ZPLS,ZMIN R1050139
001304        IF(MJ-1)3141,3142,3142                                   R1050140
001307   3141 SIGMA=6.0                                                R1050141
001311        ISIGMA=4                                                 R1050142
001312        GOTO3143                                                 R1050143
001312   3142 ISIGMA=XINTF(0.5*SIGMA+1.25)                             R1050144
001321   3143 IF(ME-1)3144,3145,3146                                   R1050145
001324   3144 IPHI=0                                                   R1050146
001325        GOTO3147                                                 R1050147
001326   3145 U=8.0                                                    R1050148
001330        DELTA=0.12                                               R1050149
001331        IPHI=1                                                   R1050150
001332        GOTO3147                                                 R1050151
001333   3146 IPHI=1                                                   R1050152
001334   3147 IF (MP-1) 3148,3149,3149                                      153
001337   3148 ZPLS=1.0                                                 R1050154
001341        ZMIN=1.0                                                 R1050155
001342   3149 WRITEOUTPUTTAPE6,3005,AGSUPO                             R1050156
001350        WRITEOUTPUTTAPE6,8006                                    R1050157
001354        WRITE OUTPUT TAPE 6,3102                                 R1050158
001360        WRITEOUTPUTTAPE6,26,SIGMA,U,DELTA,ZPLS,ZMIN              R1050159
001376        IF(MB-1)3150,105,105                                     R1050160
001401   3150 IBG=0                                                    R1050161
001402        GOTO315                                                  R1050162
001403    105 READINPUTTAPE7,25,(PE(JPI),JPI=1,NOJ1)                   R1050163
001416        WRITE OUTPUT TAPE 6,8006                                 R1050164
001422        WRITE OUTPUT TAPE 6,8011                                 R1050165
001426        WRITE OUTPUT TAPE 6,8008,(PE(JPI),JPI=1,NOJ1)            R1050166
001441        READINPUTTAPE7,25,(EM(JPI),JPI=1,NOJ1)                   R1050167
001454        WRITE OUTPUT TAPE 6,8006                                 R1050168
001460        WRITE OUTPUT TAPE 6,8012                                 R1050169
001464        WRITE OUTPUT TAPE 6,8008,(EM(JPI),JPI=1,NOJ1)            R1050170
001477        IBG=1                                                    R1050171
001500    315 IF(IAF.EQ.0)GO TO 5000
```

```
                C                                                                   172*
                C       INPUT CHANNEL F DATA                                        172*
                C                                                                   172*
001501                  WRITE(6,8006)
001505                  DO 6 IAF=1,NOK
001507                  READ(7,2666)FNU(IAF),FKAY(IAF),PSP(IAF),PSM(IAF),EZERO(IAF),
                       XHBARO(IAF),HBOTI(IAF),ALPHA(IAF)
001532           2666 FORMAT(8F10.5)
001532                  ANTA=AWT
001534              6   CONTINUE
001536                  WRITE(6,3007)
001542           3007 FORMAT(* *,2X,*FNU(K)*,3X,*K*,4X,*PSP*,2X,*PSM*,2X,*EZERO(K)*,
                       *2X,*HBARO(K)*,2X,*HBOTI(K)*,2X,*ALPHA(K)*)
001562                  DO 5 IAF=1,NOK
001544              5   WRITE(6,3006)FNU(IAF),FKAY(IAF),PSP(IAF),PSM(IAF),EZERO(IAF),
                       *HBARO(IAF),HBOTI(IAF),ALPHA(IAF)
001572           3006 FORMAT(* *,3X,F3.1,3X,F3.1,3X,F3.1,2X,F3.1,2X,F8.5,3X,F6.4,4X,
                       *F7.5,2X,F7.4)
001572           5000 CONTINUE
001572                  WRITE(6,8006)
001576                  LMAX12=2*LMAX+1
                C
                C       INPUT EXPERIMENTAL DATA
                C
001600                  DO 7043  I=1,NE
001602                  READ INPUT TAPE 7,7046,SIGMAF(I),USIGMF(I)
001611                  WRITE OUTPUT TAPE 6,7046,SIGMAF(I),USIGMF(I)
001621           7046 FORMAT(2F10.5)
001621           7043 CONTINUE
001624                  DO 218 J=1,NANGL
001625                  READ INPUT TAPE 7,217,XJ(J)
001632            217   FORMAT(F12.8)
001632            218   CONTINUE
001635                  CALL WKJ(NANGL)
001636                  DO 7045  I=1,NE
001640                  DO 7045 J=1,NANGL
001641                  READ INPUT TAPE 7,7044,WEXP(I,J) ,SIGMAW(I,J)
001654           7044 FORMAT(2F10.8)
001654           7045 CONTINUE
001661                  WRITE OUTPUT TAPE 6,7047
001665           7047 FORMAT(1HHOEXPERIMENTAL DATA//)
001665                  DO 7048 I=1,NE
001667                  WRITE OUTPUT TAPE 6,1749,I
001674           1749 FORMAT(19HOTHIS IS ENERGY NO.,I2//)
001674                  WRITE OUTPUT TAPE 6,1750
```

```
001700     1750 FORMAT(27H0ANGLE       WEXP        SIGMA)
001700          DO 7048 J=1,NANGL
001702          XXXJ = J
001703          WRITE OUTPUT TAPE 6,1751,XJ(J),WEXP(I,J),SIGMAW(I,J)
001721     1751 FORMAT(* *,F10.3,2F10.8)
001721     7048 CONTINUE                                                    R1050192
               C
               C    CALCULATE STAT. WT. FACTORS,IE, G(K),ETC.
               C                                                           R1050194
001725          FNINT=FLOAT(NINT)
001730          DO 1807 K=1,NINT                                           R1050196
001731          TEMP=FLOAT(K)
001732          TEMP1=3.141592654*(2.0*TEMP-1.0)/(2.0*FNINT)               R1050198
001740          G(K)=SIN(TEMP1)
001744          TEMP=COS(TEMP1)
001747     1807 XK(K)=0.5*(1.0+TEMP)                                       R1050201
001755          FINAWT=2.045/(2.0*HI(1)+1.0)
001761          IF(IPHI-1) 1902,1809,1901                                  R1050203
001763     1901 IERR=1701                                                  R1050204
001764          GO TO 9500                                                 R1050205
001765     1902 PHIU=1.0                                                   R1050206
001767          GO TO 1813                                                 R1050207
001767     1809 TEMP=0.0                                                   R1050208
001770          CALL PHI (DELTA,TEMP,U,PHIU)                               R1050209
001773     1813 IF(INAWT-1)1825,1814,1814                                  R1050210
001776     1814 INO=XINTF(HI(1)+1.25)
002004          TEMP1=FHALE(INO,ISIGMA)                                    R1050212
002007          INO=INO+1                                                  R1050213
002011          TEMP1=TEMP1+FHALE(INO,ISIGMA)                              R1050214
002015          GO TO 1835                                                 R1050215
002015     1825 INO=XINTF(HI(1)+0.75)
002023          TEMP1=FINT(INO,ISIGMA)                                     R1050217
002027          INO=INO+1                                                  R1050218
002031          TEMP1=TEMP1+FINT(INO,ISIGMA)                               R1050219
002035     1835 AFPHI=AGSUPO/(TEMP1*PHIU)                                  R1050220
002040          TEMP=0.5*HI(1)
002042          IF (INAWT-1) 1865,1855,1850                                R1050222
002044     1850 IERR=3472                                                  R1050223
002045          GO TO 9500                                                 R1050224
002046     1855 TEMP=TEMP+0.5                                              R1050225
002050          GO TO 1870                                                 R1050226
002051     1865 TEMP=TEMP+1.0                                              R1050227
002053     1870 TEMP=TEMP+0.25                                             R1050228
               C
               C    JUPPER = NOJ  FOR OUR CALC.
```

```
      C
002055            JUPPER=XINTF(TEMP)                                    R1050229
002061            JUPPER=JUPPER+LMAX                                    R1050230
002063            WRITEOUTPUTTAPE6,1370                                 R1050231
002066            GO TO 321
002067       321  DO 322 I =1,NE
002071            READ(7,7046)E(I)
002075       322  CONTINUE
002101            READ INPUT TAPE 7,260,IOPTION
002105       260  FORMAT(II)
      C                                                                 R1050232
      C          TRANSMISSION COEFFICIENT INPUT                         R1050233
      C                                                                 R1050234
002106            IF(LEVDEN)1131,1132,1131
002107      1132  NIE=0
002110      1135  NIE=NIE+1
002112            PHPH=0
002113            WRITE(6,3011)E(NIE)
002121            WRITE(6,3012)PHPH
002127            WRITE(6,8005)
002133            WRITE(6,3913)
002137            WRITE(6,8006)
002143            DO 1134 NLK=1,NMAX1
002145      1134  READ(7,26)(A(NLK,NN),NN=1,LMAX12)
002164            DO 1133 NLK=1,NMAX1
002165      1133  WRITE(6,3914)(A(NLK,NN),NN=1,LMAX12)
002204            GO TO 1102
002204      1131  CONTINUE
002204            NIE=0
002205       186  NIE=NIE+1                                             R1050236
002207            NMAX1=2*NMAX
002210            NOK=NOKK
002212            READINPUTTAPE7,27,RN(NIE,1),HIN(NIE,1),PIN(NIE,1)
002223            READINPUTTAPE7,26,(TN(1,NN,NIE),NN=1,LMAX12)
002240            DO 400 LKN=1,NMAX1
002242            DO 400 NN=1,LMAX12
002243            COMPTR(LKN,NN)=0.0
002247       400  CONTINUE
002254            IF(SING.EQ.0.0)GO TO 762
002255            DO 760 NLK=NMAX2,NLIM
002257       760  READ(7,26)(A(NLK,NN),NN=1,LMAX12)
002276            DO 761 NLK=NMAX2,NLIM
002300       761  WRITE(6,3914)(A(NLK,NN),NN=1,LMAX12)
002317       762  CONTINUE
002317            PHPH =0
```

```
002321          WRITE OUTPUT TAPE 6,3011,F(NIE)
002326          WRITEOUTPUTTAPE6,3012,PHPH                                  R1050240
002334          PI(1)=PIN(NIE,1)
002336          HI(1)=HIN(NIE,1)
002340          H(1)=HN(NIE,1)
002341          DO 407 NN=1,LMAX12
002343      407 A(1,NN)=TN(1,NN,NIE)
002355          DO 9888 J=1,NMAX
002357          DO 9888 L=1,LMAX1
002360     9888 RHO(J,L)=0.0
002371          DO 15 LKN=1,NMAX
002372       15 READ(7,304)(RHO(LKN,NN),NN=1,LMAX1)
002411      304 FORMAT(8E10.3)
002411          DO 404 LKN=1,NMAX1,2
002412          J=(LKN+1)/2
002414          COMPTR(LKN,1)=RHO(J,1)
002416          COMPTR(LKN+1,1)=RHO(J,1)
002420          DO 404 NN=2,LMAX12,2
002421          M=(NN+2)/2
002423          COMPTR(LKN,NN)=RHO(J,M)
002432          COMPTR(LKN+1,NN)=RHO(J,M)
002437          COMPTR(LKN,NN+1)=RHO(J,M)
002444          COMPTR(LKN+1,NN+1)=RHO(J,M)
002451      404 CONTINUE
002455          DO 790 LKN = 1,NMAX1
002457          DO 790 NN=1,LMAX12
002460          COMPTR(LKN,NN)=COMPTR(LKN,NN)*DFACT
002465      790 CONTINUE
002472          WRITE(6,229)
002475      229 FORMAT(* *,*ENERGY LEVELS ARE IN THE CONTINUUM*)
002475          IF(JSTAT.EQ.1)WRITE(6,1847)VAR(NIE),ESUP(NIE),EMINI
002511     1847 FORMAT(* *,*KZERO SQUARE=*,F10.5,/,*UPPER LIMIT OF INTEGRATION=*,
               XF10.5,/,*LOWER LIMIT OF INTEGRATION=*,F10.5)
002511          VARIAN=VAR(NIE)
002513            EMAX=ESUP(NIE)
002515          WRITEOUTPUTTAPE6,8006                                       R1050116
002520          WRITEOUTPUTTAPE6,3913                                       R1050242
002524          WRITEOUTPUTTAPE6,8006                                       R1050243
002530          IF(LPRNT.EQ.1)GO TO 1102
002532     3291 WRITE OUTPUT TAPE 6,3914,(A(      ),NN),NN=1,LMAX12)
002546          DO 18 LKN=1,NLIM
002550       18 WRITE(6,3914)(COMPTR(LKN,NN),NN=1,LMAX12)
002567     1102 CONTINUE
          C                                                                 237*
          C     Q IS QALPHA = TRANSMISSION COEFFICIENT FACTOR               237*
```

```
                C                                                                    237*
                C
                C       CALC OF CN TRANSMISSION COEFFICIENTS                         246*
                C
002567                  D = E(NIE)
002571                  IF(LEVDEN.EQ.1)NMAX1=1
002574                  DO330NN=1,LMAX12
002576                  SS = A(    1,NN)
002601                  IF (PHPH) 9003,9002,9003                                     R1050249
002602          9002    TEMP1=SS                                                     R1050250
002604                  BBB(NN)=0.0                                                  R1050251
002605                  GO TO 330                                                    R1050252
002606          9003    TEMP=SQRT(1.0-PHPH*SS)
002614                  TEMP1=SS+(1.0-TEMP)*(1.0-TEMP)/PHPH                          R1050254
002620                  BBB(NN)=0.1591549*(SS-TEMP1)                                 R1050255
002623           330    A(    1,NN) = 0.1591549*TEMP1
002632                  IF(NMAX1-1)333,333,331                                       R1050257
002635           331    DO332NLK=2,NMAX1                                             R1050258
002637                  DO332NN=1,LMAX12                                             R1050259
002640                  SS = A(   NLK,NN)
002644                  IF (PHPH) 9001,9000,9001                                     R1050261
002645          9000    TEMP1=SS                                                     R1050262
002647                  GO TO 332                                                    R1050263
002647          9001    TEMP=SQRT(1.0-PHPH*SS)
002655                  TEMP1=SS+(1.0-TEMP)*(1.0-TEMP)/PHPH                          R1050265
002661           332    A(   NLK,NN) = 0.1591549*TEMP1
002673           333    IAN=2                                                        R1050267
002674                  IF (IPHI-1) 2041,2043,2040
002677          2040    IERR=2040                                                    R1050269
002700                  GO TO 9500                                                   R1050270
002701          2041    PHIUE=1.0                                                    R1050271
002703                  GO TO 205                                                    R1050272
002703          2043    CALL PHI (DELTA,D,U,PHIUE)
002706           205    CONTINUE                                                     R1050274
002706                  IF(LEVDEN.EQ.1)GO TO 8050
002710                  DO 8051 LKN=1,NMAX1
002712                  DO 8051 NN=1,LMAX12
002713                  COMPTR(LKN,NN)=A(LKN,NN)
002722          8051    CONTINUE
002727                  IF(LTPRNT.EQ.1)GO TO 8050
002731                  DO 8052 LKN=1,NMAX1
002732          8052    WRITE(6,3914)(COMPTR(LKN,NN),NN=1,LMAX12)
002751          8050    CONTINUE
002751                  IF(SING.EQ.0.0) GO TO 765
002752                  DO 766 NLK=NMAX2,NLIM
```

```
002754          DO 766 NN=1,LMAX12
002755          A(NLK,NN)=A(NLK,NN)/6.2832
002761      766 COMPTR(NLK,NN)=A(NLK,NN)
002773      765 CONTINUE                                                    R1050275
            C                                                               276
            C       CALC  OF  THETA-MU-S                                    R1050277
            C
            C
            C       CALC  OF   T-GAMMA(J,PI)/2*PI
            C
002773          DO 423 JPI=1,JUPPER
002775          IF (INAWT-1) 405,403,402                                    R1050279
002777      402 IERR=402                                                    R1050280
003000          GO TO 9500                                                  R1050281
003001      403 TEMP=FHALF(JPI+1,ISIGMA)                                    R1050282
003005          GO TO 406                                                   R1050283
003005      405 TEMP=FINT(JPI,ISIGMA)                                       R1050284
003011      406 TEMP1=AFPHI*TEMP*PHIUF                                      R1050285
003014          AGPLUS(JPI)=TEMP1*ZPLS                                      R1050286
003016      423 AGMIN(JPI)= TEMP1*ZMIN
            C
            C       CALC  OF   T- F (J,PI)/2*PI
            C
003022          IF(IAF.EQ.0)GO TO 1213
003023          DO 16 IAF=1,NOK
003025          XKKAY=FKAY(IAF)
003027          EKZERO=EZERO(IAF)
003030          HIBOTI=HBOTI(IAF)
003032           HHAROK=HHARO(IAF)
003033          ALPHAK=ALPHA(IAF)
003035          IF(XKKAY-0.5)9,10,9
003037        9 XKDELT=0.0
003040          GO TO 11
003041       10 XKDELT = 1.0
003043       11 CONTINUE
003043          XKAY = XKKAY
003045          KK1= XKKAY+0.5
003050          EFK=0.0
003051          TFK=0.0
003052          KK2=1
003053          IF(KINDEX.EQ.0)KK2=KK1
003055          DO 12 KK=KK2,NOJ
003057          IF(KK.LT.KK1)GO TO 13
003061          EFK     = EKZERO+ HIBOTI*((XKAY*(XKAY+1.))+ALPHAK*(-1.**(XKAY+0.5))
               X*(XKAY+0.5)*XKDELT)
```

```
003077          TFK     =((1.+EXP(2.0*3.14*(EFK     -D)/HBAROK))**(-1))/(2.0*3.14)
003110          XKAY = XKAY + 1.
003112       13 AKPLUS(IAF,KK)=PSP(IAF)*TFK*2.0
003120          AKMIN(IAF,KK)=PSM(IAF)*TFK*2.0
003124          TFK=0.0
003124          EFK=0.0
003125       12 CONTINUE
003127       16 CONTINUE
003132          WRITE(6,8006)
003135          M=0
003136          N=0
003137     1212 M=N+1
003141          N=M+9
003142          IF(N.GT.NOK)N=NOK
003145          DO 2 I=M,N
003147        2 NFTR(I)=I
003152          WRITE(6,1731)(NFTR(I),I=M,N)
003165     1731 FORMAT(* *,10(*F-TRANS(*,I2,*)*),X)
003165          WRITE(6,8006)
003171          DO 8 KK=1,NOJ
003173          DO 36 IAF=M,N
003175          IF(PSP(IAF).EQ.1.0)GO TO 7
003177          TCOEFF(IAF,KK)=AKMIN(IAF,KK)
003204          GO TO 36
003205        7 TCOEFF(IAF,KK)=AKPLUS(IAF,KK)
003213       36 CONTINUE
003216        8 CONTINUE
003220          DO 1306 KK=1,NOJ
003222     1306 WRITE(6,1727)(TCOEFF(IAF,KK),IAF=M,N)
003241     1727 FORMAT(* *,10(X,F9.3,X))
003241          WRITE(6,8006)
003244          IF(N.EQ.NOK)GO TO 1213
003246          GO TO 1212
003247     1213 CONTINUE
          C
          C
          C
003247          IF(JSTAT.EQ.0)GO TO 4001
003250          EREL=EZERO(1)
003252          ALITE=AMEV(NIE)
003254          CALL DISTAT(LMAX,EMINI,EMAX,HBAROS,VARIAN,D,EX,ALITE,RIGIDI,E0,
               XTEMPER,ATOMN,IMAX,EREL,AFFCIN,A1,A2,A3)
003275          IAFF=NOK+2*NOJ
003300          KXX=NOK+1
003302          DO 4002 IAF=KXX,IAFF,2
```

C STATISTICAL TRANSMISSION COEFFICIENTS FOR FISSION

```
003303          LD=(IAF-KXX+1)/2+1
003307          DO 4002 KK=1,NOJ
003310          AKPLUS(IAF,KK)=SIGST(LD,KK)*DOBLE/6.2832
003317          AKMIN(IAF+1,KK)=SIGST(LD,KK)*DOBLE/6.2832
003325     4002  CONTINUE
003331          WRITE(6,8006)
003335          WRITE(6,4003)
003341     4003 FORMAT (* *,*STATISTICAL TRANSMISSION COEFFICIENTS FOR FISSION*)
003341          WRITE(6,8006)
003345          AE=ALITE
003347          WRITE(6,73)
003352      73  FORMAT(* *,*     A          A1         A2         E0         AE
                X EX       TEMPER     HBAROS     RIGIDI       A3*)
003352          WRITE(6,74)ATOMW,A1,A2,E0,AE,EX,TEMPER,HBAROS,RIGIDI,A3
003402      74  FORMAT(10F10.5)
003402          WRITE(6,8006)
003406          N=KXX-1
003410     4006 M=N+1
003412          N=M+9
003413          IF(N.GT.IAFF)N=IAFF
003416          DO 4004 I=M,N
003420     4004 NFTR(I)=I
003423          WRITE(6,1731)(NFTR(I),I=M,N,2)
003436          WRITE(6,8006)
003442          DO 4005 KK=1,NOJ
003444     4005 WRITE(6,1727)(AKPLUS(IAF,KK),IAF=M,N,2)
003463          WRITE(6,8006)
003466          IF(N.EQ.IAFF)GO TO 4007
003470          GO TO 4006
003471     4007 CONTINUE
003471     4001 CONTINUE
           C                                                          R1050305
           C          BG(F,J,P)                                       R1050306
           C                                                          R1050307
003471          IF (IBG-1) 502,506,501                                R1050308
003474      501 IERR=501                                              R1050309
003475          GO TO 9500                                            R1050310
003476      502 DO 504 JPI=1,JUPPER                                   R1050311
003500          BGP(JPI)=1.0                                          R1050312
003502      504 BGM(JPI)=1.0                                          R1050313
003505          GO TO 800                                             R1050314
003505      506 DO 730 JPI=1,JUPPER                                   R1050315
003507          IF (INAWT-1) 700,512,511                              R1050316
003511      511 IERR=511                                              R1050317
003512          GO TO 9500                                            R1050318
```

```
003513      512 IF (JPI-1) 513,550,515                                    R1050319
003516      513 IERR=513                                                  R1050320
003517          GO TO 9500                                                R1050321
003520      515 FTEMP1=FHALF(JPI,ISIGMA)                                  R1050322
003524          FTEMP2=FHALF(JPI+1,ISIGMA)                                R1050323
003526          FTEMP3=FHALF(JPI+2,ISIGMA)                                R1050324
003531          SUMINV=FTEMP1+FTEMP3+FTEMP2                               R1050325
003534      525 EJPI=EM(JPI-1)                                            R1050326
003536          IF (EJPI-D) 529,527,527
003540      527 SUMUPP=FTEMP1                                             R1050328
003542          GO TO 532                                                 R1050329
003542      529 CALL PSI (D,U,EJPI,DELTA,PSIBAR)
003546          TEMP=PSIBAR/PHIUE                                         R1050331
003550          SUMUPP=FTEMP1*TEMP                                        R1050332
003552      532 EJPI=EM(JPI)                                              R1050333
003554          IF (EJPI-D) 536,534,534
003556      534 SUMUPP=SUMUPP+FTEMP2                                      R1050335
003560          GO TO 539                                                 R1050336
003561      536 CALL PSI (D,U,EJPI,DELTA,PSIBAR)
003565          TEMP=PSIBAR/PHIUE                                         R1050338
003567          SUMUPP=FTEMP2*TEMP+SUMUPP                                 R1050339
003572      539 EJPI=EM(JPI+1)                                            R1050340
003574          IF (EJPI-D) 543,541,541
003576      541 SUMUPP=FTEMP3+SUMUPP                                      R1050342
003600          GO TO 546                                                 R1050343
003601      543 CALL PSI (D,U,EJPI,DELTA,PSIBAR)
003605          TEMP=PSIBAR/PHIUE                                         R1050345
003607          SUMUPP=FTEMP3*TEMP+SUMUPP                                 R1050346
003612      546 BGP(JPI)=SUMUPP/SUMINV                                    R1050347
003615          EJPI=PE(JPI-1)                                            R1050348
003616          IF (EJPI-D) 629,627,627
003620      627 SUMUPM=FTEMP1                                             R1050350
003622          GO TO 632                                                 R1050351
003623      629 CALL PSI (D,U,EJPI,DELTA,PSIBAR)
003626          TEMP=PSIBAR/PHIUE                                         R1050353
003630          SUMUPM=FTEMP1*TEMP                                        R1050354
003632      632 EJPI=PE(JPI)                                              R1050355
003634          IF (EJPI-D) 636,634,634
003636      634 SUMUPM=SUMUPM+FTEMP2                                      R1050357
003640          GO TO 639                                                 R1050358
003641      636 CALL PSI (D,U,EJPI,DELTA,PSIBAR)
003645          TEMP=PSIBAR/PHIUE                                         R1050360
003647          SUMUPM=FTEMP2*TEMP+SUMUPM                                 R1050361
003652      639 EJPI=PE(JPI+1)                                            R1050362
003654          IF (EJPI-D) 643,641,641
```

```
003656      641 SUMUPM=FTEMP3*SUMUPM                                      R1050364
003660          GO TO 645                                                 R1050365
003661      643 CALL PSI (0,U,EJPI,DELTA,PSIBAR)
003665          TEMP=PSIBAR/PHIUE                                         R1050367
003667          SUMUPM=FTEMP3*TEMP+SUMUPM                                 R1050368
003672      646 BGM(JPI)=SUMUPM/SUMINV                                    R1050369
003675          GO TO 730                                                 R1050370
003675      550 FTEMP1=FHALE(2,ISIGMA)                                    R1050371
003700          FTEMP2=FHALE(3,ISIGMA)                                    R1050372
003703          SUMINV=FTEMP1+FTEMP2                                      R1050373
003705          EJPI=EM(1)                                                R1050374
003706          IF (EJPI-0) 564,562,562
003710      562 SUMUPP=FTEMP1                                             R1050376
003712          GO TO 567                                                 R1050377
003712      564 CALL PSI (0,U,EJPI,DELTA,PSIBAR)
003716          TEMP=PSIBAR/PHIUE                                         R1050379
003720          SUMUPP=FTEMP1*TEMP                                        R1050380
003722      567 EJPI=EM(2)                                                R1050381
003724          IF (EJPI-0) 571,569,569
003726      569 SUMUPP=SUMUPP+FTEMP2                                      R1050383
003730          GO TO 574                                                 R1050384
003731      571 CALL PSI (0,U,EJPI,DELTA,PSIBAR)
003735          TEMP=PSIBAR/PHIUE                                         R1050386
003737          SUMUPP=FTEMP2*TEMP+SUMUPP
003742      574 BGP(1)=SUMUPP/SUMINV                                      R1050388
003744          EJPI=PE(1)                                                R1050389
003746          IF (EJPI-0) 664,662,662
003750      662 SUMUPM=FTEMP1                                             R1050391
003752          GO TO 667                                                 R1050392
003752      664 CALL PSI (0,U,EJPI,DELTA,PSIBAR)
003756          TEMP=PSIBAR/PHIUE                                         R1050394
003760          SUMUPM=FTEMP1*TEMP                                        R1050395
003762      667 EJPI=PE(2)                                                R1050396
003764          IF (EJPI-0) 671,669,669
003766      669 SUMUPM=SUMUPM+FTEMP2                                      R1050398
003770          GO TO 674                                                 R1050399
003771      671 CALL PSI (0,U,EJPI,DELTA,PSIBAR)
003775          TEMP=PSIBAR/PHIUE                                         R1050401
003777          SUMUPM=FTEMP2*TEMP+SUMUPM                                 R1050402
004002      674 BGM(1)=SUMUPM/SUMINV                                      R1050403
004004          GO TO 730                                                 R1050404
004005      700 IF (JPI-1) 701,702,725                                    R1050405
004010      701 IERR=701                                                  R1050406
004011          GO TO 9500                                                R1050407
004012      702 EJPI=EM(2)                                                R1050408
```

```
004014          IF (EJPI-0) 705,704,704
004016      704 BGP(1)=1.0                                              R1050410
004020          GO TO 712                                               R1050411
004020      705 CALL PSI (0,U,EJPI,DELTA,PSIBAR)
004024          BGP(1)=PSIBAR/PHIUE
004026      712 EJPI=PE(2)                                              R1050414
004030          IF (EJPI-0) 715,714,714
004032      714 BGM(1)=1.0                                              R1050416
004034          GO TO 730
004034      715 CALL PSI (0,U,EJPI,DELTA,PSIBAR)
004040          BGM(1)=PSIBAR/PHIUE                                     R1050419
004042          GO TO 730                                               R1050420
004043      725 FTEMP1=FINT(JPI-1,ISIGMA)                               R1050421
004047          FTEMP2=FINT(JPI,ISIGMA)                                 R1050422
004052          FTEMP3=FINT(JPI+1,ISIGMA)                               R1050423
004055          SUMINV=FTEMP1+FTEMP2+FTEMP3                             R1050424
004060          GO TO 525                                               R1050425
004061      730 CONTINUE                                                R1050426
                C                                                       R1050427
                C          SUMS OVER L AND K                            R1050428
                C                                                       R1050429
004064      800 NINDEX=0
004065          IF(JSTAT.EQ.1)NOK=IAFF
004071          EMIN=0.0
004072          IF(LIO)1262,1263,1262
004073     1262 WRITE(6,1302)
004077     1302 FORMAT(* *,*NN*,3X,*VLN*,3X,*VKN*,3X,*VJ*,5X,*SUMINP*,5X,
                X*SUMINM*,5X,*TEMPA0*,5X,*TEMPJ*,5X,*TEMPFA(1,JPI)*)
004077          WRITE(6,8006)
004103     1263 CONTINUE
004103          IF(LEVDEN.EQ.1)NMAX1=2*NMAX
004107          IF(SING.EQ.1.0)NMAX1=NLIM
004113          DO 1285 NN=1,LMAX12
004115          TEMPAP=0.0
004116          TEMPAM=0.0
004117          GSIG(NN)=0.0                                            R1050431
004120          DO 1717 IAF=1,NOK
004121     1717 FSIG(IAF,NN)=0.0
004127          DO 810 NLK=1,NMAX1                                      R1050434
004131          DO 810 NLKN=1,LMAX12                                    R1050435
004132      810 ENSIG(NLK,NN,NLKN)=0.0                                  R1050436
004145          CALL ELKAY (NN,VLN,VKN)                                 R1050437
004147          NINDEX=INT(VKN+0.5)
004152          DO 1261 JPI=1,JUPPER                                    R1050438
004153          INK=JPI
```

```
004154          IF(KINDEX.EQ.1)INK=NINDEX
004160          IF (INAMT-1) 860,857,856                                R1050439
004162      856 IERR=756                                                R1050440
004163          GO TO 9500                                              R1050441
004164      857 VJ=FLOAT(JPI)
004166          VJ=VJ-0.5                                               R1050443
004170          GO TO 870                                               R1050444
004170      860 VJ=FLOAT(JPI-1)
004173      870 PATOT=0.0
004174          AMTOT=0.0
004175          PATOT=PATOT+AGPLUS(JPI)
004177          AMTOT=AMTOT+AGMIN(JPI)
004201          DO 1718 IAF=1,NOK
004203          PATOT=PATOT+AKPLUS(IAF,INK)
004207          AMTOT=AMTOT+AKMIN(IAF,INK)
004213     1718 CONTINUE
004215          SUMINP=0.0                                              R1050448
004216          SUMINM=0.0                                              R1050449
004217          DO 923 LKN=1,NMAX1                                      R1050450
004220          J=(LKN-1)/2
004222          TRIAL=AMODF(LKN,2)
004225          SUMOTP=0.0                                              R1050451
004226          SUMOTM=0.0                                              R1050452
004227          DO 921 N=1,LMAX12                                       R1050453
004230          FLAGP=0.0
004231          FLAGM=0.0
004232          CALL ELKAY (N,VL,VK)                                    R1050454
004234          IF(LEVOFN.EQ.0)GO TO 8053
004235          IF(LKN.GT.(2*NMAX))GO TO 8053
004241          VI=FLOAT(J)
004242          IF(TRIAL.EQ.0.0)PIEN=-1.0
004245          IF(TRIAL.EQ.1.0)PIEN=+1.0
004250          WOFN=EMIN
004252          GO TO 8054
004252     8053 VI=HI(LKN)
004254          PIEN=PI(LKN)
004256          WOFN=R(LKN)
004257     8054 CONTINUE
004257          PIE=1.0                                                 R1050458
004261          CALL ANEJLK (VJ,VK,VL,VI,PIE,PIEN,D,WOFN,      AOFN)    R1050459
004271          IF (AOFN-1.0) 911,908,907                               R1050460
004274      907 IERR=707                                                R1050461
004275          GO TO 9500                                              R1050462
004276      908 CONTINUE
004276          ATEMPM(LKN,N)=0.0                                       R1050464
```

```
004302          FLAGP=1.0
004304          GO TO 930
004304      911 ATEMPP(LKN,N)=0.0                                          R1050466
004310          PIE=-1.0                                                   R1050467
004312          CALL ANEJLK (VJ,VK,VL,VI,PIE,PIEN,D,WOFN,AOFN)             R1050468
004322          IF (AOFN-1.0) 918,916,915                                  R1050469
004325      915 IERR=715                                                   R1050470
004326          GO TO 9500                                                 R1050471
004327      918 ATEMPM(LKN,N)=0.0                                          R1050474
004333          GO TO 920
004334      916 FLAGM=1.0
004336      930 SPECTR=COMPTR(LKN,N)
004342          IF(FLAGP.EQ.1.0)ATEMPP(LKN,N)=SPECTR
004350          IF(FLAGM.EQ.1.0)ATEMPM(LKN,N)=SPECTR
004356      920 SUMOTP=SUMOTP+ATEMPP(LKN,N)                                R1050475
004363      921 SUMOTM=SUMOTM+ATEMPM(LKN,N)                                R1050476
004371          SUMINP=SUMOTP+SUMINP                                       R1050477
004373      923 SUMINM=SUMOTM+SUMINM                                       R1050478
004377          PATOT=PATOT+SUMINP                                         R1050479
004401          AMTOT=AMTOT+SUMINM                                         R1050480
004403          IF (ATEMPP(1,NN)-0.0) 953,951,955                          R1050481
004410      951 IF (ATEMPM(1,NN)-0.0) 953,952,960                          R1050482
004416      952 GO TO 1261                                                 R1050483
004417      953 IERR=753                                                   R1050484
004420          GO TO 9500                                                 R1050485
004421      955 TEMPAO=A(1,NN)
004425          TEMPAP=TEMPAO
004426          PIE=1.0                                                    R1050487
004427          TEMPAG=AGPLUS(JPI)                                         R1050488
004431          TEMPBG=BGP(JPI)                                            R1050489
004433          DO 1719 IAF=1,NOK
004434     1719 TEMPFA(IAF)=AKPLUS(IAF,INK)
004443          TEMPA=PATOT                                                R1050492
004445          GO TO 964                                                  R1050493
004445      960 TEMPAO=A(1,NN)
004451          TEMPAM=TEMPAO
004452          PIE=-1.0                                                   R1050495
004453          TEMPAG=AGMIN(JPI)                                          R1050496
004455          TEMPBG=BGM(JPI)                                            R1050497
004457          DO 1720 IAF=1,NOK
004460     1720 TEMPFA(IAF)=AKMIN(IAF,INK)
004467          TEMPA=AMTOT                                                R1050500
004471      964 TEMPJ=2.0*VJ+1.0                                           R1050501
004474          IF (IEJPI-1) 967,1020,1020                                 R1050502
004477      967 ANAWTA=TEMPAO/TEMPA                                        R1050503
```

```
004501          GSIG(NN)=GSIG(NN)+ANAWTA*TEMPAG*TEMPBG*TEMPJ                    R1050504
004506          DO 1721 IAF=1,NOK
004510          FSIG(IAF,NN)=FSIG(IAF,NN)+ANAWTA*TEMPFA(IAF)*TEMPJ
004517    1721  CONTINUE
004521          IF(LIO)1264,1265,1264
004522    1264  WRITE(6,1303)NN,VLN,VKN,VJ,SUMINP,SUMINM,TEMPAO,TEMPJ,TEMPFA(1)
004550    1303  FORMAT(* *,I2,2X,F4.1,2X,F4.1,2X,F4.1,3X,E9.3,2X,E9.3,2X,E9.3,
                X2X,E5.2,5X,E9.3)
004550    1265  CONTINUE
004550          TEMPP=TEMPAP/PATOT
004552          TEMPM=TEMPAM/AMTOT
004554          DO 1010 NLK=1,NMAX1                                            R1050509
004556          DO 1010 NLKN=1,LMAX12                                          R1050510
004557          CALL ELKAY (NLKN,VL,VK)                                        R1050511
004561          IF(LEVDEN.EQ.0)GO TO 8055
004562          IF(NLK.GT.(2*NMAX))GO TO 8055
004566          J=(NLK-1)/2
004570          TRIAL=XMODF(NLK,2)
004573          VI=FLOAT(J)
004574          IF(TRIAL.EQ.0.0)PIEN=-1.0
004577          IF(TRIAL.EQ.1.0)PIEN=+1.0
004602          WOFN=EMIN
004604          GO TO 8056
004604    8055  VI=HI(NLK)
004606          PIEN=PI(NLK)
004610          WOFN=B(NLK)
004611    8056  CONTINUE                                                       R1050515
004611          PIEK=1.0                                                       R1050516
004613          CALL ANEJLK (VJ,VK,VL,VI,PIEK,PIEN,D,WOFN,AOFN)                R1050517
004623          IF (AOFN-1.0) 1004,1002,1001                                   R1050518
004626    1001  IERR=1001                                                      R1050519
004627          GO TO 9500
004630    1002  ATEMP=COMPTR(NLK,NLKN)                                         R1050521
004634          ENSIG(NLK,NN,NLKN)=ENSIG(NLK,NN,NLKN)+ATEMP*                   R1050522
                X                          TEMPP*TEMPJ                        R1050523
004644          GO TO 1010                                                     R1050524
004645    1004  PIEK=-1.0                                                      R1050525
004647          CALL ANEJLK (VJ,VK,VL,VI,PIEK,PIEN,D,WOFN,AOFN)                R1050526
004657          IF (AOFN-1.0) 1010,1008,1007                                   R1050527
004662    1007  IERR=1007                                                      R1050528
004663          GO TO 9500
004664    1008  ATEMP=COMPTR(NLK,NLKN)                                         R1050530
004670          ENSIG(NLK,NN,NLKN)=ENSIG(NLK,NN,NLKN)+ATEMP*                   R1050531
                X                          TEMPM*TEMPJ                        R1050532
004700    1010  CONTINUE
```

```
004705          GO TO 1261                                                      R1050534
                C                                                               R1050535
                C          CALCULATE INTEGRAND CASE 1                           R1050536
                C
004706    1020  CONTINUE
004706          IF(PIE+1.0) 1100,1061,1021
004711    1021  DO 1049 K=1,NINT                                                R1050538
004713          XK1=XK(K)
004715          TEMP1=AGPLUS(JPI)*(1.0-XK1)/(PATOT*XK1)
004723          IF (TEMP1-85.0) 5027,1025,1025
004725    1025  TEMP1=0.123456E38                                               R1050542
004727          GO TO 1028
004727    5027  TEMP3=AGPLUS(JPI)/PATOT                                         R1050544
004732          IF (TEMP3-0.0001) 5029,5029,5031                                R1050545
004734    5029  TEMP1=1.0                                                       R1050546
004736          GO TO 5527
004736    5031  TEMP1=EXP(TEMP1)
004741          GO TO 5527
004741    5527  TEMP4=ATEMPP(1,NN)/PATOT                                        R1050550
004746          IF (TEMP4-0.0001) 5529,1027,1027
004750    5529  TEMP1=XK1*XK1*TEMP1                                             R1050552
004752          GO TO 1028
004753    1027  TEMP1=XK1*XK1*TEMP1*(1.0+2.0*ATEMPP(1,NN)*                      R1050554
                X       (1.0-XK1)/(PATOT*XK1))                                  R1050555
004767    1028  PROD11=1.0                                                      R1050556
004771          DO 1047 N=1,LMAX12
004772          PROD21=1.0
004774          CALL ELKAY(N,VEL,VEK)
004776          DO 1046 LK=1,NMAX1
005000          VI=HI(LK)
005002          PIEN=PI(LK)
005003          WOFN=B(LK)
005005          PIEK=1.0
005006          CALL ANEJLK (VJ,VEK,VEL,VI,PIEK,PIEN,D,WOFN,AOFN)
005017          IF (AOFN-1.0) 1040,1042,1039
005022    1039  IERR=1037                                                       R1050567
005023          GO TO 9500                                                      R1050568
005024    1040  ANAWTP=0.0                                                      R1050569
005025          GO TO 1045
005026    1042  ANAWTP=A(     LK,N)
005032    1045  CALL PROD (ANAWTP,PATOT,XK1,DBPROD)                             R1050572
005035          CALL OVERFL(IQQQ)
005037          IF (IQQQ -1   )1044,1044,1044
005041    1044  PROD21=PROD21*DBPROD
005043          CALL OVERFL(IQQQ)
```

```
005044          IF (IQQQ-1   )4045,4045,1046
005047    4045  PROD21=0.123456E38                                    R1050576
005051    1046  CONTINUE                                              R1050577
005054          PROD11=PROD21*PROD11                                  R1050578
005055          CALL OVERFL(IQQQ)
005057          IF (IQQQ-    1) 4048,4048,1047
005062    4048  PROD11=0.123456E38                                    R1050580
005064    1047  CONTINUE                                              R1050581
005067          AE=PATOT                                              R1050582
005070          TEMPX=(1.0-XK1)/XK1                                   R1050583
005073          TEMP5=2.0/AE                                          R1050584
005075          DO 1726 IAF=1,NOK
005076    1726  ASUBFE(IAF)=AKPLUS(IAF,JPI)
005105          DO 416 IAF=1,NOK
005107          IF(ASUBFE(IAF)-1.0E-25)4026,4026,4126
005112    4126  TEMP=ASUBFE(IAF)/AE
005115          IF (TEMP-0.0001) 4026,4028,4028                       R1050589
005117    4026  TEMPNE(IAF)=1.0
005121          GO TO 416
005122    4028  TEMPNE(IAF)=(1.0+TEMP5*(ASUBFE(IAF)/FNU(IAF))*TEMPX)**(FNU(IAF)/
                X2.0)
005135    416   CONTINUE
005140          TEMP=1.0
005141          DO 49 IAF=1,NOK
005143     49   TEMP=TEMP*TEMPNE(IAF)
005147          GFUNG(K)=PROD11*TEMP1*TEMP
005152          CALL OVERFL(IQQQ)
005154          IF(IQQQ-1   )4034,4034,9220
005157    4034  GFUNG(K)=0.123456E38                                  R1050601
005161    9220  CONTINUE
005161    1049  CONTINUE                                              R1050602
005164          GO TO 1101
          C                                                           R1050604
          C          CALCULATE INTEGRAND CASE 2                       R1050605
          C                                                           R1050606
005164    1061  DO 1049 K=1,NINT                                      R1050607
005166          XK1=XK(K)
005170          TEMP2=AGMIN(JPI)*(1.0-XK1)/(AMTOT*XK1)
005176          IF (TEMP2-85.0) 5067,1065,1065
005200    1065  TEMP2=0.123455E38                                     R1050611
005202          GO TO 1068
005202    5067  TEMP3=AGMIN(JPI)/AMTOT                                R1050613
005205          IF (TEMP3-0.0001) 5069,5069,5071
005207    5069  TEMP2=1.0                                             R1050615
005211          GO TO 5567
```

```
005211     5071 TEMP2=EXP(TEMP2)
005214          GO TO 5567
005214     5567 TEMP4=ATEMPM(1,NN)/AMTOT                                  R1050619
005221          IF (TEMP4-0.0001) 5569,1067,1067
005223     5569 TEMP2=XK1*XK1*TEMP2                                       R1050621
005225          GO TO 1068
005226     1067 TEMP2=XK1*XK1*TEMP2*(1.0+2.0*ATEMPM(1,NN)*                R1050623
               X       (1.0-XK1)/(AMTOT*XK1))                           R1050624
005242     1068 PROD12=1.0                                                R1050625
005244          DO 1087 N=1,LMAX12
005245          PROD22=1.0
005247          CALL ELKAY(N,VEL,VEK)
005251          DO 1086 LK=1,NMAX1
005253          VI=HI(LK)
005255          PIEN=PI(LK)
005256          WOEN=B(LK)
005260          PIEK=-1.0
005261          CALL ANEULK (VJ,VEK,VEL,VI,PIEK,PIEN,D,WOEN,
               X                  AOFN)
005272          IF (AOFN-1.0) 1080,1082,1079
005275     1079 IERR=1077                                                 R1050637
005276          GO TO 9500                                                R1050638
005277     1080 ANAWTM=0.0                                                R1050639
005300          GO TO 1085
005301     1082 ANAWTM=A(     LK,N)
005305     1085 CALL PROD (ANAWTM,AMTOT,XK1,DBPROD)                       R1050642
005310          CALL OVERFL(IQQQ)
005312          IF (IQQQ -1  )1084,1084,1084
005314     1084 PROD22=PROD22*DBPROD
005316          CALL OVERFL(IQQQ)
005317          IF (IQQQ-1  )4085,4085,1086
005322     4085 PROD22=0.123456E38                                        R1050646
005324     1086 CONTINUE                                                  R1050647
005327          PROD12=PROD22*PROD12                                      R1050648
005330          CALL OVERFL(IQQQ)
005332          IF (IQQQ-1  )4088,4088,1087
005335     4088 PROD12=0.123456E38                                        R1050650
005337     1087 CONTINUE                                                  R1050651
005342          AE=AMTOT                                                  R1050652
005343          TEMPX=(1.0-XK1)/XK1                                       R1050653
005346          TEMPS=2.0/AE                                              R1050654
005350          DO 30 IAF=1,NOK
005351       30 ASUBFE(IAF)=AKMIN(IAF,JPI)
005360          DO 80 IAF=1,NOK
005362          IF(ASUBFE(IAF)-1.0E-25)4526,4626,4626
```

```
005365     4526 TEMP=ASUBFE(IAF)/AF
005370          IF (TEMP-0.0001) 4526,4528,4528                          R1050659
005372     4526 TEMPNE(IAF)=1.0
005374          GO TO 80
005375     4528 TEMPNE(IAF)=(1.0+TEMPS*(ASUBFE(IAF)/FNU(IAF))*TEMPX)**(FNU(IAF)/
               X2.0)
005410       80 CONTINUE
005413          TEMP=1.0
005414          DO 53 IAF=1,NOK
005416       53 TEMP=TEMP*TEMPNE(IAF)
005422          GFUNG(K)=PROD12*TEMP2*TEMP
005425          CALL OVERFL(IQQQ)
005427          IF (IQQQ-1  )4534,4534,1089
005432     4534 GFUNG(K)=0.123456E38                                     R1050671
005434     1089 CONTINUE                                                 R1050672
005437          GO TO 1101
               C                                                        R1050674
               C          SIGMA CAPTURE                                 R1050675
               C                                                        R1050676
005437     1100 IERR=1100                                               R1050677
005440          GO TO 9500                                            R1050678
005441     1101 IF (IEJPI-1) 1109,1107,1111                             R1050679
005444     1107 TEMP=TEMPAO*TEMPAG/(TEMPA*TEMPA)                        R1050680
005447          IF (TEMP-0.0001) 1109,1109,1111
005452     1109 EYE=1.0                                                 R1050682
005454          GO TO 1115
005454     1111 SUMK=0.0                                                R1050684
005455          DO 5116 K=1,NINT
005457          SUMK=SUMK+G(K)/GFUNG(K)
005462     5116 CONTINUE                                                R1050687
005464          EYE=3.141592654*SUMK/(2.0*FNINT)
005470     1115 GSIG(NN)=GSIG(NN)+TEMPAO*TEMPJ*EYE*TEMPAG               R1050689
                X          *TEMPBG/TEMPA                               R1050690
               C                                                        R1050691
               C          SIGMA FISSION                                 R1050692
               C                                                        R1050693
005500          DO 1140 IAF=1,NOK
005501          IF (IEJPI-1) 1122,1120,1124
005504     1120 TEMP=TEMPAO*TEMPFA(IAF)/(TEMPA*TEMPA)
005510          IF (TEMP-0.0001) 1122,1122,1124
005512     1122 EYE=1.0                                                 R1050697
005514          GO TO 1130
005514     1124 TEMP=2.0*TEMPFA(IAF)/(FNU(IAF)*TEMPA)
005520          SUMK=0.0
005521          DO 5131 K=1,NINT
```

```
005523          TEMP5=TEMPFA(IAF)/TEMPA
005526          IF (TEMP5-0.0001) 6131,5129,5129
005530    6131  TEMPT=1.0                                                  R1050704
005532          GO TO 5130
005532    5129  TEMPT=1.0+(1.0-XK(K))*TEMP/XK(K)                           R1050706
005537    5130  SUMK=SUMK+(G(K)/GFUNG(K))/TEMPT                            R1050707
005544    5131  CONTINUE                                                   R1050708
005546          EYE=3.141592654*SUMK/(2.0*FNINT)
005552    1130  FSIG(IAF,NN)=FSIG(IAF,NN)+TEMPAO*TEMPJ*EYE*TEMPFA(IAF)/TEMPA
005562    1140  CONTINUE
          C                                                                R1050731
          C          SIGMA SCATTERING                                      R1050732
          C                                                                R1050733
005565          DO 1260 NLK=1,NMAX1
005566    1205  DO 1260 NLKN=1,LMAX12                                      R1050735
005570    1210  CALL ELKAY (NLKN,VEL,VEK)                                  R1050736
005573    1220  VI=HI(NLK)                                                 R1050737
005575          PIEN=PI(NLK)
005577          WOFN=B(NLK)
005600    1223  CALL ANEJLK (VJ,VEK,VEL,VI,PIE,PIEN,D,WOFN,                R1050740
                X                  AOFN)                                 R1050741
005611    1224  IF (AOFN-1.0) 1226,1228,1225                               R1050742
005614    1225  IERR=1225                                                  R1050743
005615          GO TO 9500                                                 R1050744
005616    1226  AN=0.0                                                     R1050745
005617    1227  GO TO 1260                                                 R1050746
005620    1228  AN=A(     NLK,NLKN)
005624    1251  IF (KC-1) 1231,1229,1241                                   R1050748
005627    1229  TEMP=TEMPAO*AN/(TEMPA*TEMPA)                               R1050749
005632    1230  IF (TEMP-0.0001) 1231,1231,1241                            R1050750
005635    1231  EYE=1.0                                                    R1050751
005637    1232  GO TO 1255                                                 R1050752
005640    1241  IF (NLK-1) 1246,1242,1246                                  R1050753
005642    1242  IF (VLN-VEL) 1246,1243,1246                                R1050754
005644    1243  IF (VKN-VEK) 1246,1244,1246                                R1050755
005646    1244  GELTA=3.0                                                  R1050756
005650    1245  GO TO 1247                                                 R1050757
005651    1246  GELTA=1.0                                                  R1050758
005653    1247  TEMP=2.0*AN/TEMPA                                          R1050759
005656    1250  SUMK=0.0                                                   R1050760
005657    5251  DO 5256 K=1,NINT                                           R1050761
005661    6254  TEMP5=AN/TEMPA                                             R1050762
005663    6255  IF (TEMP5-0.0001) 6256,5254,5254                           R1050763
005666    6256  TEMPT=1.0                                                  R1050764
005670    6257  GO TO 5255                                                 R1050765
```

```
005671      5254 TEMPT=1.0+TEMP*(1.0-XK(K))/XK(K)                          R1050766
005676      5255 SUMK=SUMK+(G(K)*GELTA/GFUNG(K))/TEMPT                     R1050767
005703      5256 CONTINUE                                                  R1050768
005705      1254 EYE=3.141592654*SUMK/(2.0*ENINT)                          R1050769
005711      1255 ENSIG(NLK,NN,NLKN)=ENSIG(NLK,NN,NLKN)+TEMPJ*              R1050770
                X                       TEMPAO*AN*EYE/TEMPA                R1050771
005724      1260 CONTINUE                                                  R1050772
005731      1261 CONTINUE                                                  R1050773
005734      1270 TEMP=FINAWT/D                                             R1050774
005736      1271 GSIG(NN)=TEMP*GSIG(NN)                                    R1050775
005741           DO 1272 IAF=1,NOK
005742      1272 FSIG(IAF,NN)=TEMP*FSIG(IAF,NN)
005751      1280 DO 1282 NLK=1,NMAX1                                       R1050778
005753      1281 DO 1282 NLKN=1,LMAX12                                     R1050779
005755      1282 ENSIG(NLK,NN,NLKN)=TEMP*ENSIG(NLK,NN,NLKN)                R1050780
005771           IF(KKK-7)334,334,3341                                     R1050781
005773      3341 GOTO1285                                                  R1050782
005774       334 ENSIG(1,NN,NN)=ENSIG(1,NN,NN)+TEMP*BBB(NN)*TEMPJ         R1050783
006004      1285 CONTINUE                                                  R1050784
            C                                                              R1050785
            C          SUM OVER INCIDENT CHANNELS                          R1050786
            C                                                              R1050787
006007      1300 GSIGE=0.0                                                 R1050788
006010           DO 1301 IAF=1,NOK
006012      1301 FSIGE(IAF)=0.0
006015      1305 DO   66 NN=1,LMAX12
006017           GSIGE=GSIGE+GSIG(NN)
006021           DO 399 IAF=1,NOK
006023       399 FSIGE(IAF)=FSIGE(IAF)+FSIG(IAF,NN)
006033        66 CONTINUE
006035      1310 DO 1314 NLK=1,NMAX1                                       R1050795
006037      1311 ENSIGE(NLK)=0.0                                           R1050796
006041      1312 DO 1314 NN=1,LMAX12                                       R1050797
006043      1313 DO 1314 NLKN=1,LMAX12                                     R1050798
006045      1314 ENSIGE(NLK)=ENSIGE(NLK)+ENSIG(NLK,NN,NLKN)                R1050799
            C                                                              R1050800
            C          WRITE OUTPUT MATRIX                                 R1050801
            C                                                              R1050802
006064       335 CONTINUE                                                  R1050803
006064       336 IF(IITP1-1)337,338,338                                    R1050804
006067       337 WRITEOUTPUTTAPE6,1370                                     R1050805
006073           GOTO1427
006074       338 CONTINUE
006074       342 WRITEOUTPUTTAPE6,8006                                     R1050812
006100           WRITEOUTPUTTAPE6,3013                                     R1050813
```

```
006104          IAFGH=2                                                  R1050814
006105          WRITEOUTPUTTAPE6,8006                                    R1050815
006111          M=0
006112          N=0
006113    1503  M=N+1
006115           N=M+9
006116          IF(N.GT.NOK)N=NOK
006121          DO343NN=1,LMAX12                                         R1050816
006123          CALLELKAY(NN,FLN,FKN)                                    R1050817
006125    343   WRITE(6,3014)FLN,FKN,GSIG(NN),(FSIG(IAF,NN),IAF=M,N)
006153    3014  FORMAT(* *,F5.2,X,F5.2,11(X,E9.3,X))
006153          WRITE(6,8006)
006156          IF(N.EQ.NOK)GO TO 1502
006160          GO TO 1503
006161    1502  CONTINUE
006161    3431  WRITEOUTPUTTAPE6,8006                                    R1050819
006165          IF (IOPTION) 345,3441,345
006166    3441  WRITE OUTPUT TAPE 6,3015
006172          DO346NLK=1,NMAX1                                         R1050821
006174          M=NLK-1                                                  R1050822
006176          IF(D-B(NLK))346,346,344                                  R1050823
006200     344  CONTINUE                                                 R1050824
006200          WRITEOUTPUTTAPE6,3016,M,B(NLK),ENSIGE(NLK)
006212          WRITEOUTPUTTAPE6,8006                                    R1050826
006216          DO345NN=1,LMAX12                                         R1050827
006220          CALLELKAY(NN,FLN,FKN)                                    R1050828
006222          WRITEOUTPUTTAPE6,3017,FLN,FKN,(ENSIG(NLK,NN,NLKN),       R1050829
               XNLKN=1,LMAX12)                                          R1050830
006245     345  CONTINUE                                                 R1050831
006250     346  CONTINUE                                                 R1050832
006253     347  CONTINUE                                                 R1050833
006253    1501  GO TO 7051
          C                                                             R1050860
          C          FORMAT STATEMENTS                                  R1050861
          C                                                             R1050862
006254      25  FORMAT (6E12.6)                                         R1050863
006254      26  FORMAT (6F12.8)                                         R1050864
006254      27  FORMAT (2X,F8.6,30X,2F10.6)                             R1050865
006254    1370  FORMAT(1H1)                                              R1050866
006254    3001  FORMAT(I3,1246)                                          R1050867
006254    3002  FORMAT(116H1
               XWILDCAT          DECEMBER,1966        LOVELAND-NEARREX      )
006254    3003  FORMAT(I5,4I2,2I1,2I2,F13.8,5I2,F5.2)
006254    3004  FORMAT(44H ENERGY LEVELS                    KC = I2)     R1050871
006254    3005  FORMAT(13H0A(GAMMA) =  F15.9)                            R1050872
```

```
006254      3009 FORMAT(10H0'BU(H) =  F8.4)                                                    R1050876
006254      3011 FORMAT(11H0ENERGY =  F20.8)                                                   R1050879
006254      3012 FORMAT(5H                                                    Q =  F8.5)       R1050880
006254      3013 FORMAT(54H0CROSS SECTIONS FOR    CAPTURE      FISSION      OTHER)            R1050881
006254      3015 FORMAT(30H0CROSS SECTIONS FOR SCATTERING)                                     R1050883
006254      3016 FORMAT(23H0EXCITED LEVEL NUMBER  I3,14H       W(N) =F10.6,20H                 R1050884
           X     SIGMA(N,E) =F14.8)                                                           R1050885
006254      3017 FORMAT(1H 2F5.2,5H     9F11.7/(16H              9F11.7))                      R1050886
006254      3018 FORMAT(26H SCATTERING CROSS SECTIONS)                                         R1050887
006254      3021 FORMAT(21H0OTHER CROSS SECTIONS)                                              R1050891
006254      3101 FORMAT(F12.8,2I2,2I1,F6.2,4F10.5)                                             R1050893
006254      3102 FORMAT(55H0  SIGMA         U          DELTA        ZPLS        ZMIN)         R1050894
006254      3913 FORMAT(26H TRANSMISSION COEFFICIENTS)                                         R1050895
006254      3914 FORMAT(1H 9F12.8)                                                             R1050896
006254      8006 FORMAT(1H0)                                                                   R1050897
006254      8008 FORMAT (8E15.6)                                                               R1050898
006254      8011 FORMAT (31H0E SUB J AND PI FOR PI POSITIVE)                                   R1050899
006254      8012 FORMAT (31H0E SUB J AND PI FOR PI NEGATIVE)                                   R1050900
006254      8027 FORMAT(12A6)                                                                  R1050901
006254      9105 FORMAT(1X,18H************ ERR = ,I4)                                         R1050902
            C                                                                                  R1050903
006254      9500 WRITE OUTPUT TAPE 6,9105,IERR                                                 R1050904
006262           MESS = 4H0HEL
            C
            C       CALC OF ANGULAR DISTRIBUTION
            C
006264      7051 DO 6999  I=1,NANGL
006266      6999 DIST(I) = 0.0
006271           NOK=NOKK
006273           DO 7004 IAF=1,NOK
006274      7001 DO 7002 J=1,LMAX12
006276           DO 7002 I=1,NANGL
006277           XI=I
006300           XXI = XJ(I)
006302           FXKAY=FKAY(IAF)
006304           IF (FXKAY - 1.5) 7016,7017,7018
006306      7016 DIST(I)=DIST(I)+FSIG(IAF,J)*W1(J,I)
006316           GO TO 7002
006317      7017 DIST(I)=DIST(I)+FSIG(IAF,J)*W2(J,I)
006327           GO TO 7002
006330      7018 IF(FXKAY -3.5)7019,1211,8123
006333      7019 DIST(I)=DIST(I)+FSIG(IAF,J)*W3(J,I)
006343           GO TO 7002
006344      1211 DIST(I)=DIST(I)+FSIG(IAF,J)*W4(J,I)
006354           GO TO 7002
```

```
006355     8123 IF(FKAY-5.5)8120,8121,7002
006360     8120 DIST(I)=DIST(I)+FSIG(IAF,J)*W5(J,I)
006370          GO TO 7002
006371     8121 DIST(I)=DIST(I)+FSIG(IAF,J)*W6(J,I)
006401     7002 CONTINUE
006406     7004 CONTINUE
           C
           C       CALCULATION OF STATISTICAL ANGULAR DISTRIBUTION
           C
006411          IF(JSTAT.EQ.0)GO TO 4008
006412          DO 4009 KX=KXX,IAFF
006414          LD=(KX-KXX)/2 +1
006417          DO 4009 LK=1,LMAX12
006421          DO 2002 I=1,NANGL
006422          DIST(I)=DIST(I)+FSIG(KX,LK)*WS(LD,LK,I)
006435     2002 CONTINUE
006437     4009 CONTINUE
006444     4008 CONTINUE
           C
           C       OUTPUT ANGULAR DISTRIBUTION DATA
           C
006444          WRITE OUTPUT TAPE 6,7012
006450     7012 FORMAT(40H0  FISSION FRAGMENT ANGULAR DISTRIBUTION)
006450          WRITE OUTPUT TAPE 6,7013
006454     7013 FORMAT(21H0    THETA      DIST(I))
006454          DO 7015  I=1,NANGL
006456          XI=I
006457          XXI=XJ(I)
006461          WRITE OUTPUT TAPE 6,7014,XXI,DIST(I)
006470     7014 FORMAT(2F10.5)
006470     7015 CONTINUE
006473          DO 7041  I=1,NANGL
           C                                                          R1050834
           C            WRITE OUTPUT SUMMARY                          R1050835
           C                                                          R1050836
006474     7041 WCALC(NIE,I)  = DIST(I)
006503          IF(JSTAT.EQ.1)NOK=IAFF
006507     1427 GSIGN(NIE)=GSIGE                                      R1050837
006511          DO 1428 IAF=1,NOK
006513     1428 FSIGN(NIE,IAF)=FSIGE(IAF)
006522     3025 FORMAT(1H 10F11.7)
006522     1430 DO 1431 NLK=1,NMAX1                                   R1050840
006524     1431 ENSIGN(NIE,NLK)=ENSIGE(NLK)                           R1050841
006533     1432 ESUBP(NIE)=0                                          R1050842
006535          WRITEOUTPUTTAPE6,1370                                 R1050843
```

```
006541          IF (LEVDEN)3432,4000,3432
006542     3432 IF(NIE-NE)186,348,348                                    R1050844
006545     4000 IF(NIE-NE)1135,348,348
006550      348 CONTINUE                                                 R1050845
            C
            C       COMPUTATION OF CHI-SQUARE
            C
006550          CHISQS =0.0
006551          CHISQW =0.0
006552          EXPSUM=0.0
006553          CALSUM=0.0
006554          DO  7062   I=1,NE
006555          DO 7061  K=1,NANGL
006556          J = K
006557          EXPSUM = EXPSUM + WEXP(I,J)
006564          CALSUM = CALSUM + WCALC(I,J)
006567     7061 CONTINUE
006571          XXXX =EXPSUM/CALSUM
006572          DO 7070 K=1,NANGL
006574          J=K
006575     7070 CONTINUE
006577          DO 7062  K=1,NANGL
006601          J = K
006602          CHISQW=((WCALC(I,J)-WEXP(I,J))**2)/(SIGMAW(I,J)**2)+CHISQW
006613          CWCALC(I,J)= WCALC(I,J)
006617          EXPSUM =0.0
006617          CALSUM =0.0
006620     7062 CONTINUE
006625          DO 7065 I=1,NE
006627          SIGTO(I)=0.0
006630          DO 7065 IAF=1,NOK
006632          SIGTO(I)=SIGTO(I)+FSIGN(I,IAF)
006637     7065 CONTINUE
006644          DO 7066 I=1,NE
006645          CSS(I)   =  ((SIGTO(I)-SIGMAF(I))**2)/(USIGMF(I)**2)
006652          CHISQS = CHISQS + CSS(I)
006654     7066 CONTINUE
            C
            C       WRITE ITERATION OUTPUT
            C
006656          DO 1866 I=1,NE
006660          WRITE OUTPUT TAPE 6,8006
006663          DO 1866    J=1,NANGL
006665          XXJ=XJ(J)
006667     1866 WRITE OUTPUT TAPE 6,7014,XXJ,CWCALC(I,J)
```

```
006705           WRITE OUTPUT TAPE 6,7067
006711     7067 FORMAT(37H0  CHI SQUARE SIGMA   CHI SQUARE DIST)
006711           WRITE OUTPUT TAPE 6,7068,CHISQS,CHISQW
006721     7068 FORMAT(2E20.5)
           C
006721      349 WRITEOUTPUTTAPE6,3018                                  R1050846
006725           WRITE(6,8006)
006731           M=0
006732           N=0
006733      503  M=N+1
006735           N=M+4
006736           WRITE(6,8006)
006742           IF(N-NE)505,505,507
006745      507  N=NE
006747      505  WRITE(6,3020)(ESUBP(NIE),NIE=M,N)
006762     3020 FORMAT(* *,*ENERGY*,6X,5(F11.7,5X))
006762           WRITE(6,8006)
006766           DO 508 NLK=1,NMAX1
006770           LLL=NLK
006771           IF(NLK.GT.(NMAX*2))LLL=INT(HI(NLK))
006776      355  WRITE(6,3023)LLL,(ENSIGN(NIE,NLK),NIE=M,N)
007015     3023 FORMAT(* *,*LEVEL*,X,I2,4X,5(F11.7,5X))
007015      508  CONTINUE
007020           DO 514 NIE=M,N
007022           TOTAL(NIE)=0.0
007023           DO 514 NLK=1,NMAX1
007025      514  TOTAL(NIE)=TOTAL(NIE)+ENSIGN(NIE,NLK)
007037           WRITE(6,516)(TOTAL(NIE),NIE=M,N)
007051      516  FORMAT(* *,*TOTAL*,7X,5(F11.7,5X))
007051           IF(N.EQ.NE)GO TO 510
007053           GO TO 503
007054      510  CONTINUE
007054           IF(IAFGH-1)351,352,352                                R1050851
007057      351 GOTO 301
007060      352 WRITEOUTPUTTAPE6,8006                                  R1050853
007064           M=0
007065           N=0
007066     1215 M=N+1
007070           N=M+7
007071           IF(N.GT.NOK)N=NOK
007074           WRITE(6,3022)(NFTR(I),I=M,N)
007107     3022 FORMAT(* *,3X,*ENERGY*,5X,*CAPTURE*,4X,10(*FISSION*,X,I2,X))
007107           WRITEOUTPUTTAPE6,8006                                 R1050855
007113      353 DO354NIE=1,NE                                         R1050856
007115      354  WRITE(6,3025)ESUBP(NIE),GSIGN(NIE),(FSIGN(NIF,IAF),IAF=M,N)
```

```
007137          WRITE(6,8006)
007142          IF(N.EQ.NOK)GO TO 1214
007144          GO TO 1215
007145    1214  CONTINUE
007145          WRITE(6,8705)
007151    8705  FORMAT(* *,20X,*ENERGY*,5X,*FISSION TOTAL*)
007151          WRITE(6,8006)
007155          DO 8730 NIE=1,NE
007157          TOTAL1=0.0
007160          DO 8731 IAF=1,NOK
007162    8731  TOTAL1=TOTAL1+FSIGN(NIE,IAF)
007171    8730  WRITE(6,1216)ESUBP(NIE),TOTAL1
007204    1216  FORMAT(* *,17X,F11.7,4X,F11.7)
007204          GO TO 301
007204          END                                                    R1050907
```

```
                SUBROUTINE WKJ(NANGLE)
          CC
          CC      PREPARE TABLES W(K,J)  FOR PROGRAM WILDCAT
          CC
000003            DIMENSION D(2)
000003            COMMON/C/XI(9),W1(19,9),W2(19,9),W3(19,9),W4(19,9),W(19,19,10)
                 X,W5(19,9),W6(19,9)
000003            REAL K,J,M
000003            DO 55 IY=1,NANGLE
000005            Y=XI(IY)
000007            IF(XI(IY).EQ.0.0)Y=0.0001
000011            IMAX=IMAX1=IMAX2=30
000014            DO 40 KI=1,19
000016            K=FLOAT(KI)-0.5
000020            X=0.0
000021            J=-0.5
000023            DO 45 JI=1,19,2
000024            J=J+1.0
000026            IF(J.LT.K)GO TO 30
000030            DO 50 MK=1,2
000032            IF(MK.EQ.1)M=0.5
000035            IF(MK.EQ.2)M=-0.5
000041            IMAX=30
000042            DEN1=DEN2=DEN3=DEN4=1.0
000047            X=0.0
000050         28 IFLAG=0
000051            DEN1=J-K-X
000054            DEN2=J+M-X
000057            DEN3=X+K-M
000061            DEN4=X
000062            IF(DEN1)20,21,22
000064         21 IFLAG=1
000065         22 IF(DEN2)20,23,24
000067         23 IFLAG=1
000070         24 IF(DEN3)20,25,26
000072         26 IF(X.EQ.0.0)DEN4=1.0
000075            IF(IFLAG.EQ.1)GO TO 27
000077            X=X+1.0
000101            GO TO 28
000102         27 IMAX=INT(X+1.0)
000105            SUM=0.0
000106            DO 4 IE=1,IMAX
000107            X=FLOAT(IE-1)
000111            DEN1=J-K-X
```

```
000114          DEN2=J+M-K
000117          DEN3=K+K-M
000121          DEN4=K
000122          CALL FACT(DEN1,IMAX1,PROD1)
000124          CALL FACT(DEN2,IMAX1,PROD2)
000127          CALL FACT(DEN3,IMAX1,PROD3)
000132          CALL FACT(DEN4,IMAX1,PROD4)
000135          DENOM=PROD1*PROD2*PROD3*PROD4
000141          IF(DENOM.EQ.0.0)GO TO 20
000142          SEC=2.0*J-K+M-2.0*X
000150          PRIM=K-M+2.0*X
000152          AN1=SIN(Y/2.0)
000157          AN2=COS(Y/2.0)
000163          ANUM=(AN1**PRIM)*(AN2**SEC)*(-1)**INT(X)
000201          SUM=SUM+ANUM/DENOM
000203      4   CONTINUE
000207          FAC1=J+M
000211          FAC2=J-M
000212          FAC3=J+K
000214          FAC4=J-K
000215          CALL FACT(FAC1,IMAX2,PRO1)
000220          CALL FACT(FAC2,IMAX2,PRO2)
000223          CALL FACT(FAC3,IMAX2,PRO3)
000226          CALL FACT(FAC4,IMAX2,PRO4)
000231          FACTOR=(PRO1*PRO2*PRO3*PRO4)**0.5
000237     50   D(MK)=ABS(FACTOR*SUM)
000245          W(KI,JI,IY)=0.25*(2.0*J+1.0)*(D(1)**2+D(2)**2)
000262          GO TO 45
000262     30   W(KI,JI,IY)=0.0
000270     45   W(KI,JI+1,IY)=W(KI,JI,IY)
000303     40   CONTINUE
000305     55   CONTINUE
000310          DO 39 I=1,MANGLE
000311          DO 39 JI=1,19
000312          W1(JI,I)=W(1,JI,I)
000321          W2(JI,I)=W(2,JI,I)
000327          W3(JI,I)=W(3,JI,I)
000335          W4(JI,I)=W(4,JI,I)
000343          W5(JI,I)=W(5,JI,I)
000351          W6(JI,I)=W(6,JI,I)
000357     39   CONTINUE
000362          RETURN
000363     20   WRITE(6,1)X
000371      1   FORMAT(* *,*X ERROR= *,F6.3)
000371          END
```

```
                SUBROUTINE FACT(FACTOR,IMAXS,PROD)
000006          PROD=FACTOR
000006           IF(FACTOR-1.0)1,1,2
000011        2 DO 3 I2=1,IMAXS
000013          IF(FACTOR-FLOAT(I2))4,4,5
000015        5 PROD=PROD*(FACTOR-FLOAT(I2))
000020        3 CONTINUE
000022          GO TO 4
000022        1 PROD=1.0
000023        4 RETURN
000024          END
```

```
                SUBROUTINE PHI(DELTA,E,U,PHIUE)                                  R1050927
000007        5 TEMP=(.5747)*(U+E)/DELTA                                         R1050928
000012       10 TEMPR=SQRT(TEMP)
000015       15 XINV=1.0/TEMPR                                                  R1050930
000017       20 POLY4=1.0+XINV*(XINV*(45.0-105.0*XINV*(1.0-      XINV))-10.0)   R1050931
000030       25 TEMP1=TEMP*TEMP                                                 R1050932
000032       30 TEMP2=EXP(TEMPR)
000035       35 PHIUE=TEMP1*TEMP2*POLY4                                         R1050934
000042       40 RETURN                                                          R1050935
000043          END                                                             R1050936
```

```
                SUBROUTINE PSI (E,U,EJPI,DELTA,PSIBAR)                  R1050937
C                                                                       R1050938
000010      5 X=SQRT(6.57975*(U+E)/DELTA)
000021     10 XJPI=SQRT(6.57975*(U+EJPI)/DELTA)
000032     15 TEMP1=XJPI/X                                              R1050941
000034     17 TEMP1=TEMP1*TEMP1                                         R1050942
000035     20 TEMP2=1.0-TEMP1                                           R1050943
000037     25 TEMP3=TEMP2*TEMP2                                         R1050944
000041     30 TEMP4=TEMP3*TEMP2                                         R1050945
000043     35 TEMP5=X*X                                                 R1050946
000045     40 TEMP6=TEMP5*TEMP5                                         R1050947
000047     45 TEMP7=TEMP5*TEMP6                                         R1050948
000051     50 TEMP17=7.0*TEMP1                                          R1050949
000053     55 TEMP37=3.0-TEMP17                                         R1050950
000055     60 TEMP17=1.0-TEMP17                                         R1050951
000057     65 TEMP=TEMP4-TEMP3*TEMP17/XJPI-6.0                          R1050952
             X      *TEMP2*TEMP37/TEMP5+6.0*(3.0-                      R1050953
             X      TEMP1*(30.0-35.0*TEMP1))/(XJPI*                    R1050954
             X      TEMP5)                                             R1050955
000100     70 TEMPE=120.0*(TEMP37-3.0*TEMP17/XJPI)/                     R1050956
             X      TEMP6-5040.0*(1.0-1.0/XJPI)/TEMP7                  R1050957
000113     75 TEMP8=EXP(XJPI)
000116     80 PSIBAR=TEMP8*(TEMP+TEMPE)*(TEMP5*                        R1050959
             X      XJPI**5.0)/48.0                                    R1050960
000131     85 RETURN                                                    R1050961
000132        END                                                       R1050962
```

```
                SUBROUTINE ANEJLK (VJ,VK,VL,VI,PIE,PIEN,                R1050963
               X                   E,WOFN,AOFN)                         R1050964
000014      5 IF (E-WOFN) 10,15,15                                        R1050965
000020     10 AOFN=0.0                                                    R1050966
000021     11 GO TO 55                                                    R1050967
000022     15 TEMP=ABS(VJ-VI)
000025     20 IF (TEMP-VK) 25,25,10                                       R1050969
000030     25 IF (VK-VJ-VI) 30,30,10                                      R1050970
000033     30 TEMP=ABS(PIEN-PIE)
000036     31 IF (TEMP-0.25) 35,32,45                                     R1050972
000041     32 IERR=32                                                     R1050973
000042        GO TO 9500                                                  R1050974
000043     35 ITEMP=XINTF(VL+0.25)                                        R1050975
000054     36 ITEMP=XMODF(ITEMP,2)                                        R1050976
000060     37 IF (ITEMP-1) 38,10,40                                       R1050977
000066     38 AOFN=1.0                                                    R1050978
000070     39 GO TO 55                                                    R1050979
000071     40 IERR=40                                                     R1050980
000072        GO TO 9500                                                  R1050981
000073     45 TEMP=ABS(PIEN+PIE)
000076     46 IF (TEMP-0.25) 50,32,47                                     R1050983
000101     47 IERR=47                                                     R1050984
000102        GO TO 9500                                                  R1050985
000103     50 ITEMP=XINTF(VL+0.25)                                        R1050986
000114     51 ITEMP=XMODF(ITEMP,2)                                        R1050987
000120     52 IF (ITEMP-1) 10,38,40                                       R1050988
000127     55 RETURN                                                      R1050989
000130   9500 WRITE OUTPUT TAPE 6,9105,IERR                               R1050990
000136        MESS = 4HOHEL
000140   9105 FORMAT(1X,18H********** ERR = ,I4)                         R1050993
000140        END                                                         R1050994
```

```
                FUNCTION EVAL2(U,AE,A,J,W,SIGMA2)
000011          REAL J
000011          V=(1.0/(2.0*SIGMA2))*(J+0.5)**2
000015          C=2.0*SQRT(AE*U)
000025          D=C-V-W
000030          CONST0=(12.0*(AE**0.25)*(U      **1.25))**(-1.0)
000043          CONSTJ=(2.0*J+1)/(SQRT(8.0        )*(SIGMA2**1.5))
000060          EVAL2=CONST0*CONSTJ*EXP(D)
000065          RETURN
000065          END
```

```
                SUBROUTINE PELK(FPELK,EN,VLN,VKN,ALPHA,BETA,LN1)                R1050995
000012          5 TEMP=(ALPHA-BETA*(VKN*(VKN+1.0)-VLN*(VLN+1.0)-0.75))          R1050996
000022         10 Y=EN*TEMP*TEMP                                                R1050997
000024         11 YINV=1.0/Y                                                    R1050998
000026         15 GO TO (20,25,30,35,40,45,50,55,60),LN1                        R1050999
000043         20 ALNY=1.0                                                      R1051000
000045         21 GO TO 70                                                      R1051001
000046         25 ALNY=1.0+YINV                                                 R1051002
000050         26 GO TO 70                                                      R1051003
000051         30 ALNY=1.0+YINV*(3.0+9.0*YINV)                                  R1051004
000056         31 GO TO 70                                                      R1051005
000057         35 ALNY=1.0+YINV*(6.0+YINV*(45.0+225.0*YINV))                    R1051006
000066         36 GO TO 70                                                      R1051007
000067         40 ALNY=1.0+YINV*(10.0+YINV*(135.0+YINV*(1575.0+                 R1051008
                X       11025.0*YINV)))                                        R1051009
000100         41 GO TO 70                                                      R1051010
000101         45 ALNY=1.0+YINV*(15.0+YINV*(315.0+YINV*(6300.0+                 R1051011
                X       YINV*(99225.0+893025.0*YINV))))                        R1051012
000114         46 GO TO 70                                                      R1051013
000115         50 ALNY=1.0+YINV*(21.0+YINV*(630.0+YINV*(18900.0+                R1051014
                X       YINV*(496125.0+YINV*(9823275.0+                        R1051015
                X       10405603.0E1*YINV)))))                                 R1051016
000132         51 GO TO 70                                                      R1051017
000133         55 ALNY=1.0+YINV*(28.0+YINV*(1134.0+YINV*(47250.0+               R1051018
                X       YINV*(1819125.0+YINV*(58939650.0+YINV*                 R1051019
                X       (140472S3.0E2+18261468.0E3*YINV))))))                  R1051020
000152         56 GO TO 70                                                      R1051021
000153         60 ALNY=1.0+YINV*(36.0+YINV*(1890.0+YINV*(103950.0+              R1051022
                X       YINV*(5457375.0+YINV*(25540515.0E1+                    R1051023
                X       YINV*(98330983.0E2+YINV*(27392202.0E4+                 R1051024
                X       41088304.0E5*YINV)))))))                               R1051025
000174         70 TEMPR=SQRT(Y)
000177         75 FPELK=TEMPR/ALNY                                              R1051027
000204         80 RETURN                                                        R1051028
000205            END                                                           R1051029
```

```
                SUBROUTINE PROD (ASUBN,AE,XK1,DBPROD)                    R1051030
000007      11  IF (ASUBN-1.0E-25) 14,14,112                             R1051031
000012     112  TEMP=ASUBN/AE                                            R1051032
000014     113  IF (TEMP-0.0001) 14,5,5                                  R1051033
000017       5  TEMPX=(1.0-XK1)/XK1                                      R1051034
000021      10  TEMPA=2.0/AE                                            R1051035
000023      12  DBPROD=SQRT(1.0+TEMPA*ASUBN*TEMPX)
000033      13  GO TO 40                                                R1051037
000034      14  DBPROD=1.0                                              R1051038
000035      40  RETURN                                                   R1051039
000036          END                                                      R1051040
```

```
                FUNCTION XINTF(X)
000003          XINTF = X
000004          RETURN
000005          END
```

```
                    SUBROUTINE ELKAY(NN,FLN,FKN)                          R1050908
000006          1   TEMP=FLOAT(NN)
000010          5   TEMP1=TEMP/2.0                                        R1050910
000012         10   TEMP2=(TEMP-1.0)/2.0                                  R1050911
000015         15   ITEMP=XMODF(NN,2)                                     R1050912
000023         20   IF (ITEMP-1) 45,30,25                                 R1050913
000026         25   IERR=25                                               R1050914
000027              GO TO 9500                                            R1050915
000030         30   FLN=TEMP2                                             R1050916
000031         35   FKN=TEMP1                                             R1050917
000032         40   GO TO 55                                              R1050918
000033         45   FLN=TEMP1                                             R1050919
000034         50   FKN=TEMP2                                             R1050920
000035         55   RETURN                                                R1050921
000036       9500   WRITE OUTPUT TAPE 6,9105,IERR                         R1050922
000044              MESS = 4HOHEL
000046       9105   FORMAT(1X,18H********** ERR = ',I4)                   R1050925
000046              END                                                   R1050926
```

```
                FUNCTION XMODF(K,L)
000005          XMODF = K - (K/L)*L
000012          RETURN
000012          END
```

```
                      SUBROUTINE DISTAT(LMAX,EMIN,EMAX,HBARO,K02,D,EX,AE,HBOTI,E0,
                     XTEMP,A,IMAX,EREL,AFFCTN,A1,A2,A3)
                     C
                     C    CALCULATION OF COMP TRANSMISSION COEFF FOR FISSION
                     C
000025                    DIMENSION E(50)
000025                    COMMON/R/SIGMAF(20,20)
000025                    REAL K,J,K02
000025                    HBAR=1.06E-27
000026                    H=(EMAX-EMIN)/FLOAT(IMAX)
000031                    SIGMA2=TEMP/(2.0*HBOTI)
000034                    E(1)=EMIN+H
000036                    DO 1 I=2,IMAX
000040                    E(I)=E(I-1)+H
000043                1   CONTINUE
000045                    K1=LMAX+1
000047                    DO 78 KX=1,20
000050                    DO 78 LK=1,20
000051               78   SIGMAF(KX,LK)=0.0
000061                    FKN=-0.5
000062                    DO 50 LK=1,K1
000064                    FKN=FKN+1.0
000066                    SUMNOR=0.0
000067                    K=-0.5
000070                    DO 30 KX=1,LK
000072                    K=K+1.0
000074                    SUMNOR=SUMNOR+2.0*EXP(-(K**2)/(2.0*K02))
000107               30   CONTINUE
000111                    K=-0.5
000113                    DO 61 KX=1,LK
000114                    K=K+1.0
000116                    N=(K**2)/(2.0*K02)
000121                    J=FKN
000122                    TEMPJ=2.0*FKN+1.0
000125                    NINT=IMAX/2
000127                    YEVEN=YODD=0.0
000131                    YSUMO=YSUME=0.0
000133                    DO 2 N=1,NINT
000134                    I=N-1
000136                    KO=2*I+1
000137                    KE=2*I+2
000141                    EP=E(KO)
000143                    EB=E(KE)
000145                    IF(EP-EX)10,10,15
```

```
000150      10  RHO=EVAL1(EP,E0,SIGMA2,TEMP,J,W)/2.0
000157          GO TO 20
000163      15  IF(AFFCTN.EQ.1.0)AE=A1+A2*EXP(-A3*EP)
000202          FILL=A2*A3*EXP(-A3*EP)
000211          TINV=FILL*(1.0/(4*AE)-SQRT(EP/AE))+SQRT(AE/EP)-1.25/EP
000232          SIGMA2=1.0/(2.0*TINV*HBOTI)
000236          RHO=EVAL2(EP,AE,A,J,W,SIGMA2)/2.0
000245      20  Y=(EP-D+EREL)*(6.2832/HBARO)
000257          DENOM=1.0+EXP(Y)
000262          YODD=RHO/DENOM
000264          YSUMO=YSUMO+4.0*YODD
000266          IF(EB-EX)25,25,31
000275      25  RHO=EVAL1(EB,E0,SIGMA2,TEMP,J,W)/2.0
000304          GO TO 35
000310      31  IF(AFFCTN.EQ.1.0)AE=A1+A2*EXP(-A3*EB)
000327          FILL=A2*A3*EXP(-A3*EB)
000336          TINV=FILL*(1.0/(4*AE)-SQRT(EB/AE))+SQRT(AE/EB)-1.25/EB
000357          SIGMA2=1.0/(2.0*TINV*HBOTI)
000363          RHO=EVAL2(EB,AE,A,J,W,SIGMA2)/2.0
000372      35  Y=(EB-D+EREL)*(6.2832/HBARO)
000404          DENOM=1.0+EXP(Y)
000407          YEVEN=RHO/DENOM
000411          IF(N.EQ.NINT)YEVEN=YEVEN/2.0
000420          YSUME=YSUME+YEVEN*2.0
000423       2  CONTINUE
000425          SIGMAF(KX,LK)=(H/3.0)*(YSUME+YSUMO)*2.0/SUMNOR
000436      61  CONTINUE
000440      60  CONTINUE
000442          RETURN
000443          END
```

```
                FUNCTION EVAL1(EJ,E0,SIGMA2,TEMP,J,W)
000011          REAL J
000011          T=TEMP
000011          V=(1.0/(2.0*SIGMA2))*(J+0.5)**2
000016          C=(EJ-E0)/T
000020          D=C-V-W
000023          CONSTJ=(2.0*J+1)/(2.0*SIGMA2)
000027          EVAL1=CONSTJ*EXP(D)/T
000034          RETURN
000034          END
```

RA-226 SLOW NEUTRON FISSION

ENERGY LEVELS KC = 0

7
A(GAMMA) = .000200000

SIGMA	U	DELTA	ZPLS	ZMIN
6.00000000	4.53000000	.07000000	1.00000000	1.00000000

ENU(K)	K	PSP	PSM	EZERO(K)	HBARO(K)	HBOTI(K)	ALPHA(K)
1.0	1.5	0.0	1.0	3.65000	.4000	.00200	-2.0000
1.0	.5	1.0	0.0	3.67500	.7500	.00200	2.0000
1.0	2.5	0.0	1.0	3.80000	.4000	.00200	-0.0000
1.0	.5	0.0	1.0	3.88000	.1500	.00200	2.0000
1.0	1.5	0.0	1.0	3.97500	.4000	.00200	-0.0000

.00060 .00003
.00140 .00003
.00200 .00003

EXPERIMENTAL DATA

THIS IS ENERGY NO. 1

ANGLE	WEXP	SIGMA
.175	.00044040	.00005340
.350	.00035520	.00005340
.610	.00033040	.00004500
.785	.00035520	.00005340
1.048	.00024840	.00004380
1.305	.00024840	.00004380
1.570	.00027360	.00004350

THIS IS ENERGY NO. 2

ANGLE	WEXP	SIGMA
.175	.00054500	.00008240
.350	.00073130	.00008240
.610	.00078280	.00008240
.785	.00082710	.00008240
1.048	.00063650	.00007670
1.305	.00060770	.00007670
1.570	.00073130	.00007670

THIS IS ENERGY NO. 3

ANGLE	WEXP	SIGMA
.175	.00135100	.00015400
.350	.00145100	.00015400
.610	.00129800	.00013300
.785	.00113600	.00013300
1.048	.00113600	.00013300
1.305	.00078500	.00011100
1.570	.00054000	.00005400

ENERGY = 3.000000J0

Q = 0.00000

ENERGY LEVELS ARE IN THE CONTINUUM

TRANSMISSION COEFFICIENTS

F-TRANS(1)	F-TRANS(2)	F-TRANS(3)	F-TRANS(4)	F-TRANS(5)	F-TRANS(
0.	1.123E-01	0.	2.867E-06	0.	
9.187E-02	1.111E-01	0.	2.637E-06	7.833E-04	
8.196E-02	1.075E-01	1.014E-02	2.051E-06	6.698E-04	
6.931E-02	1.016E-01	8.190E-03	1.349E-06	5.378E-04	
5.520E-02	9.370E-02	6.213E-03	7.509E-07	4.056E-04	
4.116E-02	8.405E-02	4.424E-03	3.534E-07	2.872E-04	
2.861E-02	7.316E-02	2.955E-03	1.407E-07	1.910E-04	

CROSS SECTIONS FOR		CAPTURE	FISSION	OTHER		
0.00	.50	4.644E-04	0.	6.444E-05	0.	0.	0.
1.00	.50	7.541E-04	0.	0.	0.	2.667E-09	0.
1.00	1.50	1.540E-03	7.052E-05	0.	0.	2.598E-09	7.718E-07
2.00	1.50	3.754E-04	0.	6.289E-05	0.	0.	0.
2.00	2.50	1.354E-03	0.	6.698E-05	0.	0.	0.
3.00	2.50	2.269E-03	8.558E-05	0.	1.059E-05	2.142E-09	6.993E-07
3.00	3.50	3.141E-03	8.277E-05	0.	9.781E-06	1.612E-09	6.423E-07
4.00	3.50	1.145E-03	0.	4.426E-05	0.	0.	0.
4.00	4.50	1.502E-03	0.	4.849E-05	0.	0.	0.
5.00	4.50	3.554E-04	1.643E-05	0.	1.851E-06	2.238E-10	1.209E-07
5.00	5.50	1.100E-03	1.515E-05	0.	1.628E-06	1.301E-10	1.057E-07
6.00	5.50	1.215E-04	0.	3.418E-06	0.	0.	0.
6.00	6.50	1.520E-04	0.	3.817E-06	0.	0.	0.

FISSION FRAGMENT ANGULAR DISTRIBUTION

THETA	DIST(1)
.17500	.00043
.35000	.00042
.61000	.00038
.78500	.00034
1.04800	.00028
1.30500	.00025
1.57000	.00025

ENERGY = 3.50000000 Q = 0.00000

ENERGY LEVELS ARE IN THE CONTINUUM

TRANSMISSION COEFFICIENTS

F=TRANS(1)	F=TRANS(2)	F=TRANS(3)	F=TRANS(4)	F=TRANS(5)	F=TRANS(
0.	2.379E-01	0.	1.195E-02	0.	
2.878E-01	2.360E-01	0.	1.102E-02	1.717E-02	
2.831E-01	2.323E-01	1.375E-01	8.640E-03	1.479E-02	
2.756E-01	2.275E-01	1.205E-01	5.738E-03	1.198E-02	
2.640E-01	2.197E-01	1.003E-01	3.219E-03	9.114E-03	
2.466E-01	2.092E-01	7.820E-02	1.523E-03	6.507E-03	
2.214E-01	1.955E-01	5.655E-02	6.081E-04	4.356E-03	

CROSS SECTIONS FOR		CAPTURE	FISSION	OTHER		
0.00	.50	4.298E-04	0.	8.510E-05	0.	0.	0.
1.00	.50	6.752E-04	0.	0.	0.	6.748E-06	0.
1.00	1.50	1.471E-03	1.718E-04	0.	0.	6.581E-06	1.025E-05
2.00	1.50	8.038E-04	0.	8.258E-05	0.	0.	0.
2.00	2.50	1.235E-03	0.	8.951E-05	0.	0.	0.
3.00	2.50	2.040E-03	1.797E-04	0.	8.726E-05	5.484E-06	9.385E-06
3.00	3.50	2.815E-03	1.995E-04	0.	8.732E-05	4.153E-06	8.670E-06
4.00	3.50	1.135E-03	0.	6.643E-05	0.	0.	0.
4.00	4.50	1.493E-03	0.	7.594E-05	0.	0.	0.
5.00	4.50	8.734E-04	5.373E-05	0.	2.042E-05	6.552E-07	1.855E-06
5.00	5.50	1.106E-03	6.163E-05	0.	1.956E-05	3.810E-07	1.628E-06
6.00	5.50	1.544E-04	0.	7.302E-06	0.	0.	0.
6.00	6.50	1.919E-04	0.	8.711E-06	0.	0.	0.

FISSION FRAGMENT ANGULAR DISTRIBUTION

THETA	DIST(I)
.17500	.00072
.35000	.00082
.61000	.00072
.78500	.00075
1.04800	.00065
1.30500	.00063
1.57000	.00058

ENERGY = [illegible] Q = 0.00000

ENERGY LEVELS ARE IN THE CONTINUUM

TRANSMISSION COEFFICIENTS

E-TRANS(1)	E-TRANS(2)	E-TRANS(3)	E-TRANS(4)	E-TRANS(5)	E-TRANS(
0.	2.772E-01	0.	2.291E-01	0.	
3.116E-01	2.766E-01	0.	2.237E-01	6.846E-02	
3.104E-01	2.747E-01	2.500E-01	2.061E-01	6.040E-02	
3.085E-01	2.715E-01	2.375E-01	1.742E-01	5.037E-02	
3.054E-01	2.655E-01	2.192E-01	1.280E-01	3.951E-02	
3.003E-01	2.597E-01	1.943E-01	7.651E-02	2.902E-02	
2.918E-01	2.504E-01	1.624E-01	3.561E-02	1.990E-02	

CROSS SECTIONS FOR		CAPTURE	FISSION	OTHER		
0.00	.50	4.0[illegible]E-04	0.	7.807E-05	0.	0.	0.
1.00	.50	6.382E-04	0.	0.	0.	1.007E-04	0.
1.00	1.50	1.2[illegible]E-03	1.447E-04	0.	0.	1.039E-04	3.179E-05
2.00	1.50	7.677E-04	0.	7.618E-05	0.	0.	0.
2.00	2.50	1.178E-03	0.	8.303E-05	0.	0.	0.
3.00	2.50	1.925E-03	1.532E-04	0.	1.234E-04	1.018E-04	2.982E-05
3.00	3.50	2.653E-03	1.734E-04	0.	1.335E-04	9.793E-05	2.832E-05
4.00	3.50	1.130E-03	0.	6.504E-05	0.	0.	0.
4.00	4.50	1.474E-03	0.	7.546E-05	0.	0.	0.
5.00	4.50	8.805E-04	5.161E-05	0.	3.706E-05	2.163E-05	6.678E-06
5.00	5.50	1.112E-03	5.223E-05	0.	4.027E-05	1.586E-05	6.014E-06
6.00	5.50	1.673E-04	0.	8.194E-06	0.	0.	0.
6.00	6.50	2.038E-04	0.	1.005E-05	0.	0.	0.

FISSION FRAGMENT ANGULAR DISTRIBUTION

THETA	DIST(I)
.17500	.00123
.35000	.00123
.61000	.00113
.78500	.00101
1.04800	.00088
1.30500	.00079
1.57000	.00076

.17500	.00044
.35000	.00042
.61000	.00035
.78500	.00034
1.04800	.00029
1.30500	.00025
1.57000	.00025

.17500	.00072
.35000	.00068
.61000	.00062
.78500	.00060
1.04800	.00055
1.30500	.00053
1.57000	.00054

.17500	.00123
.35000	.00123
.61000	.00113
.78500	.00101
1.04800	.00094
1.30500	.00079
1.57000	.00075

CHI SQUARE SIGMA CHI SQUARE DIST
3.44313 29.95504

SCATTERING CROSS SECTIONS

ENERGY	3.6000000	3.8000000	3.9000000
LEVEL 1	.0256783	.0243898	.0237110
LEVEL 2	.0208624	.0194585	.0194697
LEVEL 3	.1855429	.1761979	.1715352
LEVEL 4	.1530507	.1459124	.1425456
LEVEL 5	.3552002	.3471153	.3387023
LEVEL 6	.2854475	.2745285	.2696440
LEVEL 7	.4333283	.4164373	.4091124
LEVEL 8	.3523234	.3445468	.3414869
LEVEL 9	.3755645	.3697729	.3682776
LEVEL 10	.3051163	.3063935	.3091824
LEVEL 11	.2339376	.2355612	.2389571
LEVEL 12	.1926804	.2012853	.2063360
LEVEL 13	.0933179	.1059446	.1101082
LEVEL 14	.0913194	.0993461	.1034479
LEVEL 15	.0351333	.0435754	.0414883
LEVEL 16	.0255615	.0296771	.0317747
LEVEL 17	.0052734	.0061858	.0066351
LEVEL 18	.0033354	.0038181	.0105639
LEVEL 19	.0015135	.0017967	.0019295
LEVEL 20	.0009738	.0011024	.0012008
LEVEL 21	.0003579	.0003852	.0000965
LEVEL 22	.0002275	.0002442	.0003143
LEVEL 23	.0000134	.0000213	.0000242
LEVEL 24	.0000004	.0000010	.0000011
TOTAL	3.1968801	3.1559705	3.1455476

ENERGY	CAPTURE	FISSION	1 FISSION	2 FISSION	3 FISSION	4 FISSION	5 FISSION
3.6000000	.0152770	.0002905	.0002943	.0000238	.0000000	.0000023	
3.8000000	.0143134	.0006863	.0004156	.0002146	.0000240	.0000316	
3.9000000	.0133414	.0005852	.0003960	.0003343	.0004418	.0001026	

ENERGY	FISSION TOTAL
3.6000000	.0006110
3.8000000	.0013523
3.9000000	.0013599

APPENDIX IV

Transition State Spectroscopy Computer Code and Sample Output

```
                      PROGRAM INTEGRO(INPUT,OUTPUT,TAPE5=INPUT,TAPE6=OUTPUT)
000003                DIMENSION TRC(30,15),RHON(10,6),RHO(6),E(15),ELIM(15)
000003                READ(5,200)ATOMW,E0,TEMPER,EX,PZ,PN
000023          200   FORMAT(8F10.5)
000023                READ(5,201)NE,NMAX,LMAX
000035          201   FORMAT(3I2)
000035                WRITE(6,202)
000041          202   FORMAT(* *,2X,*ATOMW*,7X,*E0*,6X,*TEMPER*,6X,*EX*,4X,4X,*PZ*,
                     *4X,4X,*PN*,7X,*NMAX*,6X,*LMAX*)
000041                WRITE(6,303)ATOMW,E0,TEMPER,EX,PZ,PN,NMAX,LMAX
000065          303   FORMAT(* *,6(X,F7.3,2X),4X,I2,4X,4X,I2,4X)
000065                T=TEMPER
000067                UX=EX-PZ-PN
000072                ARIT=ALIT(EX)
000074                SIG21=0.0888*SQRT(ARIT*UX)*ATOMW**(2.0/3.0)
000107                LMAX1=LMAX+1
000111                NMAX1=NMAX*2
000112                LMAX12=2*LMAX+1
000113                DO 13 I=1,NE
000115          13    READ(5,300)E(I),ELIM(I)
000127          300   FORMAT(2F10.5)
000127                DO 14 L=1,LMAX1
000130                READ(5,70)(RHON(L,IP),IP=1,6)
000142          70    FORMAT(6E10.3)
000142          14    CONTINUE
000145                DO 10 I=1,NE
000146                EMIN=ELIM(I)
000150                EMAX=E(I)
000151                DO 11 LKN=1,NMAX1
000153                DO 11 L=1,LMAX12
000154          11    TRC(LKN,L)=0.0
000165                WRITE(6,5)
000170           5    FORMAT(*0*)
000170                WRITE(6,20)E(I)
000176          20    FORMAT(* *,*THE NEUTRON ENERGY IS*,3X,F5.2)
000176                WRITE(6,5)
000202                WRITE(6,923)
000206          923   FORMAT(* *,X,*J*,3X,*PIEN*,3X,*ENERGY INTEGRATED TRANSMISSION
                     X COEFFICIENTS*)
000206                DO 1 LKN=1,NMAX1
000210                J=(LKN-1)/2
000212                VI=FLOAT(J)
000214                TRIAL=XMODF(LKN,2)
000217                IF(TRIAL.EQ.0.0)PIEN=-1.0
```

```
000221          IF(TRIAL.EQ.1.0)PIEN=+1.0
000224          DO 2 L=1,LMAX12
000226          CALL ELKAY(L,VL,VK)
000230          LVL=INT(VL+1.0)
000233          DO 18 LV=1,6
000234       18 RHO(LV)=RHON(LVL,LV)
000243          CALL AREA(EMIN,EMAX,RHO,SPECTR,E0,SIG21,T,VI,PZ,PN,ATOMW,EX)
000256          TRC(LKN,L)=SPECTR
000262        2 CONTINUE
000265          WRITE(6,926)J,PIEN,(TRC(LKN,N),N=1,LMAX12)
000304      926 FORMAT(* *,I2,1X,F4.1,3X,11(E10.3,1X))
000304        1 CONTINUE
000307       10 CONTINUE
000311          STOP
000313          END
```

```
                      SUBROUTINE AREA(EMIN,EMAX,A,SPECTR,E0,SIG21,TAU,J,PZ,PN,ATOM,EX)
000017                DIMENSION E(40),A(6)
000017                T(S,B,C,D,F,EINT)=S/(1.0+EXP(B*(C-EINT)))+D*EINT**F
000050                REAL J
000050                H=(EMAX-EMIN)/30.0
000052                YEVEN=YODD=0.0
000055                YSUMO=YSUME=0.0
000057                E(1)=EMIN+H
000060                DO 1 I=2,30
000062                E(I)=E(I-1)+H
000065           1    CONTINUE
000066                NINT=15
000067                DO 2 N=1,NINT
000071                FACTOR=FACTUR=1.0
000074                I=N-1
000075                KO=2*I+1
000076                KE=2*I+2
000100                IF(A(6).GT.E(KO))FACTOR=0.0
000105                IF(A(6).GT.E(KE))FACTUR=0.0
000112                EP=EMAX-E(KO)
000114                EB=EMAX-E(KE)
000117                IF(EP-EX)10,10,15
000122           10   RHO=EVAL1(EP,E0,SIG21,TAU,J)/2.0
000134                GO TO 20
000134           15   AE=ALIT(EP)
000136                RHO=EVAL2(U,PZ,PN,EP,AE,ATOM,J)/2.0
000160           20   YODD=RHO*T(A(1),A(2),A(3),A(4),A(5),E(KO))
000170                YODD=YODD*FACTOR
000172                IF(YODD.LT.0.0)YODD=0.0
000175                YSUMO=YSUMO+4.0*YODD
000200                IF(EB-EX)25,25,30
000203           25   RHO=EVAL1(EB,E0,SIG21,TAU,J)/2.0
000215                GO TO 35
000215           30   AE=ALIT(EB)
000217                RHO=EVAL2(U,PZ,PN,EB,AE,ATOM,J)/2.0
000231           35   YEVEN=RHO*T(A(1),A(2),A(3),A(4),A(5),E(KE))
000251                YEVEN=YEVEN*FACTUR
000253                IF(YEVEN.LT.0.0)YEVEN=0.0
000256                IF(N.EQ.NINT)YEVEN=YEVEN/2.0
000261                YSUME=YSUME+YEVEN*2.0
000264           2    CONTINUE
000266                SPECTR=(H/3.0)*(YSUME+YSUMO)/(2.0*3.14159)
000272                RETURN
000272                END
```

```
                FUNCTION XMODF(K,L)
000005          XMODF=K-(K/L)*L
000012          RETURN
000012          END
```

```
                      FUNCTION ALIT(E)
000003                ALIT = 29.2 + 205.62*EXP(-1.003*E)
000012          20    RETURN
000014                END
```

```
                SUBROUTINE FLKAY(NN,FLN,FKN)                          R1050908
000006        1 TEMP=FLOAT(NN)
000010        5 TEMP1=TEMP/2.0                                        R1050910
000012       10 TEMP2=(TEMP-1.0)/2.0                                  R1050911
000015       15 ITEMP=XMODF(NN,2)                                     R1050912
000023       20 IF (ITEMP-1) 45,30,25                                 R1050913
000026       25 IERR=25                                               R1050914
000027          GO TO 9500                                            R1050915
000030       30 FLN=TEMP2                                             R1050916
000031       35 FKN=TEMP1                                             R1050917
000032       40 GO TO 55                                              R1050918
000033       45 FLN=TEMP1                                             R1050919
000034       50 FKN=TEMP2                                             R1050920
000035       55 RETURN                                                R1050921
000036     9500 WRITE OUTPUT TAPE 6,9105,IERR                         R1050922
000044          MESS = 4HOHEL
000046     9105 FORMAT(1X,18H********** ERR = ,I4)                    R1050925
000046          END                                                   R1050926
```

```
                FUNCTION EVAL1(EJ,E0,SIG21,T,J)
000010          REAL J
000010          B=J*(J+1)/(2.0*SIG21)
000014          C=(EJ-E0)/T
000016          D=C-B
000020          CONSTJ=(2*J+1)/(2.0*SIG21)
000025          EVAL1=CONSTJ*EXP(D)/T
000034          RETURN
000035          END
```

```
                FUNCTION EVAL2(U,PZ,PN,EP,AE,A,J)
000012          REAL J
000012          U=EP-PZ-PN
000014          SIG22=0.0888*SQRT(AE*U)*A**(2./3.)
000032          B=J*(J+1)/(2.0*SIG22)
000040          C=2.0*SQRT(AE*U)
000051          D=C-B
000053           CONST0=(12.0*(AE**0.25)*(U**1.25))**(-1.0)
000066          CONSTJ=(2*J+1)/(SQRT(8.0        )*(SIG22**1.5))
000101          EVAL2=CONST0*CONSTJ*EXP(D)
000106          RETURN
000106          END
```

8 1.0	2.237E+01	3.785E+01	3.785E+01	6.829E+00	6.829E+00	3.072E+00	3.072E+00	6.580E-01	6.580E-01	7.059E-03	7.059E-03
8 -1.0	2.237E+01	3.785E+01	3.785E+01	6.829E+00	6.829E+00	3.072E+00	3.072E+00	6.580E-01	6.580E-01	7.059E-03	7.059E-03
9 1.0	1.741E+01	2.930E+01	2.930E+01	5.280E+00	5.280E+00	2.352E+00	2.352E+00	5.034E-01	5.034E-01	5.401E-03	5.401E-03
9 -1.0	1.741E+01	2.930E+01	2.930E+01	5.280E+00	5.280E+00	2.352E+00	2.352E+00	5.034E-01	5.034E-01	5.401E-03	5.401E-03
10 1.0	1.287E+01	2.154E+01	2.154E+01	3.877E+00	3.877E+00	1.708E+00	1.708E+00	3.652E-01	3.652E-01	3.917E-03	3.917E-03
10 -1.0	1.287E+01	2.154E+01	2.154E+01	3.877E+00	3.877E+00	1.708E+00	1.708E+00	3.652E-01	3.652E-01	3.917E-03	3.917E-03
11 1.0	9.063E+00	1.506E+01	1.506E+01	2.708E+00	2.708E+00	1.178E+00	1.178E+00	2.516E-01	2.516E-01	2.700E-03	2.700E-03
11 -1.0	9.063E+00	1.506E+01	1.506E+01	2.708E+00	2.708E+00	1.178E+00	1.178E+00	2.516E-01	2.516E-01	2.700E-03	2.700E-03

THE NEUTRON ENERGY IS 3.40

J	PIEN	ENERGY INTEGRATED TRANSMISSION			P=0 COEFFICIENTS		P=1		P=2		P=3		P=4		P=5	
0	1.0	8.590E+00	1.491E+01	1.491E+01	2.730E+00	2.730E+00	1.315E+00	1.315E+00	2.986E-01	2.986E-01	3.366E-03	3.366E-03
0	-1.0	8.590E+00	1.491E+01	1.491E+01	2.730E+00	2.730E+00	1.315E+00	1.315E+00	2.986E-01	2.986E-01	3.366E-03	3.366E-03
1	1.0	2.479E+01	4.299E+01	4.299E+01	7.868E+00	7.868E+00	3.782E+00	3.782E+00	8.595E-01	8.595E-01	9.681E-03	9.681E-03
1	-1.0	2.479E+01	4.299E+01	4.299E+01	7.868E+00	7.868E+00	3.782E+00	3.782E+00	8.595E-01	8.595E-01	9.681E-03	9.681E-03
2	1.0	3.813E+01	6.617E+01	6.617E+01	1.210E+01	1.210E+01	5.797E+00	5.797E+00	1.318E+00	1.318E+00	1.483E-02	1.483E-02
2	-1.0	3.813E+01	6.617E+01	6.617E+01	1.210E+01	1.210E+01	5.797E+00	5.797E+00	1.318E+00	1.318E+00	1.483E-02	1.483E-02
3	1.0	4.752E+01	8.220E+01	8.220E+01	1.501E+01	1.501E+01	7.159E+00	7.159E+00	1.629E+00	1.629E+00	1.830E-02	1.830E-02
3	-1.0	4.752E+01	8.220E+01	8.220E+01	1.501E+01	1.501E+01	7.159E+00	7.159E+00	1.629E+00	1.629E+00	1.830E-02	1.830E-02
4	1.0	5.223E+01	9.013E+01	9.013E+01	1.644E+01	1.644E+01	7.785E+00	7.785E+00	1.774E+00	1.774E+00	1.988E-02	1.988E-02
4	-1.0	5.223E+01	9.013E+01	9.013E+01	1.644E+01	1.644E+01	7.785E+00	7.785E+00	1.774E+00	1.774E+00	1.988E-02	1.988E-02
5	1.0	5.248E+01	9.058E+01	9.058E+01	1.643E+01	1.643E+01	7.719E+00	7.719E+00	1.762E+00	1.762E+00	1.968E-02	1.968E-02
5	-1.0	5.248E+01	9.058E+01	9.058E+01	1.643E+01	1.643E+01	7.719E+00	7.719E+00	1.762E+00	1.762E+00	1.968E-02	1.968E-02
6	1.0	4.903E+01	8.404E+01	8.404E+01	1.526E+01	1.526E+01	7.098E+00	7.098E+00	1.624E+00	1.624E+00	1.807E-02	1.807E-02
6	-1.0	4.903E+01	8.404E+01	8.404E+01	1.526E+01	1.526E+01	7.098E+00	7.098E+00	1.624E+00	1.624E+00	1.807E-02	1.807E-02
7	1.0	4.302E+01	7.341E+01	7.341E+01	1.330E+01	1.330E+01	6.111E+00	6.111E+00	1.401E+00	1.401E+00	1.553E-02	1.553E-02
7	-1.0	4.302E+01	7.341E+01	7.341E+01	1.330E+01	1.330E+01	6.111E+00	6.111E+00	1.401E+00	1.401E+00	1.553E-02	1.553E-02
8	1.0	3.566E+01	6.054E+01	6.054E+01	1.093E+01	1.093E+01	4.956E+00	4.956E+00	1.139E+00	1.139E+00	1.256E-02	1.256E-02
8	-1.0	3.566E+01	6.054E+01	6.054E+01	1.093E+01	1.093E+01	4.956E+00	4.956E+00	1.139E+00	1.139E+00	1.256E-02	1.256E-02
9	1.0	2.804E+01	4.734E+01	4.734E+01	8.522E+00	8.522E+00	3.802E+00	3.802E+00	8.766E-01	8.766E-01	9.611E-03	9.611E-03
9	-1.0	2.804E+01	4.734E+01	4.734E+01	8.522E+00	8.522E+00	3.802E+00	3.802E+00	8.766E-01	8.766E-01	9.611E-03	9.611E-03
10	1.0	2.094E+01	3.519E+01	3.519E+01	6.312E+00	6.312E+00	2.766E+00	2.766E+00	6.400E-01	6.400E-01	6.972E-03	6.972E-03
10	-1.0	2.094E+01	3.519E+01	3.519E+01	6.312E+00	6.312E+00	2.766E+00	2.766E+00	6.400E-01	6.400E-01	6.972E-03	6.972E-03
11	1.0	1.497E+01	2.493E+01	2.493E+01	4.454E+00	4.454E+00	1.913E+00	1.913E+00	4.442E-01	4.442E-01	4.804E-03	4.804E-03
11	-1.0	1.497E+01	2.493E+01	2.493E+01	4.454E+00	4.454E+00	1.913E+00	1.913E+00	4.442E-01	4.442E-01	4.804E-03	4.804E-03

THE NEUTRON ENERGY IS 3.90

J	PIEN	ENERGY INTEGRATED TRANSMISSION			COEFFICIENTS							
0	1.0	1.065E+01	1.857E+01	1.857E+01	3.413E+00	3.413E+00	1.667E+00	1.667E+00	3.710E-01	3.710E-01	4.421E-03	4.421E-03
0	-1.0	1.065E+01	1.857E+01	1.857E+01	3.413E+00	3.413E+00	1.667E+00	1.667E+00	3.710E-01	3.710E-01	4.421E-03	4.421E-03
1	1.0	3.074E+01	5.356E+01	5.356E+01	9.840E+00	9.840E+00	4.795E+00	4.795E+00	1.068E+00	1.068E+00	1.272E-02	1.272E-02
1	-1.0	3.074E+01	5.356E+01	5.356E+01	9.840E+00	9.840E+00	4.795E+00	4.795E+00	1.068E+00	1.068E+00	1.272E-02	1.272E-02
2	1.0	4.743E+01	8.252E+01	8.252E+01	1.514E+01	1.514E+01	7.352E+00	7.352E+00	1.639E+00	1.639E+00	1.948E-02	1.948E-02
2	-1.0	4.743E+01	8.252E+01	8.252E+01	1.514E+01	1.514E+01	7.352E+00	7.352E+00	1.639E+00	1.639E+00	1.948E-02	1.948E-02
3	1.0	5.912E+01	1.027E+02	1.027E+02	1.882E+01	1.882E+01	9.042E+00	9.042E+00	2.029E+00	2.029E+00	2.404E-02	2.404E-02
3	-1.0	5.912E+01	1.027E+02	1.027E+02	1.882E+01	1.882E+01	9.042E+00	9.042E+00	2.029E+00	2.029E+00	2.404E-02	2.404E-02
4	1.0	6.512E+01	1.129E+02	1.129E+02	2.063E+01	2.063E+01	9.882E+00	9.882E+00	2.210E+00	2.210E+00	2.611E-02	2.611E-02
4	-1.0	6.512E+01	1.129E+02	1.129E+02	2.063E+01	2.063E+01	9.882E+00	9.882E+00	2.210E+00	2.210E+00	2.611E-02	2.611E-02
5	1.0	6.561E+01	1.133E+02	1.133E+02	2.067E+01	2.067E+01	9.805E+00	9.805E+00	2.198E+00	2.198E+00	2.586E-02	2.586E-02
5	-1.0	6.561E+01	1.133E+02	1.133E+02	2.067E+01	2.067E+01	9.805E+00	9.805E+00	2.198E+00	2.198E+00	2.586E-02	2.586E-02
6	1.0	6.150E+01	1.058E+02	1.058E+02	1.925E+01	1.925E+01	9.022E+00	9.022E+00	2.029E+00	2.029E+00	2.373E-02	2.373E-02
6	-1.0	6.150E+01	1.058E+02	1.058E+02	1.925E+01	1.925E+01	9.022E+00	9.022E+00	2.029E+00	2.029E+00	2.373E-02	2.373E-02
7	1.0	5.417E+01	9.279E+01	9.279E+01	1.682E+01	1.682E+01	7.775E+00	7.775E+00	1.754E+00	1.754E+00	2.039E-02	2.039E-02
7	-1.0	5.417E+01	9.279E+01	9.279E+01	1.682E+01	1.682E+01	7.775E+00	7.775E+00	1.754E+00	1.754E+00	2.039E-02	2.039E-02
8	1.0	4.510E+01	7.687E+01	7.687E+01	1.388E+01	1.388E+01	6.312E+00	6.312E+00	1.430E+00	1.430E+00	1.650E-02	1.650E-02
8	-1.0	4.510E+01	7.687E+01	7.687E+01	1.388E+01	1.388E+01	6.312E+00	6.312E+00	1.430E+00	1.430E+00	1.650E-02	1.650E-02
9	1.0	3.565E+01	6.041E+01	6.041E+01	1.086E+01	1.086E+01	4.848E+00	4.848E+00	1.103E+00	1.103E+00	1.262E-02	1.262E-02
9	-1.0	3.565E+01	6.041E+01	6.041E+01	1.086E+01	1.086E+01	4.848E+00	4.848E+00	1.103E+00	1.103E+00	1.262E-02	1.262E-02
10	1.0	2.682E+01	4.516E+01	4.516E+01	8.081E+00	8.081E+00	3.533E+00	3.533E+00	8.074E-01	8.074E-01	9.157E-03	9.157E-03
10	-1.0	2.682E+01	4.516E+01	4.516E+01	8.081E+00	8.081E+00	3.533E+00	3.533E+00	8.074E-01	8.074E-01	9.157E-03	9.157E-03
11	1.0	1.926E+01	3.219E+01	3.219E+01	5.731E+00	5.731E+00	2.447E+00	2.447E+00	5.623E-01	5.623E-01	6.311E-03	6.311E-03
11	-1.0	1.926E+01	3.219E+01	3.219E+01	5.731E+00	5.731E+00	2.447E+00	2.447E+00	5.623E-01	5.623E-01	6.311E-03	6.311E-03

THE NEUTRON ENERGY IS 4.10